Chapter One

Introduction

1.1 Background to the Study

The green approach for metal oxide nanoparticle (NPs) synthesis is currently discussed in material science and nanotechnology, and it is quick, simple, cost-effective, and environmentally friendly. Exploring matter at the nanoscale, known as nanotechnology (typically ranging between 1-100 nm), has broadened horizons across various fields, including Nanomedicine, biotechnology, and pivotal applications like drug delivery, electronics, cosmetics, and biosensors. Nanoparticles of diverse shapes and sizes can be fabricated through physical, chemical, or biological methods. Biological processes involve the utilization of microorganisms (such as bacteria, fungi, yeast, algae, etc.) and plants. However, employing microorganisms carries inherent risks related to pathogenicity and demands the maintenance of significant cultures. Thus, it is preferable to synthesize nanoparticles using environmentally friendly or green procedures. We provide a comprehensive overview of green synthesis, a cost-effective and straightforward method for producing nanoparticles using plant components for making nanoparticles. Additionally, we delve into the various factors that could influence the ecological friendliness of nanoparticle production.

Metals are often employed in human activities because of their outstanding mechanical and electrical properties, [1, 2, 3]. Preventive maintenance is vital to protect these metals from degradation. The most common adverse circumstance that degrades metals is corrosion [4]. The term "corrosion" refers to the aging process that a material goes through due to a chemical interaction with its surroundings. When a gas or liquid interacts with an exposed metal surface, corrosion occurs. Moreover, high temperatures, acids, and salts can speed up the process.

Mild steel is most frequently employed in the construction, oil, food, energy, and chemical industries due to its many uses, the bulk of which are based on its exceptional mechanical qualities. It is thus relatively affordable and accessible. Moreover, this metal offers excellent hardness, longevity, and mechanical resistance, among other characteristics [2, 3]. Instead of the above, finding solutions to problems with the corrosion-related degradation of mild steel should be a top concern. To a lesser degree, alloys made of copper and aluminum are studied. Using corrosion inhibitors may lower the high corrosion cost resulting from the need to replace damaged metals [5].

Plant extracts have been used in a variety of ways to prevent corrosion on the surface of mineral materials. Electrochemical investigations, which include methods including electrochemical impedance spectroscopy, weight loss monitoring, and potential dynamic polarization, are widely used to assess the efficacy of these extracts.

1.2 Corrosion

Corrosion is a natural phenomenon; it's one of the most frequent occurrences in our everyday lives. This is a process in which pure metals react with elements such as water or air, forming undesirable compounds.

This reaction damages and disintegrates the metal, starting with the area exposed to the environment and progressing to the majority of the metal as a whole. The conversion of refined metals into more stable compounds like metal oxides, metal sulfides, or metal hydroxides is another way to conceptualize corrosion.

Furthermore, corrosion is a chemical process that forms a reddish-brown film, otherwise known as "rust." It is an irreversible, spontaneous process in which metals change into far more stable chemical compounds, such as oxides, sulfides, hydroxides etc [6].

Although "corrosion" is typically associated with the deterioration of metals, whether natural or man-made, both types are subject to degradation over time. High levels of air pollution can expedite this degradation.

1.2.1 Environmental Impacts of Corrosion

Corrosion threatens historical and natural sites and increases the likelihood of catastrophic system failures. This corrosion is attributed to rising levels of air pollution, which have become a prevalent issue. Developed nations have witnessed a simultaneous rise in air pollution and corrosion levels. This trend extends to items commonly found near residential areas, including vehicles, home furnishings, patio furniture, and other objects.

Locations utilized for crucial manufacturing, communication, data transfer, Industrial process control, and the preservation of cultural assets can all be harmed by corrosion. Corrosion may also cause damage to critical infrastructure, including bridges, electrical towers, parking garages, and roads with steel reinforcement.In fact, one of the main causes of corrosion is sulfur dioxide, which power plants and automobile emissions produce. Copper connections used in electronic equipment are particularly susceptible to the aggressiveness of sulfur dioxide [5].High concentrations of sulfur dioxide can harm trees and plants by damaging leaves and inhibiting new growth. A recent analysis by Greenpeace indicates that excessive sulfur dioxide leads to severe air pollution and premature mortality [5]. This occurs due to chemical reactions between liquids and solids, resulting in the generation of airborne pollutants like corrosive particulate matter (PM). Examples of such substances include black carbon and salt, which can interact with metal molecules and accelerate their deterioration. Furthermore, gaseous acidic pollutants, acting as precursors to corrosive particulate matter, exert a substantial influence on material corrosion, both directly and indirectly [6].

In essence, sulfur dioxide not only accelerates the corrosion of metals and other materials but also adversely affects human health. The US Environmental Protection Agency (EPA) has demonstrated that short-term exposure to sulfur dioxide exacerbates asthma symptoms and causes breathing difficulties [7].

Alternatively, research suggests that elevated levels of air pollution can expedite corrosion and the deterioration of metals more rapidly compared to areas with lower pollution levels. According to the study, pollution levels peak during winter, leading to accelerated rusting of metals. Several factors contribute to this increase in pollution, including heightened usage of heating systems and vehicles during winter, as well as increased emissions from nearby power and heating facilities [7].

The primary contaminants that induce corrosion are carbon dioxide, dust, humidity, and sulfur dioxide. Additionally, other pollutants significantly impacting corrosion include hydrogen sulfide emitted by waste facilities, geothermal activity, and the anaerobic digestion of organic waste [7].

1.2.2 The Impacts of Corrosion on the Economy

Similar to the inevitability of death and taxes, corrosion is a phenomenon we endeavor to evade, yet ultimately, we must come to terms with its presence. While degradation is commonly linked with metallic materials, it can occur with any type of material. For instance, degradation of polymeric insulating wire coatings has posed challenges in older aircraft. Even ceramics are vulnerable to damage through selective disintegration.

1.2.2.1 Cost of Annual Direct Corrosion

Considering the thermodynamic factors involved, it's unsurprising that corrosion comes with substantial costs. Numerous studies conducted over the past three decades have revealed that the annual direct cost of corrosion to an industrial economy amounts to approximately 3.1% of the nation's Gross National Product (GNP) [8]. In the United States alone, this translates to over $276 billion annually. The Department of Defense incurs an annual corrosion cost of $20 billion [8, 9].

Given the significant historical, economic, and safety implications of corrosion on society, coupled with the fact that corrosion of metals is an electrochemical process, it has been a focal point of society since 1903 [8, 9].

1.2.2.2 What Does Corrosion Cost on a Worldwide Scale?

The global annual cost of corrosion stands at $2.5 trillion, as reported by NACE International. This figure represents approximately 3.4 % of the global GDP. Implementing the most effective corrosion prevention measures could potentially save the world between $375 billion and $875 billion, equivalent to 15–35 % of the total cost [8, 9].

During the last 50 years, several studies have been conducted on the societal consequences of corrosion. Using varied techniques, the studies all arrived at corrosion costs that were around 3 % – 4 % of the gross domestic product (GDP) for each nation. Hence, taking a 3.4 % global GDP (2013) as a benchmark, the global cost of corrosion may be estimated to be US $2.5 trillion. According to predictions, using well-known corrosion management techniques may produce annual savings of US $375 billion to $875 billio, or 15 % to 35 % of the cost of corrosion [8, 9].

The economics of industrialized countries are significantly impacted by corrosion, which is quite expensive. There are direct expenses and indirect costs associated with corrosion on a yearly basis. The inability of a machine or system to operate in accordance with specifications or established norms is one of the effects of corrosion.

Corrosion in today's society is one of the major problems, and that could be regarded as a menace. The majority of industrial designs must constantly include corrosion when estimating an item's lifespan. Corrosion is said to have cost some corporations billions of dollars in recent industrial disasters. According to reports, several oil corporations faced corrosion-related pipeline ruptures, oil spills that definitely polluted the environment, financial losses from having to clean up this mess, and, lastly, significant ecological damage as a result of corrosion effects. Concern about the possibility of corrosion developing in an industrial facility has been high among engineers and scientists working in the disciplines of mechanical, chemical, and petroleum engineering. It is now known that corrosion may affect

the reaction and the purity of the reaction products and that corrosion products can alter the chemistry of a specific process in a number of ways [10].

1.2.3 Corrosion Prevention

Corrosion prevention is essential to save serious losses. Most of the buildings are made of metal. Roads, railways, automobile parts, and even household objects like window grills and doors. Zinc is frequently used to galvanize steel, thereby preventing corrosion. According to test data, zinc corrodes in marine environments around 20 times more slowly than common steel alloys. A thicker galvanized coating will enable the metal to resist corrosion for a longer period.

An alternative is to utilize stainless steel grades 304 or 316. However, 316 stainless steel corrodes less quickly than 304, which is considered adequate for the majority of marine environments [11]. After 40 years of water exposure, the 304 and 316 stainless steel samples used in the 1940 experiments exhibited no corrosion or loss of strength. The primary drawback of stainless steel 304 and 316 is the cost of production compared to alternative corrosion prevention methods. While the original price of corrosion protection technologies is higher, maintenance and replacement expenses are less.

1.3 Pathogenicity of Microorganisms

Pathogenicity of Microorganisms refers to the capacity of certain microorganisms to induce disease in plants, animals, or insects. These organisms, termed pathogens, can harm their host during interaction, either through direct means such as toxins or via virulence factors that indirectly impact the host's immune responses. Pathogenicity encompasses the transmission of disease or the development of disease within a host organism. The degree of pathogenicity, known as virulence, is the ability of bacteria to cause illness based on their genetic, metabolic, or structural characteristics. Virulence involves mechanisms for accessing environmental resources and nutrients, exploiting them, and subsequently moving on to infect new hosts [12].

Pathogens can be classified as facultative, obligatory, or opportunistic. Although they need living hosts to reproduce and survive, obligatory pathogens can infect healthy members of vulnerable host species. Mycobacterium tuberculosis is one example. Opportunistic pathogens grow best on organic substrates and are less dangerous to live hosts. Often targeting individuals with compromised immune systems. The interaction between hosts and pathogens depends on molecular mechanisms facilitated by genetic makeup. Genetic variations, selection of compatible hosts, and the progression into disease are key processes governing these interactions [13].

Many pathogenic microorganisms adhere to their hosts using adhesions or specialized adherence factors. They may then physically penetrate or enter the host's cells. Infections can be intracellular, as seen in *Salmonella, Mycoplasma, Mycobacterium, Legionella spp., Shigella, and Chlamydia*, or extracellular, as observed in *Pseudomonas*[14, 15] .

1.4 Statement of the Problem

Corrosion brought on by outdated infrastructure has been mostly blamed for pipeline failures. In Nigeria, the majority of the petroleum product transportation pipes are more than 60 years old. In the 35 years under consideration, there have been around 7,359 spills in Nigeria, releasing 3,114,255 barrels worth an estimated $247,957,000. This results in the most significant rate of spills worldwide, nearly 600 on average each year. Records showed that 6 %, 25 %, and 69 % of all oil spills in Nigeria occur in land, swamp, and offshore areas, respectively. Corrosion and the ineffective control of corrosion have cost many millions of dollars. Environmentalists requested that the federal government declare a state of emergency regarding oil spills and the affected areas to highlight the hazards of oil leakage. They emphasized that it poses a severe risk to people's lives and property, making it a silent murderer of Nigeria's future. There are 150 fish species and other types of animals that are threatened by spills in Nigeria. Maintaining older pipelines can be tricky, yet cutting losses is necessary. It was demonstrated that the expense of managing corrosion between 2004 and

2008 was significantly less than the estimated cost of an oil spill in 1978 alone. This was calculated to be over $38 billion; prevention is preferable to treatment. It may be crucial to stop more losses if laws and government policies establishing minimum criteria to minimize corrosion are strictly enforced and followed.

The deterioration of the country's energy and transportation infrastructures, the leaking of corrosion products into the environment, and the degeneration of an early generation of medical implants and equipment caused by interactions with human body fluids are just a few of the effects that go far beyond the purely financial. We must intensify the fight against corrosion since its harmful effects outweigh economic loss.

More so, microbial contamination of food is particularly concerning for both developed and developing nations, Food borne illnesses caused by pathogens pose a significant global public health concern, prompting countries to allocate substantial resources to address the issue. Bacterial contamination of food is particularly concerning for both developed and developing nations. P. aeruginosa can induce a wide range of severe acute and chronic life-threatening conditions, including meningitis, otitis media, urinary tract infections, and pneumonia, particularly in individuals with cystic fibrosis. It ranks among the top three causative agents of opportunistic infections in humans, affecting over 2 million patients annually and causing approximately 90,000 deaths each year. Due to its ability to secrete extracellular enzymes, P. aeruginosa is also commonly implicated as a spoilage bacterium, particularly in foods with higher water content and rich nutrient content.

1.5 Justification of the Study

Non-edible plants are often chosen for the synthesis of valuable materials to prevent any risk of depletion of species such as *Cassia javanica, Washingtonia robusta, Adonidia merrillii,* and *Casuarina equisetifolia*. These particular plants are non-edible and may even be considered as weeds. This therefore necessitates the adoption of the eco-friendly green

synthetic route using non-edible plant parts for the synthesis of Zinc oxide and aluminum oxide nanoparticles for corrosion inhibition and medical purposes.Zinc oxide and aluminum oxide nanoparticles are excellent corrosion inhibitors and have good therapeutic properties against diverse microbial strains. These nanoparticles of different shapes and sizes may be produced by physical, chemical, or biological processes. However, physical and chemical processes require the usage of potent reducing agents, which leads to excessive energy use, poor yield, high prices, and negative environmental effects.

1.6 Aims and Objectives of the Study

The primary objective of this study is to develop innovative extracts and nanoparticles that serve as effective inhibitors for both corrosion and antimicrobial purposes.

The specific objectives were to:

I. Synthesize zinc oxide and aluminum oxide nanoparticles using the following plant extracts: *Adonida merrilli*, *Washingtonia robusta*, *Cassia javanica*, *Casuarina equisetifolia.* See Appendix 1 for more details.

II. Characterize the synthesized nanoparticles using Fourier transform infrared spectroscopy (FT-IR), Energy dispersive X-ray analyzer (EDX), UV-vis spectrophotometer, Scanning Electron Microscopy (SEM), X-ray diffractometer (XRD)

III. Determine the corrosion inhibition characteristic of each of the plant extracts in an acidic medium.

IV. Evaluate inhibition studies of zinc oxide and aluminum oxide nanoparticles in an acidic medium.

V. Carry out comparative studies of the corrosion inhibition properties of each plant extract, zinc oxide, and aluminum oxide nanoparticles.

VI. Monitor and measure the degree of mild steel corrosion using the gravimetric technique with electrochemical technique at various acid concentrations.

VII. Determine kinetic study of the corrosion inhibition process.

VIII. Determine the phytochemical properties of the extracts.

IX. Determine the antimicrobial properties of plant extracts, zinc oxide, and aluminum.

Oxide nanoparticles on *Escherichia coli, Pseudomonas aeruginosa, Staphylococcus aureus, and Salmonella*.

1.7 Significance of the Study

This study is poised to advance the field of science, through the use of *Adonida merrilli, Washingtonia robusta , Cassia javanica, Casuarina equisetifolia*, and weeds or unwanted plants from being considered trash to becoming valuable resources. To develop novel corrosion inhibitors and methods to restrict microbial growth, and to synthesize zinc oxide and aluminum oxide nanoparticles using leaf extracts from *Adonida merrilli, Washingtonia robusta , Cassia javanica, and Casuarina equisetifolia.*

1.8 Scope of the Study

The goal of this study is to utilize a green chemistry approach to synthesize zinc oxide and aluminum oxide from aqueous extracts of *Casuarina equisetifolia, Adonida merrilli, Washingtonia robusta, and Cassia Javanica.* The plant extracts and the synthesized nanoparticles will be used for corrosion inhibition study at sulfuric acid concentrations to track the rate of mild steel deterioration.

The corrosion inhibition characteristics of the nanoparticles will be determined at varying concentrations of the acid. The mild steel sample metal's corrosion activity will be determined using gravimetric analysis and a Potentiostat galvanostat, and the sample metal's weight loss will be carefully observed to see whether the phenomenon may be connected to the various phases of the metal's corrosion activity.

Evaluate the antimicrobial activities of aqueous plant extracts from *Casuarina equisetifolia, Adonidia merrillii, Washingtonia robusta,* and *Cassia javanica,* as well as the zinc oxide and

aluminum oxide nanoparticles synthesized from each plant sample, against *Escherichia coli, Pseudomonas aeruginosa, Staphylococcus aureus,* and *Salmonella species.*

1.9 Limitation of the Study

Utilizing leaf extracts and their derived zinc oxide (ZnO) and aluminum oxide (Al_2O_3) nanoparticles offers a sustainable and cost-effective alternative to conventional synthetic agents in corrosion inhibition and antimicrobial studies. While this green approach is both innovative and environmentally friendly, it faces several limitations that may affect the consistency, reproducibility, and overall effectiveness of the results in practical applications.

Variability in Phytochemical Composition: The chemical composition of plant extracts can vary based on factors such as plant age, season, location, soil conditions, and extraction methods. These fluctuations affect the consistency of phytochemicals, which serve as natural reducing and stabilizing agents during nanoparticle synthesis. As a result, variations in the concentration and composition of these compounds lead to inconsistencies in particle size, shape, surface charge, and crystallinity, ultimately impacting the reliability and standardization of corrosion inhibition and antimicrobial performance.

Regulatory, Toxicological, and Environmental Concerns: Although plant extracts are natural, they may contain harmful or allergenic compounds, which, without proper safety evaluation, could limit their use in food-related or biomedical applications. Similarly, while zinc oxide (ZnO) and aluminum oxide (Al_2O_3) nanoparticles are considered environmentally friendly, they may still pose toxicity risks to aquatic life or human cells if not handled properly. These concerns highlight the need for thorough safety assessments before their application, particularly in medical or environmental contexts.

1.10 Operational Definition of Term

Phytochemicals: Phytochemicals are naturally occurring chemical compounds found in plants. These compounds, such as alkaloids, flavonoids, terpenoids, and phenolics,

contribute to the plant's color, flavor, and resistance to pathogens, and have potential health benefits for humans, such as antimicrobial, antioxidant, and anti-inflammatory properties.

Antimicrobial: Antimicrobial refers to substances that kill or inhibit the growth of microorganisms, including bacteria, fungi, viruses, and parasites. Antimicrobials are used in various applications, including medicine, food preservation, and surface disinfection.

Corrosion Inhibition: Corrosion inhibition is the process of reducing or preventing the deterioration of materials, especially metals, due to chemical reactions with environmental factors, such as oxygen, water, or acids. Inhibitors are chemicals that slow down or stop these reactions, protecting materials from damage.

Mild Steel: Mild steel, also known as carbon steel, is a type of low-carbon steel that contains a small percentage of carbon (usually 0.05-0.25%). It is commonly used in construction and manufacturing due to its strength, durability, and ease of fabrication. However, it is susceptible to rust and corrosion when exposed to moisture and oxygen.

Plant Extracts: Plant extracts are concentrated preparations made by extracting bioactive compounds from plant materials using solvents, such as water, ethanol, or methanol. These extracts contain various phytochemicals and are used in a variety of applications, including medicine, cosmetics, and food preservation.

Zinc Oxide Nanoparticles: Zinc oxide nanoparticles (ZnO NPs) are nanoscale particles of zinc oxide that exhibit unique properties, such as high surface area, antimicrobial activity, and UV absorption. These nanoparticles are widely used in applications like sunscreens, coatings, and as antimicrobial agents in various industries.

Aluminum Oxide Nanoparticles: Aluminum oxide nanoparticles (Al_2O_3 NPs) are nanoscale particles of aluminum oxide, known for their hardness, high thermal stability, and biocompatibility. They are used in applications such as drug delivery, sensors, and as corrosion-resistant coatings for metals.

Endnotes

1. Pantea Ghahremania, Mohammad Ebrahim Haji Naghi Tehrani, Mohammad Ramezanzadeha, Bahram Ramezanzadeha, *Golpar leaves extract application for construction of an effective anti-corrosion film for superior mild-steel acidic-induced corrosion mitigation at different temperatures,* **Colloids and Surfaces**, 629, 2021,127488**.**

2. Roland Tolulope Loto, Oluwatobilola Olowoyo *Synergistic effect of sage and jojoba oil extracts on the corrosion inhibition of mild steel in dilute acid solution.* **Procedia Manufacturing,** 35, 2019, 310-314.

3. Chandrabhan Verma, Eno E. Ebenso, Indra Bahadur, M.A. Quraishi. An *overview on plant extracts as environmental sustainable and green corrosion inhibitors for metals and alloys in aggressive corrosive media.* **Journal of Molecular Liquids,** 266, 2020, 577–590. https://doi.org/10.1016.

4. Yu Zhu, Li-Xiang Wang, Y. Behnamian, Shi-zhe Song, Ruiqi Wang, Zhiming Gao, Wenbin Hu, Da-Hai Xia less. *Metal pitting corrosion characterized by scanning acoustic microscopy and binary image processing.* **Corrosion Science**, 170, 2020, 108685.

5. K.T.Dauda, T.F.Owoeye, O.S.I.Fayomi, I.G.Akande. *Ethanolic extract of Chrysophyllum albidum leaves and peels as a green inhibitor for AISI 1015 carbon steel in 1M H_2SO_4 solution* **Vietnam Journal of Chemistry,** 2023 doi: 10.1002/vjch.202200094

6. Anthony Obike, Kelechi Uwakwe, E K Abraham, Wilfred Emori, *Review of the losses and devastation caused by corrosion in the Nigeria oil industry for over 30 years,* **International Journal of Corrosion and Scale Inhibition** 9 (1) ,2020,74-91, DOI: 10.17675/2305-6894-2020-9-1-5

7 Corrosion costs the world an estimated $2.5 trillion USD – RCI | English (rcinet.ca), https://www.rcinet.ca/en/2021/04/24/corrosion-costs-the-world-an-estimated-2-5-trillion-usd/

8 Annual Global Cost of Corrosion: $2.5 Trillion | GlobalSpec, https://insights.globalspec.com/article/2340/annual-global-cost-of-corrosion-2-5-trillion.

9 Surajit Dey, S.M.ASCE1 and Ravi Kiran, M.ASCE *Bio-Based Inhibitors to Mitigate Internal Corrosion in Crude Oil Pipelines*, **Pipelines** 2022. Available Online :DOI:10.1061/9780784484289.009.

10 "Different Types of Corrosion: *Pitting Corrosion - Causes and Prevention".* Corrosionclinic.com. **WebCorr** Corrosion Consulting Services.

11 Bibek Lamichhane , Asmaa M M Mawad , Mohamed Saleh , William G Kelley , Patrick J Harrington , Cayenne W Lovestad , Jessica Amezcua , Mohamed M Sarhan , Mohamed E El Zowalaty , Hazem Ramadan Melissa Morgan , Yosra A Helmy *Salmonellosis*: *An Overview of Epidemiology, Pathogenesis, and Innovative*

Approaches to Mitigate the Antimicrobial Resistant Infections. **antibiotics** 2024 13(1)76 . doi: 10.3390/13010076,PMID: 38247636,PMCID: PMC108126 83.

12 Rodríguez-Cerdeira C., Martínez-Herrera E., Carnero-Gregorio M., López-Barcenas A., Fabbrocini G., Fida M., El-Samahy M., González-Cespón J.L. *Pathogenesis and Clinical Relevance of Candida Biofilms in Vulvovaginal Candidiasis.***Front. Microbiol**. 2020; 11:2884. doi: 10.3389/fmicb.2020.544480.

13 Kevin Bouiller , Xavier Bertrand , Didier Hocquet , Catherine Chirouze *Human Infection of Methicillin-Susceptible Staphylococcus aureus CC398: A Review*. **Microorganisms.** 2020; 8:11.

14 Nour Ahmad-Mansour, Paul Loubet, Cassandra Pouget, Catherine Dunyach-Remy, Albert Sotto, Jean-Philippe Lavigne, and Virginie Molle,*Staphylococcus aureus Toxins: An Update on Their Pathogenic Properties and Potential Treatments* **Toxins (Basel).** 2021 Oct; 13(10):677, 2021 Sep 23.doi:10.3390/toxins13100677,PMCID: PMC8540901,PMID: 34678970.

Chapter Two

Literature Review

2.1 Introduction to Green Nanoparticles

The study of matter at the nanoscale, or between 1 and 100 nm, is known as nanotechnology. In comparison to microparticles (1-1000 μm), "fine particles" (100-2500 nm), and "coarse particles" (2500-10,000 nm), nanoparticles are smaller. This allows for distinct chemical and physical properties, such as colloidal properties and ultrafast optical or electrical effects. Nanoparticles generally do not settle out like colloidal particles, which are typically in the 1-1000 nm range, since they are more impacted by Brownian motion [1].

Due to their size being smaller than the wavelengths of visible light (400-700 nm), nanoparticles are invisible under ordinary optical microscopes, necessitating electron or laser microscopes for observation. Consequently, nanoparticle dispersions in transparent media can remain transparent, whereas larger particle suspensions scatter visible light. Common filters can also capture nanoparticles; hence, specific nanofiltration methods are needed to separate them from liquids.

Nanoparticles are found all throughout nature and are the subject of research in many scientific fields, including biology, chemistry, physics, and geology. They occur at the interface between atomic or molecule structures and bulk materials, displaying special behaviors not observed at either size. They play a critical role in industrial goods such as paints, plastics, metals, ceramics, and magnetic materials, as well as in air pollution. A crucial feature of nanotechnology is the production of nanoparticles with certain characteristics [2].

Nanoparticles have received accolades in several disciplines, such as nanomedicine and biotechnologies, in addition to other key applications, such as drug delivery, electronics, cosmetics, and biosensors. Microorganisms (bacteria, fungi, yeast, algae, etc.) and plants are both used in biological processes; however, utilizing microorganisms is riskier due to the issue of pathogenicity and necessitates the upkeep of large cultures. It is also better to create nanoparticles utilizing green procedures. We provide a general review of green synthesis, a

less expensive and complex way to make nanoparticles that use plants or parts of plants. The myriad factors that may affect how ecologically nanoparticles are produced are also considered and explored. [1, 2].

2.1.1 Various Methods for Synthetization Nanoparticles

There are two major methods for the synthesis of nanoparticles.

1) Top-down and

2) Bottom-up.

1) Top-Down-Synthesis Techniques

The synthesis of nano-scale structures using the top-down approach involves the use of larger devices. Traditional workshops or microfabrication methods, in which the material is cut, machined, and molded with tools, are widely used in this practice. Imperfections, such as structural faults and pollutants, may be present in nanoparticles made top-down [3].

Vander Waals forces between stacked bulk components are frequently broken as part of the top-down method for producing thin-layer crystals. While creating nanoparticles from the bottom up, ionic or covalent bonding is employed. The top-down approach frequently necessitates significant energy inputs with detrimental environmental implications. There should not be any significant negative impact from producing nanoparticles that will be utilized to restore the ecosystem. Top-down techniques include mechanical milling, ion sputtering, laser ablation, and more. Top-down approaches are frequently simpler to use, but they can be used for very small particles. The main issues with this method of manufacturing nanoparticles are changes in the physiochemical characteristics of the Nanoparticles and their surface chemistry [3].

2) Bottom-Up Technique

Brick house construction is comparable to bottom-up manufacturing. Instead of employing bricks piled on top of each other, this method layers atoms or molecules one at a time to

create the necessary nanostructure. This long process requires atoms to self-assemble. Liquid-phase and gas-phase processes are the two different categories of bottom-up methods.

In every case, nanomaterials are produced by a carefully controlled process that begins with a single atom or molecule. Examples of gas-phase techniques are plasma arcing and chemical vapor deposition, while a liquid-phase technique is sol-gel synthesis.

Atoms, molecules, or smaller particles may band together to generate nanoparticles via a bottom-up technique. The first step in creating finished nanoparticles is assembling the nano-organized building blocks of the nanomaterials. Examples of physical-chemical, mist deposition, sol-gel, hydrothermal, spray, and laser decomposition are examples of bottom-up processes [3]. The environment is negatively impacted by the employment of chemicals, extreme temperatures, and pressure to produce nanoparticles through chemical and physical processes. Nanoparticles are produced biologically using isolates, extracts, and other microbes from plants. Biological methods are the most efficient for producing nanoparticles for contaminant removal since they are less expensive, safer for the environment, scalable, and don't need dangerous chemicals, high pressure, energy, or temperature [3]. various methods have been used to synthesize nanoparticles as shown in Figure 2.1 [2,3] .

TOP – DOWN APPROACH

BOTTOM – UP APPROACH

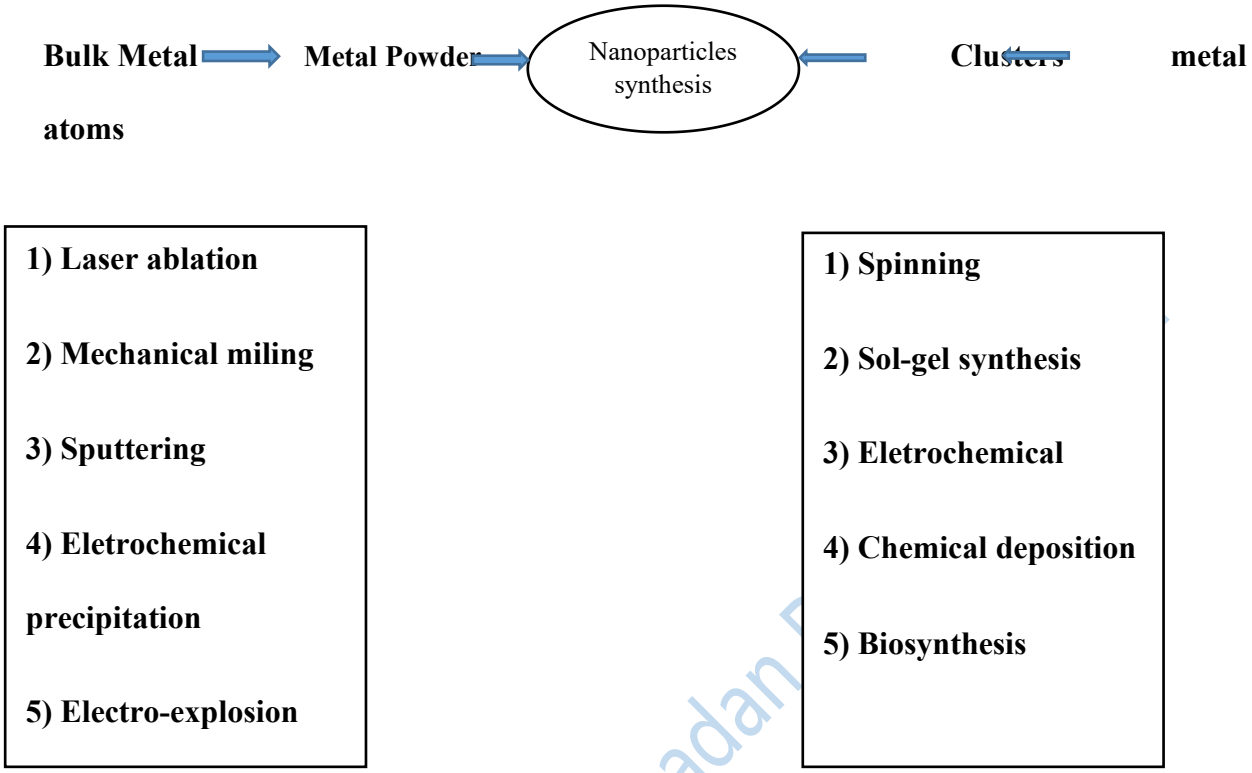

Figure 2.1: Various Methods for Synthetization Nanoparticles [1, 2]

2.1.2 Biosynthesis of Aluminum Nanoparticles

Biosynthesis is now a key trend in the globe due its low cost, high efficacy, and ecologically benign approach. In a recent work, aluminum nitrate was used as a precursor to extract aluminum oxide Nanopowder from *Muntingia calabura* leaves. Aluminum oxide (Al_2O_3) nm has been added in an attempt to improve the characteristics of hybrid composites based on sisal and coir, sisal and banana, and banana and coir. The epoxy-based natural fiber composites were produced by compression casting. Added amounts of nano Al_2O_3 granules were 0, 1, 2, and 3 wt. The results show that all combined hybrid fibers' tensile, flexural, and impact characteristics are enhanced by the addition of nano power to 3 weight percent. For the sisal/coir, banana/coir, and sisal/banana hybrid compounds, the leftover weight percentage increased by 3 % nano substitution, going from 27.15 to 29.14, 26.07 to 31.33 %, and 23.76 to 27.50 %, respectively. When hybrid combinations are in different stages, temperature deterioration becomes better. Scanning electron microscopy (SEM) images showed that the addition of alumina Nano power significantly reduced fiber breakage, matrix cracking, and void gaps [4, 5].

In a recent study, aluminum nanoparticles and *Moringaoleifera* gum-activated carbon are coupled to generate nanocomposites for effective photocatalytic removal of nitrate and phosphate in an aqueous solution. Removing nitrate and phosphate from polluted water is a problem that affects the ecosystem. The objective of the research was to create a carbon-based metal nanocomposite adsorption for improved nitrate and phosphate removal from aqueous solution utilizing a specific light spectrum. Aluminum oxide nanoparticles and *Moringaoleifera* gum-activated carbon (MOGAC) were combined to make nanocomposites using the sol-gel method (Al_2O_3NPs). A nanocomposite was also generated to assess the photocatalytic elimination of nitrate and phosphate under various LED light irradiations. The compound's surface holes, which have a honeycomb-like structure, were visible in the compound's microscopic picture. Al_2O_3 and Al_2O_3/MOGAC had bandgap values of 3.16 and 3.22 eV, respectively, and they matched the reflectance edge of 420 nm. The surface area of

Al_2O_3/MOGAC nanocomposites was found to be 176.92 m^3/gL. Under different LED light, the created nanocomposites showed photocatalytic activity against nitrate and phosphate. After 105 and 75 minutes of contact, respectively, the removal of nitrate and phosphate ions by the red LED light spectrum and ten mg/l of nanocomposite was up to 94% and 95%. After four rounds of nitrate and phosphate reduction, the Al_2O_3/MOGAC nanocomposites usually kept their stability [6].

In this study, the shelf stability of water mixes made with distributed aluminum nanoparticles using conventional and controlled bath temperature two-step procedures was investigated. pH nine water and nanoparticles in the range of 0.1 to 1.0 Vol % were used to make the Nanofluids. A bath-style ultrasonicator was used to evenly distribute the nanoparticles throughout the base fluid. During a 4-hour sonication process, all as-prepared samples were either subjected to an uncontrolled device, such as bath temperature, or temperature control between 10 and 60 °C. The steadiness of the generated as-nano suspensions was also evaluated utilizing the sedimentation snapshot capture technique by capturing pictures over the course of 12 hours at regular intervals and assessing the results using the ratios of sample sedimentation height.[7] It was discovered that the customary approach and set temperatures of 30 °C and above generated nano fluids that displayed flocculated sedimentation behavior, whereas the regulated temperature of under 30 °C produced nano fluids that exhibited dispersed sedimentation behavior. Increasing the temperature of the controlled sonication has also been shown to hasten sediment settling. Also, it was shown that as the nanoparticle concentration grew a constant temperatures, there was less fluctuation in the sedimentation height ratio among the samples [7]. When the two manufacturing processes were compared, it was found that the 30 °C nano fluids had better short- and long-term stability than the suspensions manufactured the traditional way [8,9,10].

Aluminum nanoparticle production in large numbers is difficult using the majority of the currently available synthesis methods. Cryomilling, a top-down method described in the

present work, produces a significant number of aluminum nanoparticles (Al NPs). Cryomilling is known to improve particle size to an ultra-fine level and to reduce the rate of oxidation during synthesis. Due to its high susceptibility to nanoscale oxidation and Nitridation, aluminum is a reactive metal. As a consequence, huge amounts of Al NPs have been produced using a special cryo mill that grinds powder at an extremely low temperature (123 K). This process is recognized as being safe for the environment and producing no unwanted by-products. The ultra-refined Al NPs are a potential choice for use in a range of applications, such as the manufacture of explosive formulations, nanofilms, pigments, and heat-shield coatings for aircraft, among others. The increasing demand for Al NPs will thus be satisfied by the industrial-scale bulk production of Al NPs via Cryomilling. The created nanoparticles have been described using a variety of cutting-edge techniques to establish their size, shape, dispersion stability, and purity, such as AlN. The results demonstrate that it is possible to produce Al NPs that range in size from 5 to 15 nm. Al NPs have been shown to be thermally stable up to 150 °C as a result of research on nanoparticle thermal stability. The results have been analyzed using the now available hypotheses [11].

The use of biosensor technology in the diagnosis of disease and the monitoring of its evolution is very promising. Chemical sensors that are rapid, sensitive, and almost affordable are known as electrochemical biosensors. An integrated electrochemical biosensor with a zinc oxide nano structure doped with aluminum nanoparticles has been developed to detect the dengue virus. A hard mask and thermal evaporator system were used in the construction of the Ag (silver) interdigitated electrode (IDE) embedded on Si-AZO made of Ag. (PVD). In order to set up electrical sensing for DNA probes specific to dengue in quantities of 100 fM, 100 pM, and 10 nM, (IDE/Ag)/AZO/Si) is functionalized by DNA immobilization, hybridization, and surface modification. The limit detection and quantification sensitivity are 15.46 and nM1 and 51.53 an nM1, respectively, while the wide range detection sensitivity is 55.54 an nM1 cm^2. A linear regression coefficient of 0.8563 and a present technology is very

speedy and very effective. Thus, it could aid in the development of dengue virus diagnostics in the future [12].

2.1.3 Biosynthesis of Zinc Oxide Nanoparticles

Utilizing *Cnidoscolus aconitifolius* aqueous leaf extracts, zinc oxide nanoparticles were created, and their biological functions were investigated. The following instruments were used for characterization: FT-IR, TEM, SEM, and UV-Vis spectroscopy. The tests used to evaluate the antioxidant capabilities were DPPH scavenging, ABTS, H_2O_2, NO, and FRAP. Proteinase inhibitory tests, albumin denaturation, and membrane stabilization were used to assess the anti-inflammatory properties. The well diffusion method was used to test the antibacterial effects. The ANOVA statistical analysis was carried out. A peak at 378 nm was found by UV-Vis Spectroscopy, suggesting the existence of artificial nanoparticles. Functional groups that suggested the plant extract's stabilizing effect on the nanoparticle surface were found by FT-IR analysis. SEM analysis confirmed spherical morphology, with TEM indicating a size of 100 nm. In antioxidant assays, zinc oxide nanoparticles exhibited significant potential compared to the ascorbic acid standard across various tests. They also demonstrated noteworthy anti-inflammatory properties, particularly in membrane stabilization. Moreover, the nanoparticles showed inhibitory effects against clinical pathogens compared to the standard drug Cefuroxime. These promising biological activities highlight the potential applications of these nanoparticles in various fields [13].

Biosynthesized nanoparticles have become a major contender for replacing traditional physical and chemical synthesis techniques in recent times. The production of zinc oxide nanoparticles (ZnO NPs) was done using zinc nitrate and leaf extracts from *Phoenix dactylifera L*. The purpose of the study was to evaluate these nanoparticles' effects on biochemical and biomass parameters. X-ray diffraction (XRD), transmission electron microscopy (TEM), ultraviolet-visible spectrophotometry, and Fourier transform infrared spectroscopy (FTIR) were used to characterize the biosynthesized ZnO nanostructures. The

findings showed that the nanoparticles were spherical and ranged in size from 16 to 35 nm. They also showed clear functional group peaks and a UV absorption peak at 370.5 nm. The effects of various doses (0.0 mg/L, 80 mg/L, and 160 mg/L) of biosynthesized ZnO nanoparticles on the biomass and in vitro bioactive chemical synthesis in *Juniperus procera* were also examined in the study. In vitro growth of J. *Procera* was observed to be greatly improved by concentrations of biosynthesized ZnO NPs (80 mg/L and 160 mg/L) when compared to non-treated plants. On the other hand, although the maximum concentration of ZnO NPs (160 mg/L) at first promoted plant development, after a month the calluses became brownish and the shoots turned yellow. Additionally, GC-MS analysis of the effect of ZnO NPs on phytochemical components in *Juniperus procera calluses* revealed variations across treatments [14].

Furthermore, rapid, environmentally friendly, and straightforward approach for synthesizing zinc oxide nanoparticles (ZnO-NPs) was outlined utilizing extracts from *Ducrosia anethifolia* and *Anabasis setifera* plants. The structural characteristics of the biosynthesized ZnO-NPs were examined through FT-IR, XRD, EDX, and FESEM techniques. These ZnO-NPs, synthesized from two different botanical sources, were also utilized as both support and promoters in the fabrication of Pd/ZnO nanoparticles. XRD, FESEM, EDX, and elemental mapping analyses were employed to ascertain the phase composition and morphology of the synthesized oxides. Electrochemical investigations using cyclic voltammetry revealed that the oxide synthesized from *Ducrosia anethifolia* plant extract exhibited superior promoting behavior for palladium in ethanol oxidation compared to the one from *Anabasis setifera*. This superiority can be attributed to the more porous structure of the oxide synthesized from *Ducrosia anethifolia* extract, resulting in a higher surface area and better dispersion of palladium on the promoter. [15]

2.1.4 Nanoparticles Characterization

Nanoparticles undergo a variety of characterization processes. Determining their spreads, sizes, surface features, and surface area is shown in Figure 2.2. The visual assessment of color shift is the first step in the characterization of every nanoparticle. When gold nanoparticles are produced, a color change from yellow to red may be seen. Moreover, as the particle size rises, the color shifts from a deep red to a purple tint.

Nanoparticles characterization methods

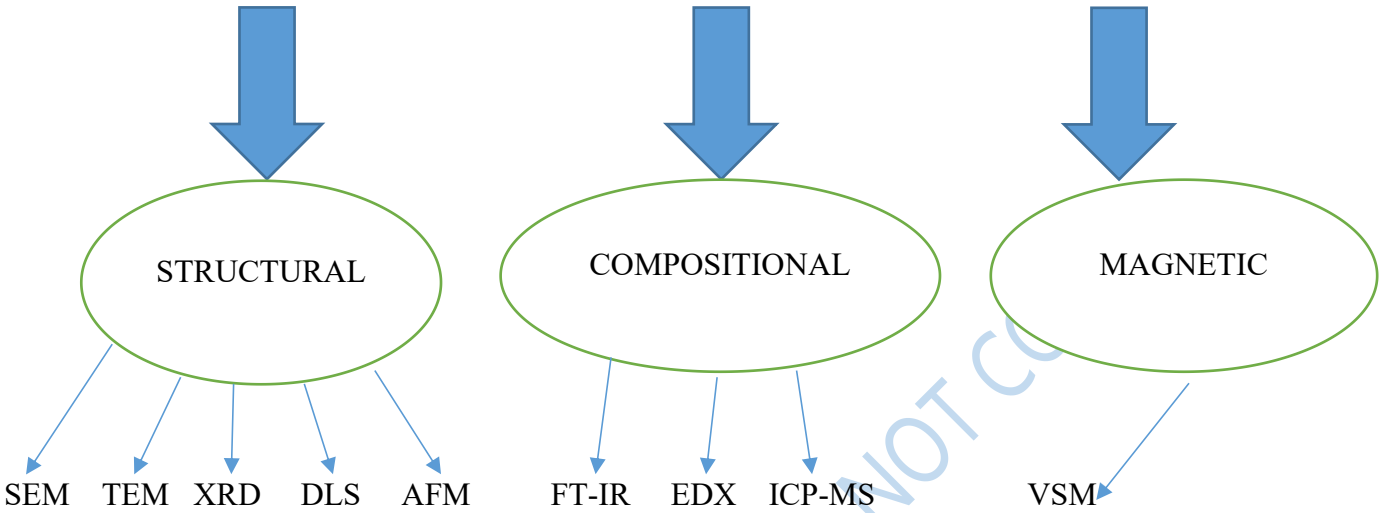

Figure 2.2 Nanoparticle Characterization Techniques [16].

2.1.4.1 The Structural Characterization Method

UV-Vis Spectroscopy

Variations in the Surface Plasmon Resonance (SPR) of the nanoparticles cause color shift. The change in color from yellow to brown can be utilized to visually confirm that nanomaterials are being produced. Like gold nanoparticles, all nanoparticles display a range of colors and tints due to size variation. Surface Plasmon Resonance (SPR) in metallic nanoparticles has demonstrated extraordinary optical properties that may be seen via UV-Vis spectroscopy. A specific SP band is generated as a result of radiation's interaction with metals, which promotes the movement of electrons from their ground state to higher energy states. This helps with the deduction of nanoparticles (nm) up to a point. AgNPs, for instance, have an absorption spectrum between 400 and 450 nm, while AuNPs have one between 500 and 550 nm. This wavelength range applies to ZnO-NPs (350–390 nm). When absorbance is determined for copper nanoparticles between 550 and 700 nm, the appearance of reddish brown color from green color indicates the creation of copper nanoparticles. The dark brown hue signifies the conversion of magnesium nitrate into magnesium nanoparticles [16].

Scanning Electron Microscopy

An electron microscope is used to carry out a SEM inspection. Sample preparation occurs often. Subsequently, carbon samples were placed onto the Grip and exposed to a mercury lamp for 15 minutes to cure. After that, copper grids were coated with tiny layers of carbon. The specimen's surface is in line with the electron beam. A three-dimensional (3D) picture of the material at different magnifications is created by the detection of back-scattered electrons, secondary electrons, and characteristic X-rays. With the use of energy dispersive spectroscopy (EDX) and field emission scanning electron microscopy (FE-SEM), the appearance, structure, and elemental composition of the zinc oxide nanoparticles were investigated.

Transmission Electron Microscopy (TEM)

Transmission electron microscopy (TEM) is another useful technique for figuring out the morphology, size, shape, and aggregation of nanoparticles. The precise restoration of a dry sample with the appropriate thickness is the primary goal in the TEM investigation of nanoparticles. The electrons that flow through the material are used to create two-dimensional TEM pictures. Details on the interior particle structures of nanocarriers and the polymeric walls of nanocapsules may be obtained from TEM images of polymeric nanoparticles with sub-nanometer resolution [17, 18].

X-Ray Diffraction (XRD)

X-ray diffraction is a safe way to analyze metallic nanoparticles (XRD). Analyzing XRD data may help to understand the structure, composition, and molecular interactions of a material. In addition to regulating sample phase and phase content, it is utilized for particle size detection. When electrons possess sufficient energy to cause the inner shell of target materials to shift, characteristic X-ray spectra are generated.

Dynamic Light Scattering (DLS)

Photon correlation spectroscopy (PCS), also referred to as dynamic light scattering (DLS), is a widely utilized technique for ascertaining the size of nanoparticles. A monochromatic laser beam illuminates a colloidal solution in a DLS experiment, and the light scatters into a photon detector. The intensity of scattered light is measured over time to estimate the hydrodynamic particle size. DLS is applicable to colloidal suspensions as well. It provides selectivity, sensitivity, ease of use, and speedier measurement intervals.

Atomic Force Microscope (AFM)

AFM is a type of scanning probe microscopy (SP) that employs a cantilever to scan the material and enable the imaging of nanoparticles. The cantilever deflection is then monitored using a laser-photodiode system that monitors variations in the photodetector output voltage. The two most used imaging methods are AFM and AFM, both in contact and tapping modes. AFM topographic imaging may be used to ascertain the growth mechanism of the

nanocrystals. An AFM was used to measure the height and roughness of cobalt oxide nanoparticles, and 3.16 nm of typical roughness was discovered. The size, aggregation, and shape of the nanoparticles may also be ascertained using AFM examination. The filamentous fungus Penicillium decumbens had silver nanoparticles that were uniformly distributed, spherical in shape, and aggregated=, according to an AFM scan.

Brunauer-Emmet-Teller (BET)

A Brunauer-Emmet-Teller (BET) study is used to determine the surface area of nanoparticles. The surface area of nanoparticles is important for environmental applications. For pollutants like heavy metals and pigments to be absorbed, nanoparticles need to have a larger surface area. The BET surface area was found to be 86.95 m^3/g in a study involving the adsorption of Ni (II) ions by supermagnetic iron oxide nanoparticles coated with green extract. Ni(II) ions might attach to nanoparticles more readily due to the region's mesoporous shape and size [19]. In agricultural contexts; nanoparticles can be employed as carrier molecules to efficiently transmit therapeutic compounds to crops. Having more surface area might be beneficial for collecting crops and distributing medicines. Smaller nanoparticles showed higher surface area-to-volume ratios, which sped up the rate at which target molecules had to dissolve to reach the microorganisms responsible for cleaning up pollution. The aggregation state of nanoparticles is determined by their surface area, which also influences their stability in particular physiological conditions required for the healing process [19].

2.1.4.2 The Magnetic Characterization Method

Vibrating Sample Magnetometers (VSM)

The Phomopsis liquidambaris silver nanoparticles included flavonoids, triterpenoids, and protein, all of which were required for the reduction and capping processes [20]. Magnetic nanoparticles have gained attention recently as a material with potential uses in many different fields. It consists of a magnetic core formed of metal ions and an outside active-

group shell. Functionalized magnetic nanoparticles bring additional challenges related to magnetization, surface effect, and magneto-mechanical effect. The basic characteristic of magnetic nanoparticles is their capacity to be modified by a magnetic force outside. These properties promote the removal of adsorption nanoparticles from the treated solutions under magnetic fields, hence increasing oil recovery. Therefore, recognizing these traits is crucial to developing an effective rehabilitation plan. Nanomaterials' magnetic properties may be evaluated using vibrating sample magnetometers (VSM). An induced current is generated proportionate to the magnetic property of the sample by creating vibration and applying a magnetic field to the embedded coil within the equipment. The produced current is sent into a hysteresis so that the sensor can follow the magnetic properties of nanoparticles. The isolated magnetic iron nanoparticles from Bacillus cereus were clearly superparamagnetic, as evidenced by the fact that they did not magnetize in the presence of an external magnetic field [21].

2.1.4.3 The Compositional Characterization Method

Fourier Transform Infrared Spectroscopy (FTIR)

A variety of nanoparticles, including metallic, carbon, and polymeric nanomaterials, may be recognized via infrared spectroscopy. Potential biomolecules that could cap nanoparticles can be found using Fourier Transform Infrared Spectroscopy. Nanoparticles that have been deposited on activated carbon can also be examined using FTIR.

Energy Dispersive X-Ray (EDX)

The elemental analysis method known as Energy Dispersive X-ray (EDX) microanalysis, which is related to electron microscopy, uses the production of distinctive Xrays to identify the elements that are present in the samples. Both semi-quantitative and semi-qualitative data are present in the EDX microanalysis spectrum. An essential tool for finding nanoparticles is EDX. The characterization of mineral bioaccumulation in the tissues is another use for EDX.

To sum up, the element detection spectroscopy (EDX) is a valuable instrument for any research project requiring the identification of endogenous or exogenous elements in tissue, cell, or other material.

Inductively Coupled Mass Spectrometer (ICP-MS)

Nanoparticles may be analyzed quantitatively and qualitatively using an inductively coupled mass spectrometer (ICP-MS). Zeta sizer analysis may be used to estimate the hydrodynamic diameter, zeta potential measurements, and particle size distribution. Ag nanoparticles were made using Fusarium oxysporum, and the process of creating the particles was accelerated by the presence of fungal filters. The magnetite nanoparticles are also characterized using zeta potential testing. The three primary forces of attraction that prevent nanoparticles from aggregating and dispersing are gravity, magnetic force, and Vander Waals force. The zeta potential test showed a shift from negative to positive values in gold nanoparticles derived from Fusarium solani. The positive values indicate lower nanoparticle stability due to enhanced clustering and less interparticle interaction [22, 23, 24].

2.1.5. Recent Developments in Green Nanoparticle Production and Challenges

Due to the expanding use of nanoscale metals in fields like engineering, health, and the environment, the subject of nanoscale metal production is significant. The majority of nanoscale metals are currently produced chemically, which has unintended effects like degradation of the atmosphere, excessive energy use, and grave health issues. Green synthesis, which substitutes plant extracts for toxic industrial agents, was created to decrease metal ions. Since green synthesis is less expensive, produces less waste, and enhances environmental and human health safety, it is more advantageous than conventional chemical synthesis. The most recent developments in the ecologically friendly synthesis of Au, Ag, Pd, Cu, and Fe NPs (gold, silver, copper, palladium, iron, and iron oxide nanoparticles) were evaluated in this paper. Large-scale studies have shown that the limitations of green synthesis are the timing and location; due to the complexity of the regional and periodic dispersal of

plants and their components, there are issues with production, low purity, and poor production. Ecological synergy, on the other hand, provides an alternative form of development, opportunities, and potential applications while taking into consideration pollution from chemical production and contemporary environmental issues [25].

2.2 Corrosion

Corrosion is one of the most common events in our daily lives. Certain iron objects eventually have a layer of orange or reddish-brown corrosion on top of them. The chemical process that results in the formation of this layer is called rusting, a kind of corrosion [26].

The process that converts refined metals into more stable compounds like metal hydroxides, metal sulfides, or oxides is known as corrosion. Iron oxides are produced when air moisture and oxygen come together, much like iron rusts. The study of corrosion suggests that metals change spontaneously and irreversibly into far more stable chemical compounds, such as oxides, sulfides, and hydroxides [27].

2.2.1 Importance of Corrosion in Various Industries

Economy, safety, and environmental preservation are the three main benefits of corrosion. Corrosion experts aim to mitigate material degradation and associated financial losses stemming from the deterioration of pipelines, tanks, metallic machinery components, ships, bridges, marine infrastructure, and other constructions, collaborating closely with corrosion scientists. The integrity of operational equipment may be jeopardized by corrosion, posing safety risks. This can lead to the failure (with catastrophic results) of items like pressure vessels, boilers, metallic containers for toxic chemicals, turbine blades and rotors, bridges, airplane parts, and automotive steering mechanisms. Safety is a key consideration in the design of equipment for nuclear power plants and the disposal of nuclear waste [26, 27].

Additionally, investments in metal, energy, water, and human resources are needed to rehabilitate rusted equipment. Direct losses and indirect losses are the two categories used to classify economic losses. In addition to the necessary work, the expenses of replacing rusted

machinery and structures, such as condenser tubes, mufflers, pipelines, and metal roofing, are considered direct losses. Other instances are (a) repainting buildings when rust avoidance is the major goal and (b) the initial investment plus ongoing maintenance of cathodic protection systems for subterranean pipes. The need to repair millions of rusted car mufflers and several million home hot water tanks per year as a result of failure from corrosion serve as examples of significant direct losses.

Direct losses also include the extra cost of galvanizing or nickel-plating steel, adding corrosion inhibitors to water, and dehumidifying storage rooms for metal equipment. These expenses are incurred when corrosion-resistant metals and alloys are used in place of carbon steel, which has adequate mechanical properties but insufficient corrosion resistance.

Coastal and marine settings are typically associated with corrosion, although they are not the only ones that might encourage corrosion. In environments that are mostly industrial, air pollution may cause corrosion. If your equipment is exposed to pollution from industries, vehicles, or power plants, it might become less durable. Industrial facilities release gases into the atmosphere, such as sulphur and nitrogen oxide, which subsequently condense back as acidic dew or acid rain. Pollution is not a worry in every industrial situation. Industrial dust particles may include hazardous metal compounds, carbon, sulphates and chlorides.These particles may be highly caustic when combined with oxygen, water, or humid environments. Considerable steps must be taken to mitigate the impacts of this natural phenomenon, which causes large financial losses for many different businesses. A significant driving force behind a lot of the present corrosion research is the economic aspect. Each year, governments and businesses both suffer losses totaling several billions of dollars [27, 28].

2.2.2 Definition of Corrosion and Its Impact

Explaining corrosion to put it simply, it is a natural process that takes place anytime unintended compounds are created when pure metals mix with substances like water or air.

This process corrodes and disintegrates the metal, starting with the part of it that is exposed to the environment and moving on to the majority of it.

2.2.3 Causes of Corrosion

The gradual degradation of desirable metal properties due to interaction with specific environmental factors is commonly termed "metal corrosion." It is well understood that Corrosion has detrimental effects on both the environment and human health. Corrosion of metals and alloys can stem from various sources [23]. Figure.2.3 these elements encompass bases or corrosive substances, salts, liquid compounds, abrasive metal cleaners, potentially hazardous gases, and other agents that can promote rust formation on metal surfaces. Additionally, ambient temperature influences Corrosion in conjunction with the aforementioned factors [24].

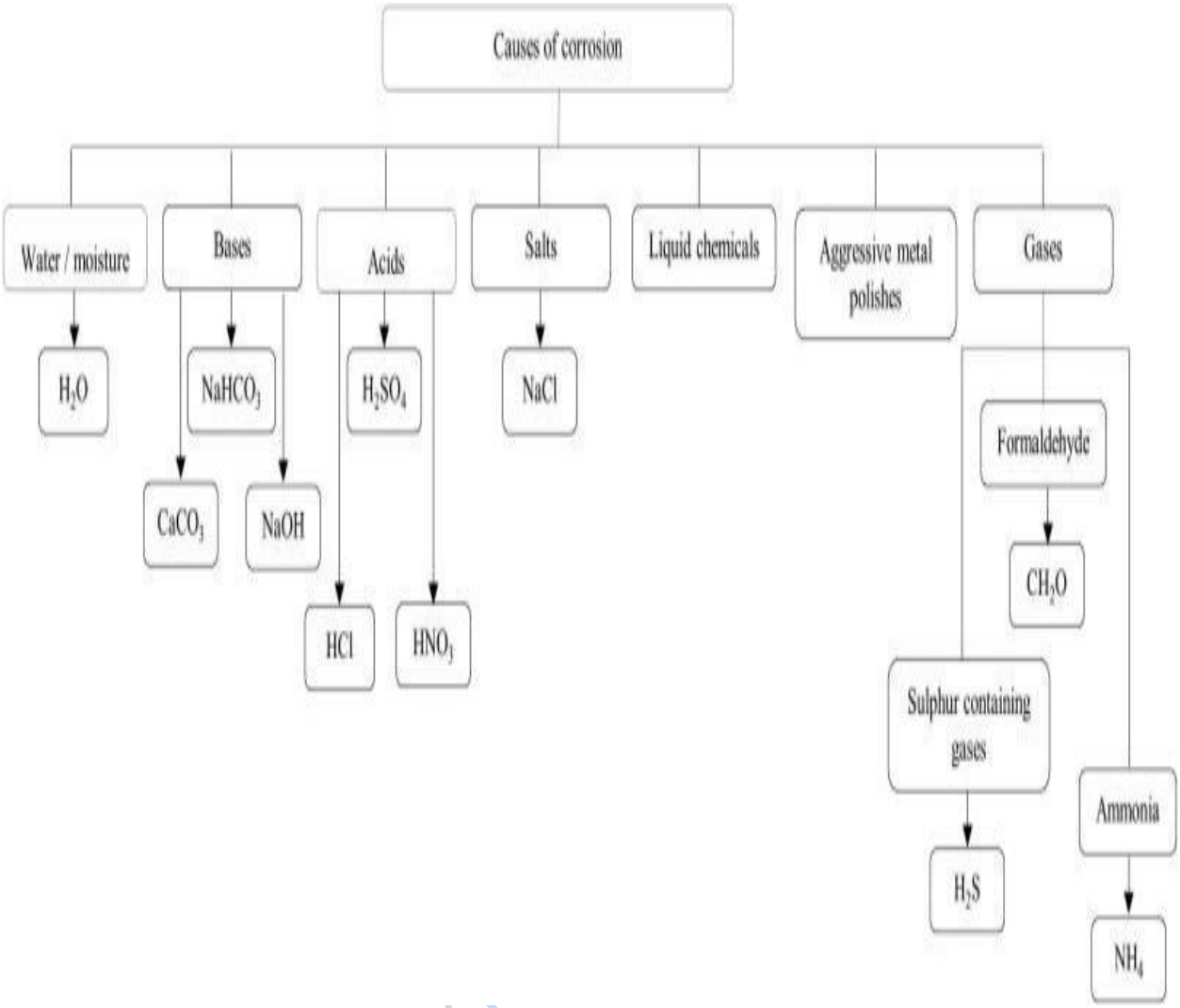

Figure 2.3: Causes of Corrosion [24]

2.2.4 Need for Corrosion Inhibitors

In order to reduce the possibility that corrosion will develop, corrosion inhibitors are chemicals that are added to corrosive surroundings or to metal surfaces in incredibly tiny quantities. On the other hand, inhibitors might be substances that are used in extremely tiny amounts to stop or lessen corrosion. As a consequence of chemical attack or ambient contact, corrosion is a normal process in which composites and metals attempt to return to a more solid thermodynamic state. Moreover, corrosion can come from both natural and man-made processes [29, 30]. "Metals corrosion" is the term used to describe how specific environmental factors combine with intended metal characteristics to cause deterioration [31]. It is widely known that corrosion is bad for the environment and for people's health.

2.2.5. Green Corrosion Inhibitor Types

In general, there are two types of green corrosion inhibitors: organic green corrosion inhibitors and inorganic green corrosion inhibitors. The family of inorganic rust inhibitors with a plant basis is extensively used because of their great output in aqueous environments, whereas the organic class is made up of synthetic compounds that are ecologically benign [32, 33].The green organic inhibitor's benefits over artificial inhibitors clarified how the best protection against abrasive media is to continuously apply organic green corrosion inhibitors to the metal surface[34, 35]. The brittle passive layers created by inorganic inhibitors make a metal surface that is prone to pitting and crevice corrosion, two localized forms of corrosion attack [36, 37].

2.2.6 Four Types of Corrosion Inhibitors

A corrosion inhibitor forms a barrier on a metal surface to thwart corrosive elements. There are a number of different types of corrosion inhibitors.

2.2.6.1 Anodic Inhibitors Anodic inhibitors are present on the metal's exterior, and oxygen mixes to create a thin coating. By oxidizing a surface layer that is less reactive to corrosive chemicals, they reduce the material's susceptibility to corrosion [38, 39].

Anodic inhibitors are present on the metal's exterior, and oxygen mixes to create a thin coating. By oxidizing a surface layer that is less reactive to corrosive chemicals, they reduce the material's susceptibility to corrosion [38, 39].

2.2.6.2 Cathodic Inhibitors

Substances that block the cathodic reaction or the access of reductive elements like oxygen or hydrogen to the metal surface are known as cathodic substances. Examples include oxygen scavengers like sulphite ions that block the flow of oxygen or cathodic poisons like arsenic and selenium ions that disrupt the process [39].

2.2.6.3 Mixed Inhibitors

Chemicals known as mixed inhibitors precipitate or form a film to obstruct both cathodic and anodic actions. Phosphates and sodium silicate are two examples of additives that are used in domestic water softener salts to stop the growth of rust in the water [39].

2.2.6.4 Inhibitors of Volatile Corrosion

In a closed environment, chemicals called volatile corrosion inhibitors are applied to the corrosion site. They create a thin, protective layer of molecules. For instance, to avoid corrosion in condenser tubes, volatile compounds like morpholine or hydrazine are delivered in boilers with steam [39].

2.2.7 Benefits of Green Corrosion Inhibitors over Plant Extracts.

Corrosion inhibitors work by adhering to the top of the substrate and creating a thin coating of defense when applied in very small doses. Efficacy at low concentrations, low toxicity, environmental tolerance, durability at various working times, and shelf life are important considerations when choosing corrosion inhibitors for a certain activity.

Green corrosion inhibitors made from plant extracts often provide a number of advantages compared to many natural corrosion inhibitors. Plant extracts can only be used in low-temperature activities since they are sensitive to heat or Biochemical Agents. Moreover, plant extracts often lose their efficiency when stored for an extended period of time.

Several studies have looked at the possibilities of modifying plant extracts to increase their stability at elevated times and bio-degradation resistance. Several additions, including potassium iodide acetylacetonate, cerium nitrate, zinc oxide, zinc salt sulfate ions, and praseodymium nitrate, have been combined with the extracts. Together, these additions improve the potency of plant extracts. Depending on the biomass (extract) content, temperature, and pH, some active chemical compounds in plant extracts may combine with metal salts to form metal ions complexes and/or nanoparticles. The efficiency of corrosion inhibitors was synergistically increased in the papers mentioned above when metal salts were utilized, but nothing was done to check if the created product was at the nanoscale, despite the fact that materials are more reactive at the nanoscale.

2.2.8. The Efficiency of Plant Extracts as Inhibitors

As it affects many sectors, including metallurgy, chemicals, materials, and the oil industry, metal corrosion is a worldwide issue. Corrosion is typically related to metals as material breakdown is brought on by interaction with ambient gases. Metals corrode and oxidize spontaneously via chemical or electrochemical processes. The production of autos, pipelines, and machinery for the chemical industry depends on the use of mild steel. Employ hydrochloric acid to pickle, descale, and chemically clean mild steel. Issues may be avoided in 90% of instances by adding the proper inhibitor to the medium, and corrosion reduction techniques include plating, painting, and using alloys and inhibitors, among others. Utilizing an inhibitor is one of the best ways to stop metal from corrosion. Sadly, the bulk of inhibitors are salts of organic or inorganic materials that are dangerous and ineffectual. Environmentally friendly inhibitors are being investigated in response to the mounting

dangers to human health and the environment. Several plant extracts are used as corrosion inhibitors for materials in pickling and cleaning processes. Plant extracts may include proteins, polysaccharides, tannin, alkaloids, and other substances. These chemicals are effective corrosion inhibitors for a variety of metals. Natural inhibitors need extra consideration because of the stringent environmental restrictions. These Inhibitors are much less expensive than organ inhibitors.

2.2.9 Factors Influencing Corrosion

2.2.9.1 Environmental Factors

Moisture and Dew: These are among the most important factors in metal corrosion. When exposed to environments with high amounts of moisture and mist, metals quickly acquire rust or corrosion. Dry and non-humid conditions are ideal for metals, especially non-alloy metals. Only dry, non-humid conditions are suitable for the usage of metals. Additionally, we will need to choose non-dry, non-humid metals. By painting and using alloy metals, corrosion, and rust may be prevented. There are specialized anti-rust coatings developed specifically to partially prevent the corrosion-induced degradation of metal.

Temperature: Temperature is a significant factor in metal corrosion and magnetization. In the automobile, pulp and paper, mining and metallurgical processing, refining, and Petrochemical, aerospace, etc. sectors, high temperature is a significant problem. When components are exposed to greater temperatures and a non-inert environment, they may be in danger. Most alloys and metals corrode and oxidize at higher temperatures. Because the active center of corrosion in a substance or metal expands as the temperature rises, corrosion accelerates when exposed to higher temperatures. Therefore, it is vital to protect machinery and metal goods from greater temperatures. The high-temperature structural coating applied to metals will help stop corrosion brought on by greater temperatures [39, 40].

Pollutants in the atmosphere: In close proximity to water and commercial areas, metals rust more quickly. This is brought on by airborne industrial pollutants such as carbon dioxide,

hydrogen sulfide, sulfur dioxide, and HCl, which are common. On the other hand, NaCl, which is found in coastal areas' ambient air, interacts with the surface layer and increases the amount of liquid present on metal surfaces. These issues led to an increase in corrosion and oxidation rates [39, 40].

Humidity: Higher humidity levels make the pace of corrosion more obvious. This is because a high concentration of moisture can hasten the oxidation and corrosion of metals. Metals and other things can experience corrosion.

2.2.9.2 Material properties

Aluminum does not rust like other metals because of its reactive nature, which is also the characteristic of the initial layer of oxide that forms. When corrosion occurs, it forms an aluminum oxide layer that prevents the metal from further interacting with the environment.

Type of metal- All metals do not corrode. Metals that are higher in the reactivity series, such as iron, zinc, etc., corrode very fast in contrast to metals that are lower in the reactivity series, such as gold, platinum, and silver, which do not corrode [40,41].

Purity of metals: In the event of corrosion, a metal's molecular composition is crucial. Pure metal is less likely to corrode. Corrosion is more likely to occur in the case of impure metals since they contain tiny electrochemical cells [39, 40].

2.2.9.3 Electrochemical Factors

Nature of metal: when the material's electrode potential is high, the corrosive impact on the substance is concentrated. Noble metals like gold, silver, and platinum corrode with the least speed, whereas magnesium, zinc, and aluminum corrode more quickly when their electrode potential is low. Corrosion is more likely when there is a large electrode potential difference between two metals that are in touch with one another. For instance, iron corrodes quickly when it comes into touch with copper. This should be taken into account when choosing the metals to employ, and the use of dissimilar metals should not be considered.

Position in electrochemical series: Less reactive metals display less corrosion than more reactive metals do. Metals with a greater reaction rate will show more corrosion. The electrochemical series is employed to determine the metals' degree of reactivity [39, 40].

2.2.9.4 Mechanical Factors

The physical state of metal: A faster corrosion rate is significantly influenced by the physical state of the metal. Corrosion happens more slowly in metal under less stress. However, the rate of corrosion will be considerable if the metal is under excessive stress [39, 40].

2.2.10 Corrosion Prevention and Control Techniques

2.2.10.1 Protective Coatings

For small spaces, painting with a brush or roller is preferable; spraying is preferable for larger coated areas such as steel decks and shoreline applications. Flexible polyurethane coatings, such as Durabak-M26, can provide an anticorrosive seal with a very strong membrane that resists slippage. Although temperature and humidity may affect how quickly painted coatings dry, both are generally simple to apply. Many organic coatings based on renewable sources are replacing organic coatings created with polymers derived from petroleum today. The most extensively researched polymer in such endeavors, among other carriers or binders, is polyurethane [41, 42].

Coatings: Metals are covered with paints and other organic coatings to prevent ambient gasses from destroying them. Depending on the type of polymer used, coatings are categorized. Typical organic coatings include:

1) Epoxy and alkyd ester coatings that encourage cross-link oxidation when air-dried

2) Urethane coatings in two parts

3) Radiation-curable epoxy and acrylic polymer coatings

4) Latex coatings with vinyl, acrylic, or styrene polymer combinations

5) Coatings soluble in water

6) Sturdy coatings

7) Coatings using powder.

Plating

1. Metallic coatings, or plating, can be used to give aesthetically pleasing, ornamental finishes in addition to preventing corrosion. Four types of metallic coatings are frequently used:
2. Electroplating: In an electrolytic bath, a thin coating of metal, usually nickel, tin, or chromium, is deposited on the substrate metal, usually steel. A water solution containing salts of the metal to be deposited is often used as the electrolyte.
3. Mechanical Plating: By spinning the component in an aqueous solution that has been treated, together with the metal powder and glass beads, you may cold weld metal powder to a substrate metal. Zinc or cadmium are frequently applied to tiny metal components mechanically.
4. Electroless: This non-electric plating method uses a chemical procedure to deposit a coating metal, such as nickel or cobalt, on the substrate metal.
5. Hot Dipping: When the substrate metal is immersed in a molten bath of the protective coating metal, a thin layer formed on it [42, 43].

2.2.10.2 Cathodic Protection

By using a metal surface as the cathode of an electrochemical cell, cathodic protection (CP) controls corrosion on metal surfaces. Steel pier piles, ships, offshore oil platforms, and pipelines and tanks are the most typical targets for cathodic protection systems.

To generate efficient CP, the potential of the steel surface is gradually polarized (pushed) negatively until it achieves a uniform potential. An even voltage stops the primary force driving the corrosion process. The anode material for galvanic CP systems eventually has to be updated since it corrodes when exposed to steel. Polarization is caused by the current flowing from the anode to the cathode due to the difference in electrode potential between the two. Aluminum, zinc, magnesium, and similar alloys are the most typical materials used as

sacrificial anodes. Magnesium is employed in places where resistance is higher since it has the highest driving voltage and the maximum capacity. Zinc serves as the foundation for galvanizing and is all-purpose [40, 42].

Cathodic protection works by converting unwanted anodic (active) sites on a metal's surface into cathodic (passive) sites by providing an opposing current. In opposition to the surrounding cathode potential, this opposing current causes free electrons to be produced and pushes adjacent anodes in the direction of polarization [43, 44].

There are two varieties of cathodic protection available. The first is the production of galvanic anodes. This method, sometimes called a sacrificial system, shields the cathode by exposing metal anodes to the electrolytic environment and letting them corrode. The metals with the biggest negative electro-potential, zinc, aluminum, or magnesium, are frequently used to build sacrificial anodes; however, the metal that requires protection may be different. The different electro-potentials are compared using the galvanic series. Also known as nobility, of metals and alloys.

Metallic ions migrate from the anode to the cathode in a sacrificial system, which causes the anode to deteriorate more quickly than it otherwise would. As a result, the anode has to be changed frequently. Impressed current protection is the name given to the second cathodic protection technique. This technique, which is frequently employed to safeguard submerged pipelines and ship hulls, calls for the electrolyte to be supplied with direct electrical current from a different source.

The positive terminal of the current source is linked to an auxiliary anode, which is added to complete the electrical circuit, and the negative terminal is connected to the metal. In contrast to a galvanic (sacrificial) anode system, an impressed current protection system does not sacrifice the auxiliary anode [44].

2.2.10.3 Inhibitors and Passivation Techniques

Corrosion inhibitors can frequently be added to a controlled environment (particularly in recirculating systems). On exposed metal surfaces, these compounds provide an impermeable or chemically insulating covering to prevent electrochemical reactions. These techniques reduce the sensitivity of the system to coating flaws or scratches since additional inhibitors may be made accessible whenever exposed metal occurs. Some of the salts found in hard water—the mineral deposits in Roman water systems are well known—as well as chromates, phosphates, polyanilines, other conducting polymers, and a wide variety of specially formulated chemicals that resemble surfactants—long-chain organic molecules with ionic end groups—inhibit corrosion [41, 42].

Inhibitor.

Corrosion-inhibiting substances interact with the metal's surface or the airborne gases that cause corrosion. Inhibitors may function by adhering to the surface of the metal and creating a barrier coating. Through the use of dispersion methods, these compounds can be applied as a solution or as a protective coating.

1. Modifying the anodic or cathodic polarization behavior is necessary for the inhibitor to slow corrosion.
2. Reducing the diffusion of ions to the surface of the metal
3. Increasing the metal's surface's electrical resistance

Petroleum refining, oil and gas exploration, chemical production, and water treatment facilities are some of the major end-use sectors for corrosion inhibitors. Corrosion inhibitors have the advantage of being able to be applied in situ to metals as a remedial measure to stop unforeseen corrosion [43, 44].

2.2.10.4 Material Selection and Design Considerations

Metal Selection and Surface Conditions: No metal is resistant to corrosion in all situations, but by keeping an eye on and comprehending the environmental elements that lead to corrosion, changes in the type of metal being used may also considerably lessen corrosion.

The optimum metals for a specific condition may be determined by combining information about the characteristics of the environment with data on metal corrosion resistance. Inhibitors may function by adhering to the surface of the metal and creating a barrier coating. Through the use of dispersion methods, these compounds can be applied as a solution or as a protective coating.

a. Modifying the anodic or cathodic polarization behavior is necessary for the inhibitor to slow corrosion.
b. Reducing the diffusion of ions to the surface of the metal
c. Increasing the metal's surface's electrical resistance

Petroleum refining, oil and gas exploration, chemical production, and water treatment facilities are some of the major end-use sectors for corrosion inhibitors. Corrosion inhibitors have the advantage of being able to be applied in situ to metals as a remedial measure to stop unforeseen corrosion [45, 46].

2.2.10.5 Maintenance and Repair Strategie

Metal and gasses in the atmosphere react chemically, which is what causes corrosion. Metal corrosion can be stopped in its tracks by taking the metal out of the environment or altering the environment altogether. This might take the form of direct modification of the environment impacting the metal or could be as straightforward as preventing contact with rain or ocean by keeping metal components indoors.

Corrosion is stopped by substances referred to as corrosion inhibitors that interact with the metal's surface or the gases in the environment that contribute to corrosion. Inhibitors may function by adhering to the surface of the metal and creating a barrier coating. Through the use of dispersion methods, these compounds can be applied as a solution or as a protective coating.

a. Modifying the anodic or cathodic polarization behavior is necessary for the inhibitor to slow corrosion.

b. Reducing the diffusion of ions to the surface of the metal

c. Increasing the metal's surface's electrical resistance

Petroleum refining, oil and gas exploration, chemical production, and water treatment facilities are some of the major end-use sectors for corrosion inhibitors. Corrosion inhibitors have the advantage of being able to be applied in situ to metals as a remedial measure to stop unforeseen corrosion [43, 44].

2.2.11 Corrosion in Specific Industries

2.2.11.1 Oil and Gas Industry

One of the most thriving industries in the world is the oil and gas industry. It generates more money than many other significant industries, including the pharmaceutical and cosmetics industries. As the need for energy keeps growing, more people and businesses are investing. Over the following few decades, this need is anticipated to keep increasing. In a sense, the extraction, transportation, and processing of these priceless resources are essential to our civilization's prosperity. Corrosion is the cause of around 50 % of all failures in the oil and gas sector. One of the biggest reasons for failure in the oil and gas sector, namely in pipelines, is corrosion. The main cause of pipeline breakdowns has been corrosion brought on by aging infrastructure. The bulk of the pipelines used to carry petroleum products in Nigeria are older than 60 years [47, 48].

2.2.11.2 Automotive Industry

Manufacturers and suppliers continue to develop advanced corrosion prevention technologies because vital elements like brake and suspension components, which are essential to driving safety can be vulnerable to rust. Recent Mazda, Toyota, Kia, and Mitsubishi recalls helped to draw attention to the issue of corrosion on suspension parts.

Mazda said in August 2016 that it was recalling more than 190,000 CX-7 crossovers from the 2007 to 2012 model years. Water might enter the front suspension ball joint fittings of the

CX-7, according to the US National Highway Traffic Safety Administration. The ball joint may corrode if the water is contaminated with impurities like salt used to de-ice roadways. The front lower control arm might detach from the automobile if the corrosion was bad enough, making the car difficult to drive and raising the danger of an accident.

This summer, Toyota issued a recall like that described above, requiring the return of more than 370,000 Toyota and Lexus vehicles to address a major suspension issue. The RAV4 crossover from 2006 to 2011 and the HS 250h sedan from 2010 are the two cars in question. The lock nuts on the rear suspension arm may not have been correctly tightened, which causes the problem. They could thus be overly slack, enabling the suspension arms to break and the thread to corrode. Once more, this would make it harder to manage the car and raise the possibility of an accident.

Mitsubishi issued yet another recall, this time involving over 174,000 cars because of possible front lower control arm corrosion. Recalls are being issued in areas that utilize salt to de-ice roadways, similar to the Kia problem. The resulting corrosion may cause the front lower control arm to separate from other suspension parts, rendering the car dangerous to drive. All recalled cars will be examined, and new and used parts will both get extra anti-corrosion coatings for future defense [49].

2.2.11.3 Marine Industry

Marine corrosion is unavoidable when metals are exposed to water, whether fresh, brackish, or saltwater. Nearly all metals attempt to revert to the state they were in before humans took them out of the ground as soon as they are made. Boaters often try to control three forms of corrosion:

1) Simple electrochemical corrosion
2) Electrolytic/stray current corrosion and
3) Galvanic corrosion [50]

The three different forms of maritime corrosion all come from an electrochemical mechanism; the only distinction is how quickly it happens. When numerous metals are involved, the process accelerates (galvanic corrosion), and it does so even more quickly (stray current corrosion) when uninvited electrical currents are used. While the damage to exposed metal caused by any of these forms of corrosion is essentially the same [50] .

2.2.11.4 Construction Industry

One of the most frequent degradation processes seen in reinforced concrete structures, corrosion of the reinforcement in the concrete affects both the structure's structural capacity and durability. Over the last several years, a lot of research has been done to minimize corrosion and extend the reinforced concrete structure's service life [51]. The reinforcing steel (here, rebar) corrodes when oxygen and moisture from the environment seep into the concrete, forming corrosion products. Because the corrosion products take up more space than the initial steel reinforcement, internal pressure builds up around the rebar, and tensile stresses arise in the concrete, which has an impact on how well the structure performs[51]. Cracking, spalling, delamination of concrete, and cross-sectional decrease of the reinforcing steel are examples of damages brought on by corrosion. It may result in aesthetic harm, a decrease in the structure's ability to support loads, and potentially deadly outcomes like structural breakdown [51].

2.2.11.5 Effects of Corrosion on Electronic Devices and Equipment

Corrosion has been acknowledged as a major factor in equipment failure; this was observed in the 19th century during the development of mechanical telephone switch centers. Lowering the risk of failure is even more important in today's society because of the widespread use of computers and other electrical devices as well as the rising pollution, especially in industrial areas and large cities. Infrastructure for communication and data transmission is crucial nowadays. One method to reduce cooling costs is to use "free cooling"

or "air-side economizers," systems that allow outside air to enter the room through filters to offer direct cooling when the outside temperature and humidity permit [49, 50].

Corrosion has been labeled to have a potential effect on a human daily routine if not properly checked. Its immediate consequences might include, but are not limited to, the following:

Electrical equipment failure in commercial aircraft or vehicles

1. Damage to computers and hard disks required to run complex systems (e.g., power plants, petrochemical facilities, or pulp and paper mills).
2. Damage to data centers and server rooms.
3. Museum artifacts are degrading.
4. The cost of buying new or fixing damaged household equipment, such as "free cooling,"

2.2.12 Factors Affecting the Corrosion Inhibition Efficiency of Nanoparticles

2.2.12.1 Temperature Effects

More water-derived chloride salts precipitate as temperatures rise, and changes occur on the metal's surface. Speeding up the chemical reactions that cause corrosion. Yet, when temperatures rise, their solubility declines and the quantity of liquid oxygen and carbon dioxide in the water has an impact on how quickly iron corrodes [52].

Corrosion is accelerated by rising temperatures. A layer of protection that is insoluble is produced by certain oxides, such as Al_2O_3, and may prevent further corrosion. This describes the characteristics of the first oxide layer that forms. Others, like rust, are easily broken down to show the metal that is still there. Acidic environment: Acids have the power to significantly accelerate the corrosion process [53].

2.2.12.2 Compatibility with Different Metals and Alloys

Metals and composites, in particular, demonstrated a noticeable propensity to corrode due to the presence of acid. Metals are defenseless against corrosion in an acidic solution. The use of acid solutions in industrial processes, like descaling with acid and pickling with acid, are a

few examples [54, 55]. This may be related to rust in the oil and gas business when it happens because of the characteristics of crude oil, which promotes corrosion due to its toxic components, including sulfur and naphthenic acid.

2.2.12.3 pH Solution

The rate of corrosion increases with an increase in the acidity of the medium due to the presence of hydrogen ion concentration, which changes the corrosion process [56].

2.2.12.4 Presence of Other Corrosion Species

Corrosion may happen more rapidly in certain media than others because some components, including oxygen and chlorine, speed up the process. Also, because of the acidic compounds that bacteria create, their presence accelerates corrosion. Moreover, the mechanical movement of the medium may speed up corrosion as it erodes the metal's surface [56].

2.2.12.5 The Time Spent Immersed

Since the metal layer shielding cannot rebuild itself, the immersion time has a significant influence on how corrosion behaves. During longer immersion times, the rate of corrosion increases proportionally [56].

2.2.12.6 Carbon Steel

Due to the carbon element's inclusion in a range of ratios between 0.2 % and 2.1 % of the weight of the steel alloy, it is an iron alloy with specific additions and varied proportions of the components. The steel alloy's hardness and tensile strength increase with its carbon content. Since various alloys' carbon contents vary, they all have unique qualities.

Moreover, the steel alloy comprises silicon up to 0.3 %, phosphorus up to 0.5 %, manganese up to 1 %, and sulfur up to 0.05 %. Similar to how these elements' concentrations, formation, and thermal treatment influence how an alloy's mechanical characteristics behave, it was discovered that steel naturally contains a lot of carbon. The composition of carbon is predetermined before it is ever created. Other substances are then added to it in order to increase its qualities and ensure they are in line with use specifications before it is distributed

after being put into molds. Steel carbon is essential to both the economy and the environment since it can be recycled without losing any of its original properties [56].

2.2.12.7 Stainless Steel

It has a minimum of 50 % iron, a maximum of 30% chromium, 85 % nickel and molybdenum, and just 2 % carbon. It prevents rust by creating a chromium oxide layer that adheres to the surface and is transparent, thin, and cohesive. Although it may still corrode and rust sometimes, the alloy becomes more corrosion-resistant as its chromium content increases. In an acid solution of 1M hydrochloric acid, Terminalia Catappa leaf extract was tested to see if it serves as a green corrosion inhibitor for stainless steel. Studied weight decrease data. The findings show that the used extract complies with physisorption adsorption and decreases the stainless steel corrosion rate in HCl solution by up to 96.8 % [57].

2.2.12.8 High-Carbon Steel

The strongest type of steel is high-carbon steel, which has a carbon concentration that ranges from 0.6 to 1.4 %. Nonetheless, cast iron is used to make a variety of cutting tools when the carbon concentration is greater than 0.2–4.5 %. It is important to remember that an increase in carbon may, in certain circumstances, exacerbate steel corrosion since heat treatment may alter a metal's resistance to corrosion.

2.2.12.9 Mid-Carbon Steel

In medium-carbon steel, manganese content varies from 0.26 to 0.49 percent, whereas carbon content ranges from 0.22 to 0.49 percent. Because the amount of carbon has increased, it is less ductile and stiffer than low-carbon steel. It is commonly used in the construction of equipment and railways . Using electrochemical impedance spectroscopy and the Polarization Technique methodology, examined the effect of eucalyptus leaf extract as an inhibitor of medium carbon steel corrosion in 0.5 M H_3PO_4 and 0.5 M H_2SO_4 acidic conditions. Results revealed that in H_2SO_4 solution, as opposed to H_3PO_4, the extract had a higher inhibitory impact on mild steel corrosion [58].

2.2.12.10 Low-Carbon Steel

Low-carbon steel has a carbon content that varies from 0.5 % to 0.19 %, whereas manganese is 0.4 %. It has a limited range of Industrial applications and is known as "light steel" due to its mechanical characteristics. When the carbon concentration is 0.15 to 0.3 %, it is used in buildings [59]. As a result, aqueous extracts prevented anodic corrosion reactions, whereas methanolic and ethanolic extracts hindered cathodic corrosion reactions. Alloys of metal together with trace quantities of chromium, nickel, molybdenum, vanadium, titanium, and niobium, carbon makes up less than 0.05 % of alloy steel. Low-alloy steel is one of its varieties and is used in both storage tanks and marine projects [60].

2.2.13 The Impact of Chemical Anti-Corrosion

While most chemicals have excellent anti-corrosion properties, their toxicity and possible risks to human and environmental health make them a big concern on a worldwide scale [61, 62]. The kidneys, livers, or other organs may suffer short- or long-term damage by the use of pharmacological inhibitors. Hence, they disrupt metabolic processes or how biological enzymes function [61, 63]. Traditional corrosion inhibitors, such as chromium-based therapies, are sometimes forbidden from use because they are based on compounds that could be harmful to human health [61, 63].

2.2.14 Avoiding the Mechanism of Green Corrosion Inhibitors

Plant extracts are used as corrosion inhibitors because the inhibitory effect is caused by the inhibitor molecules attaching to the metal surface. Physical/electrostatic, chemisorption, and other methods are used for the adsorption of organ molecules [64].

Adsorption inhibitors may work by reducing the reaction area on the metal surface as a result of their geometrical size. As the rate of activation energy barriers changes for anodic and cathodic reactions, the electrocatalytic impact of the reaction's byproducts may also prevent corrosion [65]. Physical adsorption is a mechanism for the occurrence of electrostatic attraction between inhibitor molecules containing electron donor atoms like (O, N, S), heterocyclic

rings, and the orbitals of metal atoms, which causes the adsorption of the inhibitor molecules to increase [66]. This electrostatic attraction occurs in addition to an increase in temperature. Adsorption of inhibitor molecules results in the inhibitory mechanism of metal surfaces. Hence, the kind of metal, its surface, and its composition all have an impact on the adsorption phenomena. Medium charge and the inhibitor's chemical makeup. As a consequence, it's conceivable that the ability of inhibitor compounds to attach to surfaces is due to the development of interactions between the orbitals of metal atoms and the electron pairs that occur on the nitrogen and oxygen atoms of heterocyclic rings. Adsorption of inhibitors may occur as a consequence of electrostatic interactions between the negatively charged metal surface and the positively charged nitrogen atom, which likewise holds true for the removal of water molecules from metal surfaces. Ring stability through resonance or ring removal from certain sub-inhibitors may be the cause of some inhibitors' capacity to halt corrosion in response to a material's resistance to oxidation (acidic or alkaline). Sometimes, there are enough inhibitors around to stop them from being absorbed. This organic process is brought about by the electrochemical reaction of metals with their corrosive surroundings. The interactions between the metal surface and the corrosive fluid result in the production of sulfides, oxides, and other substances [67].

2.2.15 Why Green Corrosion Inhibitors?

During the last ten years, green chemistry has increasingly focused on the need to safeguard both the environment and human health while simultaneously lowering waste and halting the use of potentially toxic or dangerous compounds [68]. As people's understanding of the environment grew, natural materials were shown to be safer. As they are thought to be much more cost-effective than organic inhibitors, plant extracts from the peels, seeds, stems, and leaves are widely utilized [69]. Also, they are secure. By lowering electrochemical rates, green corrosion inhibitors may perform both anodic and cathodic activity. The inhibitory process is commonly linked to the adsorption of double and triple-bound ions with single electron pairs,

which may interact with and cling to the metal surface. These molecules often include the elements phosphorus, sulfide, nitrogen, and oxygen. The location of attachment inside the metal affects the electron density, delaying the cathode or anode contacts[70]. In the area of protection, organic inhibitors have so far been shown to be very efficient, as shown by the development of a thin coating that touches the surface of the metal and separates the core. An extract is created when the energetic components or chemicals of a plant interact with a certain solvent[71, 72]. The processes or methods used and the polarity of the solvent used both have an effect on the extraction results. The characteristics required for a particular reason are given to the extract by its active principles. As a result, depending on its active ingredients and amounts, a specific plant may be associated with a particular benefit. These extracts' antimicrobial, antioxidant, antiviral, or anti-inflammatory properties are commonly recognized. It is possible to think of their corrosion-inhibitory qualities as interacting with one another. Extractions are typically made from the whole plant or the areas of the plant that have the greatest concentrations of active chemicals or phytochemicals [73]. According to the study, plant extracts made from fruits, seeds, flowers, and leaves contain active substances that may be able to prevent corrosion under difficult circumstances. Moreover, these substances develop into readily available, inexpensive, and renewable corrosion inhibitor substitutes[74, 75, 76]. Hence, research into the unique it is necessary to use plant compounds that have proven to be powerful Rust inhibitors. In this article, a variety of newly discovered plant extracts are discussed that may prevent corrosion in steel, aluminum, and copper alloys.Theoretical modeling, characterization approaches, fundamentals of extraction procedures, and adsorption processes are also addressed.

Newer methods make use of organic chemicals that are present in old prescription medications, plant extracts, and mushroom extracts [77,78,79,80]. A number of green organic substances, such as chitosan derivatives, phenylmethanimine derivatives, imidazoline derivatives, and ionic liquid derivatives, act as corrosion inhibitors and have excellent

shielding properties for metal surfaces. These substances should take the place of the hazardous corrosion inhibitors that are often used. These molecules have led to the development of highly efficient corrosion inhibitors, innovative drug recycling and reuse methods, and corrosion inhibitors derived from sustainable, ecological, and ecologically acceptable sources. Plant extracts stand out among them. These extracts provide a different, interesting alternative since they could help discover a class of organized compounds that slow down the rusting process. It has the benefit of increasing the efficiency of both extraction and testing these compounds since it is sometimes assumed that producing an extract from any plant is a straightforward process [81, 82]

2.2.16 Green Corrosion Inhibitor (GCI) Based on Plant Extracts

The creation of GCIs based on plant extracts has been the subject of one of the most comprehensive research studies on corrosion inhibition. The growing amount of research suggest that plant extract-based GCIs have great promise for reducing corrosion.Corrosion inhibitors have been the subject of extensive study. One of the most intense study projects is the development of ecological rust inhibitors. The majority of research has been concentrated on GCIs made from plant material because they are accessible, recyclable, biodegradable, and, most importantly, safe for both people and the ecosystem. Gravimetric measurements, electrochemical testing, theory, and computationally-based studies are used to assess the efficacy of GCIs [83]. It is common knowledge to aggregate the inhibitory performance as assessed by different methods under various conditions. Plant extracts have shown an inhibitory efficiency of over 80 % in preventing corrosion. Its exceptional efficacy is due to the high concentration of phytochemicals, which are active substances. It is also possible to learn more about the functionality of GCIs by identifying the inhibitor type and inhibition mechanism. The manufacture, effectiveness and characterization of the inhibitory mechanisms of utilizing plant compounds as GCIs in ferrous metal alloys are covered in this work.[84]. According to this study, employing plant extracts as GCIs might be a useful way to

successfully prevent corrosion in ferrous metal alloys. Nevertheless, further development efforts are still needed to reach the maximal inhibitory effectiveness of around 100% [85, 86, 87].

2.3 Phytochemicals in Plant Extraction

Since studies have shown that plant extracts contain a large number of these molecules, several industrial systems have introduced organic substances or bioactive compounds, which are naturally generated chemical compounds, to their devices that prevent rust [88, 89]. Numerous studies have been done on the flower, leaf, root, and complete plant, as well as other plant components that may be used to prevent rusting. Depending on the plant components, different compounds such as saponins, flavonoids, polyphenols, alkaloids, organic acids, and anthraquinones can be found present in both the leaves and stem extract as well as in the leaves only in the stem extract, according to the Phytochemical components of silicate. Researchers were motivated to consider plant extract as GCIs because Phytochemicals are found in variable quantities and kinds in various plant parts [88, 90].

The quantities of different phytochemicals, such as condensed tannins, proanthocyanidins, and anthocyanins, in the extract, depend on a number of variables, including the age of the plant, its growth cycle, its position, and the influence of the environment [88, 90]. For instance, it has been discovered that the developmental state of the plant affects the quantity and distribution of the active components in Aloe Vera gel extract [88, 89]. The plant extract has molecular structures that are similar to those of normal organic compounds with previously reported corrosion inhibitor properties, so it may be used as one. Phytochemicals were classified according to their physical and chemical properties into six main groups. Studies have shown that these chemicals play a key role in preventing rust. They are classified based on their corrosion-inhibiting properties during characterization, Figure 2.3 [88, 89, 90].

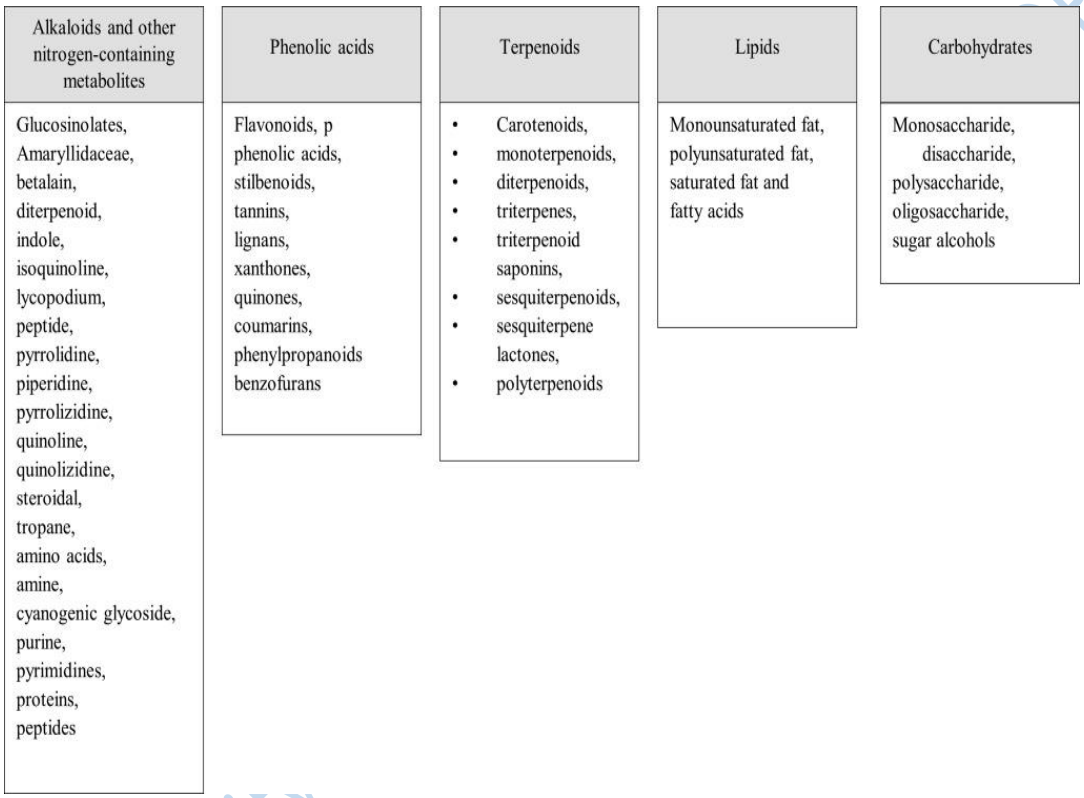

Figure 2.4: Description of Several Phytochemicals from Plant Extract [88, 89, 90].

Determining the chemical components and plant compounds is essential in order to predict how effective they will be in preventing corrosion. Plant samples are chemically analyzed to seek for and identify phytochemicals such as toxic ions, fatty acids, and amino acids, as well as volatile and non-volatile organic compounds (VOCs) [91].

2.4 Pathogens

Pathogens, which are organisms capable of inducing disease, exhibit a wide array of types and varying degrees of disease severity. This research delves into various pathogens, their effects on human health, and the diseases they instigate.

2.4.1 *Salmonella* Pathogens

Salmonellosis stands as the second most frequently reported gastrointestinal ailment within the EU, resulting from the consumption of foods contaminated with *Salmonella* bacteria. Its symptoms include gastroenteritis, abdominal cramps, bloody diarrhea, fever, myalgia, headache, nausea, and vomiting. In 2018, *Salmonella* infections constituted over half of the reported cases of foodborne outbreaks in the EU. While *Salmonella* contamination is often linked with poultry, cattle, and their feed, other products like dried foods, infant formula, fruits, vegetables, and pets have also become significant sources [92].

Various efforts are being undertaken to control *Salmonella*. For instance, legislative measures implemented have contributed to a decrease in hospitalizations between 2014 and 2015. However, hospitalizations began to rise again in 2016, highlighting the need for more rigorous controls from both governmental and private sectors. Food handlers, particularly

those involved in the processing of meat and Ready-to-Eat foods, play a critical role in the transmission of *Salmonella* and thus require heightened attention [92].

Salmonella stands as a significant foodborne pathogen, playing a prominent role in causing gastroenteritis in both humans and animals. Characterized by its high pathogenicity, *Salmonella* comprises over 2600 serovars. Transmission of *Salmonella* to humans typically occurs along the farm-to-fork continuum and is frequently associated with the consumption of animal-derived food items. Poultry and poultry products rank as the primary sources of *Salmonella* contamination, followed by beef, pork, fish, and non-animal-derived foods such as fruits and vegetables. Although antibiotics are commonly used to treat salmonellosis, the emergence of antibiotic-resistant strains, including multidrug-resistant (MDR) *Salmonella*, underscores the pressing need for alternative treatment options [93].

2.4.2 *Escherichia coli* Pathogens

Escherichia coli, which are rod-shaped bacteria classified as gram-negative and belonging to the Enterobacteriaceae family, was initially discovered in infant stool samples and described by Theodor Escherich in 1885. *Escherichia coli* exhibit remarkable versatility and are significant constituents of the normal intestinal microbiota in both humans and animals.While typically harmless as commensal organisms, they have the capacity to acquire diverse mobile genetic elements containing genes encoding virulence factors. This transformation can lead to their emergence as human pathogens capable of causing a wide range of intestinal and extraintestinal diseases. Nine distinct enteric *E. coli* pathotypes have been extensively characterized, contributing to conditions spanning various gastrointestinal disorders to urinary tract infections. These pathotypes deploy numerous virulence factors and effectors to undermine host cell functions, thereby facilitating their virulence and pathogenesis [94].

Escherichia coli (*E. coli*), a gram-negative bacillus, is implicated in various diarrheal diseases, such as traveler's diarrhea and dysentery. Additionally, it is the primary pathogen responsible for uncomplicated cystitis and can also lead to other extraintestinal conditions like pneumonia,

bacteremia, and abdominal infections like spontaneous bacterial peritonitis. The illnesses caused by *E. coli* impose a significant burden on patients and healthcare systems, underscoring the importance of prompt recognition and appropriate treatment. This review examines different strains of *E. coli* associated with human illnesses, outlines methods for identifying and managing these conditions, and emphasizes the collaborative role of the interprofessional healthcare team in patient care [94, 95, 96].

2.4.4 *Staphylococcus aureus* Pathogens

Staphylococcus aureus stands out as a highly notorious and prevalent bacterium, responsible for a significant count of uncomplicated skin infections and likely hundreds of thousands to millions of more severe, invasive infections worldwide annually. It plays a prominent role as a causative agent in pneumonia and various respiratory tract infections, surgical site infections, prosthetic joint infections, cardiovascular infections, and nosocomial bacteremia [97, 98].

Staphylococcus aureus ranks among the leading global contributors to illness and death caused by infectious agents. This pathogen is capable of inducing a diverse array of diseases, ranging from moderately severe skin infections to life-threatening conditions such as pneumonia and sepsis. Managing *S. aureus* infections is challenging due to the prevalence of antibiotic resistance, and as of now, there is no effective vaccine. There is growing interest in understanding the significant number of toxins and other virulence factors produced by S. aureus and their influence on disease progression. *Staphylococcus aureus* remains among the most prevalent bacteria in human illnesses. It resides within the typical skin microbiota of animals and humans, with a prevalence ranging from 20 to 30 % in healthy individuals. This bacterium is responsible for various conditions in humans, including abscesses, lung infections, bacteremia, endocarditis, and osteomyelitis [98, 99].

2.4.5 *Pseudomonas aeruginosa* Pathogens

Pseudomonas aeruginosa is a type of gram-negative rod-shaped bacterium known for its resilience against high salt concentrations, dyes, weak antiseptics, and many commonly prescribed antibiotics. Most instances of *Pseudomonas*-related diseases in humans are opportunistic infections.

This bacterium is notably linked to various human infections, particularly those associated with healthcare settings. Within hospitals, *Pseudomonas aeruginosa* strains often exhibit resistance to multiple antibiotics, posing significant challenges for effective treatment. However, treating *Pseudomonas aeruginosa* infections is further complicated by the formation of biofilms. An opportunistic pathogen is responsible for numerous infections in humans. It has emerged as a significant contributor to nosocomial infections and antibiotic resistance. The intricate structure of these biofilms adds an extra layer to the bacterium's pathogenicity, contributing to treatment failures, evasion of the immune system, and the development of chronic infections that prove difficult to eliminate [100,101].

Pseudomonas aeruginosa (*P. aeruginosa*) is widely recognized as a harmful gram-negative microorganism due to its array of virulence factors, capacity to form biofilms, and resistance to antimicrobials. The emergence of antibiotic-resistant strains, a consequence of antibiotic misuse and overuse, significantly heightens morbidity and mortality rates, particularly among immunocompromised individuals. Despite this, its role as a foodborne pathogen has often been overlooked across various food categories such as water, milk, meat, fruits, and vegetables. Moreover, the use of chemical preservatives aimed at inhibiting the growth of microorganisms in food sources can pose challenges to food safety. Hence, the quest for effective, safe, and natural alternative antimicrobial agents for use in food processing is of utmost importance [102,103].

2.5 Summary of the Effectiveness of Nanoparticles as Corrosion Inhibitors and Anti-Bacteria

The fabrication of metal oxide nanoparticles represents a convergence of nanotechnology and biotechnology, providing environmentally friendly material synthesis techniques. Due to their high surface-to-volume ratio, metallic nanoparticles can be produced through various methods, including chemical, electrochemical, physical, and biological techniques. However, many of these methods are costly and potentially harmful to the environment. Studies indicate that the biological synthesis of nanoparticles is both more economical and environmentally beneficial. Since the early 2000s, significant efforts have been made to synthesize nanoparticles such as gold and platinum, leveraging the antioxidant and reducing properties of plants. Recent research has demonstrated that certain plants can produce high-quality metal nanoparticles with superior biomedical applications, including antibacterial and anti-inflammatory ingredients in cosmetics, medical devices, cancer therapies, and cancer diagnostics.

Endnotes

1. S.Shishodia , B.Chouchene , T.Gries, R.Schneider *"Selected I-III-VI2 Semiconductors: Synthesis, Properties and Applications in Photovoltaic Cells"*. **Nanomaterials.** 13 (21) 2023, 2889. doi:10.3390/nano13212889. ISSN 2079-4991. PMC 10648425. PMID 37947733. (31 October 2023.

2. Samira Shahriyari Rad , Ali Mohamadi Sani , Sharareh Mohseni , *Biosynthesis, characterization and antimicrobial activities of zinc oxide nanoparticles from leaf extract of Mentha pulegium* (L.),**Microbial Pathogenesis** 131, 2019,239 245, https://doi.org/10.1016/j.micpath.2019.04.022.

3. S.Shishodia , B.Chouchene , T.Gries , R.Schneider *"Selected I-III-VI2 Semiconductors: Synthesis, Properties and Applications in Photovoltaic Cells"*. **Nanomaterials.** 13 (21),2023, 2889. doi:10.3390/nano13212889. ISSN 2079-4991. PMC 10648425. PMID 37947733.

4. K.Kanthavel , *Green Synthesis of Aluminum Oxide Nanoparticles and its Applications in Mechanical and Thermal Stability of Hybrid Natural Composites*, **Journal of Polymers and the Environment**, 27, 10, 2019, 2189–2200.

5. N.Kisku, *Strengthening of High-Alloy Steel through Innovative Heat Treatment Routes.* **Welding-Modern Topics**. 2020. DOI:10.5772.

6. ManikandanVelu, Balamuralikrishnan Balasubramanian,Palanivel Velmurugan,Hesam Kamyab, Arumugam Veera Ravi, Shreeshivadasan Chelliapan, Chew Tin Lee , Jayanthi Palaniyappan, *Fabrication of nanocomposites mediated from aluminium nanoparticles/Moringa oleifera gum activated carbon for effective photocatalytic removal of nitrate and phosphate in aqueous solution,* **Journal of Cleaner Production,** 281, 25 ,2021, 124553https://doi.org/10.1016/.

7. Naser Ali, Joao Amaral Teixeira, Abdulmajid Addali, *Aluminium Nanofluids Stability: A Comparison between the Conventional Two-Step Fabrication Approach and the Controlled Sonication Bath Temperature Method,* **Journal of Nanomaterials** 2019 *DOI: 10.1155/2019/3930572.*

8. Abdul Malek, Anusha Ganta, Govindaraj Divyapriya, Indumathi M. Nambi, Tiju Thomas *Hydrogen production from human and cow urine using in situ synthesized aluminium nanoparticles.* **International Journal of Hydrogen Energy**, 46, Issue 54, 2021, 27319-27329.https://doi.org/10.1016/.

9. N.S. Shashikumar , B.J. Gireesha, B. Mahanthesh, B.C.Prasannakumara , A.J. Chamkha, *Entropy generation analysis of magneto-nanoliquids embedded with aluminium and titanium alloy nanoparticles in microchannel with partial slips and convective conditions,* **International Journal of Numerical Methods for Heat & Fluid Flow**,0961-5539,29, 10, .2019.

10. A.De, Swarupa Ghosh, Manoswini Chakrabarti, Ilika Ghosh, Ritesh Banerjee, A. Mukherjee. *Effect of low-dose exposure of aluminium oxide nanoparticles in Swiss albino mice: Histopathological changes and oxidative damage,* **Toxicology and Industrial Health,** 36, Issue 8 2020,https://doi.org/10.1177/0748233720936828.

11. Nirmal Kumar Krishanu Biswas, Cryomilling: *An environment friendly approach of preparation large quantity ultra refined pure aluminium nanoparticles,* **Journal of Materials Research and Technology**, 8, 1, 2019,63-74. https://doi.org/10.1016/j.jmrt .2017.05.017.

12. Y. Al-Douri, K. Gherab, Khalid Mujasam Batoo, E. Raslan *Detecting the DNA of dengue serotype 2 using aluminium nanoparticle doped zinc oxide nanostructure: Synthesis, analysis and characterization,* **Journal of Materials Research and Technology** 9, 3, 2020, 5515-5523 https://doi.org/10.1016/j.jmrt.2020.03.076.

13. Reuben Samson Dangana, Reama Chinedu George, Femi Kayode Agboola, *The biosynthesis of zinc oxide nanoparticles using aqueous leaf extracts of Cnidoscolus aconitifolius and their biological activities*, Article: 2169591 | Published online: 29 Jan 2023**Green Chemistry Letters and Reviews**, Volume 16, 2023 - Issue 1. https://doi.org/10.1080/17518253.2023.2169591.

14. M.Abdalrhaman Salih, Fahad Al-Qurainy, Salim Khan, Mohamed Tarroum, Mohammad Nadeem, O. Hassan Shaikhaldein, Abdel-Rhman Zakaria Gaafar & Norah S. Alfarraj, *Biosynthesis of zinc oxide nanoparticles using Phoenix dactylifera and their effect on biomass and phytochemical compounds in Juniperus procera,* **Scientific Reports** volume 11, Article number: 19136 (2021).

15. Y.InasYounis, S.Seham El-Hawary, A.Omayma Eldahshan, M.Marwa Abdel-Aziz, Y.Zeinab Ali (2021). *Green synthesis of magnesium nanoparticles mediated from Rosa floribunda charisma extract and its antioxidant, antiaging and antibiofilm activities*, **Scientific Reports**,11, (2021) (1) doi: 10.1038/s41598-021-96377-6.

16. C.R. Rajith Kumar, Virupaxappa S. Betageri, G. Nagaraju, B. P. Suma, M. S.Kiran, M. S. Latha. *One-pot synthesis of ZnO nanoparticles for nitrite sensing, photocatalytic and antibacterial studies.* **Journal of Inorganic and Organometallic Polymers and Materials**. 30, 2020, 3476–3486.https: //doi. org/10.1007/s1090 4-020-01544 -3.

17. P. Vijaya Kumar, S. Mary Jelastin Kala, K.S. Prakash, *Green synthesis of gold nanoparticles using Croton Caudatus Geisel leaf extract and their biological studies.* **Materials Letters,** 236, 2019, 19-22, https://doi.org/10.1016.

18. S. Z. Salleh, A. H. Yusoff, Siti Koriah Zakaria, M. Taib, A. Abu Seman, M. N. Masri, M. Mohamad, S. Mamat, Sharizal Ahmad Sobri, Arlina Ali, P. Teo less. *Plant extracts as green corrosion inhibitor for ferrous metal alloys: A review*, **Journal of Cleaner Production**, 2021.127030. https://doi.org/10.1016/

19. N.Mahmoud El-Haddad, A.S. Fouda, A.F. Hassan. *Data from Chemical, electrochemical and quantum chemical studies for interaction between Cephapirin drug as an eco-friendly corrosion inhibitor and carbon steel surface in acidic medium.* **Chemical Data Collections.** 22, 100251, 2019. https://doi.org/10.1016.

20. Ravi Mani, Parameswaran Vijayakumar, T.Stalin Dhas, Karthick Velu , D. Inbakandan , C. Thamaraiselvi , Babett Greff , Murugesan Chandrasekaran ,Saeedah Musaed Almutairi , Faris S Alharbi , DinaS. Hussein , Maisari Utami , *Synthesis of biogenic silver nanoparticles using butter fruit pulp extract and evaluation of their*

antibacterial activity against Providencia vermicola in Rohu **jksus** 34, 3, 2022, 101814. https://doi.org/10.1016/

21. Yu Zhu, Li-Xiang Wang, Y. Behnamian, Shi-zhe Song, Ruiqi Wang, Zhiming Gao, Wenbin Hu, Da-Hai Xia less. *Metal pitting corrosion characterized by scanning acoustic microscopy and binary image processing.* **Corrosion Science**, 170, 2020, 108685.

22. Minha Naseer , Usman Aslam , Bushra Khalid , Bin Chen *Green route to synthesize Zinc Oxide Nanoparticles using leaf extracts of Cassia fistula and Melia azadarach and their antibacterial potential* **Scientific Reports** 10, 9055,2020. DOI: 10.1038/s41598-020-65949-3.

23. Stefania Marzorati , Luisella Verotta , Stefano P Trasatti *Green corrosion inhibitors from natural sources and biomass wastes.* **Molecules**, 24(1), 2018,.48. DOI: 10.3390/molecules24010048.

24. R. Farahati, S. M. Mousavi-khoshdel, A. Ghaffarinejad, H. Behzadi *Experimental and computational study of penicillamine drug and cysteine as water-soluble green corrosion inhibitors of mild steel.* **Progress in Organic Coatings** 2020.105567 DOI:10.1016.

25. Shuaixuan Yinga Zhenru Guana Polycarp C.Ofoegbub Preston Clubbb Cyren Ricob Feng Hea JieHonga, *Green synthesis of nanoparticles: Current developments and limitations* **Environmental Technology & Innovation,** 26,2022, 102336 https://doi.org/10.1016/j.eti.2022.102336. ISSN:2352-1864**.**

26. R. Winston Revie and H.Herbert Uhlig, *Corrosion and Corrosion Control*, Book, **John Wiley&Sons,**Inc,Globalwebicon,https://onlinelibrary.wiley.com/doi/book/10.1002/9780470277270

27. H.H.Uhlig, R.W Revie, *Corrosion and corrosion control.* Third edition (Book) | **OSTI.GOV**, https://www.osti.gov/biblio/7195167, Publication Date:1985-01-01, OSTI Identifier:7195167.

28. Derek Pletcher & C.Frank Walsh , *Corrosion and its control*,Book Chapter, **Industrial Electrochemistry** pp 481–542.

29. Ashwath Narayana, A. Sachin Bhat, Almas Fathima, S. V. Lokesh, Sandeep G. Suryad and C. V. Yelamaggad Green and low-cost synthesis of zinc oxide nanoparticles and their application in transistor-based carbon monoxide sensing. **RSC Advances** ,Issue 23, 2020,DOI https://doi.org/10.1039/D0RA00478B.

30. Lisa Zimmermann , Andrea Dombrowski , Carolin Völker , Martin Wagner *Are bioplastics and plant-based materials safer than conventional plastics? In vitro toxicity and chemical composition* **Environment International,** 145, 2020,106066.

31. A.Saviour Umoren, M.Moses Solomon, B.Ime Obot, K.Rami Suleiman *A critical review on the recent studies on plant biomaterials as corrosion inhibitors for industrial metals.* **Journal of Industrial and Engineering Chemistry.** 76, 25, 2019, 91-115,https://doi.org/10.1016/j.jiec.2019.03.057.

32. Kausalya Tamalmani, Hazlina Husin.*Review on Corrosion Inhibitors for Oil and Gas Corrosion* Issues, **Applied Sciences**, 10, 3389 ,2020,3389, ISSN 2076-3417 https://doi.org/10.3390/app10103389.http://www.mdpi.com/journal/applsci

33. P.Wei, W. Xue, Y.Zhao, G. Ning,J Wang, *CRISPR-based modular assembly of a UAS-cDNA/ORF plasmid library for more than 5500 Drosophila genes conserved in humans*. **Genome Research.** 30 (1),2019, 95--106.

34. Chandrabhan Verma , Eno E. Ebenso , Indra Bahadur , M.A. Quraishi .*An overview on plant extracts as environmental sustainable and green corrosion inhibitors for metals and alloys in aggressive corrosive media.* **Journal of Molecular Liquids,** 266, 2020, 577–590. https://doi.org/10.1016.

35. K. Ishraq Ibrahim, A.Juman Naser *Corrosion inhibition of carbon steel in sodium chloride solution using artemisia plant extract.* **Plant Archives,** 20 (1), 2020,3315-3319.

36. K. M. O. Goni, M. Mazumder, **Materials Science** *Green Corrosion Inhibitors***, Book Chapter** , 2019,DOI:10.5772/INTECHOPEN.81376

37. Surajit Dey, S.M.ASCE1 and Ravi Kiran, M.ASCE *Bio-Based Inhibitors to Mitigate Internal Corrosion in Crude Oil Pipelines*, **Pipelines** 2022. Available Online :DOI:10.1061/9780784484289.009

38. Dynagard/Riserclad International Inc. Site Design. *Different-types-corrosion-inhibitors,* Available Online: https://www.dynagard.info/different-types-corrosion-inhibitors/

39. Muhammad Imran Din, Summiya Jabbar, Jawayria Najeeb, Rida Khalid, Tayabba Ghaffar, Muhammad Arshad, Safyan A. Khan, Shahid Ali, *Green synthesis of zinc ferrite nanoparticles for photocatalysis of methylene blue,* **Int J Phytoremediation** 22(13): 2018,1440-1447. doi: 10.1080/15226514.2020.1781783.

40. Roland Tolulope Loto, Oluwatobilola Olowoyo *Synergistic effect of sage and jojoba oil extracts on the corrosion inhibition of mild steel in dilute acid solution.* **Procedia Manufacturing,** 35, 2019, 310-314.

41. Unacademy, *Factors Affecting Corrosion*,https://unacademy.com/content/jee/study-material/chemistry/factors-affecting-corrosion/

42. What is Corrosion?: *Factors Affecting, Types, Causes - What is Corrosion?:* **Embibe**,https://www.embibe.com/exams/corrosion

43. The Monticello News, *The Different Factors Affecting Corrosion*,Book (2020), Y. Al-Douri, K. Gherab, Khalid Mujasam Batoo, E. Raslan *Detecting the DNA of dengue serotype 2 using aluminium nanoparticle doped zinc oxide nanostructure: Synthesis, analysis and characterization,* **Journal of Materials Research and Technology** 9, 3, 2020, 5515-5523 https://doi.org/10.1016/j.jmrt.2020.03.076

44. Reuben Samson Dangana,Reama Chinedu George, Femi Kayode Agboola.*The biosynthesis of zinc oxide nanoparticles using aqueous leaf extracts of Cnidoscolus aconitifolius and their biological activities,*Article: 2169591 | Published online: 29 Jan

2023 **Green Chemistry Letters and Reviews** ,Volume 16, 2023 - Issue 1. https://doi.org/10.1080/17518253.2023.2169591.

45. https://themonticellonews.com/the-different-factors-affecting-corrosion-p17173-147.htm

46. A.Juman Naser, W. Zainab Ahmed, H.Enas Ali, *Plant Leaves Extracts as Green Inhibitors for Corrosion of Carbon Steel; a Review* **Annals of R.S.C.B**., ISSN:1583-6258, 25, 4, 2021, 5332 - 5340.

47. "Different Types of Corrosion: *Pitting Corrosion - Causes and Prevention".* corrosionclinic.com. **WebCorr** Corrosion Consulting Services.

48. [Lecture Text],*Strategies of metal corrosion protection*,**Su-Il Pyun, ChemTexts** volume 7, Article number: (2)2021, Published: 21 November 2020

49. Corrosion Prevention for Metals **thoughtco.com** https://www.thoughtco.com/

50. Anass Nassef, Michael Keller, Shokrollah Hassani, Siamack Shirazi & Kenneth Roberts, *A Review of Erosion-Corrosion Models for the Oil and Gas Industry Applications*.Book Chapter, 2022. **Recent Developments in Analytical Techniques for Corrosion Research** pp 205–233, https://link.springer.com/chapter/10.1007/978-3-030-89101-5_10.

51. Muhammad Idrees,Saima Batool,Tanzila Kalsoom,Sadaf Raina,Hafiz M. Adeel Sharif,Summera Yasmeen., *Biosynthesis of silver nanoparticles using Sida acuta extract for anti-microbial actions and corrosion inhibition potential*, **Environmental Technology**, 40(8)2019 1-26,DOI:10.1080/09593330.

52. Muhammad Imran Din, Summiya Jabbar, Jawayria Najeeb, Rida Khalid, Tayabba Ghaffar, Muhammad Arshad, Safyan A. Khan, Shahid Ali, *Green synthesis of zinc ferrite nanoparticles for photocatalysis of methylene blue,* **Int J Phytoremediation** 22(13): 2018,1440-1447. doi: 10.1080/15226514.2020.1781783.

53. A. Kadhim, A.A. Al-Amiery, R. Alazawi, M.K.S. Al-Ghezi, R.H. Abass1, *Corrosion inhibitors. A review* **Int. J. Corros. Scale Inhib**., 2021, 10, no. 1, 54–67 54, doi: 10.17675/2305-6894-2021-10-1-3

54. Jingkuang Liu, Zhengjie Huang, Xuetong Wang. *Economic and Environmental Assessment of Carbon Emissions from Demolition Waste Based on LCA and LCC.* **Sustainability**,12, 6683,2020. p. 6683. https://doi.org/10.3390/su12166683,

55. Roland Tolulope Loto, Oluwatobilola Olowoyo *Synergistic effect of sage and jojoba oil extracts on the corrosion inhibition of mild steel in dilute acid solution.* **Procedia Manufacturing,** 35, 2019, 310-314.

56. Arpit Goyal, Homayoon Sadeghi Pouya, Eshmaiel Ganjian & Peter Claisse *A Review of Corrosion and Protection of Steel in Concrete* **Arabian Journal for Science and Engineering** , 43, 2018,5035–5055. doi:10.1007/s13369-018-3303-2

57. Chandrabhan Verma , Eno E. Ebenso , Indra Bahadur , M.A. Quraishi .*An overview on plant extracts as environmental sustainable and green corrosion inhibitors for metals and alloys in aggressive corrosive media.* **Journal of Molecular Liquids,** 266, 2020, 577–590. https://doi.org/10.1016.

58. J.O. Madu, C. Ifeakachukwu, U. Okorodudu, F.V. Adams, I.V. Joseph, *Corrosion Inhibition Efficiency of Terminalia Catappa Leaves Extracts on Stainless Steel in Hydrochloric Acid.* **Journal of Physics**: 1378, Issue,2,2019,1378 (2), 022092.**DOI** 10.1088/1742-6596.

59. Kisku, N. *Strengthening of High-Alloy Steel through Innovative Heat Treatment Routes.* **Welding-Modern Topics**. 2020. DOI:10.5772

60. A. M. Abdel-Gaber., H. T. Rahal and F. T. Beqai. *Eucalyptus leaf extract as a ecofriendly corrosion inhibitor for mild steel in sulfuric and phosphoric acid solutions*.**International Journal of Industrial Chemistry** 11, 2020, pages123–132.

61. I.Ahanotu, Onyeachu, M.Moses Solomon, S.Ikechukwu Chikwe, B.Oluchukwu Chikwe, C. Eziukwu. *Pterocarpus santalinoides leaves extract as a sustainable and potent inhibitor for low carbon steel in a simulated pickling medium.* **Sustainable Chemistry and Pharmacy**, 15, 2019, 100196. DOI:10.1016.

62. Pello Uranga, Cheng Jia Shang, Takehide Senuma, Jer Ren Yang, Ai Min Guo, Hardy Mohrbacher. *Molybdenum alloying in high-performance flat-rolled steel grades.* **Advances in Manufacturing,** 8,1, 2020,15-34.

63. S. Z. Salleh, A. H. Yusoff, Siti Koriah Zakaria, M. Taib, A. Abu Seman, M. N. Masri, M. Mohamad, S. Mamat, Sharizal Ahmad Sobri, Arlina Ali, P. Teo less. *Plant extracts as green corrosion inhibitor for ferrous metal alloys: A review*, **Journal of Cleaner Production**, 2021.127030. https://doi.org/10.1016/

64. D.K.Akinlabu, T.F. Owoeye, F.E. Owolabi, O.Y.Audu, C.O. Ajanaku, F.Falope, O.O.Ajani, *Phytochemical and proximate analysis of African oil bean (Pentaclethra macrophylla Benth) seed.* **Journal of Physics,**1378, Issue 3, 2019, DOI 10.1088/1742-6596/1378/3/032057

65. Olawale Olayinka Ajani, Taiwo Felicia Owoeye, Kehinde Deborah Akinlabu, Oladotun Bolade, E. Oluwatimilehin Aribisala, M.Bamidele Durodola. *Sorghum extract: Phytochemical, proximate, and GC-MS analyses* November 2021, **Foods and Raw Materials** ,9 (2),(2021. 371-378, DOI:10.21603/2308-4057.

66. K.T.Dauda,T.F.Owoeye, O.S.I.Fayomi , I.G.Akande. *Ethanolic extract of Chrysophyllum albidum leaves and peels as a green inhibitor for AISI 1015 carbon steel in 1M H_2SO_4 solution* **Vietnam Journal of Chemistry,** 2023 doi: 10.1002/vjch.202200094

67. M.Hany. Abd El Lateef1, Abdel Rahman El Sayed, S.Hossnia Mohran , Hoda Abdel Shafy Shilkamy. *Corrosion inhibition and adsorption behavior of phytic acid on Pb and Pb–In alloy surfaces in acidic chloride solution.* **International Journal of Industrial Chemistry**, 10(1), (2019). 31-47. https://doi.org/10.1007/s40090-019-0169-4

68. A.Juman Naser, W. Zainab Ahmed, H.Enas Ali, *Plant Leaves Extracts as Green Inhibitors for Corrosion of Carbon Steel; a Review* **Annals of R.S.C.B**., ISSN:1583-6258, 25, 4, 2021, 5332 - 5340.

69. Minha Naseer , Usman Aslam , Bushra Khalid , Bin Chen *Green route to synthesize Zinc Oxide Nanoparticles using leaf extracts of Cassia fistula and Melia azadarach and their antibacterial potential* **Scientific Reports** 10, 9055,2020. DOI: 10.1038/s41598-020-65949-3

70. Tse-Lun Chen , Hyunook Kim , Shu-Yuan Pan , Po-Chih Tseng , Yi-Pin Lin , Pen-Chi Chiang *Implementation of green chemistry principles in circular economy system towards sustainable development goals: Challenges and perspectives.* **Science of the Total Environment,**716, 2020,136998. https://doi.org/10.1016

71. R. Farahati, S. M. Mousavi-khoshdel, A. Ghaffarinejad, H. Behzadi *Experimental and computational study of penicillamine drug and cysteine as water-soluble green corrosion inhibitors of mild steel.* **Progress in Organic Coatings** 2020.105567 DOI:10.1016.

72. K.Ishraq Ibrahim, A.Juman Naser. *Corrosion inhibition of carbon steel in sodium chloride solution using artemisia plant extract.* **Plant Archives,** 20 (1), 2020,3315-3319.

73. Minlan Gao , Jie Zhang , Qiaona Liu , Jinling Li , Rongjun Zhang , Gang Chen *Effect of the alkyl chain of quaternary ammonium cationic surfactants on corrosion inhibition in hydrochloric acid solution.* **Comptes Rendus Chimie**, 22, 5, 2019, 355-362,https://doi.org/10.1016/

74. Tao Gao , Rongjun Bian , Stephen Joseph , Sarasadat Taherymoosavi ,R.G David. Mitchell, Paul Munroe, Jianhong Xu, Jianrong Shi *Wheat straw vinegar: A more cost-effective solution than chemical fungicides for sustainable wheat plant protection.* **Science of The Total Environment,** 725, 2020, 138359. https://doi.org/10.1016.

75. A.Marsoul , M. Ijjaali , F. Elhajjaji , M. Taleb , R. Salim , A. Boukir *Phytochemical screening, total phenolic and flavonoid methanolic extract of pomegranate bark (Punica granatum L): Evaluation of the inhibitory effect in acidic medium 1 M HCl.* **Mater. Today Proc.** ,2020, 27, 4, 2020, Pages 3193-3198, https://doi.org/10.1016/j.matpr.2020.04.202

76. A.Sedik , D. Lerari , A. Salci , S. Athmani , K. Bachari , İ.H. Gecibesler , R. Solmaz *Dardagan Fruit extract as eco-friendly corrosion inhibitor for mild steel in 1 M HCl: Electrochemical and surface morphological studies* **Journal of the Taiwan Institute of Chemical Engineers**,107, 2020, 189-200

77. Ali Dehghani , Ghasem Bahlakeh , Bahram Ramezanzadeh , Mohammad Ramezanzadeh *Aloysia citrodora leaves extract corrosion retardation effect on mild-steel in acidic solution: Molecular/atomic scales and electrochemical explorations* **Journal of Molecular Liquids,** 310, 113221. 2020,https://doi.org/10.1016/

78. N.Chaubey, V.K.Savita Singh, M.A. Quraishi, *Corrosion Inhibition Performance of Different Bark Extracts on Aluminium in Alkaline Solution.* **Journal of the Association of Arab Universities for Basic and Applied Sciences,** 22, 38-44. 2017,.https://doi.org/10.1016/j.jaubas.2015.12.003

79. N.Mahmoud El-Haddad , A.S. Fouda , A.F. Hassan. *Data from Chemical, electrochemical and quantum chemical studies for interaction between Cephapirin drug as an eco-friendly corrosion inhibitor and carbon steel surface in acidic medium.* **Chemical Data Collections.** 22, 100251,2019. https://doi.org/10.1016

80. M. Gholamhosseinzadeh, H. Aghaie, M. Zandi, M. Giahi, *Rosuvastatin drug as a green and effective inhibitor for corrosion of mild steel in HCl and H_2SO_4 solutions.***Materials Research and Technology, 8,** 2019, 5314–5324**.** DOI:10.1016

81. R. Farahati, S. M. Mousavi-khoshdel, A. Ghaffarinejad, H. Behzadi *Experimental and computational study of penicillamine drug and cysteine as water-soluble green corrosion inhibitors of mild steel.* **Progress in Organic Coatings** 2020.105567 DOI:10.1016.

82. Olawale Olayinka Ajani, Taiwo Felicia Owoeye, Kehinde Deborah Akinlabu, Oladotun Bolade, E. Oluwatimilehin Aribisala, M.Bamidele Durodola. *Sorghum extract: Phytochemical, proximate, and GC-MS analyses* November 2021, **Foods and Raw Materials** ,9 (2),(2021. 371-378, DOI:10.21603/2308-4057.

83. D.K.Akinlabu, T.F.Owoeye, F.E. Owolabi, O.YAudu, C.O. Ajanaku, F.Falope, O.O.Ajani. *Phytochemical and proximate analysis of African oil bean (Pentaclethra macrophylla Benth) seed.* **Journal of Physics,**1378, Issue 3, 2019, DOI 10.1088/1742-6596/1378/3/032057

84. A Saravanan , P Senthil Kumar, S Karishma , Dai-Viet N Vo , S Jeevanantham 1, P R Yaashikaa , Cynthia Susan George ,*A review on biosynthesis of metal nanoparticles and its environmental applications*, **Chemosphere**, 264, 2, 2020, 128580, https://doi.org/10.1016/j.

85. S. Z. Salleh, A. H. Yusoff, Siti Koriah Zakaria, M. Taib, A. Abu Seman, M. N. Masri, M. Mohamad, S. Mamat, Sharizal Ahmad Sobri, Arlina Ali, P. Teo less. *Plant extracts as green corrosion inhibitor for ferrous metal alloys: A review*, **Journal of Cleaner Production**, 2021.127030. https://doi.org/10.1016/

86. Pantea Ghahremania, Mohammad Ebrahim Haji Naghi Tehrani, Mohammad Ramezanzadeha, Bahram Ramezanzadeha , *Golpar leaves extract application for construction of an effective anti-corrosion film for superior mild-steel acidic-induced corrosion mitigation at different temperatures,* **Colloids and Surfaces** , 629,2021,127488**.**

87. R M Soliman , S A Younis , N Sh El-Gendy , S S M Mostafa , S A El-Temtamy , A Espinoza-Vázquez, A.; Rodríguez-Gómez, F.J.; Negrón-Silva, G.E.; González-Olvera, R.; Ángeles-Beltrán, D.; Palomar-Pardavé, M.; Miralrio, A.; Castro, M. *Fluconazole and fragments as corrosion inhibitors of API 5L X52 steel immersed in 1 M HCl.* **Corros. Sci.** 174, 2020,108853.

88. Adnan Munis , Tianyu Zhao , Maosheng Zheng , Ata Ur Rehman , Feng Wang *A newly synthesized green corrosion inhibitor imidazoline derivative for carbon steel in 7.5% NH_4Cl solution.* **Sustainable Chemistry and Pharmacy**, 16, 2020, 100258, 16, 100258.https://doi.org/10.1016/

89. Chandrabhan Verma , Eno E. Ebenso , Indra Bahadur , M.A. Quraishi .*An overview on plant extracts as environmental sustainable and green corrosion inhibitors for metals and alloys in aggressive corrosive media.* **Journal of Molecular Liquids,** 266, 2020, 577–590. https://doi.org/10.1016.

90. S. Z. Salleh, A. H. Yusoff, Siti Koriah Zakaria, M. Taib, A. Abu Seman, M. N. Masri, M. Mohamad, S. Mamat, Sharizal Ahmad Sobri, Arlina Ali, P. Teo less. *Plant extracts as green corrosion inhibitor for ferrous metal alloys: A review*, **Journal of Cleaner Production**, 2021.127030. https://doi.org/10.1016/

91. Bibek Laha, Sabyasachi Maiti, Kalyan Kumar Sen,Subrata Jana, *Nanoscale polysaccharide-based particles for the delivery of therapeutic molecules.* **Micro and Nano Technologies,** 2019, 347-368 https://doi.org/10.1016/B978-0-08-102579-6.00014-9.

92. Xianchun Zhu Kavitha Pathakoti, Huey-Min Hwang, *Green synthesis of titanium dioxide and zinc oxide nanoparticles and their usage for antimicrobial applications and environmental remediation,* **Micro and Nano Technologies** 2019,223-263, https://doi.org/10.1016/B978-0-08-102579-6.000101.

93. Olugbenga Ehuwa, Amit K. Jaiswal, Swarna Jaiswal Salmonella, *Food Safety and Food Handling Practices,* **Foods.** 2021 May; 10(5): 907.Published online 2021 Apr 21. doi: 10.3390/foods10050907,PMCID: PMC8143179,PMID: 33919142.

94. Bibek Lamichhane , Asmaa M M Mawad , Mohamed Saleh , William G Kelley , Patrick J Harrington , Cayenne W Lovestad , Jessica Amezcua , Mohamed M Sarhan , Mohamed E El Zowalaty , Hazem Ramadan Melissa Morgan , Yosra A Helmy Salmonellosis: *An Overview of Epidemiology, Pathogenesis, and Innovative Approaches to Mitigate the Antimicrobial Resistant Infections*. (1) :76. 2024 Jan 13;13 doi: 10.3390/ **antibiotics**13010076, PMID: 38247636, PMCID: PMC10812683

95. Babak Pakbin, Wolfram M. Brück, John W. A. Rossen,Virulence *Factors of Enteric Pathogenic Escherichia coli: A Review,* **Int J Mol Sci**. 22(18): 9922,2021 Sep;.Published online 2021 Sep 14. doi: 10.3390/ijms22189922,PMCID: PMC8468683,PMID: 34576083

96. Jasminka Talapko,Martina Juzbašić,Tatjana Matijević,Emina Pustijanac, Sanja Bekić, Ivan Kotris, Ivana Škrlec., *Candida albicans—The Virulence Factors and Clinical Manifestations of Infection,***J Fungi (Basel).** 2021 Feb; 7(2): 79.Published online 2021 Jan 22. doi: 10.3390/jof7020079,PMCID: PMC7912069,PMID: 33499276

97. Garcia-Rubio R., de Oliveira H.C., Rivera J., Trevijano-Contador N. *The Fungal Cell Wall: Candida, Cryptococcus, and Aspergillus Species.* **Front. Microbiol**. 2020;10:2993. doi: 10.3389/fmicb.2019.02993.W

98. Kevin Bouiller , Xavier Bertrand , Didier Hocquet , Catherine Chirouze, *Human Infection of Methicillin Susceptible Staphylococcus aureus CC398:A Review.* 8(11) 2020, Nov 5;1737.PMID: 33167581,PMCID: PMC7694499,DOI: 10.3390/microorganisms 8111737

99. Nour Ahmad-Mansour, Paul Loubet, Cassandra Pouget, Catherine Dunyach-Remy, Albert Sotto, Jean-Philippe Lavigne, and Virginie Molle, *Staphylococcus aureus Toxins: An Update on Their Pathogenic Properties and Potential Treatments* **Toxins (Basel).** 2021 Oct; 13 (10): 677, Published online 2021 Sep 23. doi:10.3390/toxins13100677, PMCID: PMC8540901, PMID: 34678970.

100. Felipe Francisco Tuon, Leticia Ramos Dantas, Paula Hansen Suss, and Victoria Stadler Tasca Ribeiro. *Pathogenesis of the Pseudomonas aeruginosa Biofilm: A Review* **Pathogens.** 2022 Mar; 11(3): 300. 2022 Feb 27. doi: 10.3390/ pathogens 11030300, PMCID: PMC8950561, PMID: 35335624

101. Ito C.A.S., Bail L., Arend L., Nogueira K.D.S., Tuon F.F. *The activity of ceftazidime/avibactam against carbapenem-resistant Pseudomonas aeruginosa.* **Infect. Dis.** 2021;53:386–389. doi: 10.1080/23744235.2020.1867763.

102. Xuejie Li, Nixuan Gu, Teng Yi Huang, Feifeng Zhong, Gongyong Peng., *Pseudomonas aeruginosa: A typical biofilm forming pathogen and an emerging but underestimated pathogen in food processing*. **Front Microbiol**. 2022; 13: 1114199, Published online 2023, Jan 25. doi: 10.3389/fmicb.2022.1114199, PMCID: PMC 9905436, PMID: 36762094

Chapter Three

Methodology

3.1 Materials

3.1.1 Chemical and Reagents

Analytical-grade materials were all employed directly as sources without additional purification. All solutions were prepared using distilled water and metal salts such as Aluminum Chloride ($AlCl_3.6H_2O$) and Zinc Sulfate Heptahydrate ($ZnSO_4.7H_2O$) as precursors. Solutions of H_2SO_4 were used as corrosive substances. Drying was done with ethanol and acetone. Glacial acetic acid, ferric chloride, concentrated sulphuric acid, sodium hydroxide, hydrochloric acid, 10 % alcoholic ferric chloride, chloroform, and 5 % ferric chloride are used to carry out phytochemical analyses of their presence in the extract samples.

3.1.2 Apparatus

250 mL volumetric flasks, 100 mL beakers, 250 mL conical flasks, 10 mL and 50 mL measuring cylinders, a spatula, a glass rod, watch glasses, sample bottles, a glass funnel, filter paper, and crucibles.

3.1.3 Other Materials Needed for Analysis

Materials needed for Analysis include Emery Paper (Grade 320,1200), Cotton wool (for cleaning the metal surface), Leaf extracts from *Adonidamerrilli, Caryota mitis, Cassia javanica,* and *Casuarina equisetifolia.*, Sticks and threads (for suspending the coupons), a bowl to wash the coupons, Scissor to cut the suspending thread, and a brush (for polishing the coupon during washing), Paper-Tape (for labeling) and medium glass container (for immersion and retention of circulations).

3.2. Appliances

The following equipment was used: a muffle furnace, a centrifuge, a potentiostat galvanostat system (Auto lab Nova 2.1.1), a weighing scale (AE ADAM) with 0.1 mg sensitivity, a hot air oven (Uniscope SM9053), a rotary evaporator (IKA RV8), and desiccator.

3.3. Mild Steel Composition and Preparations

The Corrosion analysis will use mild steel (MS) in thicknesses of 1 mm, 2 mm, and 3 mm, which were physically pressed into coupons measuring 30 mm by 20 mm. These samples were polished using different grades of emery papers to remove oxide layers and corrosive scales from the surface. After polishing, the samples were weighed, then cleaned in acetone, dried in 100% ethanol, reweighed, and stored in moisture-free desiccators until use. The mild steel plate, whose composition is indicated in Table 3.1, was procured in Ogun State, Nigeria. Characterization of the steel revealed approximately 0.152% carbon and 99.154% iron.

Table 3.1: Composition of AISI 1015 Carbon Steel Used (wt. %)

Element	C	Mn	Si	P	S	Al	Ni	Fe
Composition	0.152	0.451	0.186	0.011	0.0318	0.0053	0.009	99.154

3.4 Extract Preparation

Cassia javanica, Adonida merrilli, Washingtonia robusta, and Casuarina equisetifolia leaves were cut into pieces after being properly cleaned under running water and with double distilled water. The leaves were air-dried and ground. About 500 g of dried samples were soaked in about 1000 mL of double-distilled water and boiled for 30 minutes. The resulting

extracts were filtered using cotton wool, and the filtrate was then transferred to a 1000 mL Erlenmeyer flask and refrigerated for further use [1].

3.5 ZnO Nanoparticle Synthesis

Adonida merrilli, Washingtonia robusta, Cassia javanica, and Casuarina equisetifolia extract was slowly added gradually into the solution of 1 M of Zincsulphate hexahydrate ($ZnSO_4.7H_2O$) in ratio 2:4 under magnetic stirring at 80 °C for about 4 hours to obtain a complex formation. The mixture was centrifuged for 15 minutes at 4500 rpm. The formed complex was then cleaned with distilled water and centrifuged for 10 minutes at 4500 rpm. The supernatant was discarded, and the nanoparticles were calcined at 450 °C in a muffle furnace after being dried at 40 °C for eight hours [1].

3.6 Aluminum Oxide Nanoparticles Synthesis

Plant leaf extracts were effectively used to produce aluminum oxide nanoparticles. *Adonida merrilli, Washingtonia robusta, Cassia javanica, and Casuarina equisetifolia* extract was slowly added into the solution of 1 M of aluminum chloride ($AlCl_3.6H_2O$) in ratio 2:4 under magnetic stirring at 50 °C for about 2 hours to obtain a complex formation. Centrifugation was used to separate the complex that had developed at 15 minutes for 4500 rpm. The formed complex was then cleaned with distilled water and centrifuged for 10 minutes at 4500 rpm. The resultant nanoparticles were calcined at 450 °C in a muffle furnace after being dried at 40 °C for eight hours [2].

3.7 The Electrolytes' Preparation.

The tests used 0.5 M of H_2SO_4 electrolytes as the acidic medium, which was made by gradually adding 30 mL of concentrated sulfuric acid to roughly 1000 mL of water while stirring.

3. 8 Used Inhibitors

(1) Aqueous extracts from *Casuarina equisetifolia, Cassia javanica, Adonida merrilli, and Washingtonia robusta.*

(2) All zinc nanoparticles were synthesized using leaf extracts of *Adonida merrilli, Washingtonia robusta , Cassia javanica,* and *Casuarina equisetifolia* at concentrations of 500 ppm, 1000 ppm, 1500 ppm, and 2000 ppm, respectively.

(3) Aluminum nanoparticles synthesized using extracts from *Adonida merrilli, Washingtonia robusta , Cassia javanica,* and *Casuarina equistifolia* were used at concentrations of 500 ppm, 1000 ppm, 1500 ppm, and 2000 ppm, respectively.

3.9 Phytochemical Screening

3.9.1 Alkaloids Test (Wagner's Reagent)

Wagner's reagent, which contains 1.27 grams of iodine and 2 grams of potassium iodide in 100 milliliters of water, was applied to a portion of the extract. The production of a reddish brown precipitate was checked for (or colouration) [3, 4].

3.9.2 The Cardiac Glycosides Keller

5 mL of each extract was placed in a test tube, which received 2 mL of glacial acid treatment and a drop of ferric chloride solution. Over this, 1 mL of concentrated H_2SO_4 acid was carefully placed in a thin coating. The appearance of a brown ring at the interface indicated the presence of the cardenolide-specific deoxysugar. A violet ring may appear under the ring, and a greenish ring may form in the acid layer [3].

3.9.3 Test for Phenols in (Ferric Chloride Test)

A portion of the extracts were subjected to an aqueous solution containing 5 % ferric chloride, and the production of a deep blue or black color was checked [3, 5].

3.9.4 Test for Saponins (Foam Test)

6 mL of water was added to 2 mL of extract in a test tube. Shaking the mixture briskly allowed the presence of saponins to be confirmed by looking for the development of persistent foam [4, 5].

3.9.5 Tannin Test (Braymer's Test)

A 10 % alcoholic ferric chloride solution was applied to 2 mL of the extract, and the production of a blue or greenish-colored solution was checked [4, 5].

3.9.6 Salkowki's Test for Terpenoids

2 mL of each extract was combined with 1 mL of Chloroform and a few drops of concentrated H_2SO_4 acid. Terpenoids were present because a reddish brown precipitate was generated right away, [4].

3.9.7 Test for Quinones

Concentrated HCl was used to treat a small quantity of extract, and the appearance of a yellow precipitate was monitored (or colouration) [3, 4].

3.9.8 Oxalate Test

A few drops of glacial ethanoic acid were added to a 3 mLportion of the extracts. Oxalates are present when coloration is greenish-black [3].

3.10 Gravimetric Method

On test coupons with dimensions of 2 x 3 x 0.5 mm and 2 x 3 x 1 mm, gravimetric experiments were performed. All tests were performed in rated and undisturbed test solutions. The test coupons were cleaned with a brittle brush, rinsed, degreased, dried, and reweighed after being recovered at 1 day intervals and increasingly over the course of 4 days. The difference between the coupons' starting and final weights was used to calculate the weight reduction. The previously established weighing balance was used to obtain measurements [6, 7, 8].

3.11 Electrochemical Method

A three-electrode glass cell with an Auto-Lab Nova 2.1.1 Potentiostat galvanostat device was used to evaluate the linear polarization resistance. A platinum rod serves as the counter electrode, with a Saturated Calomel electrode serving as the reference electrode. At a scan rate of 0.5 mV/s, the polarization curves for corrosion current were recorded from 100 mA to 100 nmA. To determine corrosion current density, the linear Tafel segments of the cathodic curves, the computed anodic Tafel lines, and the Tafel plots of potential (V) versus log current (I) were extrapolated to the point of junction (Icorr).The following relationship was used to compute the corrosion inhibition effectiveness (%) from the corrosion current density measurements.

$$IE\% = \frac{I\_o, corr - I\_i, corr}{I\_o, corr} \times 100$$

Where I_o, corr = substrate's corrosion current densities in the absence of leaf extracts or nanoparticles , I_i, corr = substrate's corrosion current densities in the presence of leaf extracts or nanoparticles,*(Cassia javanica, Adonida merrilli, Washingtonia robusta, Casuarina equisetifolia,)* and nanoparticles at a scanning rate of 0.5 mV/s, respectively [6,8].

3.12 Scanning Electron Microscopy (SEM)

PHENOM PRO X Scanning Electron Microscopy,Serial number:MVE0224651193, Model number:800-07334 was used to analysed the samples. The samples were mounted on stubs with adhesive carbon and coated in 20 nm Carbon with a QUORUM Q15OR ES mini sputter coater,and then analysed with a Phenom PRO-X SEM equipped with an Oxford XMax 50 Silicon Drift Energy Dispersive X-ray detector at 15 KV under high vacuum.

3.13 Energy Dispersive Analysis (EDX)

Energy dispersive spectroscopy (EDS) is frequently used to ascertain the elemental composition of metal nanoparticles. It was completed in a SEM unit coupled to an EDX analyzer.

3.14 X-Ray Diffractometer (XRD)

Angstrom ADX2700 X-Ray Diffractometer was used to analysed the samples, The XRD analysis parameters are graphite-monochromatic Cu radiation sources at 40 kV and 30 mA. The diffraction intensities were recorded in the 2Θ = 50 - 70° with a step size of 0.2 and a scan speed of 1.0 second. X-rays penetrate the nanomaterial, and the resultant diffusion pattern is compared with standards to get structural information. XRD was utilized for phase identification and characterization of the crystal structure of the nanoparticles. The Scherrer formula was employed to estimate the crystallite size of the primary zinc oxide and aluminum oxide nanoparticle phases present in the sample based on their X-ray diffraction (XRD) patterns.

$$C = \frac{K\lambda}{\beta \cos\theta}$$

Where:C is the crystallite size (in nanometers),

K is the Scherrer constant (typically around 0.9, depending on shape),

λ is the wavelength of the X-ray source (commonly 1.5406 Å for Cu Kα radiation),

β is the full width at half maximum (FWHM) of the most intense diffraction peak (in radians),

θ is the Bragg angle (in degrees, but converted to radians in calculation).

3.15 UV-Visible Spectrophotometer

An Orion AquaMate 8100 UV-Visible Spectrophotometer (Serial No. 9A8Y052002) was employed to record absorption wavelengths (in nanometers) and confirm the presence of zinc oxide and aluminum oxide nanoparticles over a scan range of 200–900 nm.

3.16 Fourier Transform Infrared Spectroscopy (FT-IR)

Agilient Technologies Cary 630 FTIR ZnSe,Part Number:G8043 64002,Model Number:MY19322004 FTIR spectroscopy has been employed to characterize the surface chemistry of extracts, ZnONPs and AI_2O_3NPs. which also allows for the detection of additional surface chemical residues. The sythesis of zinc oxide and aluminum oxide nanoparticles in the wave number range of 4000- 700 cm^{-1} has also been proven.

3.17 Antimicrobial

The antimicrobial properties of both the extracts of *Adonida merrilli, Washingtonia robusta , Cassia javanica, and Casuarina equisetifolia* and their nanofluid (Zinc oxide and Aluminum oxide nanoparticles) were determined using the Agar-well diffusion method. A stock concentration of 100 mg/mL of ethanol produced by combining 1 g of the ethanol extract with 10 mL of distilled water was used for the testing. 25 mL of prepared Meullerhinton agar was added to each sterile Petri plate.The suspension of the test bacterial (*Escherichia coli, Pseudomonas aeruginosa, Staphylococcus aureus, and Salmonella.)* isolates was added to the solidified Meullerhinton as an inoculant. Three equally spaced holes were bored into each plate of the set Agar using a sterile cock-borer with a diameter of 4 mm. After that, the wells (holes) were filled with 0.2 mL of the extracts, ZnONPs and AI_2O_3NPs solution. The plates were incubated at 37 °C for 24 hours. The resultant zone of inhibition (replicates) of the different plant extracts was observed and measured using a transparent meter rule [9].

3.18 Minimum Inhibitory Concentration (MIC)

The *Adonida merrilli, Washingtonia robusta , Cassia javanica, and Casuarina equisetifolia*, as well as their nano fluid samples, were prepared to a stock concentration of 100 mg/mL in sterile distilled water and serially diluted (two-fold) to a working concentration ranging from 500-1.95 mg/ mL before being mixed with an equal amount of nutrient broth. The test organisms' (*Escherichia coli, Pseudomonas aeruginosa, Staphylococcus aureus, and Salmonella.)* 0.2 mL suspension was used to inoculate the dilutions. The test tubes were checked for turbidity after 24 hours of incubation at 37 °C. The Minimum Inhibitory

Concentration (MIC) value was identified as the lowest concentration at which no turbidity was seen. [9, 1]

Endnotes

1. Essien, Enobong R. Atasie, Violette N.;Nwude, Davies O.;Adekolurejo, Ezekiel;Owoeye, Felicia T. *Characterisation of ZnO nanoparticles prepared using aqueous leaf extracts of Chromolaena odorata (L.) and Manihot esculenta (Crantz)* **South African Journal of Science**,Volume 118, Issue 1122022 Article number #11225,2022

2. K.U.Efemwenkiekie, S.O Oyedepo, S.O Giwa, M.Sharifpur,T.F. Owoeye,K.D. Akinlabu,J.P Meyer. *Experimental investigation of heat transfer performance of novel bio-extract doped mono and hybrid nanofluids in a radiator.Case Studies in Thermal Engineering*, **j.csite**,Volume 28December 2021 Article number 101494,Gold Open Access Journal, 2214157X, 10.1016/.2021.101494

3. Olawale Olayinka Ajani, Taiwo Felicia Owoeye, Kehinde Deborah Akinlabu, Oladotun Bolade, E. Oluwatimilehin Aribisala, M.Bamidele Durodola. *Sorghum extract: Phytochemical, proximate, and GC-MS analyses*, **Foods and Raw Materials** ,9 (2),2021. 371-378, DOI:10.21603/2308-4057.

4. D.K.Akinlabu, T.F.Owoeye, F.E. Owolabi, O.YAudu, C.O. Ajanaku, F.Falope, O.O.Ajani. *Phytochemical and proximate analysis of African oil bean (Pentaclethra macrophylla Benth) seed.* **Journal of Physics,**1378, Issue 3, 2019,DOI 10.1088/1742-6596/1378/3/032057

5. Adnan Munis , Tianyu Zhao , Maosheng Zheng , Ata Ur Rehman , Feng Wang *A newly synthesized green corrosion inhibitor imidazoline derivative for carbon steel in 7.5% NH_4Cl solution.* **Sustainable Chemistry and Pharmacy**, 16, 2020, 100258, 16, 100258.https://doi.org/10.1016/

6. K.T.Dauda,T.F.Owoeye,O.S.I. Fayomi ,I.G.Akande. *Ethanolic extract of Chrysophyllum albidum leaves and peels as a green inhibitor for AISI 1015 carbon steel in 1M H_2SO_4 solution* **Vietnam Journal of Chemistry,** 2023 doi: 10.1002/vjch.202200094

7. Araceli Espinoza-Vázquez, Francisco Javier Rodríguez-Gómez, Ivonne Karina Martínez-Cruz, Deyanira Ángeles-Beltrán, Guillermo E. Negrón-Silva, Manuel Palomar-Pardavé, Leticia Lomas Romero, Diego Pérez-Martínez and Alejandra M. Navarrete-López , Adsorption and corrosion inhibition behaviour of new theophylline–triazole-based derivatives for steel in acidic medium, **Royal Society Open Science** (2019) https://doi.org/10.1098/rsos.181738.

8. Ahmed Al-Amiery, Lina M. Shaker, Nadia Betti Corrosion inhibition effect and adsorption behaviour of nicotinic acid derivative on mild steel in HCl media, **Materials Today: Proceedings,**Volume 56, Part 4, 2022, Pages 2204-2208 https://doi.org/10.1016/j.matpr.2021.11.529

9. Taye Kebede, Eshetu Gadisa, Abreham Tufa, *Antimicrobial activities evaluation and phytochemical screening of some selected medicinal plants: A possible alternative in the treatment of multidrug-resistant microbes,* ***Pone**.0249253* (2021),https://doi.org/10.1371.

10. Baye Sitotaw, Fikremariam Ayalew , Abayneh Girma , Amare Bitew Mekonnen , Yousef A. Bin Jardan , Hiba-Allah Nafidi and Mohammed Bourhia. *Isolation and identification of promising antibiotic-producing bacteria* **Open Chemistry**, 2022 https://doi.org/10.1515/chem-2022-0233.

Chapter Four

Results and Discussion of Findings

4.1 Phytochemical Result

Phytochemicals are naturally occurring, biologically active chemical compounds found in plants. Table 4.1 lists the chemical compounds present in the plant samples used for this study. The Oxalates, Phenol, and Cardiac glycosides were absent in aqueous extracts of *Casuarina equisetifolia, Cassia javanica, Adonida merrilli, and Washingtonia robusta* . Saponin was present in all the aqueous extracts (*Casuarina equisetifolia, Cassia javanica, Adonida merrilli, and Washingtonia robusta).* Quinines was present in all except *Casuarina equisetifolia,* while Tannis was absent in all except *Adonida merrilli.*Alkaloid was only present in *Casuarina equisetifolia* while absent in the others. When compared with ethanolic extracts of *Chrysophyllum albidum* peel, which is very effective at corrosion inhibiton[1], possess terpenoids, Terpenoids were present in *Adonida merrilli and Casuarina equisetifolia* but absent in *Cassia javanica* and *Washingtonia robusta.* Aqueous leaf extracts of *Casuarina equisetifolia* are the most effective when compared with other aqueous leaves extracts used in this study it exhibited similar results with ethanolic extracts of *Chrysophyllum albidum* peel. They both have alkaloids, saponins, and terpenoids, and both also lack oxalate, phenols, quinines, and cardiac glycosides. The next aqueous leaf extract is *Adonida merrilli,* which exhibits similar results with ethanolic extracts of *Chrysophyllum albidum* peel. They both have tannins, saponins, and terpenoids, but both lack oxalate, phenols, and cardiac glycosides. More so, *Adonida merrilli* was also observed to possess the same phytochemical component when compared with *Casuarina equisetifolia*; they both have tannins, saponin, and terpenoids, but both lack oxalate, phenols, and cardiac glycosides. *Cassia javanica* and *Washingtonia robusta* both have similar results. They all have saponin but lack these: oxalate, phenols, and cardiac glycosides.[1]

Table 4 1: Phytochemical Screening of Aqueous Leaf Extracts of *Casuarina equisetifolia, Cassia javanica, Adonida merrilli, and Washingtonia robusta* .

Constituent	C	E	M	NM

Oxalates	-	-	-	-
Phenols	-	-	-	-
Quinines	++	-	++	++
Tannins	-	-	-	++
Alkaloid (dragendorf)	-	++	-	-
Cardiac glycosides	-	-	-	-
Saponins	++	++	++	++
Terpenoids	-	++	-	++

Casuarina equisetifolia (E), Cassia javanica (C), Adonida merrilli (NM) and Washingtonia robusta (M).

Keys: (++) abundant (+) present, (-) absent.

Source: Author's Field Work 2025

4.2 Characterization of Nanoparticles

4.2.1 UV-Visible Analysis of the Plant Extracts and Metal Oxide

4.2.1.1 UV-Visible Analysis of the Plant Extracts

The UV analysis indicated a λmax at 292 nm for *Cassia Javanica* (C), 290 nm for *Adonida merrilli* (NM), 296 nm for *Washingtonia robusta* (M), 288 nm for *Casuarina equisetifolia* (C) with log emax calculated through absorbance utilizing Beer-Lambert law. This occurred due to the transition from π- π*.Transition peculiar to C=C functionality. No visible sign of any light has been absorbed, making *Cassia Javanica* (C), *Adonida merrilli* (NM), *Washingtonia robusta* (M), *Casuarina equisetifolia* (C) aqueous extracts colourless, The important band of UV absorption was discovered according to their UV-Vis spectra. Figure 4.1 (a) (b) (c) (d) [2,3]. When comparing the wavelengths of various aqueous extracts, *Cassia javanica* (C) exhibits a wavelength of 292 nm, *Adonida merrilli* (NM) 290 nm, *Washingtonia robusta* (M) 296 nm, and *Casuarina equisetifolia* (E) 288 nm. The UV absorption of these extracts ranges from 285 nm to 296 nm, all within the UV region. This is in good agreement with previous studies on UV-Vis spectroscopic analysis of *Eucalyptus globulus* leaf extract revealed an absorption peak at 300 nm, indicating its relevance within the specified UV range, which falls within the same range [2].

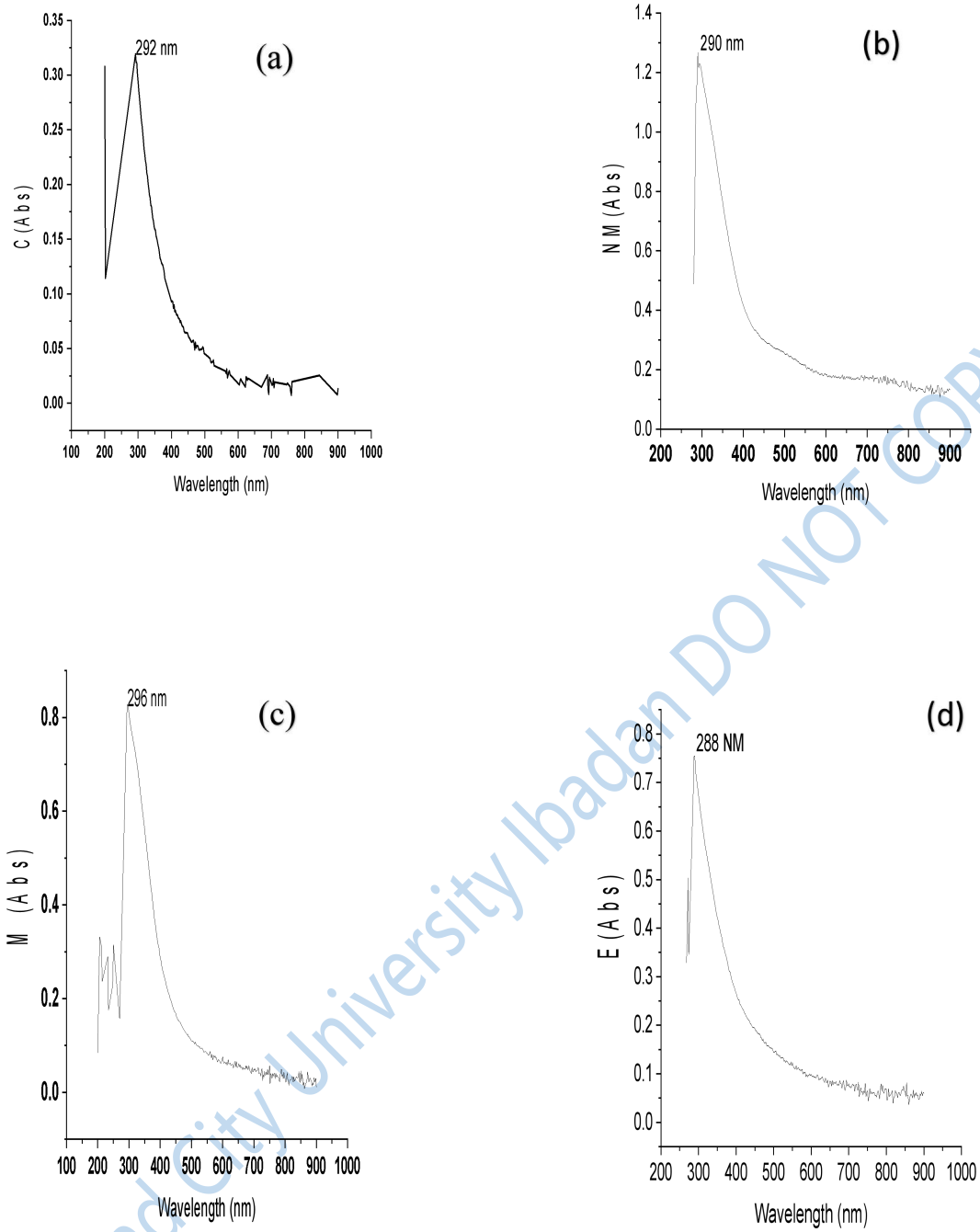

Figure 4.1: UV-Visible Spectra of the Plant Extracts (a): *Cassia javanica* extracts(C) (b) *Adonida merrilli* extracts (NM), (c) *Washingtonia robusta* extracts (M) (d) *Casuarina equisetifolia* extracts (E)

Source: Author's Field Work 2025

4.2.1.2 UV-Visible Analysis of ZnO Nanoparticles

Zinc oxide nanoparticles exhibit light absorption across a spectrum from visible to near-infrared, influenced by their size and structure. This absorption is attributed to the collective oscillation of surface electrons, known as surface plasmon resonance (SPR). The dispersion of plasmonic nanoparticles manifests one or more peaks, indicative of SPR characteristics, which can be harnessed to glean essential information about nanoparticle dimensions, morphology, and size distribution. The UV-Vis analysis of the zinc nanoparticles shows an important band of UV absorbance at 300 nm (C-ZnONP), 302 nm (NM-ZnONP), 300 nm (M-ZnONP) and 308 nm (E-ZnONP), in the spectra, according to Figure 4.2.The band is caused by the ZnO nanoparticles' valence electrons being excited, which are produced by the interaction between the leaves extracts and zinc sulphate hexahydrate ($ZnSO_4.7H_2O$) [4, 5, 6] .

Different Zinc Oxide nanoparticles exhibit varying UV absorption results. C-ZnONP shows UV absorbance at 300 nm, NM-ZnONP at 302 nm, M-ZnONP at 300 nm, and E-ZnONP at 308 nm. The UV absorbance of these Zinc Oxide nanoparticles ranges from 300 nm to 334 nm, all occurring within the same region. When these results were compared with zinc oxide nanoparticles (ZnO-NPs) synthesized from the novel medicinal plant *Lagerstroemia indica*, The UV–Vis spectroscopy, showing a peak at 302 nm. This peak falls within the same region as previously reported, demonstrating good agreement with this earlier findings.

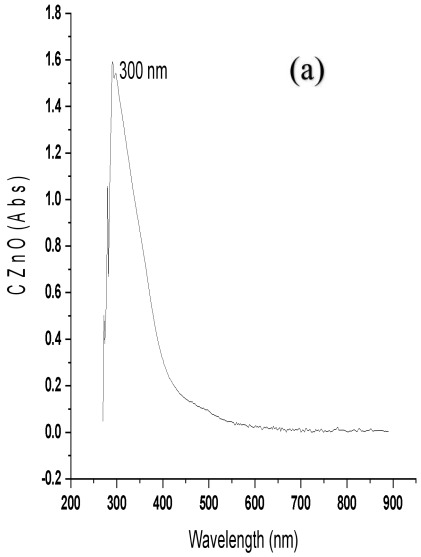

(b)

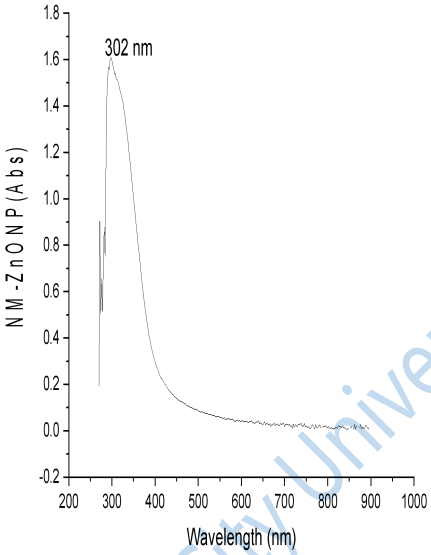

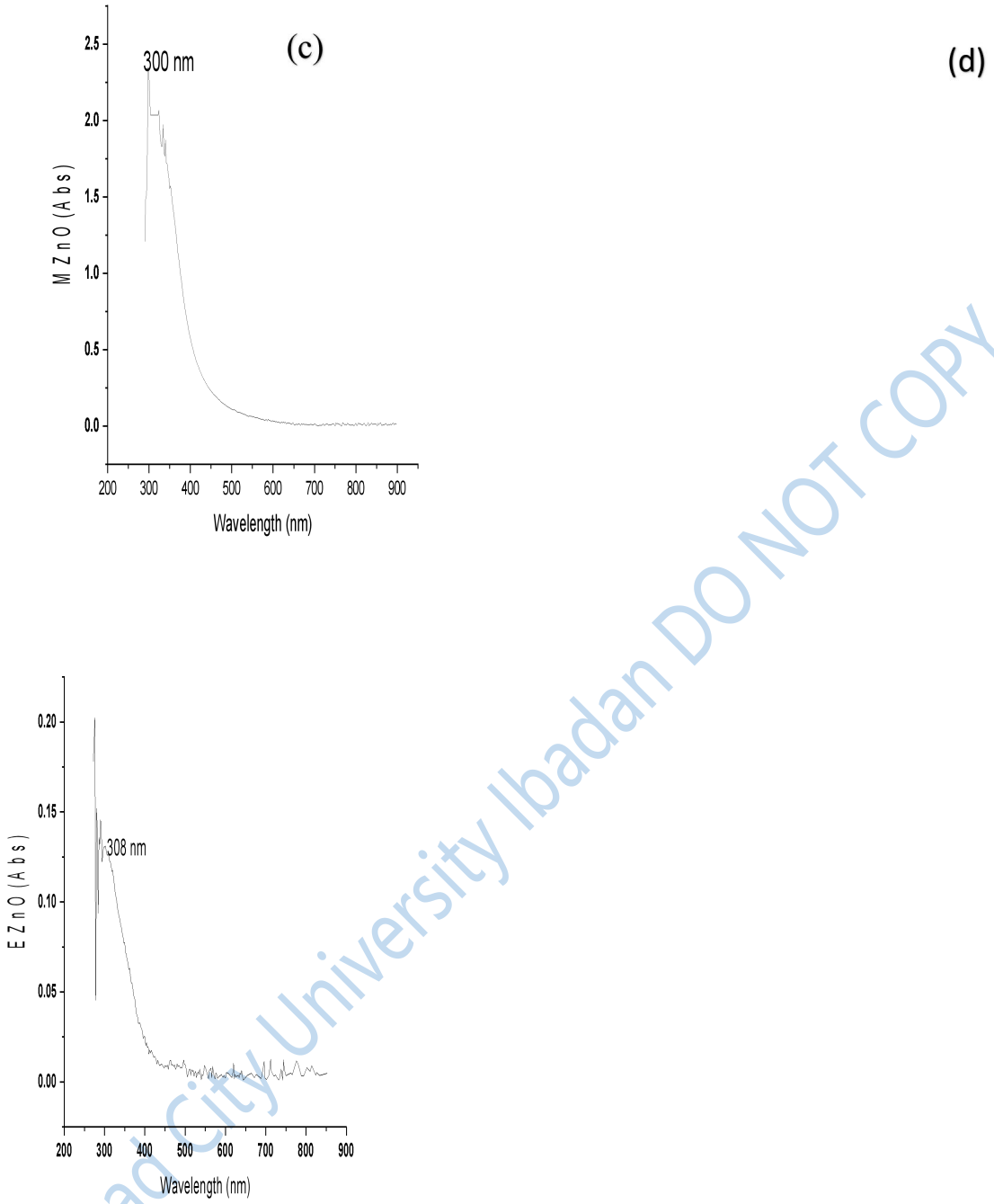

Figure 4.2 : UV-Visible Plots of ZnONP (a) C-ZnONP (b) NM-ZnONP, (c) M-ZnONP (d) E-ZnONP

Source: Author's Field Work 2025

4.2.1.3 UV-Visible Analysis of Aluminum Oxide Nanoparticles

Depending on their size and shape, nanoparticles have the ability to absorb visible to near-infrared light. This absorption phenomenon is attributed to the collective oscillation of surface electrons on nanoparticles, known as surface plasmon resonance (SPR). The SPR characteristic leads to the dispersion of plasmonic nanoparticles, resulting in one or more peaks that can provide valuable insights into their dimensions, size distribution, and morphology.

During the UV-Vis analysis of Aluminum oxide nanoparticles, an important UV absorption band at 335 nm and 401 nm (C-Al_2O_3NP), at 336 nm and 401nm (NM-Al_2O_3NP), at 333 nm and 401 nm (M-Al_2O_3NP) and at 317 nm and 401 nm (E-Al_2O_3NP) were identified from their UV-Vis spectra (Figure 4.3). These peak were generated when the valence electrons of aluminum oxide within the nanoparticles undergo excitation due to the interaction between *Cassia javanica* extract and aluminum chloride (Al_2Cl_3) [7,8,]

Different aluminum oxide nanoparticles show varying UV absorption results. C-Al_2O_3NP exhibits UV absorbance at 335 nm and 401 nm, NM-Al_2O_3NP at 336 nm and 401 nm, M-Al_2O_3NP at 333 nm and 401 nm, and E-Al_2O_3NP at 317 nm and 401 nm. The UV absorbance of these Aluminum Oxide nanoparticles occurs within the same region. These results align with previous studies on aluminum oxide nanoparticles synthesized via picosecond laser ablation and *Lyngbya majuscula extract,* which displayed a surface plasmon resonance peak around 326 nm and 340 nm [7, 8] .

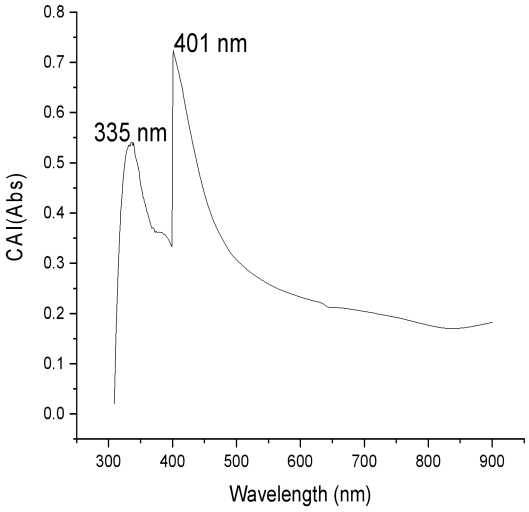

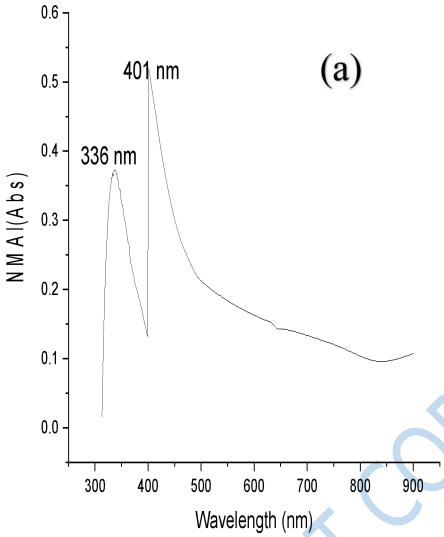

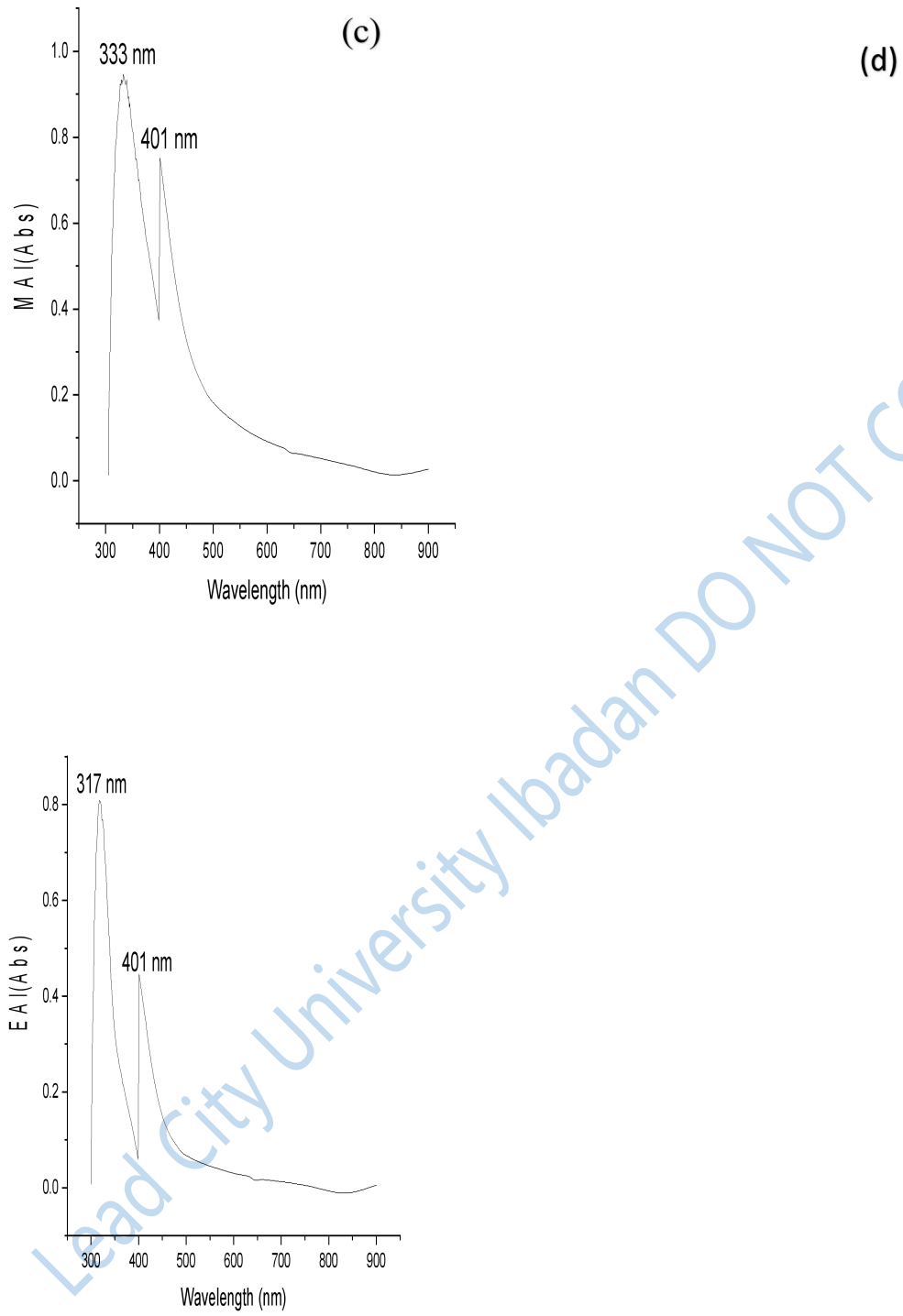

Figure 4.3: UV-Visible Spectra of AI_2O_3NP (a): C-AI_2O_3NP (b) NM-AI_2O_3NP (c) M-AI_2O_3NP (d) E-AI_2O_3NP

Source: Author's Field Work 2025

4.2.2 FTIR Analysis of the Plant Extracts and Metal Oxide

4.2.2.1 FTIR Analysis of the Plant Extracts

The bioactive components in the plant extracts (*Casuarina equisetifolia, Washingtonia robusta, Cassia javanica* and *Adonida merrilli*) were examined using FTIR. Figure 4.4 Infrared spectroscopy is also utilized in the field of natural products to identify certain biomolecules.

For instance, aqueous *Casuarina equisetifolia* leaf extract stretching vibrations are represented by the peaks at a range of 1073 cm^{-1} to 3209 cm^{-1}.; C-C vibrations is represented by a band at 1073 cm^{-1} Aromatic nitro compounds is related to the peak at 1509 cm^{-1} , Alkenyl C=C stretching vibration represented by the peak at 1640 cm^{-1}; Hydroxyl group, H-bonded OH, OH-stretching alcohols and phenols are responsible for the peak at 3209 cm^{-1} [9,10,] It is evident from the observation of distinct IR bands that aqueous *Washingtonia robusta* leaf extract has various biomolecules with distinct functional groups on their surface. C-stretching is represented by a band at 1084 cm^{-1}; C=C is related to the peak at 1640 cm^{-1}; C≡C stretching is represented by a band at 2105 cm^{-1}; and OH-stretching alcohols responsible for the peak at 3239 cm^{-1} [10, 11]

Cassia javanica leaf extract stretching vibrations are represented by these peaks; C-C represented by the peak at 1077 cm^{-1}; C=C-C stretching is represented by a band at 1509 cm^{-1}; C=C is related to the peak at 1640 cm^{-1}; C≡C is represented by a band at 2113 cm^{-1};NH is represented by a band at 2325 cm^{-1};Hydroxyl group, H-bonded OH, OH-stretching alcohols responsible for the peak at 3220 cm^{-1} [9,10]

In *Adonida merrilli*, it is evident from the observation of distinct IR bands that C-C stretching is represented by a band at 1080 cm^{-1}; 'C=C' is related to the peak at 1640 cm^{-1}; Cyanide ion and thiocyanate ions are represented by the peaks at 2087 cm^{-1} and 2292 cm^{-1}, respectively; and OH-stretching alcohols responsible for the peak at 3231 cm^{-1} [9, 10]

When Compared FTIR spectra analysis of various leaf extracts, According to Figure 4.4, all the extracts demonstrate skeletal C-C vibrations, alkenyl C=C stretching, and hydroxyl group with H-bonded OH stretching.which is in agreement with the previous study of *Adenanthera pavonina* leaf extracts [9,10]. Additionally, *Casuarina equisetifolia* and *Cassia javanica* exhibit aromatic nitro compounds. *Casuarina equisetifolia* and *Adonida merrilli* exhibit cyanide ions and thiocyanate ions, *Cassia javanica* and *Washingtonia robusta* exhibit C≡C terminal alkyne (monosubstituted), while *Washingtonia robusta and Adonida merrilli* exhibit aliphatic cyanide/nitrile.

.

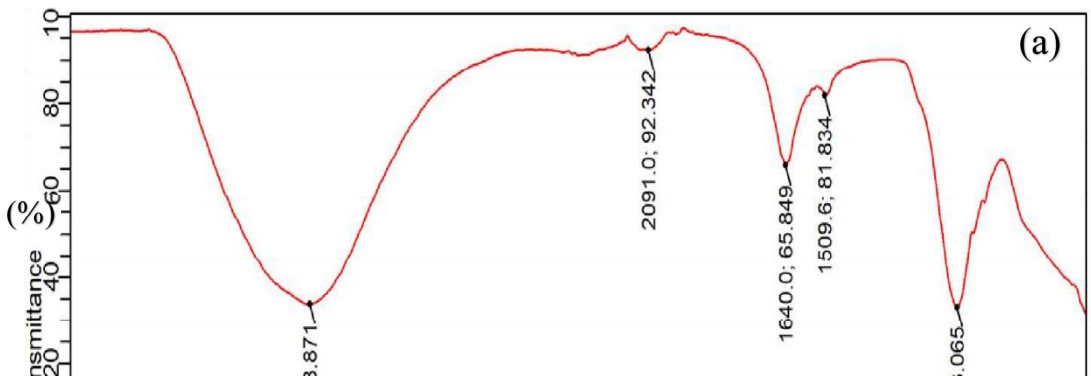

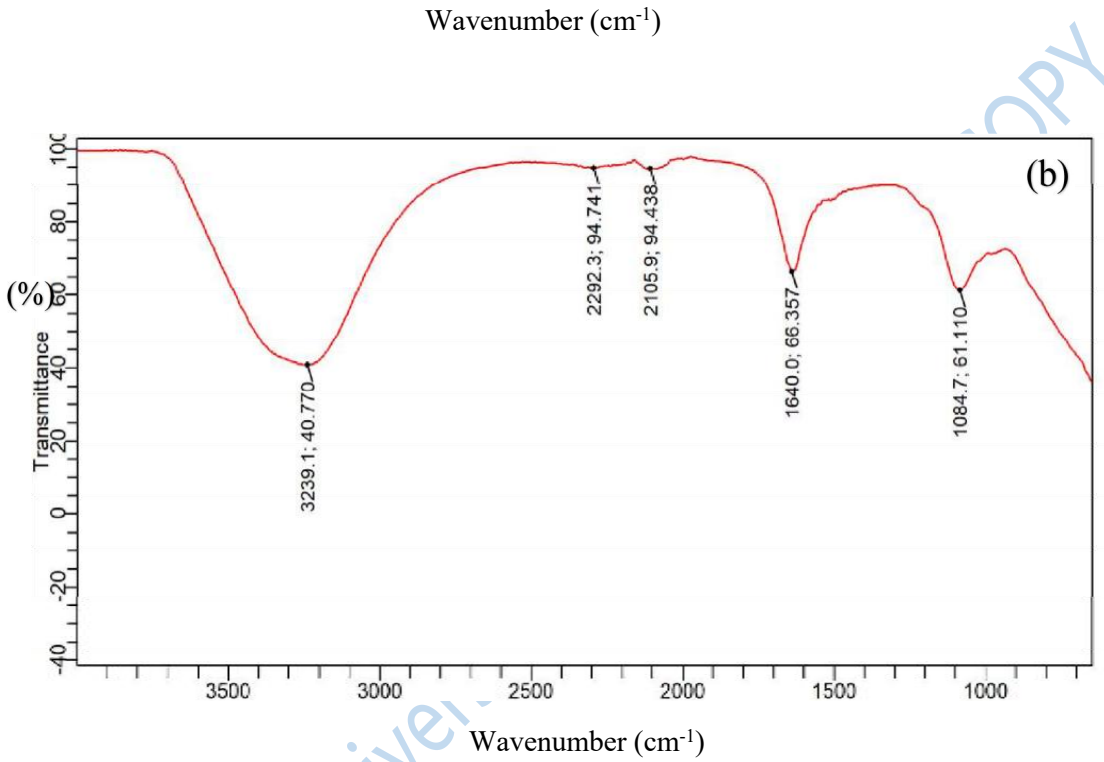

Figure 4.4: FTIR Spectra of (a): *Casuarina equisetifolia* extracts (E) (b) *Washingtonia robusta* extracts (M)

Source: Author's Field Work 2025

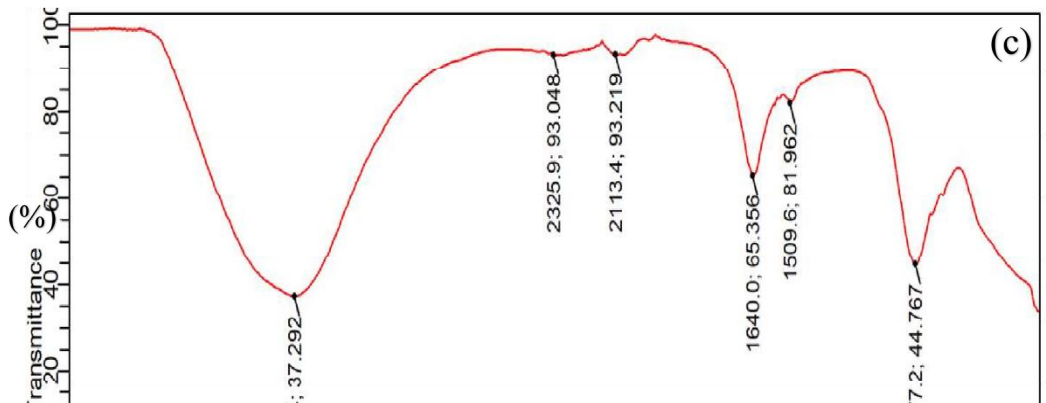

Wavenumber (cm^{-1})

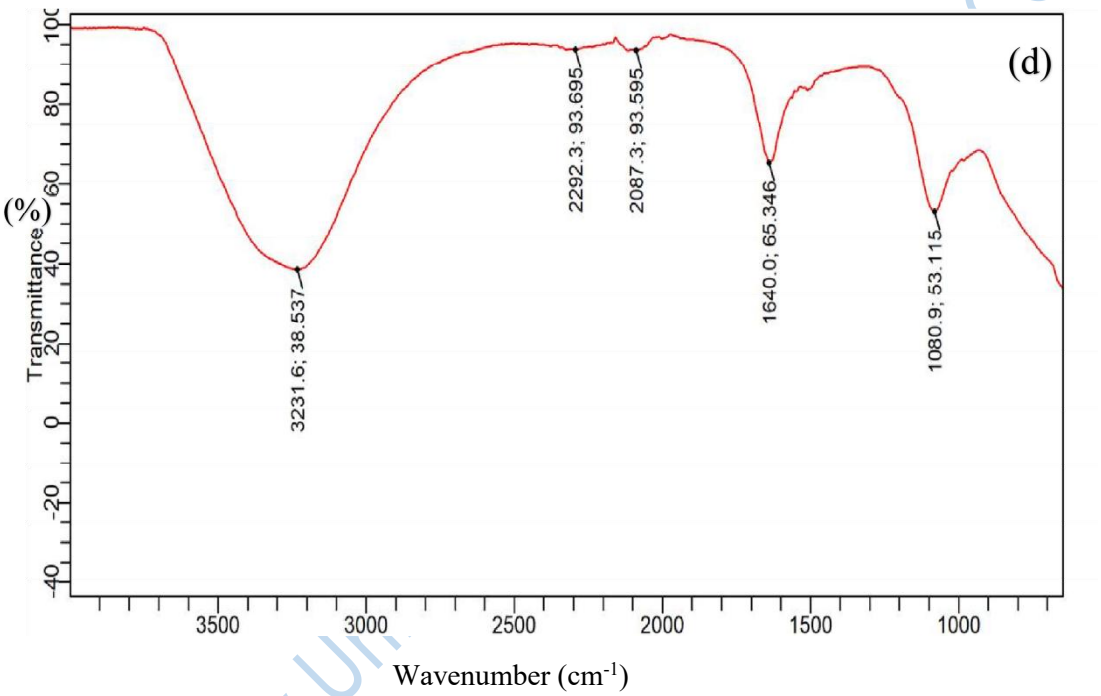

Figure 4.4: FTIR Spectra of (c) *Cassia javanica* extracts (C) (d) *Adonida merrilli* extracts (NM),

Source: Author's Field Work 2025

Table 4.2 : Comparison Studies of FT-IR Spectra Analysis of Leaf Extracts

Wavenumber (cm^{-1})	Literature Wavenumber (cm^{-1}) Range	Assignment	Leaf extracts

1073	1300–700	Skeletal C-C vibrations	*Casuarina equisetifolia*
1077			*Cassia javanica*
1084			*Washingtonia robusta*
1080			*Adonida merrilli*
1509	1555-1485	Aromatic nitro compounds.	*Casuarina equisetifolia*
1509			*Cassia javanica*
1640	1680-1620	Alkenyl C=C stretch.	*Casuarina equisetifolia*
1640			*Cassia javanica*
1640			*Washingtonia robusta*
1640			*Adonida merrilli*
2091	2200-2000	Cyanide ion, thiocyanate ion,	*Casuarina equisetifolia*
2087		and related ions.	*Adonida merrilli*
2113	2140 -2100	C≡C Terminal alkyne	*Cassia javanica*
2105		(monosubstituted).	*Washingtonia robusta*
2292	2280-2240	Aliphatic cyanide/nitrile	*Washingtonia robusta*
2292			*Adonida merrilli*
3209	3570–3200	Hydroxyl group, H-bonded OH	*Casuarina equisetifolia*
3209	(broad).	stretch	*Cassia javanica*
3239			*Washingtonia robusta*
3231			*Adonida merrilli* [8,9]

Source: Author's Field Work 2025

4.2.2.2 FTIR Analysis of Zinc Oxide Nanoparticles

The bioactive components in E-ZnONP, C-ZnONP, M-ZnONP and NM-ZnONP were examined using FTIR Figure 4.5 Infrared spectroscopy is employed to identify certain

biomolecules. It is evident from the observation of distinct IR bands that ZnONPs have adsorbed various biomolecules with distinct functional groups on their surface. These substances validated acting as stabilizers and reducers during the production of ZnONPs. Figure 4.5 For E-ZnONP, ZnO stretching vibrations are represented by the peaks at a range of 857 cm^{-1} to 3168 cm^{-1}; C-C vibrations is represented by a band at 857 cm^{-1}; C-C is related to the peak at 1017 cm^{-1}; C-C stretching vibrations represented by the peak at 1066 cm^{-1}; C=C-C stretching vibrations represented by the peaks at 1505 cm^{-1}, C=C represented by the peaks at 1640 cm^{-1}; OH stretching vibration represented by the peak at 3168 cm^{-1} OH-stretching alcohols and phenols are responsible for the peak at 3168 cm^{-1}. However, the existence of transition metal was the reason for the 2091 cm^{-1} (Figure 4.5) [8, 9].

For C-ZnONPs according to Figure 4.5. The band recorded at 700 cm^{-1} indicated that biosynthesized ZnONPs well formed, the band at 857 cm^{-1} (C–C) with a stretch type of vibration, C-C stretching is represented by a band at 1066 cm^{-1}; C=C-C is related to the peak at 1505 cm^{-1}, C=C is related to the peak at 1617 cm^{-1}, and OH-stretching alcohols and phenols are responsible for the peak at 3213 cm^{-1}. However, the existence of transition metal was the reason for the 1994 cm^{-1} and 2102 cm^{-1} [8, 9, 10].

According to Figure 4.2.2.2 shows M-ZnONPs: CH3-S-(C-Stretching is represented by a band at 663 cm^{-1}; C-C is related to the peak at 857 cm^{-1}; C-C stretching vibrations are represented by the peaks at 1017 $cm^{-1}$and 1088 cm^{-1}, respectively; Aromatic nitro compounds is related to the peak at 1505 cm^{-1}; C=C is related to the peak at 1625 cm^{-1}; However, the existence of transition metal was the reason of the 2083 cm^{-1} and OH stretching alcohols responsible for the peak at 3138 cm^{-1} [8, 9].

For NM-ZnONP, the band recorded at 715 cm^{-1} indicated that biosynthesized ZnO NPs was formed, the band at 861 cm^{-1} (C–C) with a stretch type of vibration, 1058 cm^{-1} (C=O) stretch mode of vibration, 1509 cm^{-1} (C=C-C) bending vibration; 1625 cm^{-1} (C=C). The peaks at 1990 cm^{-1} and 2083 cm^{-1} in the spectra of ZnO NPs were caused by the presence of transition

metal. Broad absorption band with a center at 3235 cm-[1] is connected to O-H stretching vibrations; the obtained spectrum of FTIR analysis is represented in (Figure 4.5) [8, 9, 10]. According to Table 4.5 shows the comparison study of FTIR spectra analysis of different ZnONP, all the Zinc Oxide nanoparticles display consistent results, showing skeletal C-C vibrations, C=C-C aromatic ring stretch, alkenyl C=C stretch, transition metal presence, and hydroxyl group H-bonded OH stretch. This is consistent with the results of a previous study on *Adenanthera pavonina* leaf extracts, which exhibit a peak at 1640 cm^{-1}. (C=C) and 795 cm^{-1} (C–C) [9, 10].

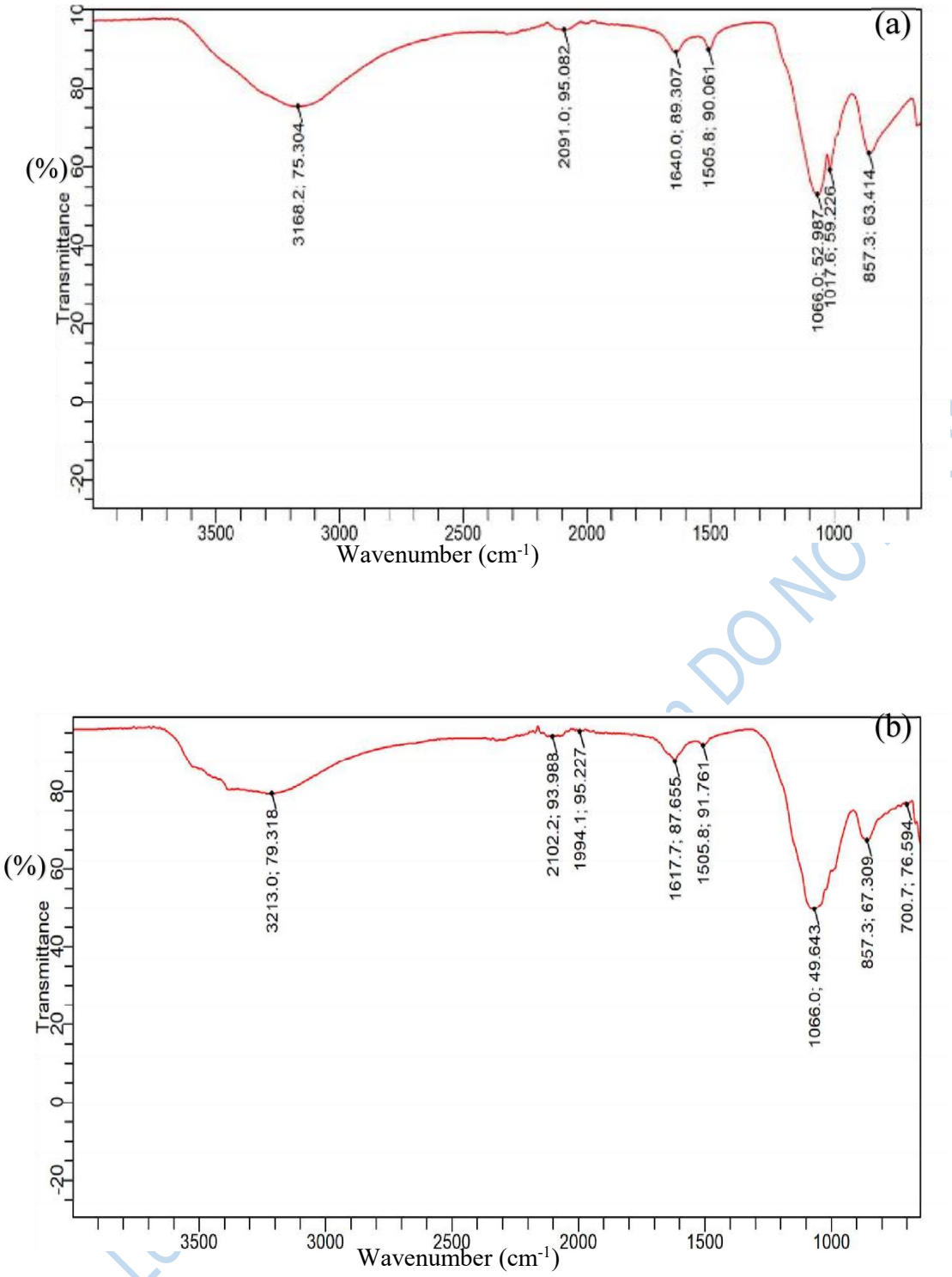

Figure 4.5: FTIR Spectra of (a) E-ZnONP (b) C-ZnONP,

Source: Author's Field Work 2025

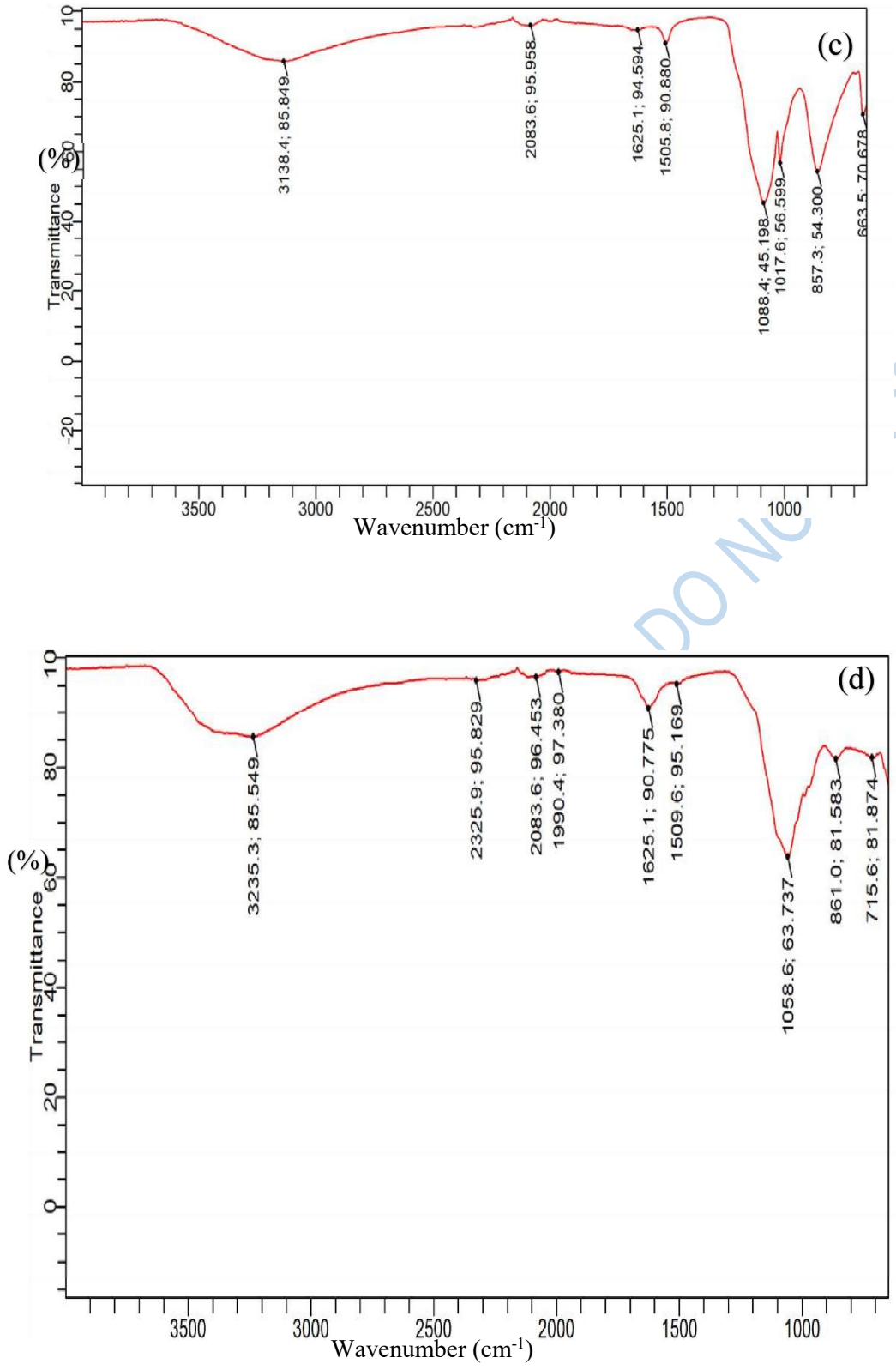

Figure 4.5: FTIR Spectra of (c) M-ZnONP (d) NM-ZnONP

Source: Author's Field Work 2025

Table 4.3. Comparison Studies of FT-IR Spectral Analysis of Different ZnONP

Wavenumber (cm^{-1})	Literature Wavenumber(cm^{-1}) Range	Assignment	ZnONP Leaf extracts
857	1300–700.	Skeletal C-C vibrations	*Casuarina equisetifolia,*
700, 857			*Cassia javanica*
663, 857			*Washingtonia robusta*
715,861			*Adonida merrilli*
1017,1066	1300–700.	Skeletal C-C vibrations	*Casuarina equisetifolia,*
1066			*Cassia javanica*
1017,1088			*Washingtonia robusta*
1058			*Adonida merrilli*
1505	1510–1450.	C=C-C Aromatic ring stretch	*Casuarina equisetifolia,*
1505			*Cassia javanica*
1505			*Washingtonia robusta*
1509			*Adonida merrilli*
1640	1680-1620	Alkenyl C=C stretch.	*Casuarina equisetifolia,*
1617			*Cassia javanica*
1625			*Washingtonia robusta s*
1625			*Adonida merrilli*
2091	2100-1800	Transition metal	*Casuarina equisetifolia,*
1994			*Cassia javanica*
2083			*Washingtonia robusta*
1990			*Adonida merrilli*
2102	2200-2000	Transition metal carbonyls	*Cassia javanica*
2083			*Adonida merrilli,*
3168	3570–3200	Hydroxyl group, H-bonded OH stretch	*Casuarina equisetifolia,*
3213	(broad).		*Cassia javanica*
3138			*Washingtonia robusta*
3235			*Adonida merrilli*

4.2.2.3. FTIR of Aluminum Oxide Nanoparticles

The technique of infrared spectroscopy is also employed to identify certain biomolecules in the E-Al_2O_3NP. It is evident from the observation of distinct IR bands that Aluminum

OxidesNPs have adsorbd various biomolecules with distinct functional groups on their surface. These

substances validated acting as stabilizers and reducers during the production of Aluminum OxidesNPs (Figure 4.6). For instance, Aluminum Oxide NPs stretching vibrations are represented by the peaks at 1643 cm^{-1} and 3417 cm^{-1}, respectively; C=C is related to the peak at 1643 cm^{-1}. OH-stretching alcohols and phenols are responsible for the peak at 3417 cm^{-1}. (Figure 4.6) [9].The C-Al_2O_3NP stretching vibrations are represented by peak 1505 cm^{-1}; C=C-C, C=C is related to the peak at 1632 cm^{-1}; NH stretching vibrations are represented by the peak at 2351 cm^{-1}, and OH-stretching alcohols and phenols are responsible for the peak at 3399 cm^{-1} [8, 9].

According to Figure 4.2.2.3 M-Al_2O_3NPs stretching vibrations are represented by the following peaks: C=C-C stretching is represented by a band at 1505 cm^{-1}; C=C is related to the peak at 1636 cm^{-1}; N-H stretching vibrations are represented by the peak at 2348 cm^{-1}; and OH-stretching alcohols responsible for the peak at 3391 cm^{-1} [8,9].

NM-Al_2O_3NP vibrations are represented by these peaks. C=C is related to the peak at 1640 cm^{-1}, and OH-stretching alcohols responsible for the peak at 3436 cm^{-1}, [9] Figure 4.6.

The comparison studies of FT-IR spectra analysis of different Al_2O_3NP**,** according to Table 4.4, all the aluminum oxide nanoparticles exhibit similar results, possessing alkenyl C=C stretch and hydroxyl group H-bonded OH stretch.This corresponds with the results of a previous study on *Adenanthera pavonina* leaf extracts, which exhibit a peak at 1640 cm^{-1} for C=C and 3457 cm^{-1} for O-H stretching [9, 10].

Additionally, *Cassia javanica* and *Washingtonia robusta* display C=C-C aromatic ring stretch and NH component amino-related components.

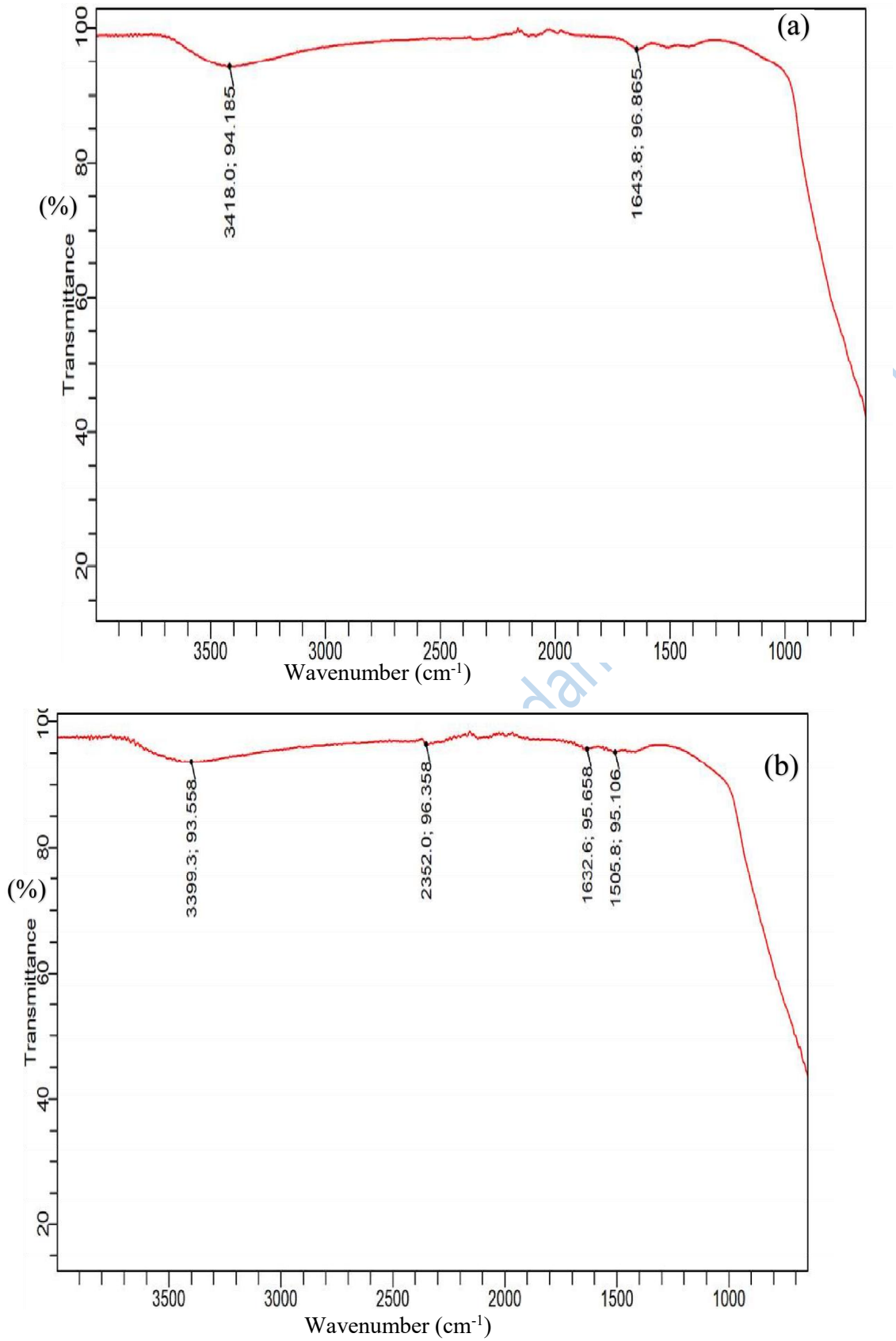

Figure 4.6: FTIR Spectra of (a): E-AI_2O_3NP (b) C-AI_2O_3NP

Source: Author's Field Work 2025

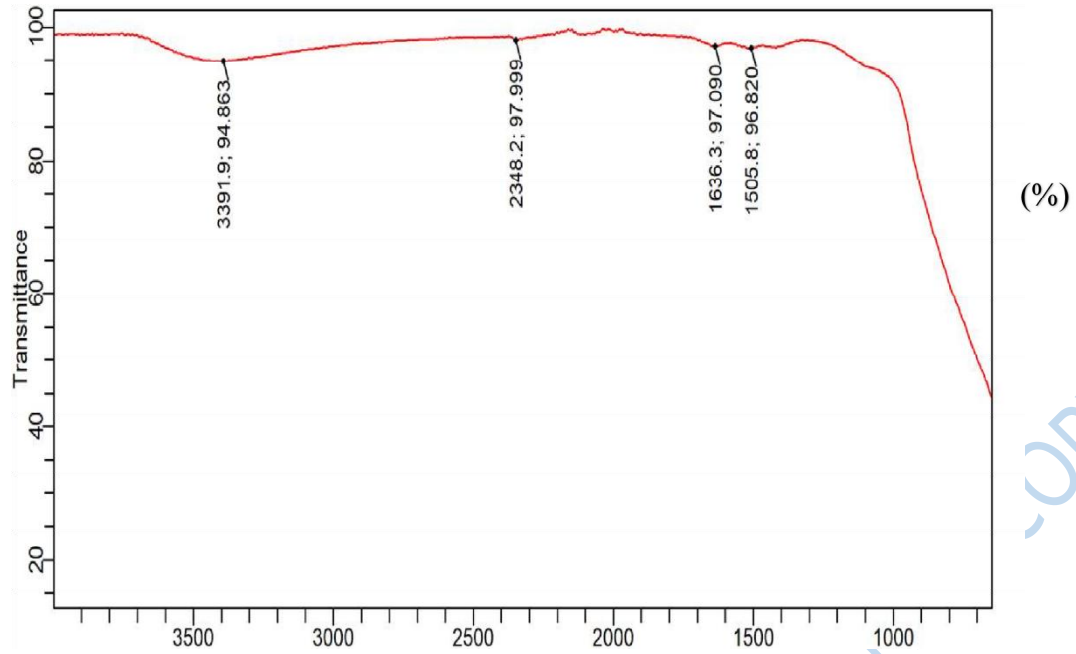

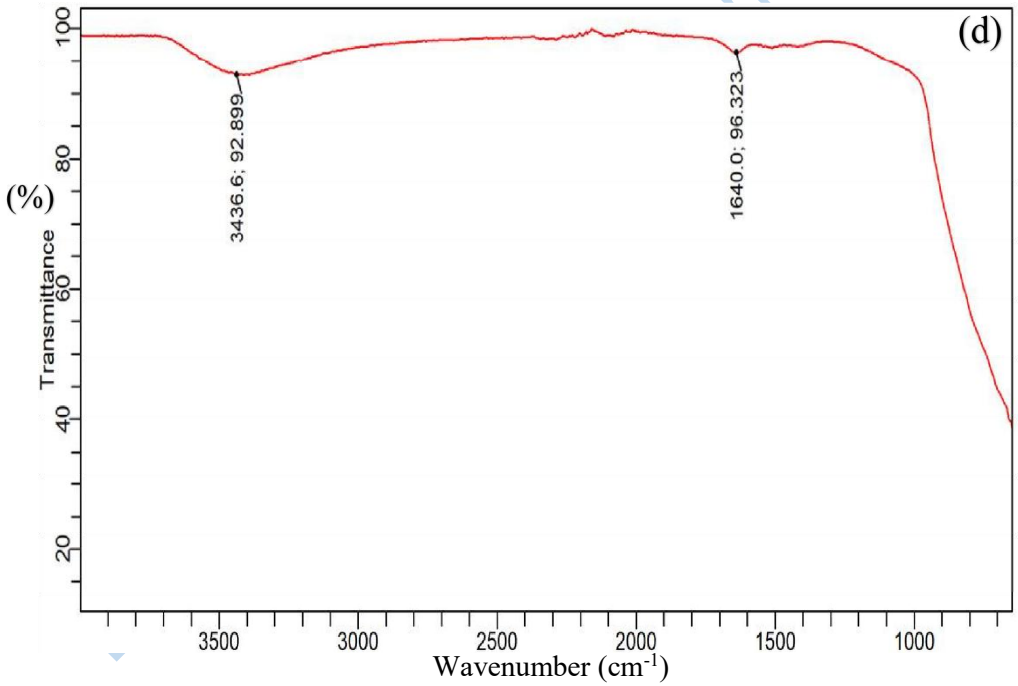

Figure 4.6: FTIR Spectra of (c) M-AI_2O_3NP (d) NM-AI_2O_3NP

Source: Author's Field Work 2025

Table 4.4: Comparison Studies of FT-IR Spectral Analysis of Different Al_2O_3NP

Wavenumber (cm^{-1})	Literature Wavenumber (cm^{-1}) Range	Assignment	Leaf extracts
1505	1510–1450.	C=C-C Aromatic ring stretch	*Cassia Javanica*
1505			*Washingtonia robusta*
1643	1680-1620	Alkenyl C=C stretch	*Casuarina equisetifolia,*
			Cassia Javanica,
1632			*Washingtonia robusta,*
1636			*Adonida merrilli,*
1640			
2351	About 2350	NH component Amino-	*Cassia Javanica*
2348		related component	*Washingtonia robusta*
3417	3570–3200 (broad)	Hydroxy group, H-bonded	*Casuarina equisetifolia*
3399		OH stretch	*Cassia Javanica*
3391			*Caryota mitis*
3436			*Adonida merrilli*

Source: Author's Field Work 2025

4.2.3 XRD Analyses of Metal Oxide Nanoparticles

4.2.3.1 XRD Analyses of Zinc Oxide Nanoparticles

X-ray Diffraction (XRD) analysis is a quick analytical method that primarily determines the phase of a crystallite material and give acurate size of each cell.XRD is one of the best techniques. It characterizes the purity and phase of the nanomaterial. XRD gives details of the diffraction angle, the interlayer spacing, and mainly the crystallite size.

The hexagonal phase is seen in the XRD pattern of the produced NM-ZnONPs, Figure 4.7 (a) shows strong and sharp diffraction peaks. The diffraction peaks are connected with the (100), (002), (101), (102), (110), (200), (112), and (201) planes, respectively, and are located at 30.8°, 35.6°, 37.6°, 46.8°, 57.2°, 66.2°, 67.6°, and 68.8°. The data match up well with the ZnO standard cards (JCPDS file number 79-2205). The X-indexed peak represents impurity, which could arise as a result of a secondary reaction with impurities cations. The particle recorded a mean particle size of 73.82 nm[12, 14].

C-ZnONPs is shown in Figure 4.7 (b). The Miller-Bravais indices of (100), (002), (101), (102), (110), (311) and (112) are responsible for the emergence of the conspicuous peaks at 30.4°, 33.8°, 36.0°, 46.6°, 56.0 °, 64.2° and 67.2°, respectively. All of the ZnO nanopowder's diffraction peaks are in good accordance with the ZnO JCPDS (card No. 89-0510) pattern, which is associated with the ZnO NPs' hexagonal wurtzite crystal structure. The X-indexed peak represents impurity, which could arise as a result of a secondary reaction with impurities. The crystallinity of the nanoparticles, with their calculated size, is evidence that their application in biomedical procedures would be seamless. The size of the ZnO NPs calculated using Scherrer's formula showed an average particle size of 41.85 nm[14].

Figure 4.7(c) shows the XRD pattern of M-ZnNPs. The peaks at 34.6, 36.0, 46.6, 55.2, 62.2, which corresponded to (002), (101), (102), (110), (103) crystalline planes of ZnO and were in good agreement with the JCPDS Card no. 01-079-2205. All these peaks exactly match the one in Literature [12] which clearly indicates the formation of zinc oxide. The average crystallite size of ZnO NP's was 71.5 nm, calculated using the Scherrer equation based on the full width at half-maximum of the diffraction plane [14]

XRD spectra of the biosynthesized E-ZnONP powder were detected by X-ray diffractor, which resulted in different crystal planes such as (100), (101), (102), (103), (200), were assigned to the 2θ values of XRD 31.57°; 36.05°; 47.34°; 62.75°; 67.82°; which showed hexagonal phase of Zinc Oxide and good crystallinity of the products. Figure 4.7(d). The average crystallite size of ZnO NPs was 22.06 nm, calculated using the Scherrer equation based on the full width at half-maximum of the diffraction plane.These presented planes matched well with the wurtzite ZnO hexagonal structure having JCPDS card No. 36-1451, which was reported by [14,] Figure 4.7(d).

The XRD results of (NM-ZnONPs, C-ZnONPs, M-ZnONPs, E-ZnONPs) align with previous studies on the green synthesis of zinc oxide nanoparticles using *Elaeagnus angustifolia L.* leaf extracts [12], *Eucalyptus globulus Labill* leaf extract [13], and *Passiflora subpeltata* [14].Figure 4.7 (a-d).

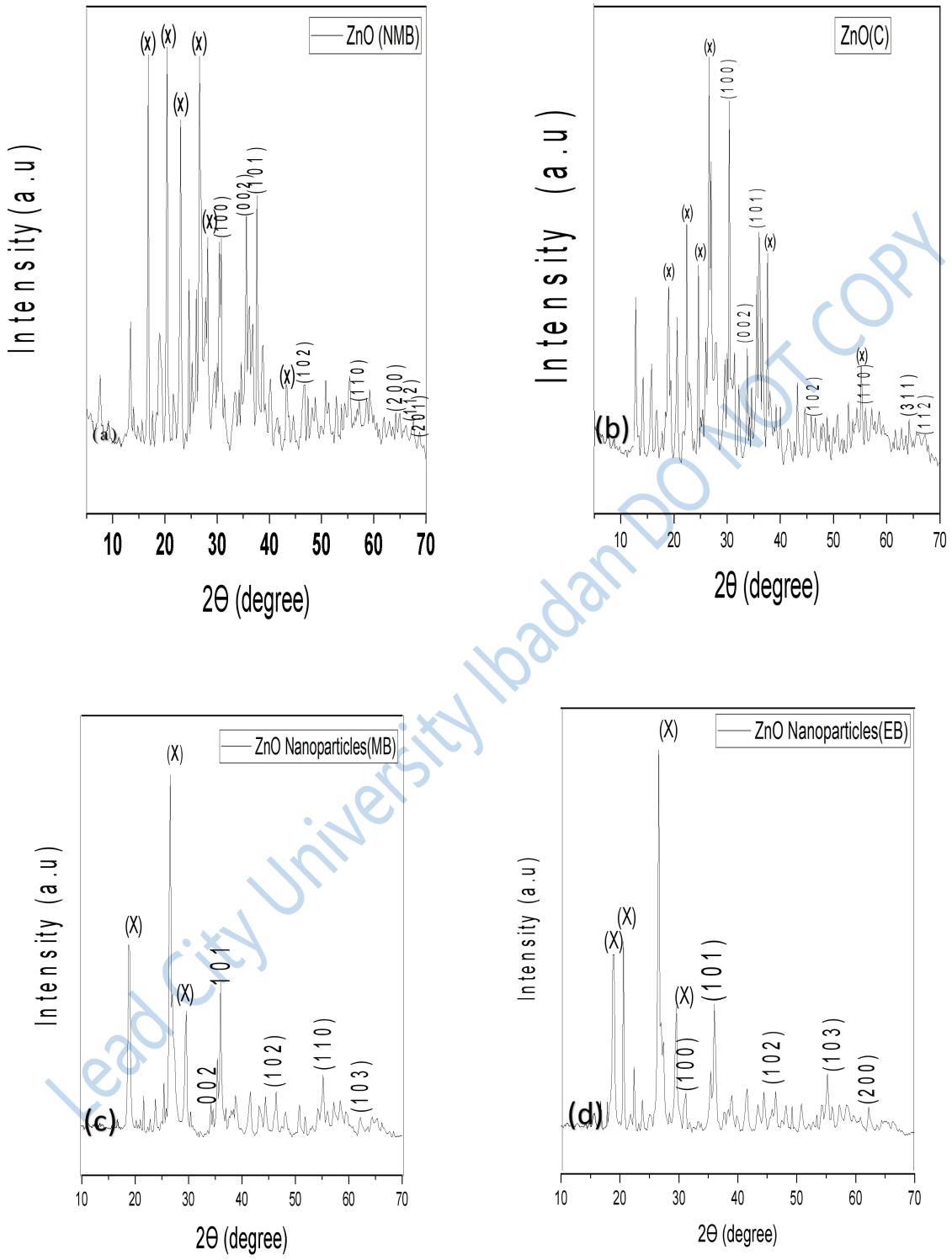

Fi

gure: 4.7 XRD Spectra of (a) NM-ZnONP (b) C-ZnONP, (c) M-ZnONP (d) E-ZnONP

Source: Author's Field Work 2025

4.2.3.2 XRD Analyses of Aluminum Oxide Nanoparticles

XRD Spectra of the biosynthesized C-Al_2O_3 powder was detected by X-ray diffractor, which resulted in different crystal planes such as (103), (112), (106), (201), (117), (205), (206), (119), (222), (300), (11 12), (2 1 11), (309), (21 13), (403) and (1 0 17) were assigned to the 2θ values of XRD 19.4°; 23.2°; 27.8°; 32.2°; 34.6°; 37.4°; 39.8°; 41.2°, 46.4°, 48.8°, 51.8°, 56.6°, 60.8°, 63.0°, 67.7°, and 69.4°; which showed cubic phase of aluminum oxide. Figure 4.8 (a). These presented planes match well with the quartzite Al_2O_3 cubic structure having JCPDS card No.00-153-1489 (Figure 4.8) XRD shows spherical crystalline nanoparticles with an average particle size of 10.13 nm [1].

E-Al_2O_3 powder was detected by X-ray diffractor, which resulted in (111), (220), (311), (222), (400), (331), (422), (511) and (440), were assigned to the 2θ values of XRD 19.6°; 32.2°; 37.8°; 39.6°; 46.0°; 50.8°; 57.0°; 60.6° and 67.2°; which showed cubic phase of aluminum oxide. Figure 4.8 (b) These presented planes match well with the wurtzite Al_2O_3 Cubic structure having JCPDS card No. 00-153-1489; Figure 4.2.3.2 (b), XRD shows nanoparticles with an average particle size of 8.63 nm.

NM-Al_2O_3 powder was detected by X-ray diffractor, which resulted in different crystal planes such as (007), (106), (115), (202), (117), (206), (222), (224) (324) and (402), were assigned to the 2θ values of XRD 26.0°; 27.6°; 29.8°; 32.8°; 34.8°; 37.6°; 39.4°; 46.4°;48.6;61.6 and 67.4°; which showed tetragonal phase of aluminum oxide. Figure 4.8 (c). These presented planes match well with the Al_2O_3 tetragonal structure, which has JCPDS card No. 00-153-7011 Figure 4.8 (c). XRD shows nanoparticles with an average particle size of 5.86 nm [13]. Calculated using the Scherrer equation based on the full width at half-maximum of the diffraction plane. 2θ (degree)

M-Al_2O_3NPs powder was detected by X-ray diffractor, which resulted in different crystal planes such as (104), (112), (200), (212), (109), (215), (208), (222), (304),(1113),(2012),(324),(2211) and (402), were assigned to the 2θ values of XRD 21.6°;

23.6°; 36.8°; 37.8°; 40.8°; 44.2°; 46.0.°; 51.4°, 55.6, 57.0, 62.0, 63.8, and 67.4°, which showed the tetragonal phase of aluminum oxide (Figure 4.8(d)). These presented planes match well with the aluminum oxide nanoparticles' tetragonal structure, which has JCPDS card No. 00-153-7011 (Figure 4.8). XRD shows nanoparticles with an average particle size of 8.68 nm calculated using Scherrer equation based on the full width at half-maximum of the diffraction plane.

The XRD results of (NM-Al_2O_3NPs, C-Al_2O_3NPs, M-Al_2O_3NPs, E-Al_2O_3NPs) are consistent with previous studies on the green synthesis of Al_2O_3 nanoparticles using leaf extracts of *Calligonum comosum L.*[15] and seed extracts of *Carica papaya* [16].

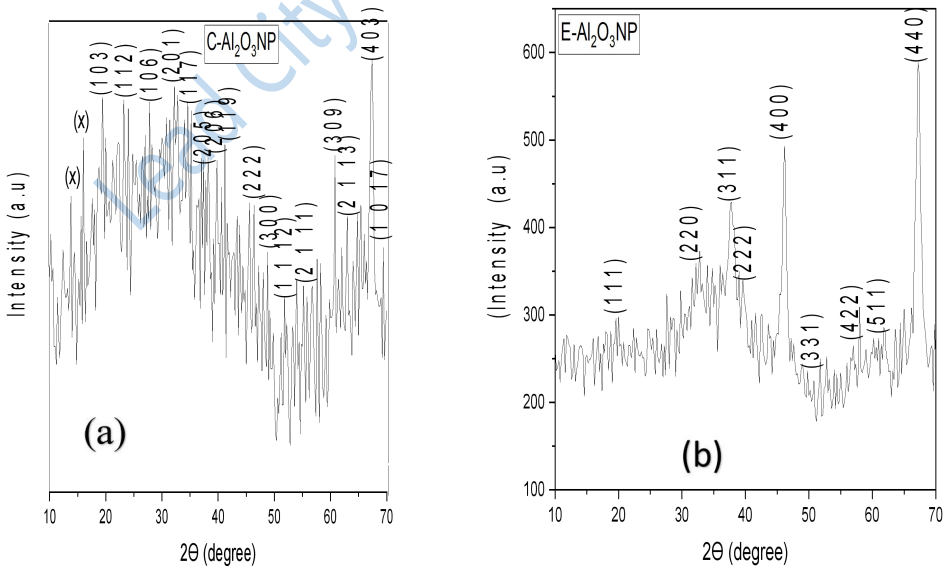

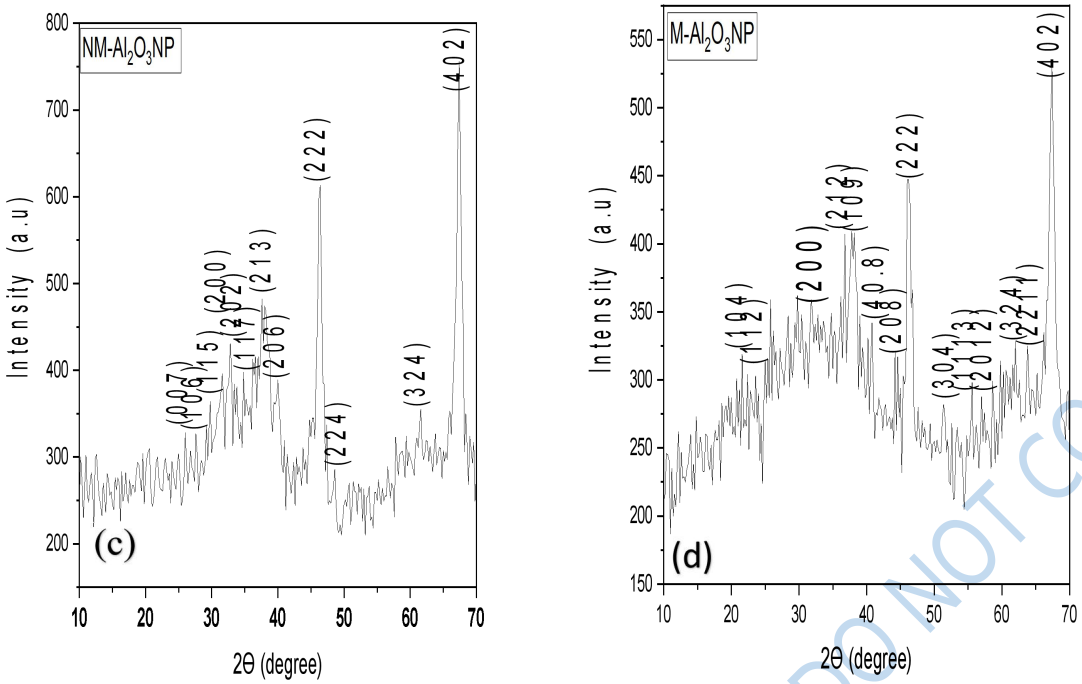

Figure 4.8: XRD Spectra of (a): C-AI_2O_3NP (b) E-AI_2O_3NP, (c) NM-AI_2O_3NP (d) M-AI_2O_3NP

Source: Author's Field Work 2025

4.2.4. SEM Analysis of Metal Oxide Nanoparticles

4.2.4.1 SEM Analysis of Zinc Oxide Nanoparticles

The SEM micrographs of C-ZnONPs are presented in Figure 4.9 (a). The Figure shows that the nanoparticles are heterogeneous having an uneven hexagonal wurtzite crystal structure while some are agglomerate, and some are not [13].

The SEM images of E-ZnONPs were revealed by SEM testing. The SEM images show that the nanoparticles are heterogeneous. The surface of zinc oxide has a hexagonal phase; some are agglomerates, and some are not [14], according to Figure 4.9 (b).

M-ZnONPs size and structure were revealed by SEM testing ZnO nanoparticles. The SEM images show that the nanoparticles are heterogeneous; the surface morphology of zinc oxide has some agglomerate and some are not [14, 17]. Figure 4.9 (c)**.**

SEM analysis unveiled the size and hexagonal phase sphericity of NM-ZnNPs. The presence of ZnO nanoparticles is depicted in Figure 4.9 (d) and are heterogeneous and some are not [17].

The SEM results of (NM-ZnONPs, C-ZnONPs, M-ZnONPs, E-ZnONPs) are consistent with previous studies on the green synthesis of zinc oxide nanoparticles using *Eucalyptus globulus Labill.* Leaf extract [13], *Passiflora subpeltata* [14], and the aqueous leaf extract of *Sida acuta* [17].

(a)

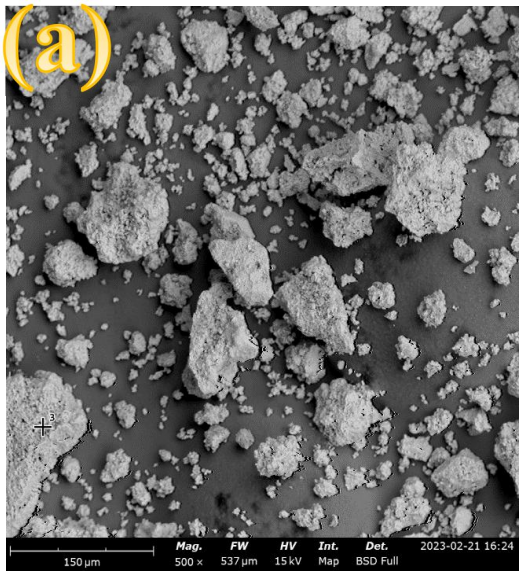

(b)

(c)

(d)

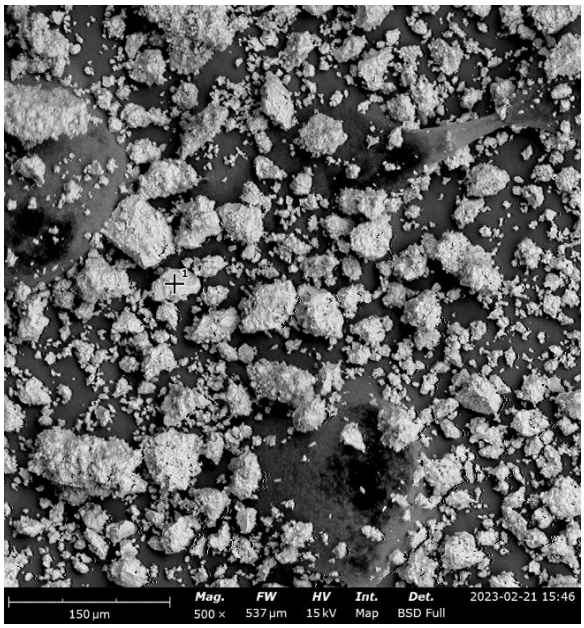

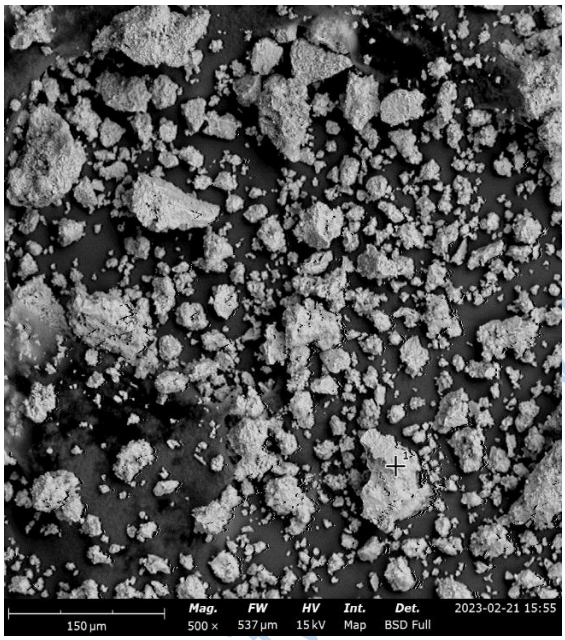

Figure 4.9: SEM Micrographs of (a) C-ZnONP (b) E-ZnONP, (c) M-ZnONP (d) NM-ZnONP

Source: Author's Field Work 2025

4.2.4.2 SEM Analysis of Aluminum Oxide Nanoparticles

The SEM images of C-Al_2O_3NPs display Cubic structures. The variation in surface morphology was attributed to intermolecular interaction, lattice mismatch, and the existence of residual oxides [15]. The SEM images show that the nanoparticles are homogeneous, not agglomerate. Figure 4.10 (a).

The SEM images of E-Al_2O_3NPs display cubic phase. The variation in surface morphology was attributed to intermolecular interaction, lattice mismatch, and the existence of residual oxides [13].The SEM images show that the nanoparticles are homogeneous; the surface morphology of Aluminum oxide nanoparticles has a cubic phase and grain size. They are not agglomerate [16]. Figure 4.10 (b) revealed the detailed structure.

The SEM images of NM-Al_2O_3 nanoparticles display tetragonal structures. The variation in surface morphology was attributed to intermolecular interaction, lattice mismatch, and the existence of residual oxides. The SEM images show that the nanoparticles are homogeneous; the surface morphology of aluminum oxide nanoparticles oxide has a tetragonal structure. They are not agglomerate [15, 16] according to Figure 4.10 (c)

The SEM images of M-Al_2O_3NPs display a tetragonal phase. The variation in surface morphology was attributed to intermolecular interaction, lattice mismatch, and the existence of residual oxides [16] The SEM images show that the nanoparticles are homogeneous; the surface morphology of aluminum oxide nanoparticles has a tetragonal phase. They are not agglomerate [15, 16]. Figure 4.10 (d).

The SEM results of (NM-Al_2O_3NPs, C-Al_2O_3NPs, M-Al_2O_3NPs, E-Al_2O_3NPs) align with previous studies on the green synthesis of Al_2O_3NPs using leaf extracts of *Calligonum comosum* L[15]. and seed extracts of *Carica papaya* [16]

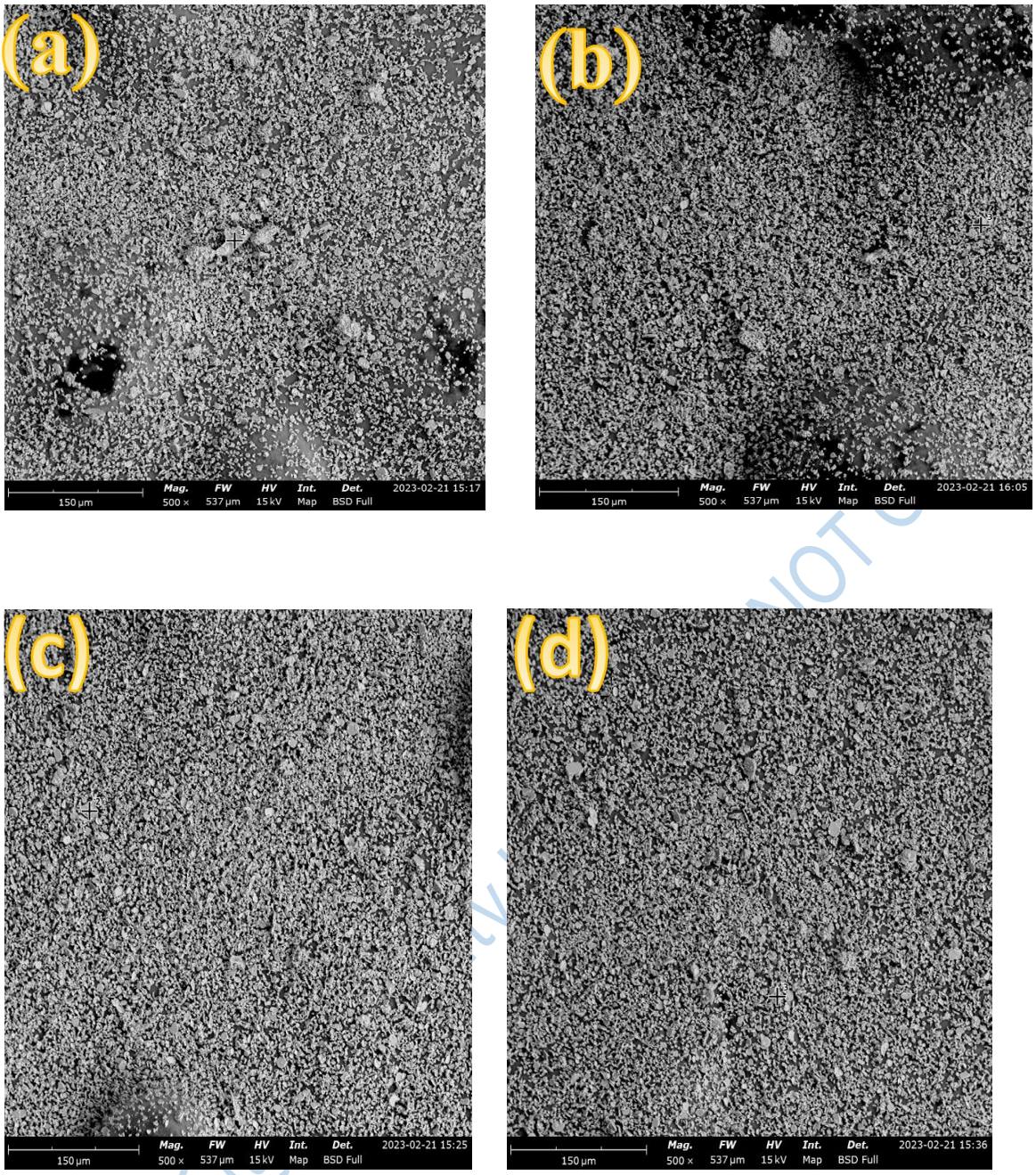

Figure 4.10: SEM Microghraphs Results of (a): C-AI_2O_3NP (b) E-AI_2O_3NP, (c) M-AI_2O_3NP (d) NM-AI_2O_3NP

Source: Author's Field Work 2025

4.2.5 EDX Analyses of Metal Oxide Nanoparticles

4.2.5.1 EDX Analyses of Zinc Oxide Nanoparticles

EDX analysis of C-ZnONPs is shown in Table 4.5.This shows the purity of ZnO nanoparticles. According to the analysis, sulphur, and zirconium were recorded to be present with recorded percentage values of 9.31 and 0.57% respectively, which indicate the presence of impurities. While the percentage values of O and Zn were found to be 48.51 and 41.60%, respectively. The two additional elements that were observed in the EDX spectrum might represent the remnants of the initial elements found in the plant extract. However, this signifies the synthesis of ZnO NP, which is in agreement with the FTIR analysis [14, 17].

E-ZnONPs are shown in EDX (Table 4.5).The purity of ZnO nanoparticles was displayed by EDX analysis, which only detects sulphur(S) with recorded percentage composition of 11.48% percentage values % of O and Zn was found to be 56.89% and 31.63%, respectively. The additional element that was detected in the EDX spectrum might represent the remnants of the initial elements found in the plant extract [17].

M-ZnONP are shown in EDX analysis (Table 4.5). The purity of ZnO nanoparticles was displayed by EDX analysis, which only detects sulphur(S) with recorded percentage composition of 12.11%. The percentage values of O and Zn was found to be 32.89 and 55.0%, respectively. The additional elements that were detected in the EDX spectrum might represent the remnants of the initial elements found in the plant extract [14, 17].

Furthermore, Table 4.5.showcases the surface elemental composition of NM-ZnONP, where zinc exhibits the highest intensity while silicon shows the least. Three additional elements were detected in the EDX spectrum; they might represent the remnants of the initial elements found in the plant extract.

The SEM results of (NM-ZnONPs, C-ZnONPs, M-ZnONPs, E-ZnONPs) are consistent with previous studies on the green synthesis of zinc oxide nanoparticles using *Passiflora subpeltata* [14] and the aqueous leaf extract of *Sida acuta* [17].

ZnONP	Element Number	Element Symbol	Element Name	Atomic Conc.	Weight Conc.
C-ZnONP	8	O	Oxygen	48.51	20.18
	30	Zn	Zinc	41.60	70.70
	16	S	Sulfur	9.31	7.76

	40	Zr	Zirconium	0.57	1.36
E-ZnONP	8	O	Oxygen	56.89	27.20
	30	Zn	Zinc	31.63	61.80
	16	S	Sulfur	11.48	11.00
M-ZnONP	30	Zn	Zinc	55.00	79.73
	8	O	Oxygen	32.89	11.67
	16	S	Sulfur	12.11	8.61
NM-ZnONP	30	Zn	Zinc	52.85	76.69
	8	O	Oxygen	35.22	12.51
	16	S	Sulfur	9.95	7.08
	14	Si	Silicon	0.72	0.45
	40	Zr	Zirconium	0.62	1.26

Table 4.5 EDX Analysis Results of Zinc Oxide Nanoparticles

4.2.5.2 EDX Analysis of Aluminum Oxide Nanoparticles

The purity of C-Al_2O_3NPs was demonstrated by EDX analysis, which only detects Carbon 1.77 %. The average atomic % of O and Al were found to be 54.60 and 43.14,% respectively. The additional element that was detected in the EDX spectrum might represent the remnants of the initial elements found in the plant extract [15].Table 4.6

The purity of E-Al_2O_3NPs was demonstrated by EDX analysis, which only detected the average atomic % of O and Al, which were found to be 17.98 and 82.02%, respectively. Table 4.6 revealed the detailed structure.

The purity of M-Al_2O_3NPs was demonstrated by EDX analysis, Table 4.6, which only detects nitrogen at 6.37%. The average atomic percentage of O and Al was found to be 41.85 and 51.62% respectively. The additional element that was detected in the EDX spectrum might represent the remnants of the initial elements found in the plant extract.

The purity of NM-Al_2O_3NPs was demonstrated by EDX analysis, which only detected Nitrogen at 7.03%. The average atomic percentage of O and Al were found to be 49.75 and 43.08% respectively. The additional element that was detected in the EDX spectrum might represent the remnants of the initial elements found in the plant extract, Table 4.6.

The EDX results of (NM-Al_2O_3NPs, C-Al_2O_3NPs, M-Al_2O_3NPs, E-Al_2O_3NPs) are consistent with previous studies on the green synthesis of Al_2O_3NPs using leaf extracts of *Calligonum comosum L.*[15] and seed extracts of *Carica papaya* [16].

Table 4.6: EDX Analysis of Aluminum Oxide Nanoparticles

	Element Number	Element Symbol	Element Name	Atomic Conc.	Weight Conc.
C-AI_2O_3NP	13	Al	Aluminium	54.60	65.74
	8	O	Oxygen	43.14	30.80
	6	C	Carbon	1.77	0.95
E-AI_2O_3NP	13	Al	Aluminum	82.02	88.49
	8	O	Oxygen	17.98	11.51
M-AI_2O_3NP	13	Al	Aluminum	51.62	64.23
	8	O	Oxygen	41.85	30.88
	7	N	Nitrogen	6.37	4.12
NM-AI_2O_3NP	8	O	Oxygen	49.75	38.42
	13	Al	Aluminum	43.08	56.11
	7	N	Nitrogen	7.03	4.75

4.3 Applications of Plant Extracts and Nanoparticles for Corrosion Inhibition Studies

4.3.1 Gravimetric Method

The study of the aqueous extracts of *Casuarina equisetifolia, Cassia javanica, Adonida merrilli, and Washingtonia robusta,* all Zinc nanoparticles and Aluminum nanoparticles of *Adonida merrilli, Washingtonia robusta , Cassia javanica, and Casuarina equisetifolia* at concentrations of 500,1000,1500 and 2000 ppm, respectively on mild steel at room temperature in 0.5 M H_2SO_4 were evaluated from one day to four days. Thier effect on weight loss of low carbon steel at room temperature for four days using gravimetric method as shown in figures below, It was observed that there is a weight loss decrease with increasing concentrations of the inhibitors during their exposure period in all tested solutions. See Appendix 2 for more details.

Figures 4.13 (a) - Figures 4.13(p) shows the weight loss and Figures 4.14 (a) - 4.14(p) shows the corrosion rate (mpy) determined at concentrations (500 ppm, 1000 ppm,1500 ppm and 2000 ppm). The weight loss was measured for four days. It was observed that weight loss of the coupons reduced as the concentration of the inhibitor increased, which might be due to an increased surface coverage and adherence of the inhibitor to the metal. A comparison of the blank and the inhibited corrosion study showed that the inhibitors influenced the rate of corrosion of mild steel in 0.5 M H_2SO_4. The study was done at room temperature.

This study aligns with previous research on the corrosion inhibition of welded X-52 steel pipelines using sodium molybdate in a 3.5% NaCl solution[18], also on recent advancements in sustainable corrosion inhibitors regarding their design, performance, and industrial applications [19], as well as the effects of aqueous *Chrysophyllum albidum* leaf and peel extracts on mild steel in an acidic medium [20].

4.3.1.1 Weight Loss at Various Time against Concentration of Inhibitors

Weight loss at various time from one day to four days with different inhibitors (extracts, zinc oxide nanoparticles and aluminum oxide nanoparticles) at 500 ppm to 1000 ppm of 0.5 M of H_2SO_4 concentration.

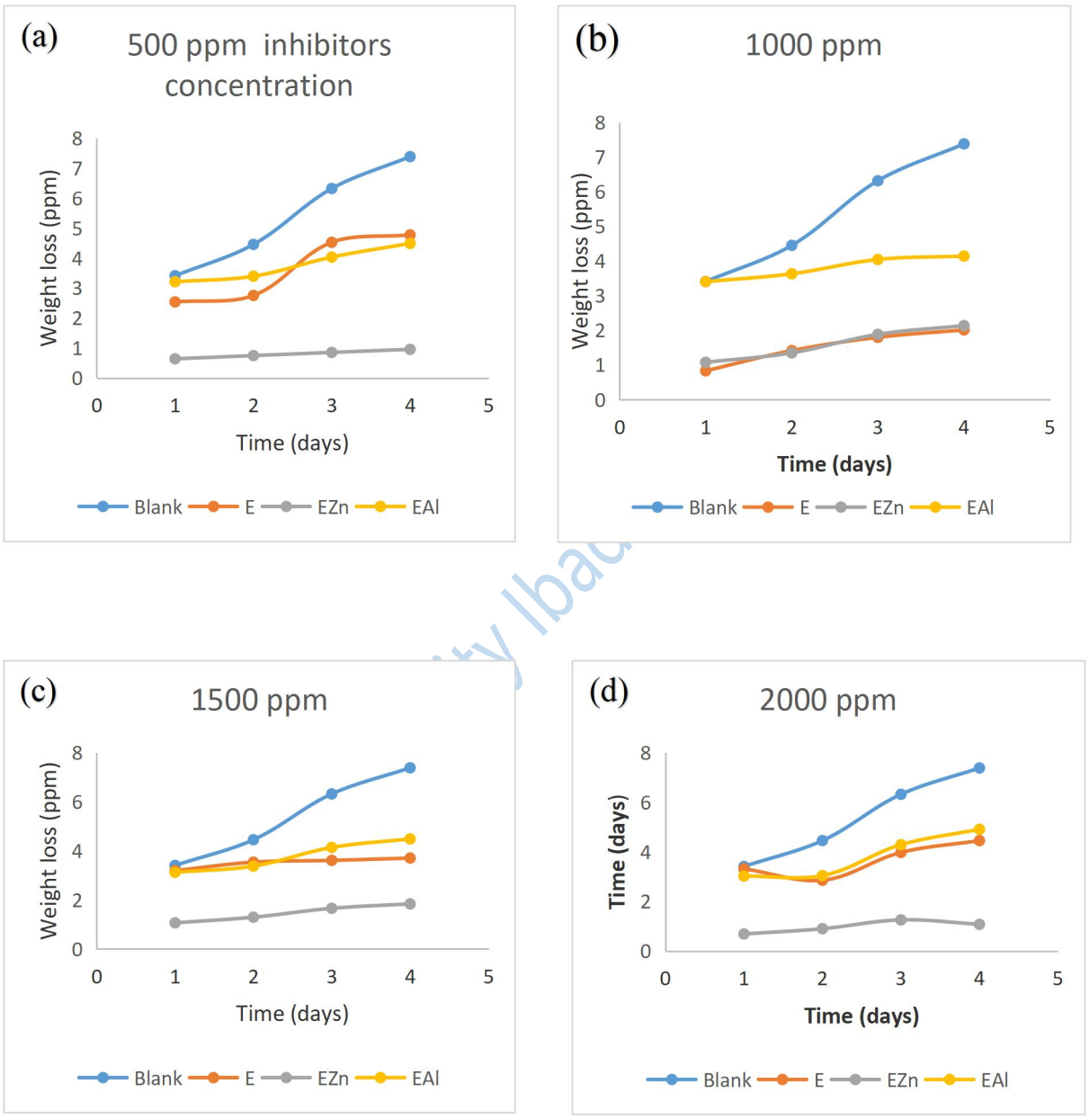

Figure 4.11 :The plots of Weight loss against time for (a) 500 ppm, (b) 1000 ppm,(c)1500 ppm and (d) 2000 ppm of (*Casuarina equisetifolia* extracts, E-ZnONP and E-AI_2O_3NP) Inhibitors concentration

Source: Author's Field Work 2025

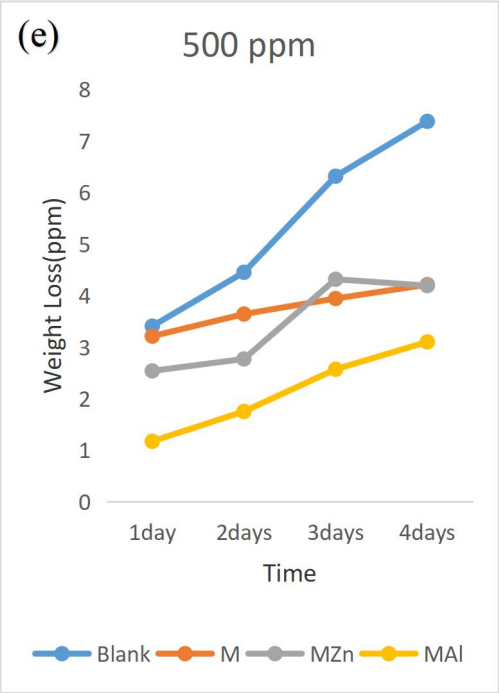

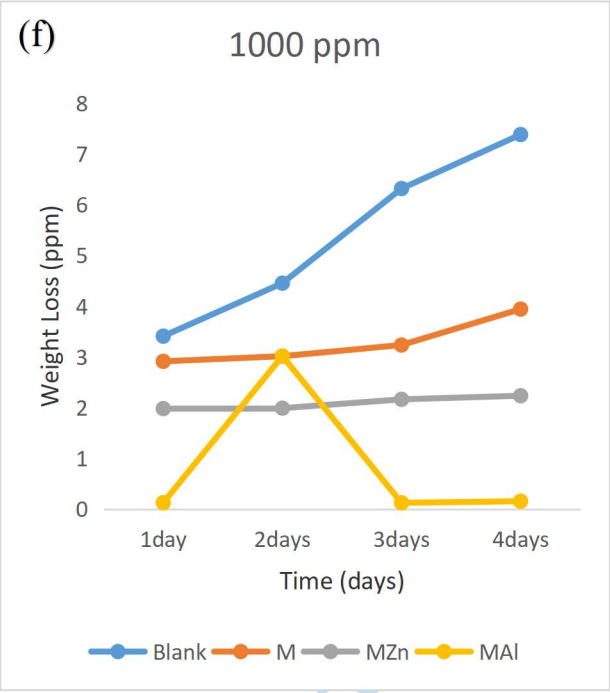

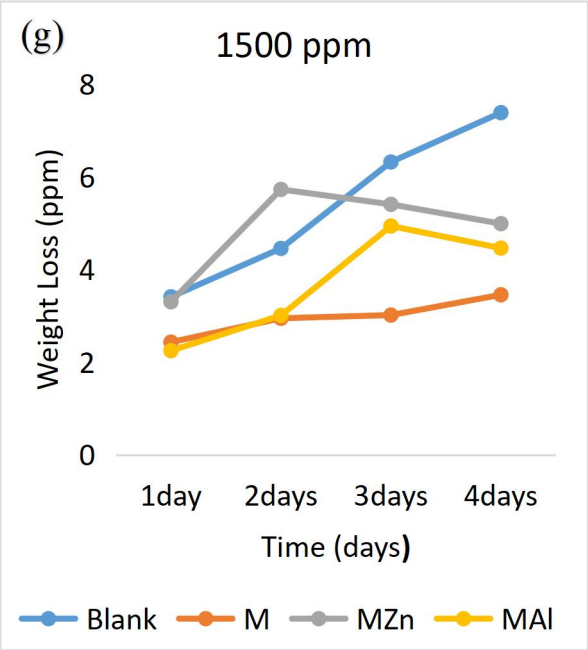

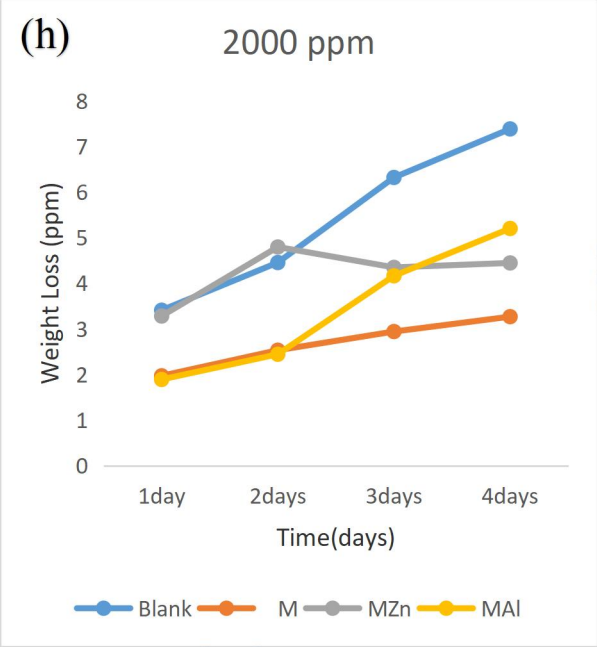

Figure 4.12 :The plots of Weight loss against time for (e) 500 ppm, (f) 1000 ppm,(g)1500 ppm and (h) 2000 ppm (*Washingtonia robusta* extracts, M-ZnONP and M-AI_2O_3NP) Inhibitors concentration

Source: Author's Field Work 2025

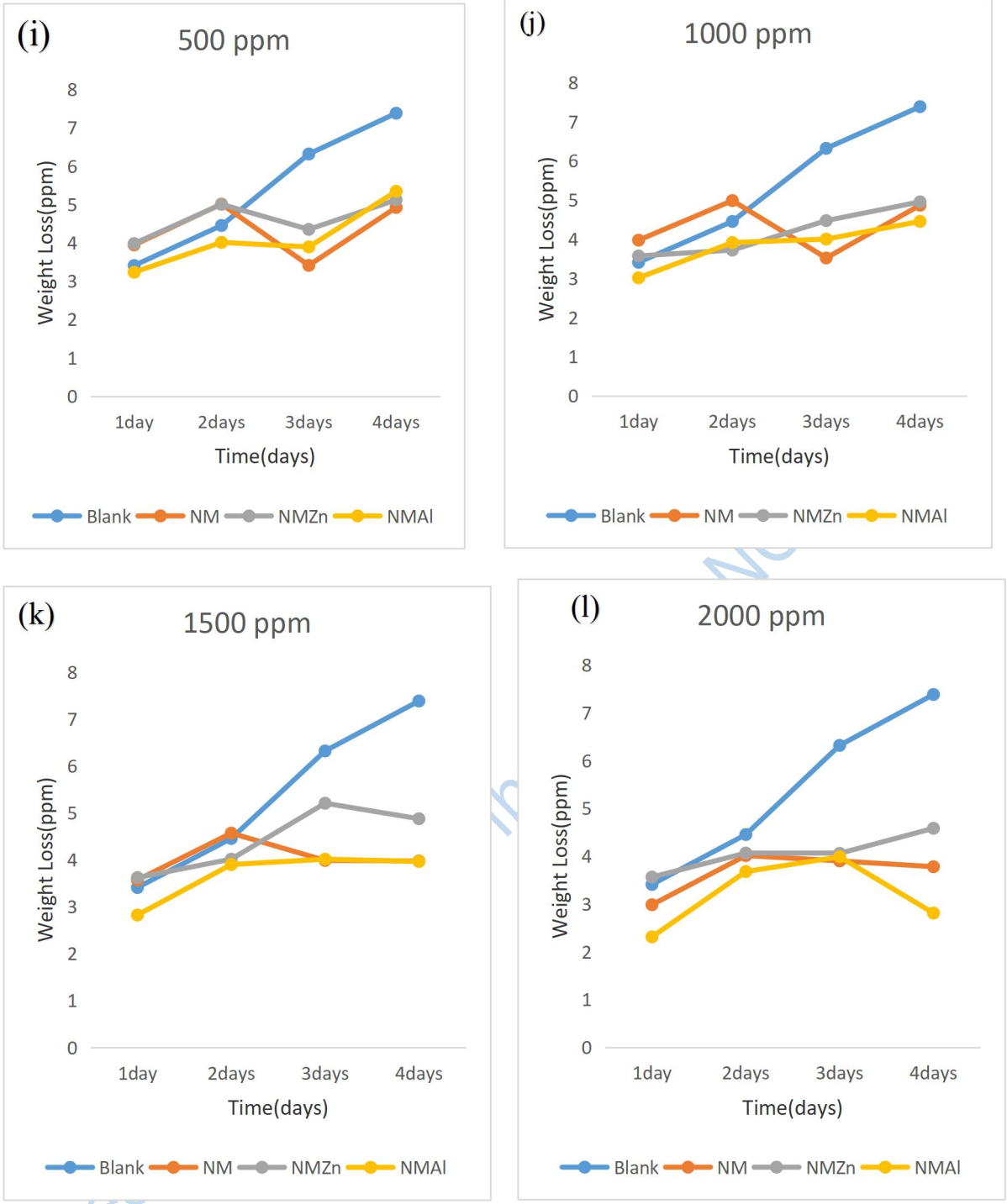

Figure 4.13 :The plots of Weight loss against time for (i) 500 ppm, (j) 1000 ppm,(k)1500 ppm and (l) 2000 ppm of *Adonida merrilli* extracts, NM-ZnONP and NM-AI_2O_3NP) Inhibitors concentration

Source: Author's Field Work 2025

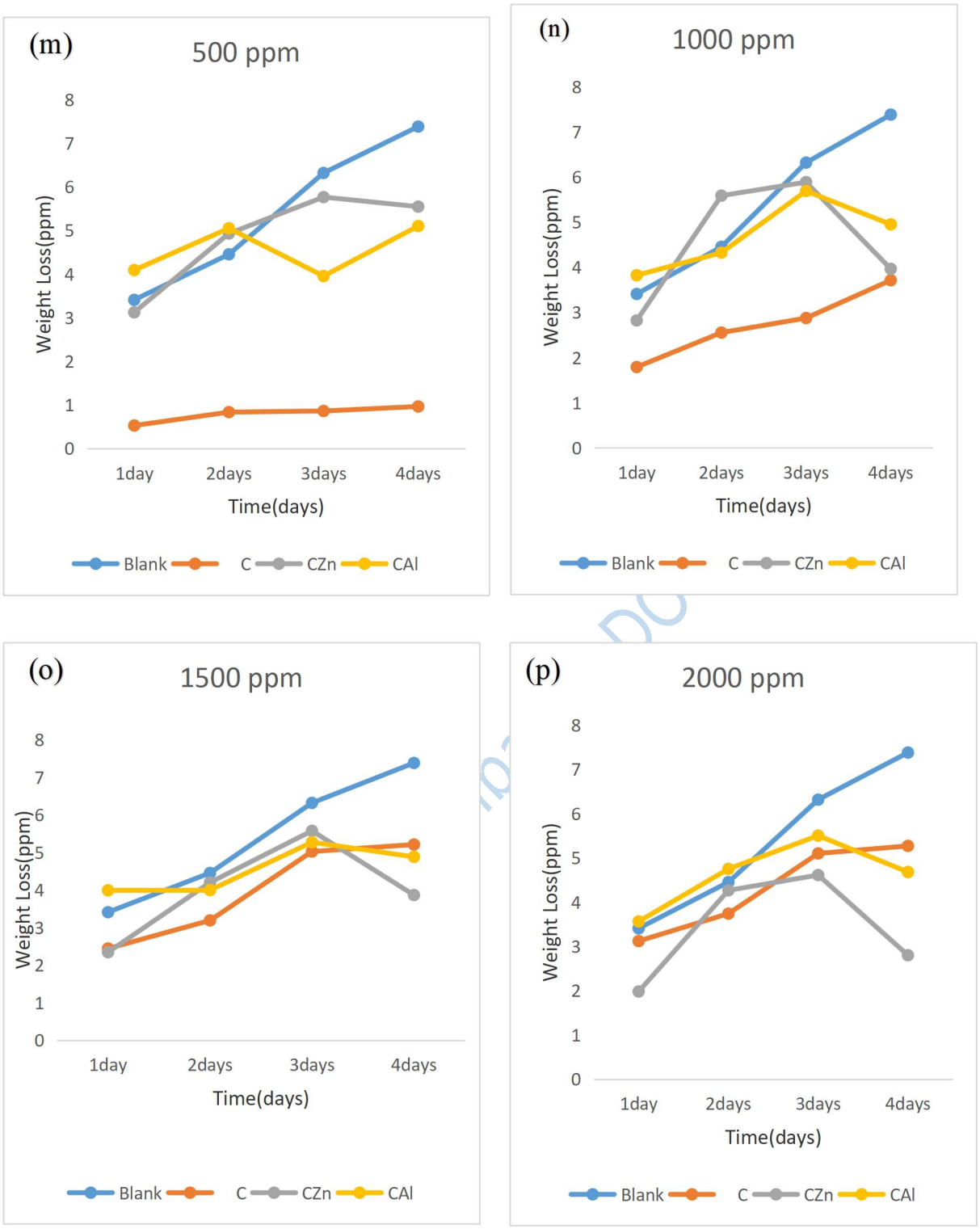

Figure 4.14 :The plots of Weight loss against time for (m) 500 ppm, (n) 1000 ppm,(o)1500 ppm and (p) 2000 ppm of (*Cassia javanica* extracts, C-ZnONP and C-AI_2O_3NP) Inhibitors Concentration.

Source: Author's Field Work 2025

4.3.1.2 Corrosion rate at Various Time against Concentration of Inhibitors

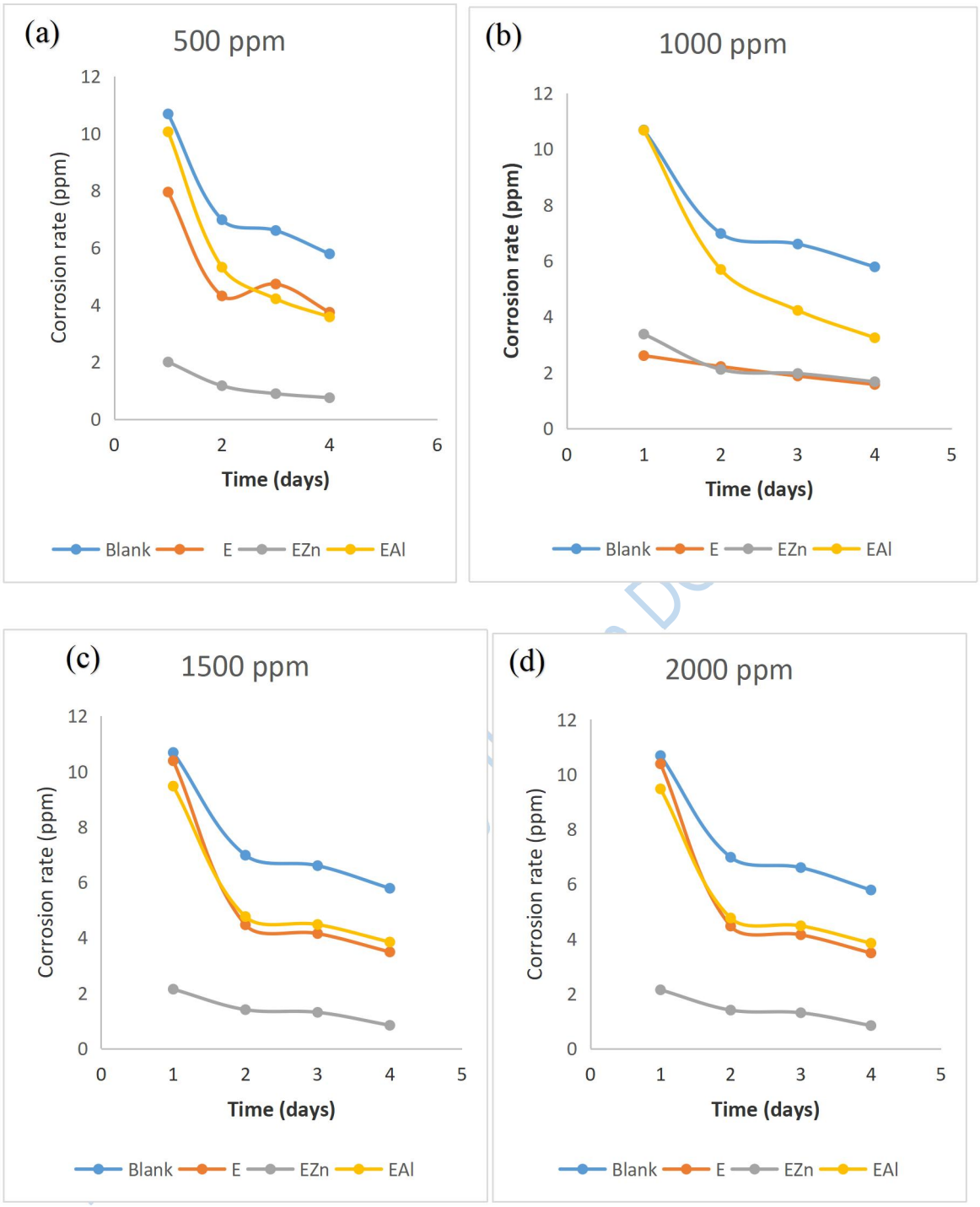

Figure 4.15 :The plots of Corrosion rate against time for (a) 500 ppm, (b) 1000 ppm,(c)1500 ppm and (d) 2000 ppm of (*Casuarina equisetifolia* extracts, E-ZnONP and E-AI_2O_3NP) Inhibitors Concentration

Source: Author's Field Work 2025

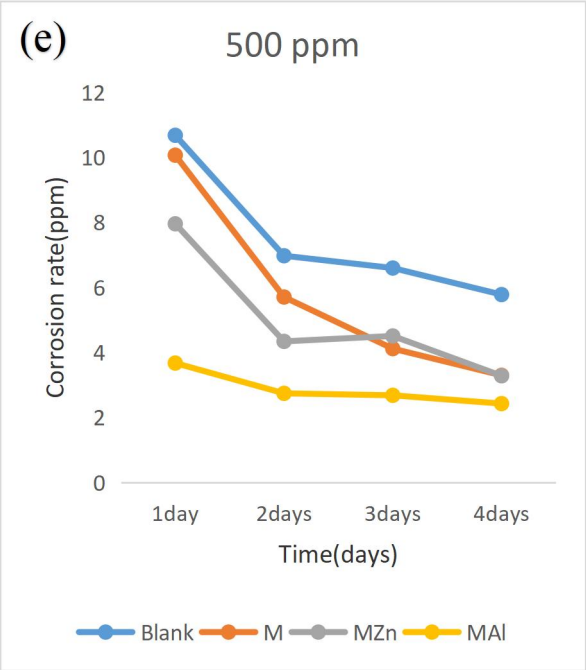

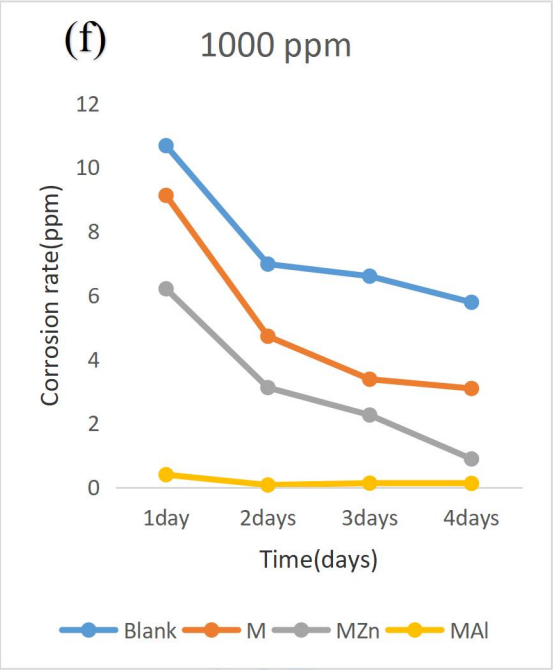

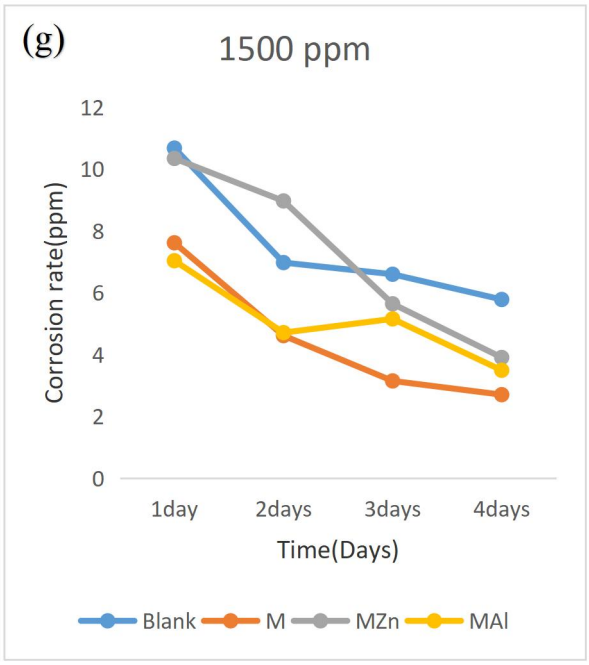

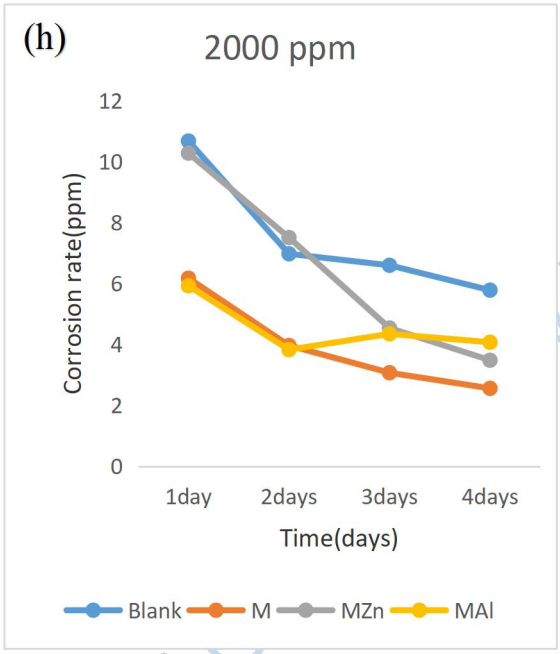

Figure 4.16 :The plots of Corrosion rate against time for (e) 500 ppm, (f) 1000 ppm,(g)1500 ppm and (h) 2000 ppm of *Washingtonia robusta* extracts, M-ZnONP and M-AI_2O_3NP) Inhibitors Concentration

Source: Author's Field Work 2025

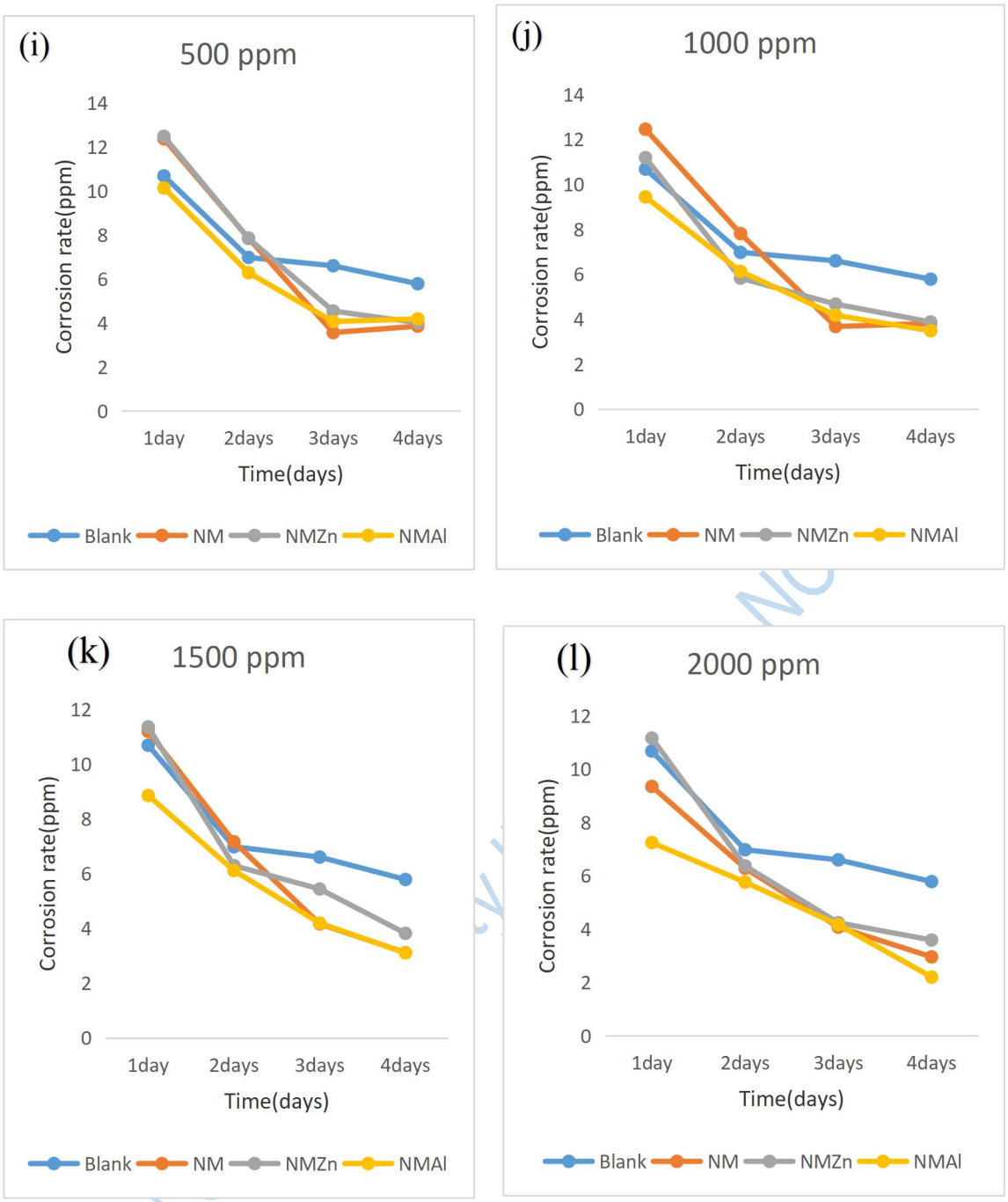

Figure 4.17 :The plots of Corrosion rate against time for (i) 500 ppm, (j) 1000 ppm,(k)1500 ppm and (l) 2000 ppm of (*Adonida merrilli* extracts, NM-ZnONP and NM-AI_2O_3NP) inhibitors Concentration

Source: Author's Field Work 2025

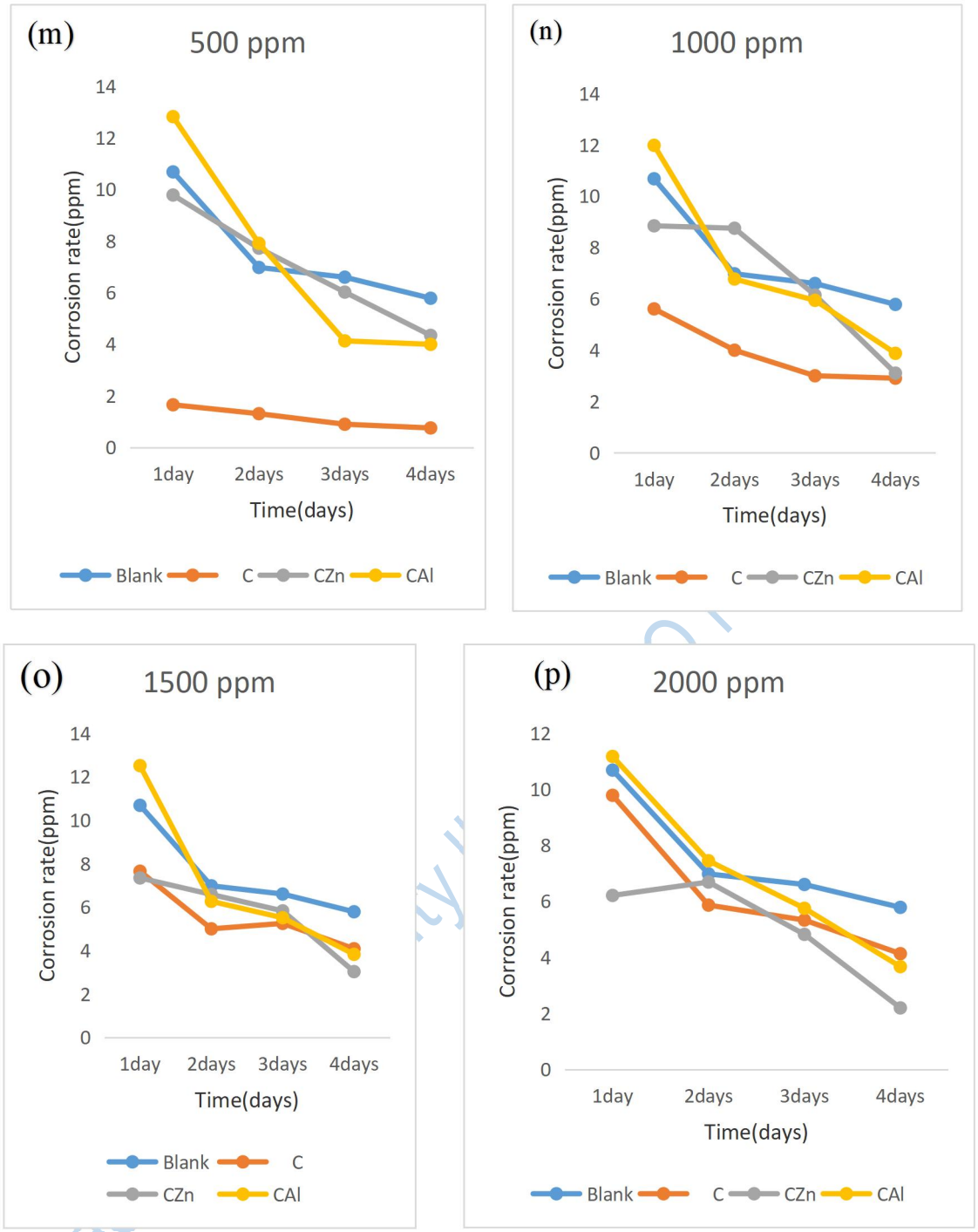

Figure 4.18 :The plots of Corrosion rate against time for (m) 500 ppm, (n) 1000 ppm,(o)1500 ppm and (p) 2000 ppm of *(Cassia javanica* extracts, C-ZnONP and C-AI_2O_3NP) Inhibitors Concentration

Source: Author's Field Work 2025

4.3.2 Electrochemical Method

The study examined the corrosion inhibition of extracts of *Casuarina equisetifolia, Cassia javanica, Adonida merrilli, and Washingtonia robusta*. The concentrations of zinc and aluminum nanoparticles of *Adonida merrilli, Washingtonia robusta, Cassia javanica, and Casuarina equisetifolia* were 500 ppm, 1000 ppm, 1500 ppm, and 2000 ppm, respectively, on mild steel at room temperature in 0.5 M H_2SO_4 were studied, See Appendix C for more details. The results were presented as curves, as seen in Figures 4.15 (a - l) [20].The corrosion current density (Icorr), corrosion potential (Ecorr), and cathodic and anodic potentiodynamic polarization plot slopes were the characteristics obtained from this curve.

A very effective and practical method for researching corrosion causes is polarization analysis. Polarization curve simplifies understanding of the anodic and cathodic reaction kinetics. A defined potential range and scan rate are used to collect the readings [21, 22]. The kinetics of corrosion processes may be measured with the use of polarization methods. The electrochemical parameters are calculated using the polarization method. The mechanism of the process—whether it be cathodic, anodic, or combined cathodic and anodic reactions—will decide the Tafel slope, and the Ecorr value will specify the kind of inhibitor being employed. The Potentiodynamic polarization plots, Figures 4.15 (a - l) have shown that when the extracts concentration increased to 500 ppm, 1000 ppm, 1500 ppm, and 2000 ppm, respectively, the current potential values went closer to the positive values. Current rises in tandem with potential differences. Current density from both the cathodic and anodic sides dropped as the inhibitor's concentration rose. They fall under mixed inhibitors because they inhibit both cathodic and anodic inhibitors. One can classify an inhibitor as anodic or cathodic if its concentration shifts to more than 0.85 mV.But Figure 4.15 (j) did not [22, 23].

From the comprehensive study of all the inhibitors, it was found that E-ZnONP, figure 4.3.2 (b) performed the best. This result aligns with aqueous *Chrysophyllum albidum* leaves and peels extract on mild steel in an acidic medium [20].This was evident in the potentiodynamic polarization plots, where its potential difference value shifted more towards the positive zone

than any other inhibitor. The inhibitor's mixed type was further confirmed by the potentiodynamic polarization plots, which showed that the anodic and cathodic zones were of equal length and did not differ from one another. The value of the inhibitor did not exceed 0.85 mV, and as its concentration increased, the current potential values shifted more toward the positive range. This comprehensive study of the inhibitors and their performance in the potentiodynamic polarization plots provides a clear understanding of their effectiveness and these findings are consistent with the corrosion results of aqueous *Chrysophyllum albidum* leaf and peel extracts on mild steel in an acidic medium [20], the corrosion inhibition effects of *Euphorbia heterophylla* L. extract in 1.5 M HCl [21], the inhibition of mild steel corrosion by a nonanedioic acid derivative in hydrochloric acid solution [22], and the corrosion protection performance of *acarbose* on mild steel in an acidic medium [24].

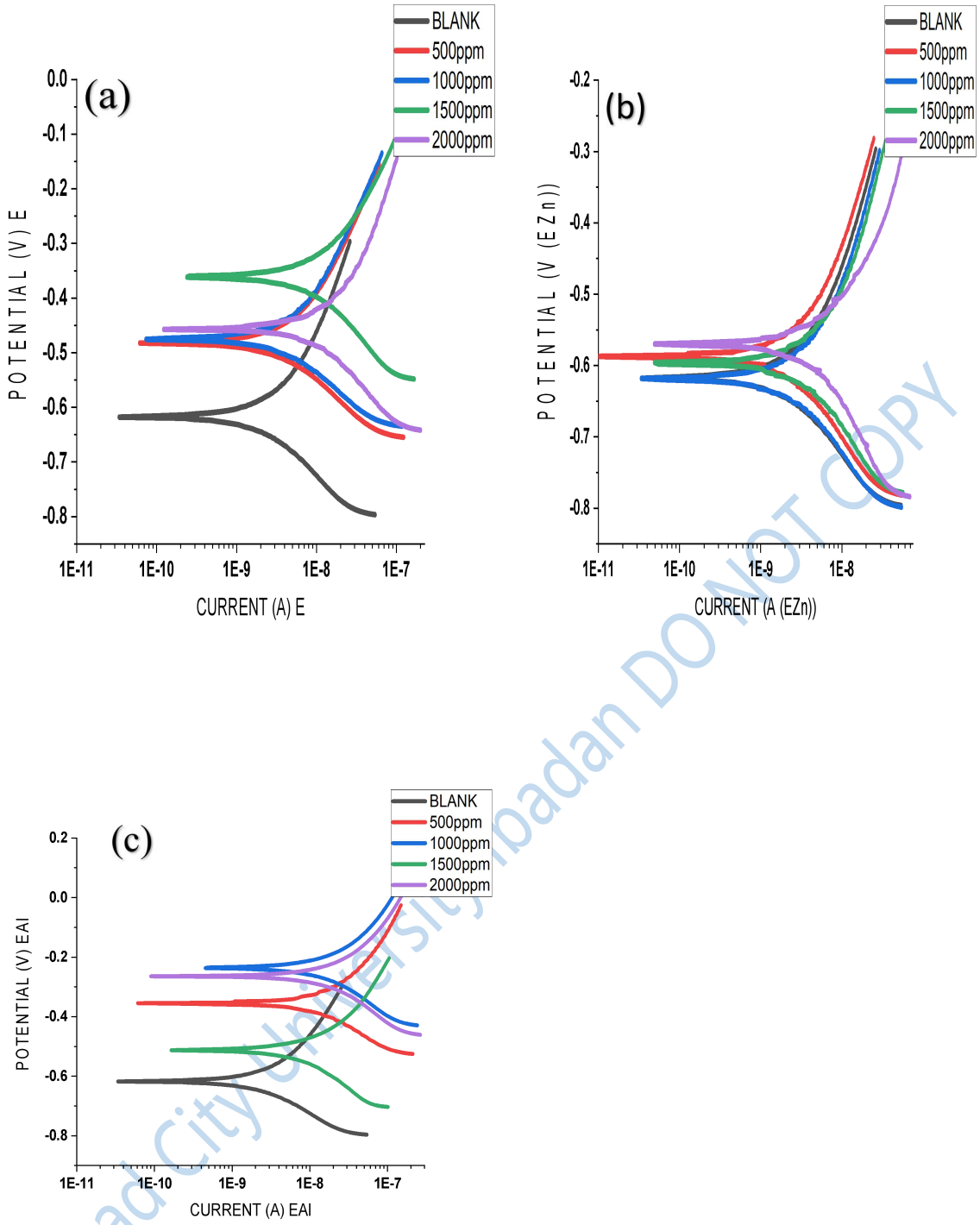

Figure 4.19: Potentiodynamic Polarization Plot of (a) *Casuarina equisetifolia* (E), (b) E-ZnONP (c) E-AI_2O_3NP

Source: Author's Field Work 2025

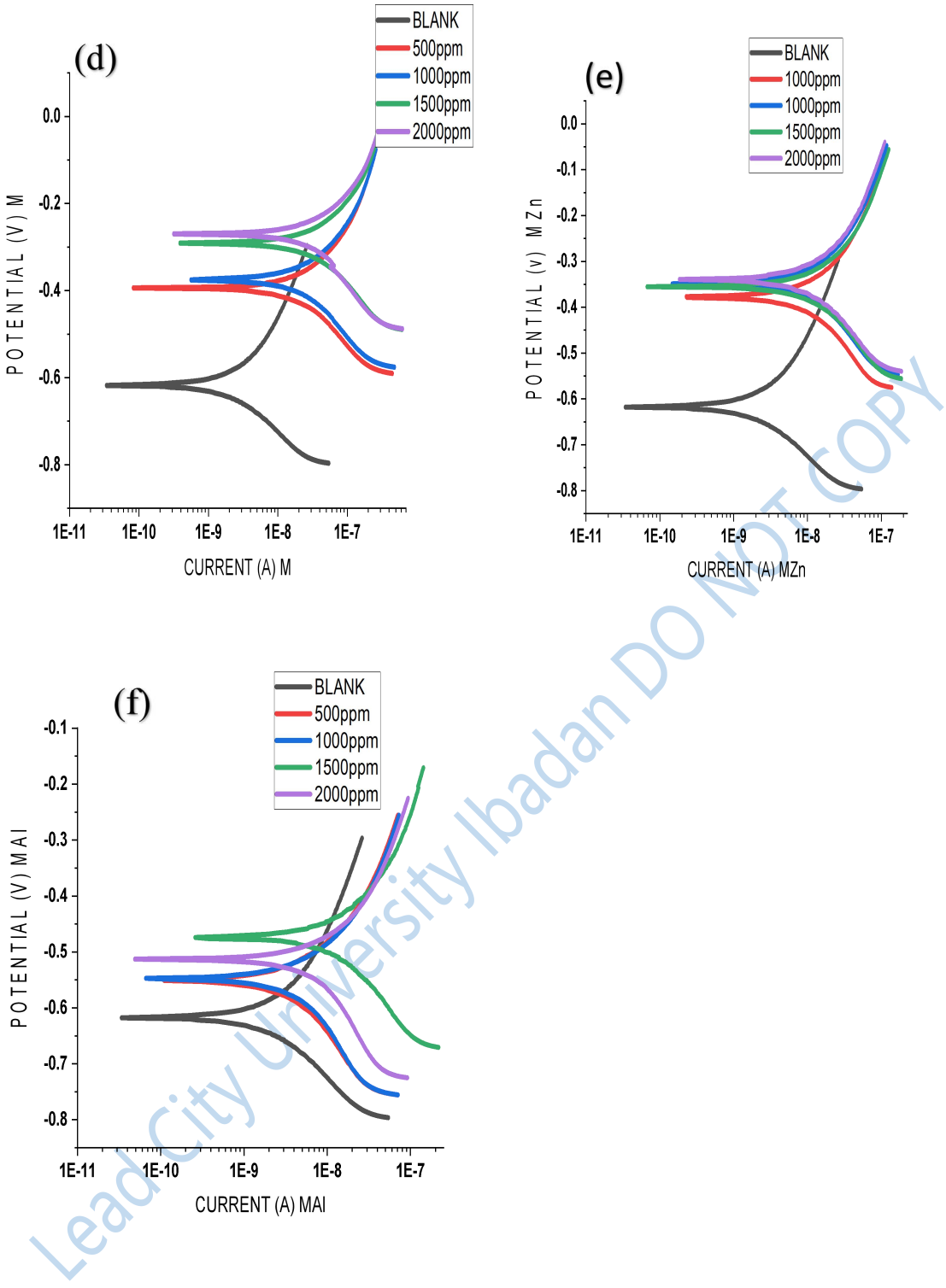

Figure 4.20: Potentiodynamic Polarization Plot of (d) *Washingtonia robusta* (C), (e) M-ZnONP (f) M-AI_2O_3NP

Source: Author's Field Work 2025

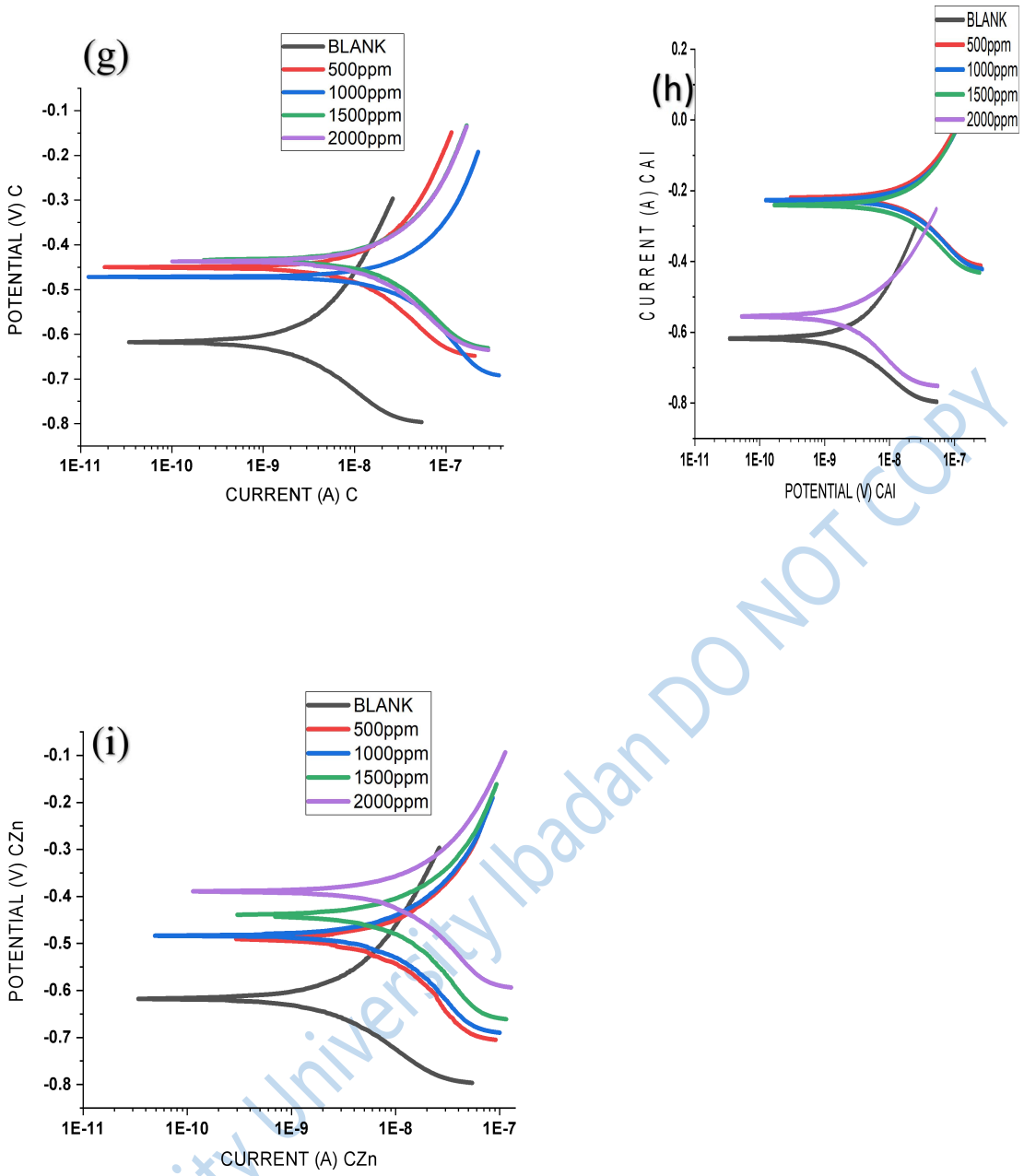

Figure 4.21: Potentiodynamic Polarization Plot of (g) *Cassia javanica* (C), (h) C-AI_2O_3NP (i) C-ZnONP

Source: Author's Field Work 2025

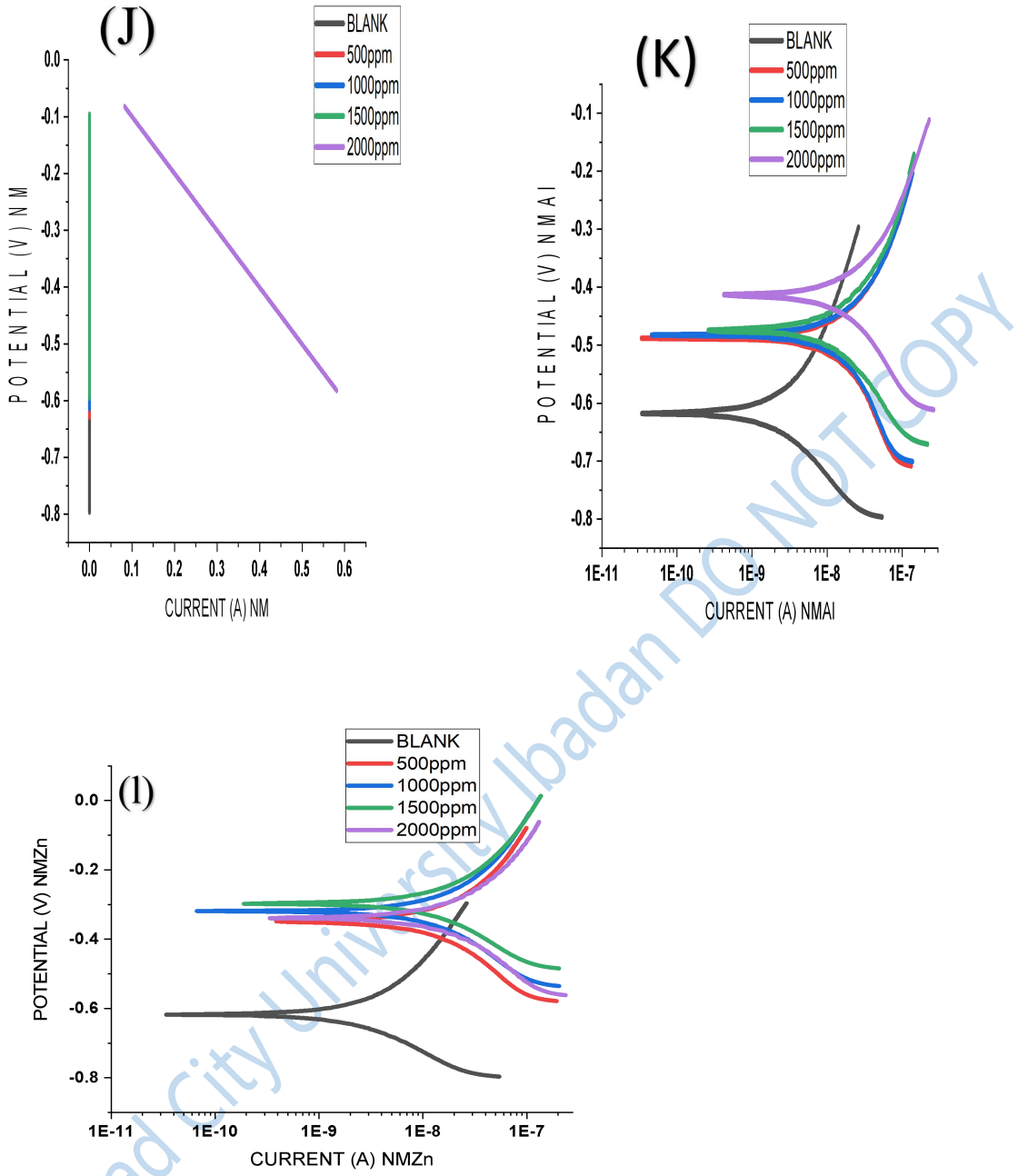

Figure 4.22: Potentiodynamic Polarization Plot of (j) *Adonida merrilli* (NM), (k) NM-AI_2O_3NP (l) NM-ZnONP

Source: Author's Field Work 2025

4.3.2.1 Inhibitors Efficiency (%) of Potentiodynamic Polarization Measurement of Corrosion Inhibition of Extracts *Casuarina equisetifolia, Cassia javanica, Adonida merrilli, and Washingtonia robusta* and their Zinc Oxide Nanoparticles and Aluminum Oxide Nanoparticles.

According to the Figure 4.16 (a) The best inhibition efficiency of these extracts concentration is 500 ppm of (C) *Cassia javanica* extract while the least efficient is (M) *Washingtonia robusta*

Refering to the Figure 4.16 (b), the least efficient zinc oxide nanoparticles are the synthesis from *Adonida merrilli*, while the best inhibition efficiency of this zinc oxide nanoparticles concentration is 500 ppm to 2000 ppm of (E-ZnONP) synthesis from extract leaf of *Casuarina equisetifolia*.

Based on Figure 4.16 (c),The best inhibition efficiency among aluminum oxide nanoparticles is M-Al_2O_3NP. In contrast, the least efficient aluminum oxide nanoparticles are NM-Al_2O_3NPs.

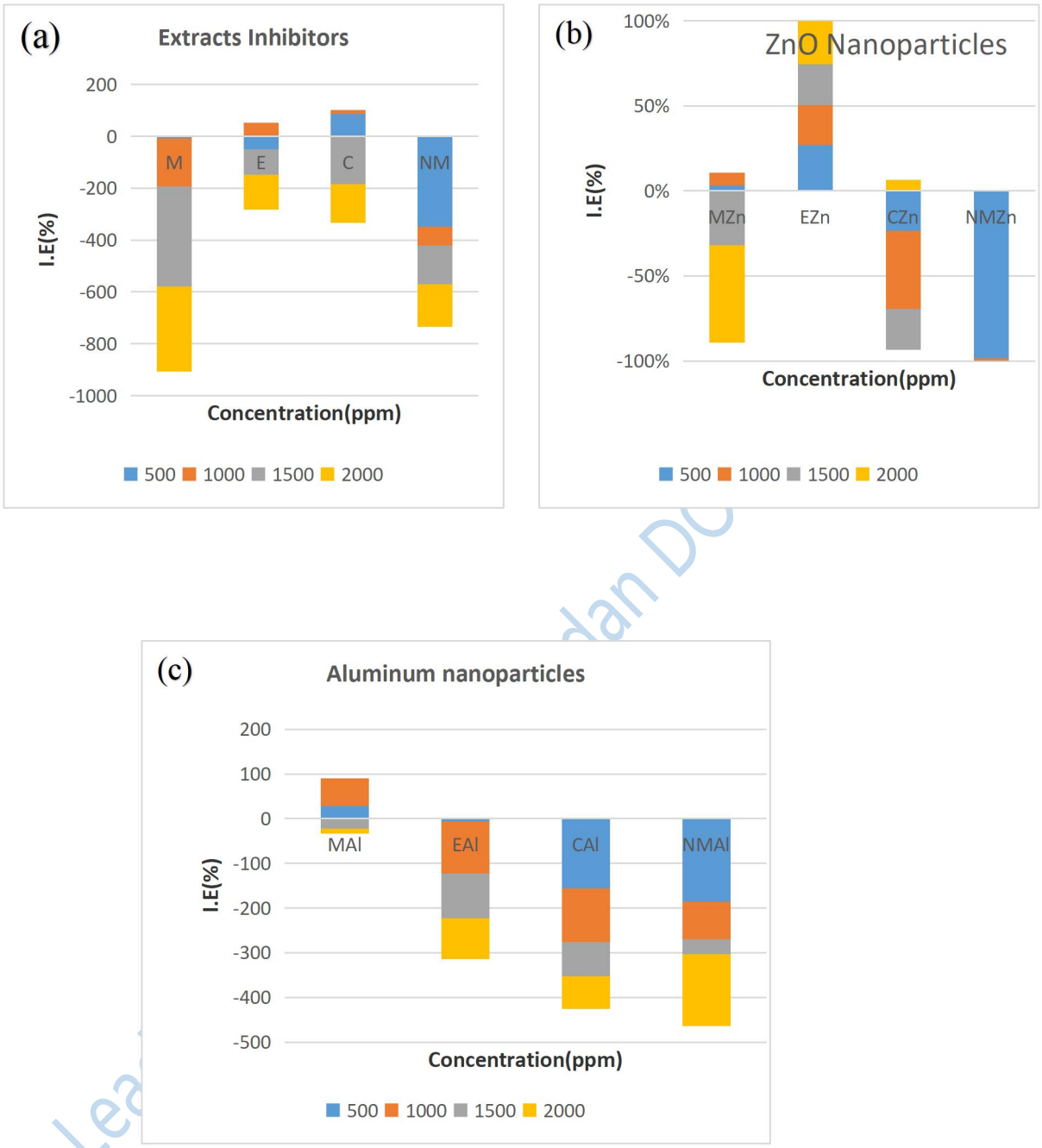

Figure 4.23 : Inhibitors Efficiency (%) of (a) Extracts (b) ZnONPs (c) Al_2O_3NPs

Source: Author's Field Work 2025

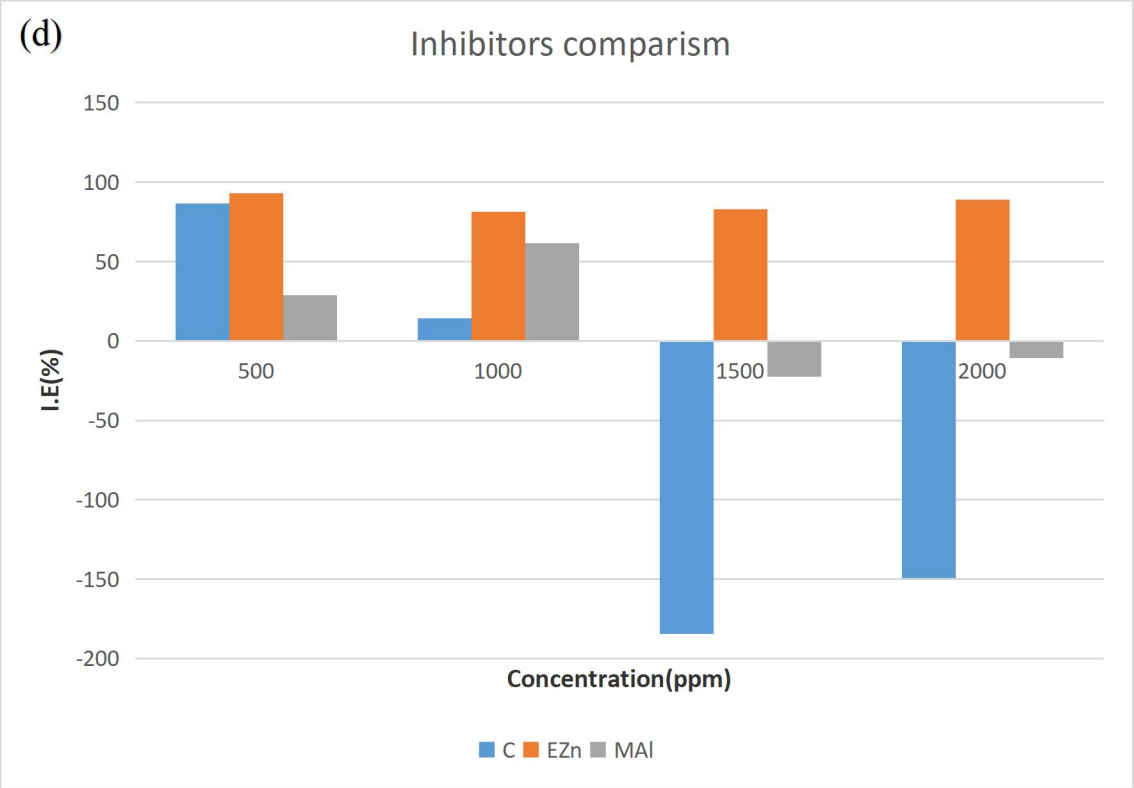

Figure 4.24 (d): Inhibitors Efficiency (%) of Selective Best Inhibitors

Source: Author's Field Work 2025

4.3.3 Morphological Study (SEM) for Surface Analysis

The surface morphology of the steel microstructures was analyzed by SEM. This provides detailed, high-resolution, accurate photographs of the sample which can be used to monitor the process [20]. SEM can be used to confirm the formation of a protective layer of inhibitor on the surface of metal [1, 20, 23] . SEM micrographs show details of rough and damaged surfaces of the metal in the absence of an inhibitor and smoother in the presence of inhibitor [21]. In the absence of an inhibitor, the roughness is due to a high rate of corrosion and uncontrolled dissolution [24, 25, 26]. This technique gives only qualitative information

Mild steel surface exposed to the corrosive media, 0.5 M of H_2SO_4 was severely corroded, very rough, and non-uniform. Figure 4.17 (a) shows the significant corrosion damage done to the steel surface. The surface of mild steel immersed in inhibitors is significantly improved and shows a smoother surface with scratches left behind when compared with the one without inhibitors, Figures 4.17 (b) and (d) but Figure 4.17 (c) showed little corrosion damage.

When the mild steel surface without inhibitors is compared to that submerged in inhibitors, the differences in surface morphologies are striking. The steel with inhibitors exhibits a noticeably better surface, with scratches left behind, and most importantly, no evident corrosion damage, except for in Figure 4.17 (d). This stark contrast underscores the significant impact of inhibitors on steel surfaces. These results align with the previous study on ethanolic extract of *Chrysophyllum albidum* leaves and peels as a green inhibitor for AISI 1015 carbon steel in 1M H_2SO_4 solution [1],and aqueous *Chrysophyllum albidum* leaves and peels extract on mild steel in acidic medium [20] .

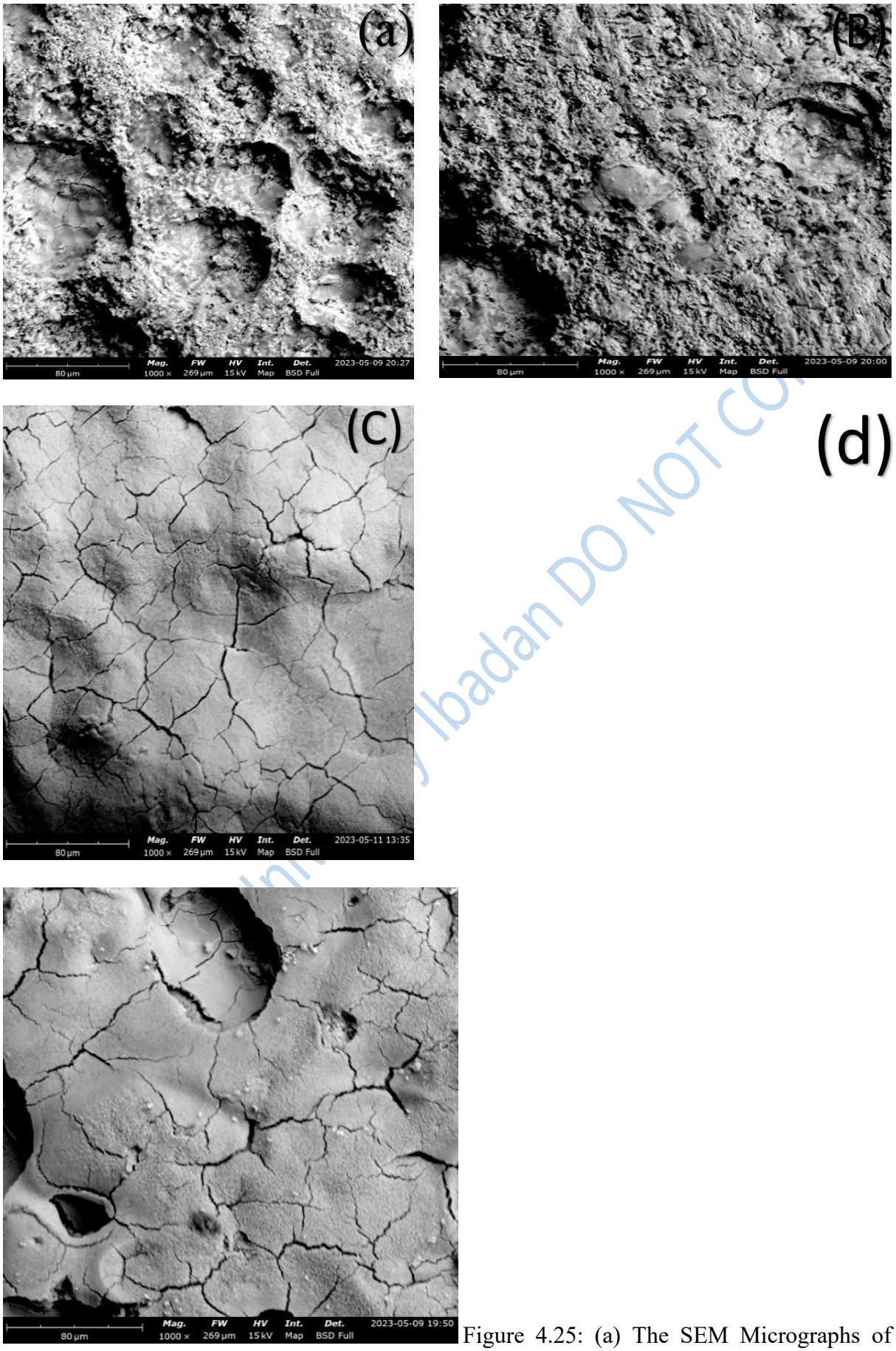

Figure 4.25: (a) The SEM Micrographs of Untreated Mild Steel (b) SEM micrographs of Mild Steel Treated with Extracts C (c) The

SEM micrographs of mild steel treated with E-ZnONP (d):The SEM Micrographs of Mild Steel treated with M-Al_2O_3NP

Source: Author's Field Work 2025

4.3.4 Adsorption Isotherm

If we want to know more detail about the corrosion process, then we need to study adsorption isotherm. We can get the idea about the equilibrium between inhibitor adsorbed and present in the bulk with the help of adsorption isotherm [20]. Adsorption isotherms are one of the key factors to describe the interaction between sample and inhibitor. Adsorption is confirmed if surface coverage data fitted in any isotherm. Various adsorption isotherm models can be used to get important details based on inhibitor molecules adsorption on the MS surface and as the linear regression coefficient is close to one, the Langmuir isotherm was considered appropriate to describe the inhibitor molecules' adsorption on the Mild steel surface [20, 21]

The adsorption isotherms of different extracts are shown on Figures 4.18 (a) - 4.18 (d) below using the Langmuir adsorption isotherms. They were determined to provide information on the interaction among the adsorbed molecules on the surface. The surface coverage was fitted to a series of different Langmuir isotherm adsorption.

Langmuir Adsorption Isotherm Equation

$$\frac{C}{\theta} = \frac{1}{kads} + C$$

C = concentration of inhibitor (mol/L or g/L) θ = surface coverage

Kads = adsorption constant

The Langmuir adsorption isotherm was observed to be the best adsorption characteristics. The plotting values of log $\frac{C}{\theta}$ versus log C shows a straight line graph with the correlation regression coefficient, R^2 = 0.99 for E-ZnONP, R^2 = 0.87 for M-Al_2O_3NP, R^2 = 0.21 for C, R^2 = 0.3976 for E. The Langmuir isotherm, best explaining the relationship between the molecules and the mild steel. The Figures indicated the interaction between the adsorbed extract molecules and the metal surface. These R^2 values revealed that the molecules of the extracts adsorbed and interact with the surface of the steel, thus reducing the ingression of ions into the acidic medium [26, 27] . It is significant to note that the degree of coverage depends on the concentration of inhibitors. According to the Langmuir isotherm, this assumption can only be accepted as a first approximation [20].The best results out of the figures above are R^2 = 0.99 for E-ZnONP and R^2 = 0.87 for M-Al_2O_3NP while R^2 = 0.21 for C and R^2 = 0.39 for E are not.

These results are consistent with findings from previous studies on the kinetics and thermodynamics of glycyrrhizic acid adsorption using S-8 macroporous resin [26], the adsorption and thermodynamic investigation of mild steel corrosion inhibition in an H_2SO_4 medium using *Vernonia amygdalina* [27], and the facile one-pot synthesis of Ag@MOF(Ag) nanocomposites for the highly selective detection of 2,4,6-trinitrophenol in an aqueous phase [28].

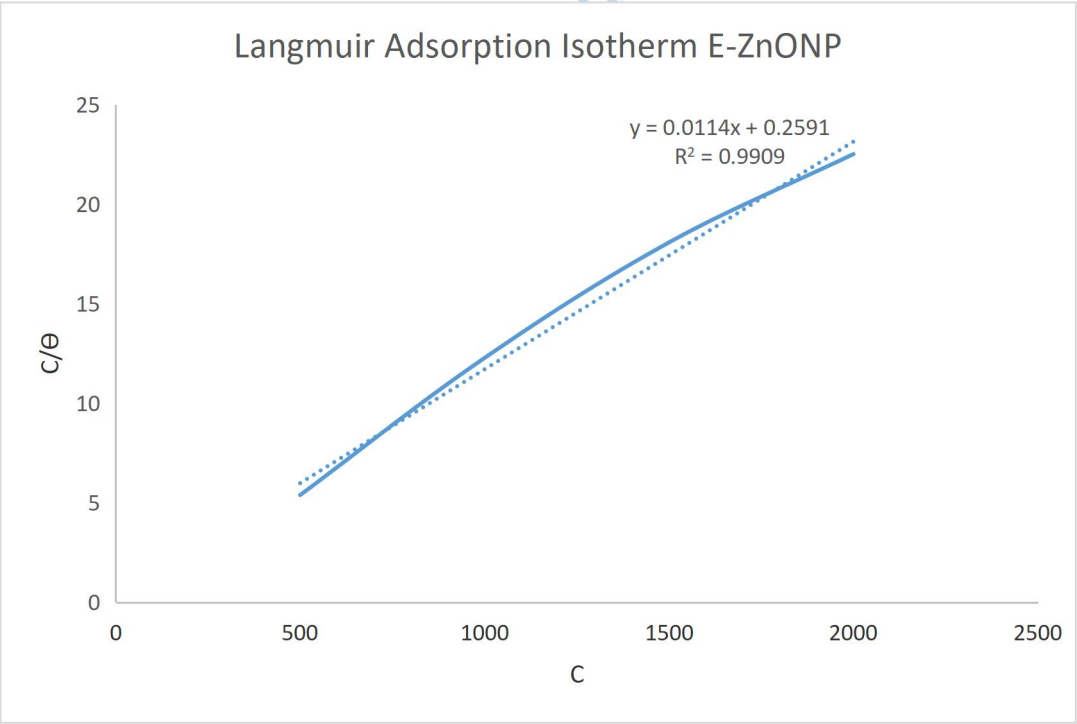

Figure 4.26: Langmuir Adsorption Isotherm of E-ZnONP

Source: Author's Field Work 2025

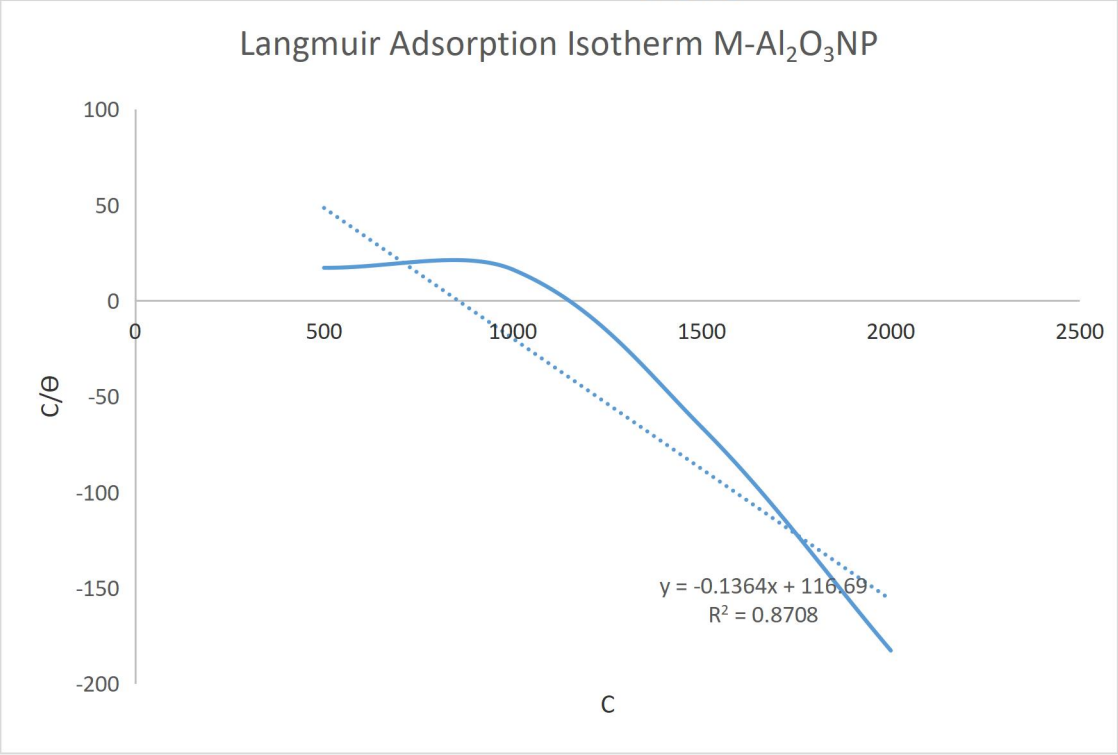

Figure 4.27 : Langmuir Adsorption Isotherm of M- Al_2O_3NP

Source: Author's Field Work 2025

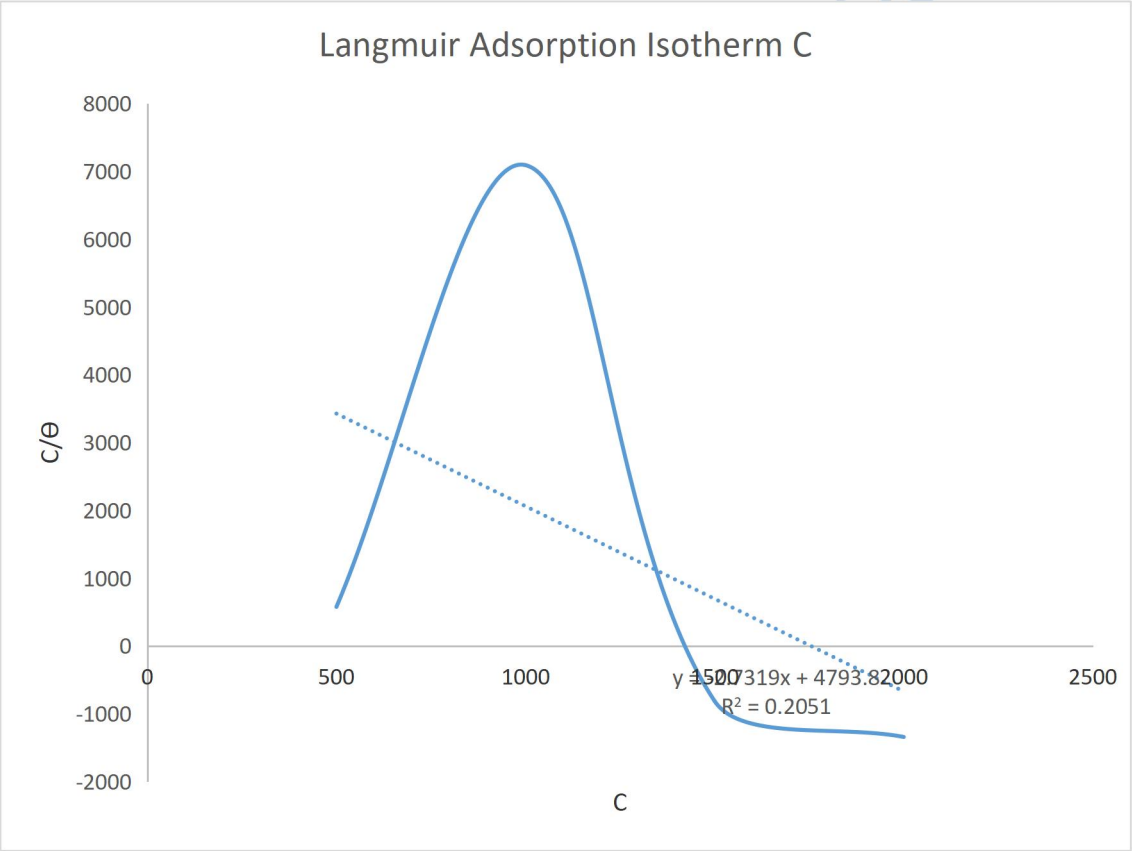

Figure 4.28: Langmuir Adsorption Isotherm of C

Source: Author's Field Work 2025

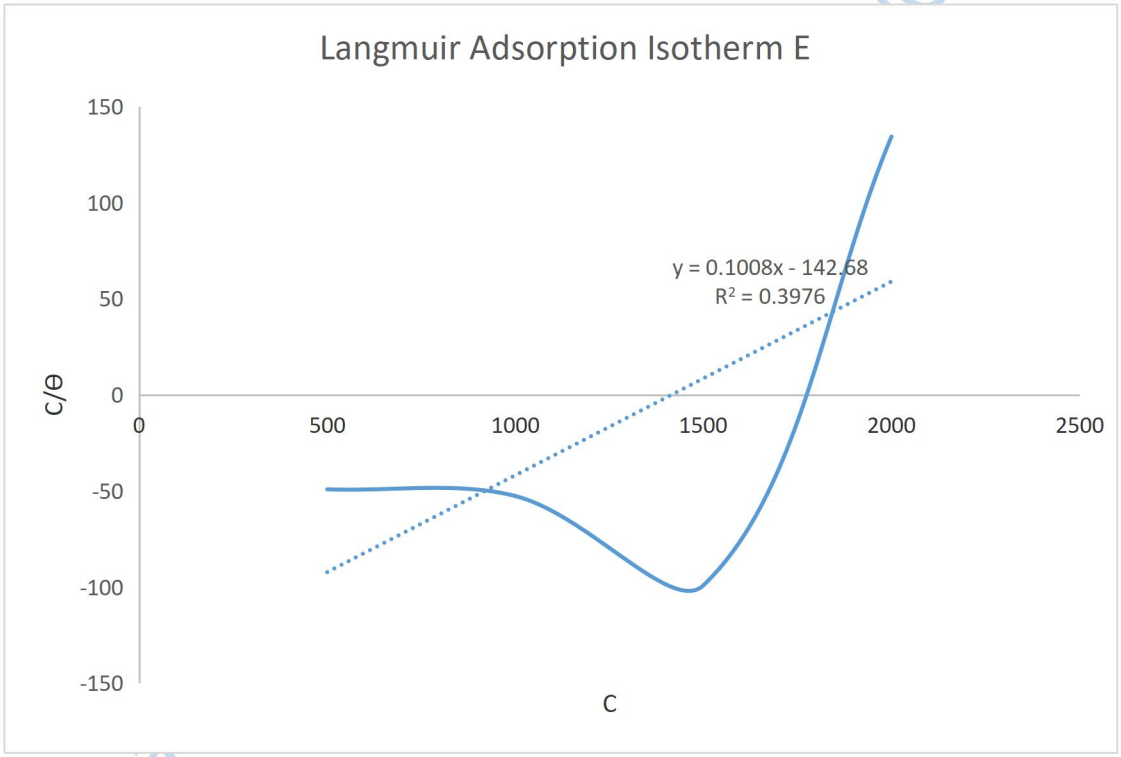

Figure 4.29: Langmuir Adsorption Isotherm of E**.**

Source: Author's Field Work 2025

4.3.5. Properties of Inhibition of Nanoparticles on Metal Surface

The thermodynamic properties of corrosion are covered in this section. Thermodynamics clarifies the energy shifts that take place during corrosion processes. It enhances our understanding of the mechanics behind the processes of corrosion. Thermodynamics evaluates the stability of chemical species and their interactions with metal surfaces to estimate the probability of corrosion. We can predict if corrosion will occur under specific conditions by examining the thermodynamic characteristics. In summary, thermodynamics provides essential information for evaluating corrosion behavior and explains the energy components of corrosion. Using the Langmuir adsorption isotherm, we will start by discussing the concepts of Gibbs free energy, adsorption equilibrium constant, etc.

In Table 4.7, E-ZnONPs, when zinc oxide nanoparticles are synthesized from *Casuarina equisetifolia* leaf extract, the Kads value of 124.3897233 mol^{-1} indicates that inhibitor molecules are adsorbed on to the metal surface with strength and efficiency, thus preventing corrosion. ΔGads = -22.27273061 (kJ/mol^{-1}) denotes a negative adsorption process. Gibbs-free is spontaneous and energetically advantageous, Gibbs-free energy significantly reduces corrosion. It implies that there is a strong bond between the metal and the adsorbate, providing significant corrosion resistance. A good correlation coefficient (RSQ) of 0.98 in corrosion adsorption suggests that both the observed data and the model accurately depict the adsorption process, making them potentially useful for predicting future behavior.

While the synthesis of M-Al_2O_3NPs, which refers to Aluminum nanoparticles from *Washingtonia robusta*, displays these: Kads in this case is 0.858570488 mol^{-1}. This value is positive for the corrosion inhibition's efficacy, which refers to the effectiveness of the

inhibitor in preventing corrosion, since it shows that the inhibitor's adsorption is rather strong and that the process is likely going to be beneficial. ΔGads - 9.74 (kJ/mol^{-1}) is a spontaneous, energetically advantageous adsorption process that has a negative Gibbs free energy and reduces corrosion. It demonstrates the robust connection between the metal and the adsorbate, which stops corrosion. 0.870189342 is the RSQ. In this instance, a high R-squared value is ideal as it indicates that the model has good predictive ability and that the independent variables are important predictors of the corrosion adsorption process.

Table 4.7: Properties of Inhibition of Nanoparticles on Metal Surface

Inhibitors	$K_{ads}(mol^{-1})$	ΔG_{ads} (kJ/mol^{-1})	RSQ
M- Al_2O_3NP	0.858570488	-9.735457952	0.870189342
E-ZnONP	124.3897233	-22.27273061	0.978289153

4.4. Antimicrobial Study of Plant Extracts and Nanoparticles

Antibacterial properties using the agar-well-diffusion method, extracts from *Adonida merrilli, Washingtonia robusta, Cassia javanica, and Casuarina equisetifolia,* as well as their ZnONPs and Al_2O_3NPs, were tested for antimicrobial sensitivity in vitro against four different species [27]. Test organisms were injected into the medium. Following a 24-hour incubation period, the zones of inhibition (ZI) in millimeters were measured and appropriately documented, as indicated in Table 4.8.

These nanoparticles C-ZnONP, E-ZnONP, M-ZnONP, and NM-ZnONP inhibited the growth of *S. aureus* effectively with ZI ranging from 30.00 mm for E-ZnONP, 34.00 mm for C-ZnONP, 36.00 mm for M-ZnONP to 40.00 mm for NM-ZnONP while ZI of Ofloxacin against the same organism was 30.00 mm. Ofloxacin is an antibacterial agent of the Fluoroquinolone group. It is useful against gram-positive and gram-negative organisms. It is also used as an additional agent in the treatment of multidrug resistance tuberculosis. Ofloxacin is used to treat bacterial infections of the skin, lungs, prostate, or urinary tract (bladder and kidneys). Ofloxacin is also used to treat pelvic inflammatory disease and Chlamydia and/or gonorrhea. These nanoparticles E-ZnONP, M-ZnONP, C-ZnONP, and NM-ZnONP inhibited the growth of *Pseudomonas aeruginosa* effectively with ZI ranging from 20.00 mm for C-Al_2O_3NP, 22 mm for M-Al_2O_3NP, 23.00 mm for NM-Al_2O_3NP, 30.00 mm for E-ZnONP, 36.00 mm for NM-ZnONP, 38.00 mm for M-ZnONP to 40.00 mm for C-ZnONP while ZI of Ofloxacin against the same organism was 26.00 mm. The antimicrobial activity against *Pseudomonas aeruginosa* revealed that C-ZnONP had the largest ZI of 40.00 mm, while the least growth inhibitor was C-Al_2O_3NP with ZI of 20.00 mm. The antimicrobial activity against *Salmonella* revealed that M-ZnNP had the largest ZI of 36.00 mm while the least growth inhibitor was E-ZnONP and NM-ZnONP with ZI of 30.00 mm. The

antimicrobial activity against *Escherichia coli* showed that M-ZnONP and NM-ZnONP revealed 30.00 mm and 32.00 mm, respectively, C-ZnONP was 19.00 mm, C-Al_2O_3NP was 22.00 mm, E-ZnONP was 18.00 mm, NM.- Al_2O_3NP was 21.00 mm, M-Al_2O_3NP was 19.00 mm [29, 30]

Nevertheless, noticeable activities were observed during the screening against *Staphylococcus aureus, Escherichia coli, Pseudomonas aeruginosa, and Salmonella*. The in vitro screening of the samples showed that all (C-ZnONP, E-ZnONP, M-ZnONP, and NM-ZnONP) Zinc Oxide nanoparticles were probably more active than Ofloxacin. Overall, it exhibited the highest level of activity among the strains of Gram-positive and Gram-negative bacteria tested in this investigation.

Table 4.8: The Zones of Inhibition of Plant Extracts and their ZnONP and Al_2O_3 Nanoparticles.

	Organisms used and ZI (mm)			
Sample Code	*Staphylococcus aureus*	*Escherichia coli*	*Pseudomonas aeruginosa*	*Salmonella typhi*
1 C	0.00	0.00	0.00	0.00
2 C-ZnONP	34.00	19.00	40.00	32.00
3 C- Al_2O_3NP	21.00	22.00	20.00	0.00
4 E	0.00	0.00	0.00	0.00
5 E-ZnONP	30.00	18.00	30.00	30.00
6 E- Al_2O_3NP	0.00	0.00	0.00	0.00
7 M	0.00	0.00	0.00	0.00
8 M-ZnONP	36.00	30.00	38.00	36.00
9 M- Al_2O_3NP	25.00	19.00	22.00	0.00
10 NM	0.00	0.00	0.00	0.00
11 NM-ZnONP	40.00	32.00	36.00	30.00
12 NMAl_2O_3NP	20.00	21.00	23.00	0.00

Control for *Staphylococcus aureus (30.00), Escherichia coli (28.00), Pseudomonas aeruginosa (26), and Salmonella typhi (28) is Ofloxacin.*

Source: Author's Field Work 2025

Based on the broad activity spectrum noticed during the antibacterial screening, MIC of the different types of extracts and nanoparticles was carried out against the four organisms using serial dilution method [29], [32] with varying concentrations from 250 to 1.95 (mg/mL) as shown in Table 4.9.The most effective nanoparticles that give best result are M-ZnONP and NM-ZnONP which inhibited *Staphylococcus aureus* at MIC value of 1.95 (mg/mL), and *Pseudomonas aeruginosa* at MIC value of 3.90 mg/mL.

Thus, zinc oxide nanoparticles synthesized herein could pave the way for new drug development to combat infectious diseases caused by *Staphylococcus aureus* and *Pseudomonas aeruginosa.* These extracts (C, E, M, and N.M.) and aluminum nanoparticles E-Al_2O_3NP could not inhibit the growth of *Staphylococcus aureus, Escherichia coli, Pseudomonas aeruginosa and Salmonella* [29].

Based on the result of visual screening of MIC values across the gram-positive and Gram-negative organisms used here in, C-ZnONP, M-ZnONP, NM-ZnONP, and E-ZnONP emerged as the most potent antimicrobial agent with MIC, But NM-ZnONP emerged as best when compared with others samples used in this study. *Staphylococcus aureus,* NM-ZnONP (1.95 mm), *Escherichia coli* NM-ZnONP (7.81 mm), *Pseudomonas aeruginosa* NM-ZnONP (3.90 mm) while NM-ZnONP and C-ZnONP exhibited 7.81 mm for *Salmonella*. Therefore, it is a valuable endeavor to research the cytotoxicity profile of these compounds in order to better -harness and identify their potential for future innovative medication development. This is necessary, particularly in light of the current drug resistance issue, which has developed into a potent weapon for threats to world health and an unfavorable pathway for high rates of death in both humans and animals [29, 30, 31].

Over the previous 20 years, there has been a rise in S. aureus infections that are both hospital-acquired and related to the community. The skin and soft tissue (impetigo) infection, scalded skin syndrome (Ritter disease), folliculitis, furuncle, bone infections (osteomyelitis) in children [29], septic arthritis, toxic shock syndrome, thrombophlebitis, deep tissue abscess, and

infection are among the types and presentations of S. aureus infection, which consequently results in a high mortality rate [29, 31, 32, 33].

Table 4.9 The Minimum Inhibitory Concentration (MIC) of Plant Extracts and their ZnONP and Al_2O_3-Nanoparticles.

	Organisms used and (MIC) (mg/mL).			
Sample Code	***Staphylococcus aureus***	***Escherichia coli***	***Pseudomonas aeruginosa***	***Salmonella typhi***
1 C	-	-	-	-
2 C-ZnONP	31.25	-	7.81	7.81
3 C-Al_2O_3NP	-	-	-	-
4 E	-	-	-	-
5 E-ZnONP	31.25	-	31.25	31.25
6 E-Al_2O_3NP	-	-	-	-
7 M	-	-	-	-
8 M-ZnONP	125.00	250.00	62.50	31.25
9 M-Al_2O_3NP	-	-	-	-
10 NM	-	-	-	-
11 NM-ZnONP	1.95	7.81	3.90	7.81
12NM-Al_2O_3NP	-	-	-	-

Source: Author's Field Work 2025

4.4.1 Microbial Plates of *Staphylococcus aureu*

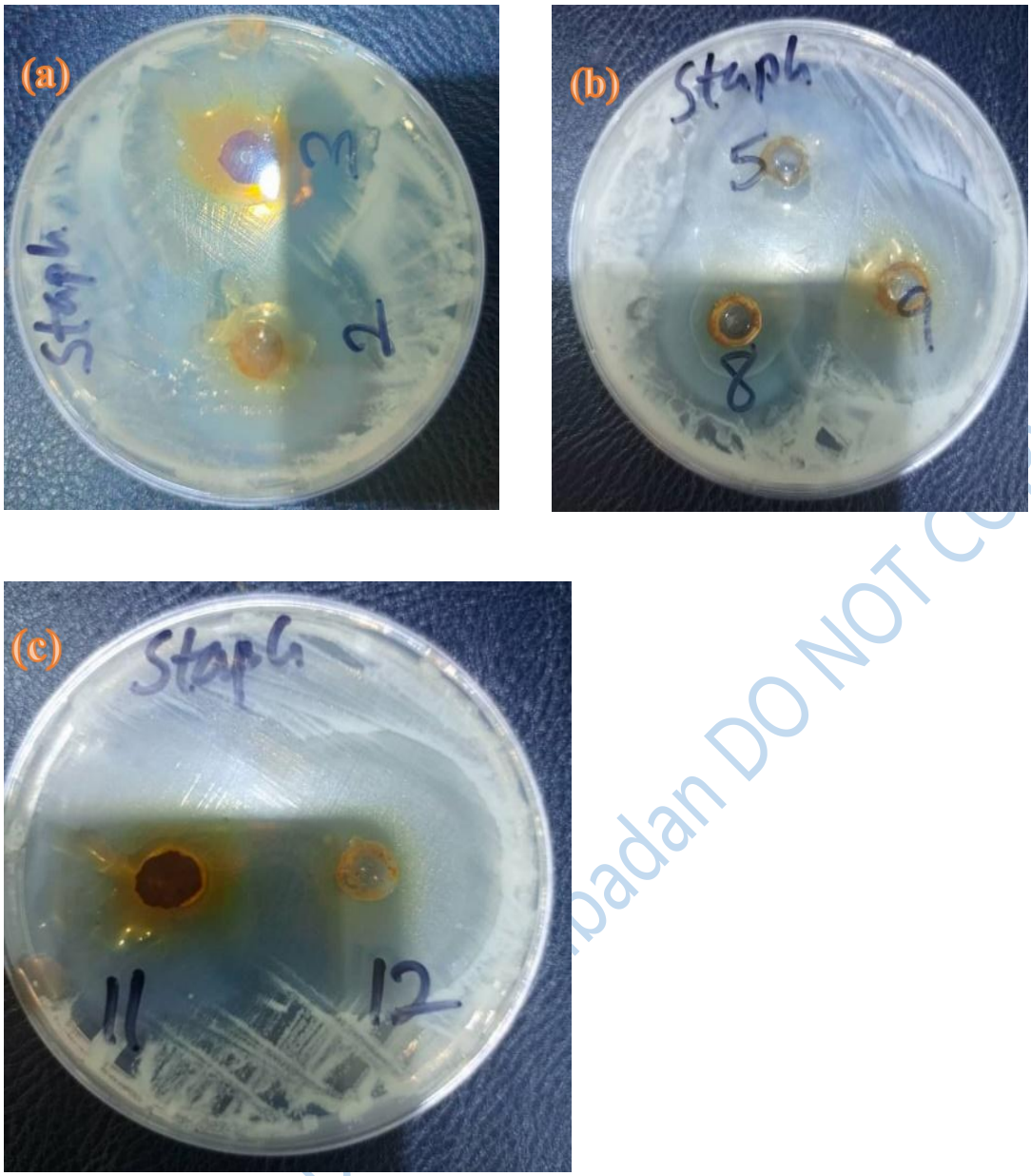

Figure 4.30: Microbial Plates of *Staphylococcus aureus* Treated with (a) C-ZnONP (2), C-Al_2O_3NP (3) (b) E-ZnONP (5), M-ZnONP (8) , C- Al_2O_3NP (9) (c) NM-ZnONP (11) and C-Al_2O_3NP (12).

Source: Author's Field Work 2025

4.4.2 Microbial Plates of *Escherichia coli*

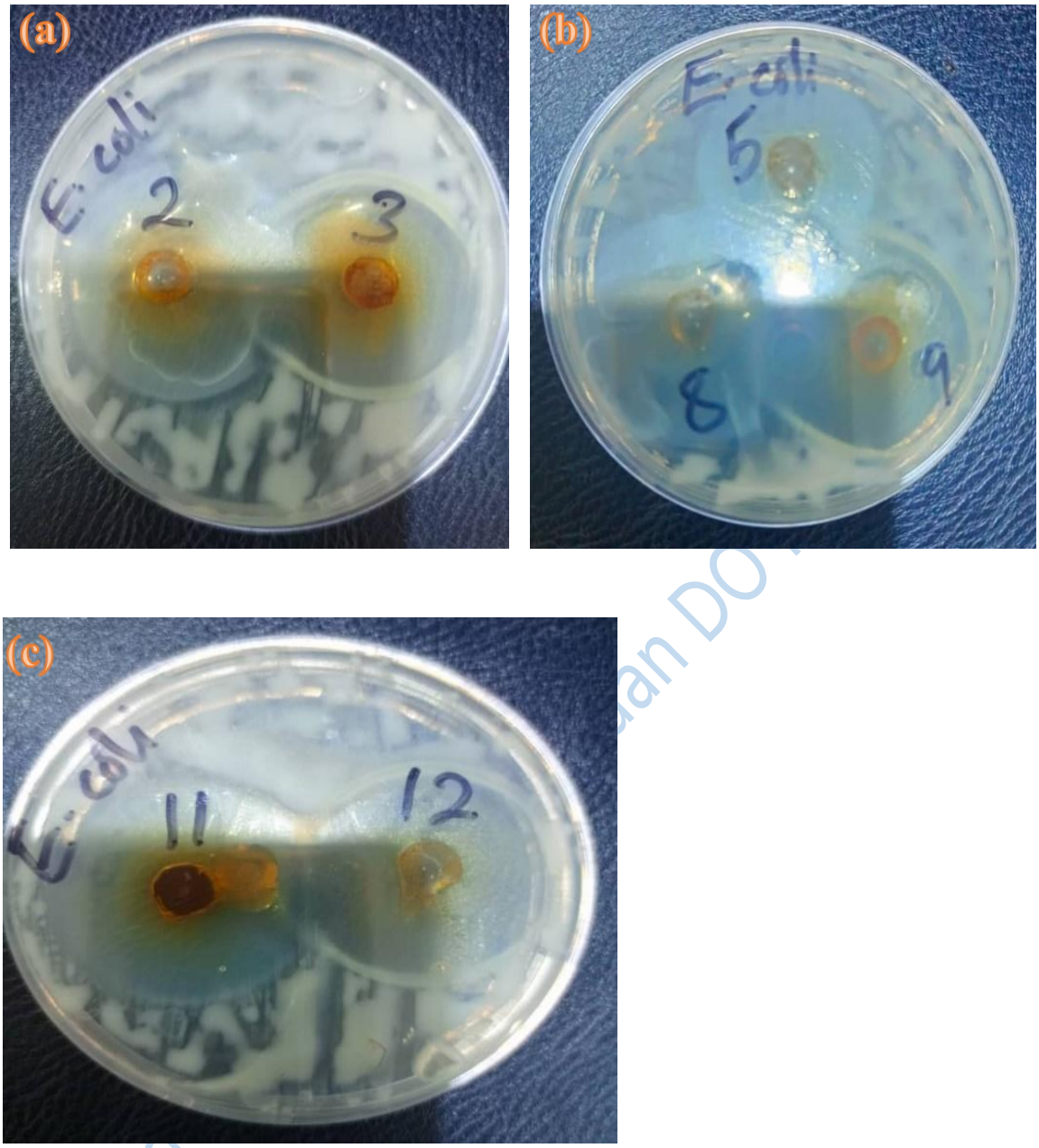

Figure 4.31: Microbial Plates of *Escherichia coli Treated with* (a) C-ZnONP (2), C-Al_2O_3NP (3) (b) E-ZnONP (5), M-ZnONP (8) and C- Al_2O_3NP (9) (c) NM-ZnONP (11) and C- Al_2O_3NP (12)

Source: Author's Field Work 2025

4.4.3 Microbial Plates of *Pseudomonas aeruginosa*

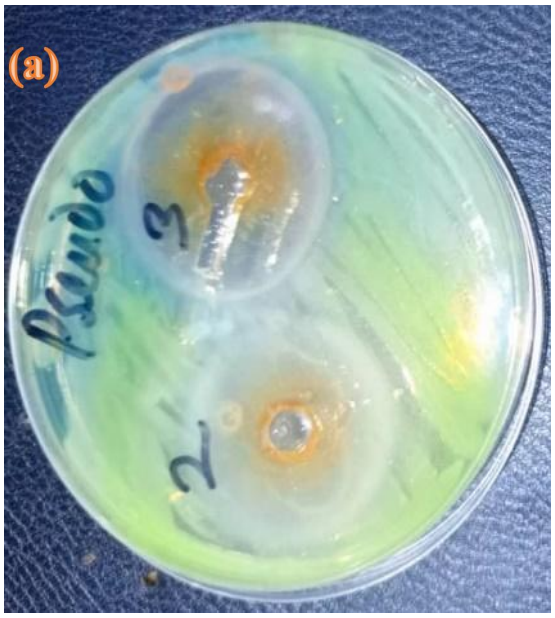

(b)

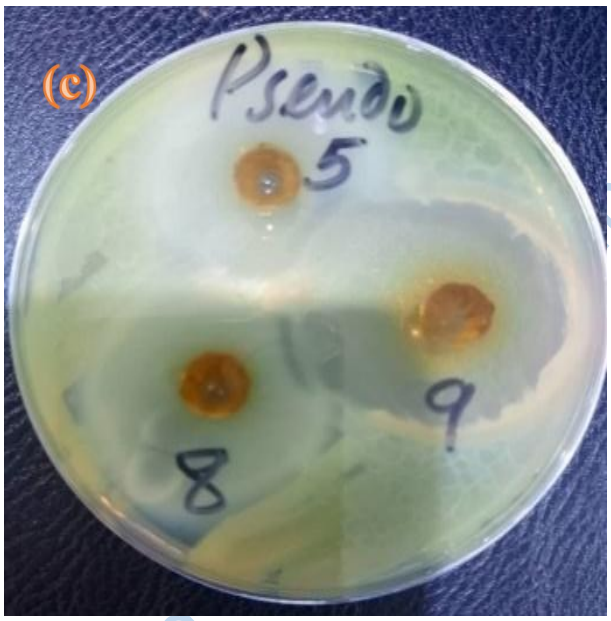

Figure 4.32: Microbial Plates of *Pseudomonas aeruginosa* (a) C-ZnONP (2), C- Al_2O_3NP (3) (b) E-ZnONP (5), M-ZnONP (8) and C- Al_2O_3NP (9) (c) NM-ZnONP (11) and C- Al_2O_3NP (12)

Source: Author's Field Work

4.4.4 Microbial Plates of *Salmonella typhi*

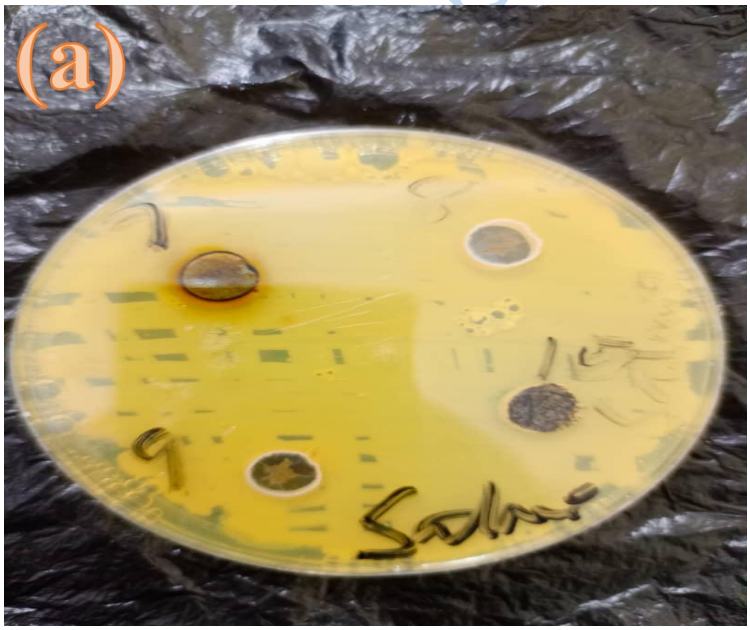

(b)

Figure 4.33: Microbial Plates of *Salmonella typhi Treated with* (a) E-Al_2O_3NP (6) M (7), and (b) C (1), E (4)

Source: Author's Field Work 2025.

Endnotes

1. K.T. Dauda ,T.F.Owoeye , O.S.I.Fayomi , I.G.Akande. *Ethanolic extract of Chrysophyllum albidum leaves and peels as a green inhibitor for AISI 1015 carbon steel in 1M H2SO4 solution* **Vietnam Journal of Chemistry**, 2023 doi: 10.1002/vjch.202200094

2. Muhammad Usman Sadiq , Afzal Shah , Abdul Haleem , Syed Mujtaba Shah , Iltaf Shah *Eucalyptus globulus Mediated Green Synthesis of Environmentally Benign Metal Based Nanostructures*: *A Review*, **Nanomaterials.** (Basel). 2023 Jul 6;13(13):2019. doi: 10.3390/nano13132019,PMCID: PMC10343597 PMID: 37446535

3. Peraman Manimegalai, Kuppusamy Selvam,Aboud Ahmed Awadh Bahajjaj,*Green synthesis of zinc oxide (ZnO) nanoparticles using aqueous leaf extract of Hardwickia binata: their characterizations and biological applications,* **Biomass Conversion and Biorefinery** 2023

4. A.Yasser Selim, A.Maha Azb, Islam Ragab, H.M Mohamed, Abd El-Azim, *Green Synthesis of Zinc Oxide Nanoparticles Using Aqueous Extract of Deverra tortuosa and their Cytotoxic Activities,* **Scientific Reports** volume 10, Article number: 3445 (2020)

5. Ambik Behera, Shruti Awasthi, *Anticancer, Antimicrobial and Hemolytic Assessment of Zinc Oxide Nanoparticles Synthesized from Lagerstroemia indica* **BioNanoScience** 2 August 2021 © LLC, part of Springer Nature, https://doi.org/10.1007/s12668-021-00889-4,

6. Bassant Naiel, Manal Fawzy, Alaa El Din Mahmoud,*Green synthesis of zinc oxide nanoparticles using Sea Lavender (Limonium pruinosum L. Chaz.) extract: characterization, evaluation of anti-skin cancer, antimicrobial and antioxidant potentials,* **Scientific Reports** (2022)

7. A Brahma Swamulu,Venugopal Rao Soma,Gopala Krishna Podagatlapalli], *Non-spherical aluminum nanoparticles fabricated using picosecond laser ablation* June 2020, **International Journal of Minerals Metallurgy and Materials** 27(7):1-7,DOI:10.1007/s12613-020-2032-1

8. A.Palani Manogar, A.Jobu Esther Morvinyabesh, B.Ponnusamy Ramesh, C.Gnanasekar Dayana Jeyaleela, D.Venkatesan Amalan, S.Jamaan, E.Ajarem, A.Ahmed ,F.Allam, G.Jong Seong Khim, D.Natesan Vijayakumar. *Biosynthesis and antimicrobial activity of aluminium oxide nanoparticles using Lyngbya majuscula extract*. Volume 311, 15 March 2022, 131569, **Materials Letters** https://doi.org/10.1016/j.matlet.2021.131569

9. A.B.D.Nandiyanto, R.Oktiani, R.Ragadhita, (2019). *How to read and interpret FTIR spectroscope of organic material***. Indonesian Journal of Science and Technology**, 4(1), 97–118. doi:10.17509/ijost.v4i1.15806

10. Taiwo.F Owoeye, D. Kehinde Akinlabu, O. Olayinka Ajani, *Proximate composition, phytochemical screening and mineral content studies of leaves extract of Adenanthera pavonina,* **Arab Journal of Basic and Applied Sciences**, 30:1, 317-328,2023 DOI: 10.1080/25765299.2215437

11. O.Y. Audu, J.Jooste, F.P.Malan, O.O.Ajani, N.October. *Synthesis, characterization, molecular structure, and computational studies on 4(1H)-pyran-4-one and its derivatives.* **Journal of Molecular Structure**, 2021.1245, 131077. 16[1]

12. Javed Iqbal, Banzeer Ahsan Abbasi, Tabassum Yaseen, Syeda Anber Zahra, Amir Shahbaz, Sayed Afzal Shah, Siraj Uddin, Xin Ma, Blqees Raouf, Sobia Kanwal, Wajid Amin, Tariq Mahmood, Hamed A. El-Serehy & Parvaiz Ahmad, *Green synthesis of zinc oxide nanoparticles using Elaeagnus angustifolia L. leaf extracts and their multiple in vitro biological applications,* **Scientific Reports** volume 11, Article number: 20988, 2021.

13. A.A. Barzinjy, H.H. Azeez, *Green synthesis and characterization of zinc oxide nanoparticles using Eucalyptus globulus Labill. leaf extract and zinc nitrate hexahydrate salt,* **SN Applied Sciences**, 2, pp. 1-14.2020

14. Chunchegowda UA, Shivaram AB, Mahadevamurthy M, Ramachndrappa LT, Lalitha SG, Krishnappa HKN, *Biosynthesis of zinc oxide nanoparticles using leaf extract of Passiflora subpeltata: characterization and antibacterial activity against Escherichia coli*

isolated from poultry faeces. **J Clust Sci**. ;32:1663–72. 2021 10.1007/s10876-020-01926-0.

15. Ahlam Hacine Gharbi ,Salah Eddine Laouini ,Hadia Hemmami ,Abderrhmane Bouafia ,Mohammed Taher Gherbi ,Ilham Ben Amor,Gamil Gamal Hasan ,Mahmood M. S. Abdullah ,Tomasz Trzepieciński Johar Amin Ahmed Abdullah*, Eco-Friendly Synthesis of Al2O3 Nanoparticles: Comprehensive Characterization Properties, Mechanics, and Photocatalytic Dye Adsorption Study.* **Journals Coatings** Volume 14 Issue 7 10.3390/coatings14070848,Coatings2024,14(7),848;https://doi.org/10.3390/coatings14070848
16. Indrani Laskar & Rajib Saha, *Synthesis of aluminum oxide nanoparticles using seeds of Carica papaya and evaluation of it for antimicrobial, antioxidant, and photocatalysis activity* . **Journal of Analytical Science and Technology** volume 15, Article number: 52 2024 Published: 19 November 2024
17. Abhilash Mavinakere Ramesh, Kaushik Pal, Anju Kodandaram , Bangalore Lakshminarayana Manjula , Doddarasinakere Kempaiah Ravishankar , Hittanahallikoppal Gajendramurthy Gowtham , Mahadevamurthy Murali , Abbas Rahdar and George Z. Kyzas, *Antioxidant and photocatalytic properties of zinc oxide nanoparticles phyto-fabricated using the aqueous leaf extract of Sida acuta*. **Green Processing and Synthesis**, 2022, https://doi.org/10.1515/gps-2022-0075
18. H. Tristijanto, M.N. Ilman, P. Tri Iswanto, *Corrosion inhibition of welded of X – 52 steel pipelines by sodium molybdate in 3.5% Na.Cl solution,* **Egypt. J. Pet.,** 29 pp. 155-162, doi:10.1016,2020,/j.ejpe.2020.02.001
19. Chandrabhan Verma, E.Eno Ebenso, M. A. Quraishi and Chaudhery Mustansar Hussain *Recent developments in sustainable corrosion inhibitors: design, performance and industrial scale applications*.**Materials Advances** Issue 12, 2021
20. K. T. Dauda, Taiwo Felicia Owoeye, Godwin Akande, Ojo Sunday Isaac Fayomi*, Evaluation of Corrosion Inhibition and Adsorption Effect of Aqueous Chrysophyllum Albidum Leaves and Peels Extract on Mild Steel in Acidic Medium*, December 2023, **Protection of Metals and Physical Chemistry of Surfaces** 59(6), DOI:10.1134/S2070205123701137
21. O.A. Akinbulumo, O.J. Odejobi, E.L. Odekanle, *Thermodynamics, and adsorption study of the corrosion inhibition of mild steel by Euphorbia heterophylla L. extract in 1.5M HCl,* **Results Mater.,** 5 2020, 10.1016/j.rinma.2020.100074 10074
22. A.Ahmed. Al-Amiery, Abu Bakar Mohamad, H.Abdul Amir Kadhum, M.Lina Shaker, Wan Nor Roslam Wan Isahak S. Mohd Takriff . *Experimental and theoretical study on the corrosion inhibition of mild steel by nonanedioic acid derivative in hydrochloric acid solution,* **Scientific Reports** volume 12, Article number: 4705, 2022
23. Shveta Sharma, Ashish Kumar *Recent advances in metallic corrosion inhibition: A review,* **Journal of Molecular Liquids** Volume 322, 114862, 2021,. https://doi.org/10.1016/j.molliq.2020.114862
24. S. Bashir, A. Thakur, H. Lgaz, I.M. Chung, A. Kumar, *Corrosion inhibition performance of acarbose on mild steel corrosion in acidic medium: an experimental and*

computational study, **Arab. J. Sci. Eng.,** 45 pp. 4773-4783,2020, 10.1007/s13369-020-04514-6

25. A. Singh, X. Dayu, E. Ituen, K. Ansari, M.A. Quraishi, S. Kaya, Y. Lin,*Tobacco extracted from the discarded cigarettes as an inhibitor of copper and zinc corrosion in an ASTM standard D1141-98(2013) artificial seawater solution* **J. Mater. Res. Technol.,** 9 pp. 5161-5173, 2020,10.1016/j.jmrt.2020.03.033

26. X. He, J. Dan, and C. Hong, *Kinetics and thermodynamics studies of glycyrrhizic acid adsorption using s-8 macroporous resin*, **Asian Journal of Chemistry**, vol. 25, no. 17, 2013, doi: 10.14233/ajchem.2013.15042.

27. J. T. Nwabanne and V. N. Okafor, *Adsorption and thermodynamics study of the inhibition of corrosion of mild steel in H2SO4 medium using vernonia amygdalina*, **Journal of Minerals and Materials Characterization and Engineering**, vol. 11, no. 9, 2012.

28. H. Guo, Y. Zhang, Z. Zheng, H. Lin, and Y. Zhang, *Facile one-pot fabrication of Ag@MOF(Ag) nanocomposites for highly selective detection of 2,4,6-trinitrophenol in aqueous phase*,Talanta, vol. 170, 2017, doi: 10.1016/**j.talanta**.2017.03.096.

29. O.Oduselu, Gbolahan, V. Aderohunmu, Damilola, O. Olayinka Ajani, F.Elebiju, Oluwadunni, A. Ogunnupebi, Temitope, Ezekiel Adebiyi. *Synthesis, in silico and in vitro antimicrobial efficacy of substituted arylidene-based quinazolin-4(3H)-one motifs.* ISSN 22962646, DOI 10.3389/**fchem**.2023.1264824 Volume 112023 Article number 1264824,.**Frontiers in Chemistry** Volume 112023 Article number 1264824.

30. Bahareh Nowruzi, Samaneh Jafari Porzani. *Study of pesticidal activity of bioactive compounds of Neowestiellopsis persica strain A1387 in improving the antioxidative and antimicrobial activity of wheat to sunn pest,* **Microbial Pathogenesis,** Volume 187, 2024, 106500,https://doi.org/10.1016/j.micpath.2023.106500.

31. Yingchao Cui , Daosheng Wang , Clarissa,J. Nobile , Danfeng Dong , Qi Ni , Tongxuan Su , Cen Jiang , Yibing Peng, *Systematic identification and characterization of five transcription factors mediating the oxidative stress response in Candida albicans.*Volume 187, 2024, 106507,https://doi.org/10.1016/j.**micpath**.2023.106507

32. Shalini Anand, Jyoti Lamba, Pramod Kumar Rai,*Azolla microphylla extract ZnO nanoparticles and antibacterial activity: eco-friendly wastewater treatment, Nanotechnology for Environmental Engineering*, **Journal of Inorganic and Organometallic Polymers and Materials** 2023

33. A.M.Al-Mohaimeed, W.A. Al-Onazi, M.F.El-Tohamy. *Multifunctional eco-friendly synthesis of ZnO nanoparticles in biomedical applications.* **Molecules** 27, 25, 2022.

Chapter Five: Conclusion

5.1 Summary of Findings

This study thoroughly examined the potential applications of *Casuarina equisetifolia, Cassia javanica, Adonida merrilli,* and *Washingtonia robusta* plants in synthesizing zinc oxide and aluminum oxide nanoparticles. The nanoparticles were successfully synthesized using the leaf extract of *the* above-mentioned plants.

Adonida merrilli, Washingtonia robusta, Cassia javanica, and *Casuarina equisetifolia* aqueous extracts did not contain phenol, cardiac glycosides, or oxalates. All aqueous extracts of *Casuarina equisetifolia, Cassia javanica, Adonida merrilli,* and *Washingtonia robusta* contained saponin. More so, except *Casuarina equisetifolia*, all had quinines. Also, all

contained tannins except *Adonida merrilli*. Only *Casuarina equisetifolia* contained alkaloids; the other plants did not. While terpenoids were lacking in *Cassia javanica* and *Washingtonia robusta*, they were found in *Adonida merrilli* and *Casuarina equisetifolia.* The SEM micrographs showed spherical nanoparticles. The XRD spectra showed crystalline nanoparticles with an average particle size of 73.82 nm (NM-ZnONP), 10.13 nm (C-Al_2O_3NP), 41.85 nm (C-ZnONP), 71.50 nm (M-ZnONP), 22.06 nm (E-ZnONP), 8.63 nm (E-Al_2O_3NP), 5.86 nm (NM Al_2O_3-NP), 8.68 nm (M-Al_2O_3NP). The *Cassia javanica* plant recorded the highest corrosion inhibitory characteristics when compared with other plants. Furthermore, the Zinc Oxide nanoparticles used include E-ZnONP, and M-Al_2O_3NP. E-ZnONP demonstrated the highest inhibition efficiency, while *Cassia javanica* was the least effective.

The best inhibitory efficiencies were determined to be 92.93 % (500 ppm), 81.49% (1000 ppm), 82.99 % (1500 ppm), and 88.84% (2000 ppm) for E-ZnONP, 61.41 % for M-Al_2O_3, and 86.63% (500 ppm) for C extracts in acidic medium.

The SEM was utilized to verify that an inhibitory layer had formed to protect the metal showing a smooth surface when an inhibitor is present and ridged and damaged surfaces was observed with the untreated metal. The E-ZnONP, C-ZnONP, M-ZnONP, NM-ZnONP, C-Al_2O_3, and M-Al_2O_3 were observed to be biopotent, and as such regarded as a good antibacterial agents when compared to other samples.

5.2 Conclusion

The study evaluated the potential of *Casuarina equisetifolia, Cassia javanica, Adonida merrilli,* and *Washingtonia robusta* plants and the synthesized zinc oxide and aluminum oxide nanoparticles for corrosion inhibition in an acidic medium. The following conclusion are inferred from the findings of this study:

The Potentiodynamic and gravimetric analyses shows that as the concentration of the inhibitors rises, the corrosion rate reduces, indicating an interaction between the inhibitor

molecules and the substrate.The optimum inhibitory efficiency recorded are 92.93% (500 ppm), 81.49%

(1000 ppm), 82.99% (1500 ppm), 88.84% (2000 ppm) for E-ZnONP, 61.41% for M-Al_2O_3, and 86.63% (500 ppm) for C extracts in acidic medium.

The inhibitors' absorption and the Langmuir adsorption isotherms' subsequent analysis demonstrated the presence of surface contact, and that adsorption occurs at the surface layer.The adsorption-related Gibbs free energy of E-ZnONP and M-Al_2O_3 are negative, with ΔG_{ads} = -22.27 (E-ZnONPS) and = -9.74 (M-Al_2O_3) respectively meaning the following:

- The adsorption process is considered spontaneous. In a different manner, the adsorbate (a corrosion inhibitor, for example) readily binds to the metal surface without needing further energy, meaning that, adsorption occurs naturally due to the favorable interaction between the adsorbate and the metal surface.
- This energy can be used to produce protective layers or stabilize the metal surface. This shows that, in the event of corrosion, the inhibitor molecules effectively adhere to the metal, reducing its reactivity and delaying the corrosion process.
- High affinity between the adsorbate and the metal surface. It is quite probable that the inhibitor will effectively halt rusting process.

The adsorption equilibrium constant of Kads with a recorded value of 124.39 mol^{-1} (E-ZnONPs) and 0.86 mol^{-1} (M-Al_2O_3) respectively, suggests a considerable link between the inhibitor molecules and the metal surface. This implies:The inhibitor molecules' significant tendency to adsorb onto the metal surface is indicated by a high Kads value. This may lead to effective corrosion prevention since it indicates a strong bond between the inhibitor and the metal.And also a strong correlation exists between the value of Kads and the inhibitor's efficiency. An inhibitor's inhibition effectiveness, which is measured by a higher Kads value, is frequently connected with its capacity to inhibit corrosion.

The adsorption data of E-ZnONPs and M-Al_2O_3NP were effectively fitted into Langmuir isotherms with recorded R^2 value of 0.98 (E-ZnONPs) and 0.87 (M-Al_2O_3NP) respectively which shows that the model accurately predicts the adsorption process,

There is good agreement between the potentiodynamic and gravimetric results.

Of the twelve samples utilized, E-ZnONP, C-ZnONP, M-ZnONP, and NM-ZnONP proved to be the most effective antibacterial agent.

5.3 Recommendations

1. This study demonstrates that a biological approach can serve as a cost-effective alternative to conventional physical and chemical synthesis methods for ZnONPs. By utilizing non-edible plants such as *Casuarina equisetifolia, Cassia javanica, Adonida merrilli, and Washingtonia robusta,* which are typically discarded as waste, nanoparticle production becomes more sustainable.
2. These plant species—*Casuarina equisetifolia, Cassia javanica, Adonida merrilli, and Washingtonia robusta* —represent valuable renewable resources for developing an eco-friendly, large-scale biological synthesis process for Al_2O_3NPs.

5.4 Contributions to Knowledge

The findings of this research have the following contributions to the field of medicine, corrosion control, and prevention:

1. The E-ZnONP and M-Al_2O_3NP offer a less expensive, more sustainable option for inhibiting corrosion.
2. Using leaf extracts from *Casuarina equisetifolia, Adonida merrilli, Washingtonia robusta,* and *Cassia javanica*, a new biosynthetic pathway for zinc oxide and aluminium oxide nanoparticles was established.
3. E-ZnONP, C-ZnONP, M-ZnONP, and NM-ZnONP nanoparticles might be helpful in antibacterial and biological applications. It can also be utilized for drug delivery purposes.Unwanted plants or weeds such as *Adonida merrilli, Washingtonia robusta ,*

Cassia javanica, and *Casuarina equisetifolia* may serve as potential raw materials for industrial use.

4. ZnO nanoparticles (E-ZnONP) synthesis from extract leaf of *Casuarina equisetifolia* and Aluminum Oxide nanoparticles (M-Al_2O_3NP) synthesis from aqueous leaf extracts of *Washingtonia robusta* are promising for the formulation of inhibitor cocktail for acid wash.

5.5 Suggested Areas for Further Research

Based on the findings of this investigation, the following actions are advised:

1. For additional research, the active components of the materials that cause the inhibitors should be isolated.

2. Of the twelve samples utilized, E-ZnONP, C-ZnONP, M-ZnONP, and NM-ZnONP proved to be the most effective antibacterial agent. Therefore, more research into their cytotoxicity profile is required to maximize and pinpoint their potential for medication development.

3. With an emphasis on the particle sizes in this work, the antiviral qualities of the nanoparticles produced via biosynthesis should be evaluated.

Bibliography

Conference Proceeding

E K Arya1 and B S Dhanya, *Corrosion control of reinforced concrete structures in construction industry: A review,* IOP Conf. Series: Materials Science and Engineering 1114 2021 012006, IOP Conf. IOP Publishing doi:10.1088/1757-899X/1114/1/012006.

Journal

Abdul Malek , Anusha Ganta , Govindaraj Divyapriya , Indumathi M. Nambi , Tiju Thomas *Hydrogen production from human and cow urine using in situ synthesized aluminium nanoparticles.* **International Journal of Hydrogen Energy**, 46, Issue 54, 27319-27329, 2021,https://doi.org/10.1016/.

A Brahma Swamulu,Venugopal Rao Soma,Gopala Krishna Podagatlapalli], *Non-spherical aluminum nanoparticles fabricated using picosecond laser ablation* **International Journal of Minerals Metallurgy and Materials** 27(7):1-7,June 2020,DOI:10.1007/s12613-020-2032-1

A.A. Barzinjy, H.H. Azeez, *Green synthesis and characterization of zinc oxide nanoparticles using Eucalyptus globulus Labill. leaf extract and zinc nitrate hexahydrate salt,* SN **Applied Sciences**, 2 , 2020, pp. 1-14.

Abhilash Mavinakere Ramesh , Kaushik Pal , Anju Kodandaram , Bangalore Lakshminarayana Manjula Doddarasinakere Kempaiah Ravishankar , Hittanahallikoppal Gajendramurthy Gowtham , Mahadevamurthy Murali, Abbas Rahdar and George Z. Kyzas, *Antioxidant and photocatalytic properties of zinc oxide nanoparticles phyto-fabricated using the aqueous leaf extract of Sida acuta.* **Green Processing and Synthesis,** gps-2022-0075,https://doi.org/10.1515/gps

A.De, Swarupa Ghosh, Manoswini Chakrabarti, Ilika Ghosh, Ritesh Banerjee, A. Mukherjee. *Effect of low-dose exposure of aluminium oxide nanoparticles in Swiss albino mice: Histopathological changes and oxidative damage,* **Toxicology and Industrial Health,** 36, Issue 8 2020,https://doi.org/10.1177/0748233720936828.

Adnan Munis , Tianyu Zhao , Maosheng Zheng , Ata Ur Rehman , Feng Wang *A newly synthesized green corrosion inhibitor imidazoline derivative for carbon steel in 7.5% NH_4Cl solution.* **Sustainable Chemistry and Pharmacy**, 16, 2020, 100258, 16, 100258.https://doi.org/10.1016/

A.M.Al-Mohaimeed, W.A.Al-Onazi, M.F. El-Tohamy. *Multifunctional eco-friendly synthesis of ZnO nanoparticles in biomedical applications.* **Molecules** 27, 25, 2022.

O.Olayinka,Ajani,Taiwo Felicia Owoeye, Kehinde Deborah Akinlabu, Oladotun Bolade, Oluwatimilehin E.Aribisala, Durodola Bamidele M. . *Sorghum extract: Phytochemical, proximate, and GC-MS analyses* November 2021, **Foods and Raw Materials** ,9(2), 2021. 371-378, DOI:10.21603/2308-4057.

D.K.Akinlabu,T.F.Owoeye,F.E.Owolabi,O.Y.Audu,C.O.Ajanaku, F.Falope,O.O.Ajani, *Phytochemical and proximate analysis of African oil bean (Pentaclethra macrophylla Benth) seed.* **Journal of Physics,**1378, Issue 3, 2019, DOI 10.1088/1742-6596/1378/3/032057

I.Ahanotu Onyeachu, M.Moses Solomon, S.Ikechukwu Chikwe, B.Oluchukwu Chikwe, C. Eziukwu *Pterocarpus santalinoides leaves extract as a sustainable and potent inhibitor for low carbon steel in a simulated pickling medium.* **Sustainable Chemistry and Pharmacy**, 15, 2019, 100196. DOI:10.1016.

A.Ahmed Al-Amiery, Abu Bakar Mohamad, H. Abdul Amir Kadhum, M.Lina Shaker, Wan Nor Roslam Wan Isahak, Mohd S. Takriff . *Experimental and theoretical study on the corrosion inhibition of mild steel by nonanedioic acid derivative in hydrochloric acid solution,* **Scientific Reports** volume 12, Article number: 4705 2022.

Ahlam Hacine Gharbi ,Salah Eddine Laouini,Hadia Hemmami ,Abderrhmane Bouafia ,Mohammed Taher Gherbi ,Ilham Ben Amor,Gamil Gamal Hasan ,Mahmood M. S. Abdullah ,Tomasz Trzepieciński Johar Amin Ahmed Abdullah*, Eco-Friendly Synthesis of Al2O3 Nanoparticles: Comprehensive Characterization Properties, Mechanics, and Photocatalytic Dye Adsorption Study.* **Journals Coating** Volume 14 issue 710. 14(7), 848;3390/coatings14070848, Coatings 2024, https://doi.org/10.3390/coatings14070848

A. Kadhim, A.A. Al-Amiery, R. Alazawi, M.K.S. Al-Ghezi, R.H. Abass1, *Corrosion inhibitors. A review* **Int. J. Corros. Scale Inhib**., 10, no. 1, 54–67 54, 2021, doi: 10.17675/2305-6894-2021-10-1-3

Ali Dehghani , Ghasem Bahlakeh , Bahram Ramezanzadeh , Mohammad Ramezanzadeh *Aloysia citrodora leaves extract corrosion retardation effect on mild-steel in acidic solution: Molecular/atomic scales and electrochemical explorations* **Journal of Molecular Liquids,** 310, 113221. 2020, https://doi.org/10.1016/

A.Ismail, A. Farag . *Experimental, theoretical and simulation studies of extracted crab waste protein as a green polymer inhibitor for carbon steel corrosion in 2 M H_3PO_4.* **Surfaces and Interfaces** 19, 2020),100483. DOI:10.1016

A. M. Abdel-Gaber, H. T. Rahal, F. T. Beqai , *Eucalyptus leaf extract as a ecofriendly corrosion inhibitor for mild steel in sulfuric and phosphoric acid solutions*.**International Journal of Industrial Chemistry** 11, pages123–132,2020.

Anthony Obike, Kelechi Uwakwe, E K Abraham, Wilfred Emori, *Review of the losses and devastation caused by corrosion in the Nigeria oil industry for over 30 years,* **International Journal of Corrosion and Scale Inhibition** 9(1):74-91,2020, DOI: 10.17675/2305-6894-2020-9-1-5

Ashwath Narayana, A.Sachin Bhat, Almas Fathima, S. V. Lokesh, G. Sandeep Suryad, C. V. Yelamaggad. *Green and low-cost synthesis of zinc oxide nanoparticles and their application in transistor-based carbon monoxide sensing* **RSC Advances** ,Issue 23, 2020,DOI https://doi.org/10.1039/D0RA00478B,

Ashwini Jayachandran, Aswathy T.R., Achuthsankar S. Nair, *Green synthesis and characterization of zinc oxide nanoparticles using Cayratia pedata leaf extract.* **Biochemistry and Biophysics, Reports**, Volume 26, July 2021, 100995, https://doi.org/10.1016/j.bbrep.2021.100995

A Marsoul , M. Ijjaali , F. Elhajjaji , M. Taleb , R. Salim , A. Boukir *Phytochemical screening, total phenolic and flavonoid methanolic extract of pomegranate bark (Punica granatum L): Evaluation of the inhibitory effect in acidic medium 1 M HCl.* **Mater. Today Proc.** ,2020, 27, 4, 2020, Pages 3193-3198, https://doi.org/10.1016/j.matpr.2020.04.202

Ambik Behera, Shruti Awasthi, *Anticancer, Antimicrobial and Hemolytic Assessment of Zinc Oxide Nanoparticles Synthesized from Lagerstroemia indica* **BioNanoScience**, https://doi.org/10.1007/s12668-021-00889-4,Accepted: 2 August 2021 © LLC, part of Springer Nature (2021)

A.Sedik , D. Lerari , A. Salci , S. Athmani , K. Bachari , İ.H. Gecibesler , R. Solmaz *Dardagan Fruit extract as eco-friendly corrosion inhibitor for mild steel in 1 M HCl: Electrochemical and surface morphological studies* **Journal of the Taiwan Institute of Chemical Engineers**,107, 2020, 189-200.

A Saravanan , P Senthil Kumar, S Karishma , Dai-Viet N Vo , S Jeevanantham 1, P R Yaashikaa , Cynthia Susan George ,*A review on biosynthesis of metal nanoparticles and its environmental applications***, Chemosphere***,* 264, 2, 2020, 128580, https://doi.org/10.1016/j.

A. Singh, X. Dayu, E. Ituen, K. Ansari, M.A. Quraishi, S. Kaya, Y. Lin, *Tobacco extracted from the discarded cigarettes as an inhibitor of copper and zinc corrosion in an ASTM standard D1141-98(2013) artificial seawater solution* **J. Mater. Res. Technol.,** 9 (2020), pp. 5161-5173, 10.1016/j.jmrt.2020.03.033

O. Y Audu, J.Jooste, Malan, F. P., Ajani, O. O., October, N. *Synthesis, characterization, molecular structure, and computational studies on 4(1H)-pyran-4-one and its derivatives*. **Journal of Molecular Structure**, 1245, 131077. 16[1].2021.

Chandrabhan Verma, Eno E. Ebenso, M. A. Quraishi and Chaudhery Mustansar Hussain, *Recent developments in sustainable corrosion inhibitors: design, performance and industrial scale applications*. **Materials Advances** Issue 12, 2021.

Babak Pakbin, M.Wolfram. Brück, John W. A. Rossen, Virulence *Factors of Enteric Pathogenic Escherichia coli: A Review,* **Int J Mol Sci**. Sep; 22(18):2021 9922.Published online 2021 Sep 14. doi: 10.3390/ijms22189922,PMCID: PMC8468683,PMID: 34576083

Baye Sitotaw , Fikremariam Ayalew , Abayneh Girma , Amare Bitew Mekonnen , Yousef A. Bin Jardan , Hiba-Allah Nafidi and Mohammed Bourhia. *Isolation and identification of promising antibiotic-producing bacteria* **Open Chemistry**, 2022 https://doi.org/10.1515/chem-2022-0233.

Bahareh Nowruzi, Samaneh Jafari Porzani. *Study of pesticidal activity of bioactive compounds of Neowestiellopsis persica strain A1387 in improving the antioxidative and antimicrobial activity of wheat to sunn pest,* **Microbial Pathogenesis,** Volume 187, 2024, 106500,https://doi.org/10.1016/j.micpath.2023.106500

Bassant Naiel, Manal Fawzy, Alaa El Din Mahmoud,*Green synthesis of zinc oxide nanoparticles using Sea Lavender (Limonium pruinosum L. Chaz.) extract: characterization, evaluation of anti-skin cancer, antimicrobial and antioxidant potentials,* **Scientific Reports** (2022)

Bibek Laha, Sabyasachi Maiti, Kalyan Kumar Sen,Subrata Jana, *Nanoscale polysaccharide-based particles for the delivery of therapeutic molecules* **Micro and Nano Technologies,** 347-368, 2019 https://doi.org/10.1016/B978-0-08-102579-6.00014-9.

Kevin Bouiller , Xavier Bertrand , Didier Hocquet , Catherine Chirouze, *Human Infection of Methicillin Susceptible Staphylococcus aureus CC398: A Review.* 8(11):1737.2020 Nov 5;,PMID: 33167581,PMCID: PMC7694499,DOI: 10.3390/microorganisms8111737

N.Chaubey, V.K. Savita, Singh, M.A.Quraishi. *Corrosion Inhibition Performance of Different Bark Extracts on Aluminium in Alkaline Solution.* **j.jaubas** 22, 38-44. 2017,. https://doi.org/10.1016/. 2015. 12.003

Chandrabhan Verma , Eno E. Ebenso , Indra Bahadur , M.A. Quraishi .*An overview on plant extracts as environmental sustainable and green corrosion inhibitors for metals and alloys in aggressive corrosive media.* **Journal of Molecular Liquids,** 266,577–590,2020. https://doi.org/10.1016.

U.A.Chunchegowda,A.B. Shivaram, M.Mahadevamurthy, L.T.Ramachndrappa, S.G.Lalitha, HKN Krishnappa, *Biosynthesis of zinc oxide nanoparticles using leaf extract of Passiflora subpeltata: characterization and antibacterial activity against Escherichia coli isolated from poultry faeces.* **J Clust Sci**. 32: 1663–72,2021. 10.1007/s10876-020-01926-0.

Chandrabhan Verma, E.Eno Ebenso, M. A. Quraishi, Chaudhery Mustansar Hussain Recent developments in sustainable corrosion inhibitors: design, performance and industrial scale applications.**Materials Advances** Issue 12, 2021.

C.R. Rajith Kumar, Virupaxappa S. Betageri, G. Nagaraju, B. P. Suma, M. S.Kiran, & M. S. Latha *One-pot synthesis of ZnO nanoparticles for nitrite sensing, photocatalytic and antibacterial studies.* **Journal of Inorganic and Organometallic Polymers and Materials.** 30, 2020, 3476–3486.https: //doi. org/10.1007/s1090 4-020-01544 -3

K.T.Dauda,T.F. Owoeye, O.S.I.Fayomi,I.G. Akande. *Ethanolic extract of Chrysophyllum albidum leaves and peels as a green inhibitor for AISI 1015 carbon steel in 1M H_2SO_4 solution* **Vietnam Journal of Chemistry,** 2023 doi: 10.1002/vjch.202200094

R.Enobong Essien, N.Violette Atasie, O.Davies Nwude,Ezekiel Adekolurejo, T.Felicia Owoeye, *Characterisation of ZnO nanoparticles prepared using aqueous leaf extracts of Chromolaena odorata (L.) and Manihot esculenta* (Crantz, **Afr J Sci**.118(1/2),2022 Art. #11225. https://doi.org/10.17159

A.Espinoza-Vázquez,F.J Rodríguez-Gómez,G.E Negrón-Silva, R.González-Olvera, D.Ángeles-Beltrán, M.Palomar-Pardavé, A. Miralrio, M.Castro. *Fluconazole and fragments as corrosion inhibitors of API 5L X52 steel immersed in 1 M HCl.* **Corros. Sci.** 174,108853,2020.

Felipe Francisco Tuon, Leticia Ramos Dantas, Paula Hansen Suss, and Victoria Stadler Tasca Ribeiro. *Pathogenesis of the Pseudomonas aeruginosa Biofilm: A Review* **Pathogens.**;11(3): 300. 2022 Feb 27. 2022 Mar doi: 10.3390/pathogens11030300,PMCID: PMC8950561,PMID: 35335624

O.Oduselu, Gbolahan,V.Aderohunmu, Damilola, O.Olayinka Ajani ,F.Elebiju, Oluwadunni ,A.Ogunnupebi, Temitope, Ezekiel Adebiyi. *Synthesis, in silico and in vitro*

antimicrobial efficacy of substituted arylidene-based quinazolin-4(3H)-one motifs. ISSN 22962646,DOI 10.3389/**fchem**.1264824 Volume 112023 Article number 1264824, 2023.Frontiers in Chemistry

R.Garcia-Rubio, H.C.de Oliveira, J.Rivera, N.Trevijano-Contador N. *The Fungal Cell Wall: Candida, Cryptococcus, and Aspergillus Species.* **Front. Microbiol**. 2020;10:2993. doi: 10.3389/fmicb.2019.02993.

H. Guo, Y. Zhang, Z. Zheng, H. Lin, and Y. Zhang, *Facile one-pot fabrication of Ag@MOF(Ag) nanocomposites for highly selective detection of 2,4,6-trinitrophenol in aqueous phase.* vol. 170, 2017, doi: 10.1016/**j.talanta**.2017.03.096.

Hadis Koopi, Foad Buazar (2018).*A Novel One-pot biosynthesis of pure alpha aluminum oxide nanoparticles using the macroalgae Sargassum ilicifolium : A green marine approach*,February **ceramint**, 44(8) (2018),DOI:10.1016/j..2018.02.091.

M.Hany. Abd El Lateef1, Abdel Rahman El Sayed, S.Hossnia Mohran , Hoda Abdel Shafy Shilkamy. *Corrosion inhibition and adsorption behavior of phytic acid on Pb and Pb–In alloy surfaces in acidic chloride solution.* **International Journal of Industrial Chemistry**, 10(1),31-47,2019. https://doi.org/10.1007/s40090-019-0169-4

H. Tristijanto, M.N. Ilman, P. Tri Iswanto, *Corrosion inhibition of welded of X – 52 steel pipelines by sodium molybdate in 3.5% NaCl solution,* **Egypt. J. Pet.,** 29, pp. 155-162, 10.1016/j.ejpe.2020.02.001

Y.Inas Younis, S.Seham El-Hawary, A.Omayma Eldahshan, M.Marwa Abdel-Aziz, Y. Zeinab.Ali *Green synthesis of magnesium nanoparticles mediated from Rosa floribunda charisma extract and its antioxidant, antiaging and antibiofilm activities*, **Scientific Reports**,11, (2021) (1) doi: 10.1038/s41598-021-96377-6.

Indrani Laskar & Rajib Saha, *Synthesis of aluminum oxide nanoparticles using seeds of Carica papaya and evaluation of it for antimicrobial, antioxidant, and photocatalysis activity* .**Journal of Analytical Science and Technology** volume 15, Article number: 52 (2024) Published: 19 November 2024.

Inès Hammami , Nadiyah M. Alabdallah , Amjad Al jomaa , Madiha kamoun. *Gold nanoparticles: Synthesis properties and applications* **Journal of King Saud University-**Science, .101560,2021 https://doi.org/10.1016

C.A.S. Ito, L. Bail , L. Arend, K.D.S, Nogueira, F.F.Tuon . *The activity of ceftazidime/avibactam against carbapenem-resistant Pseudomonas aeruginosa.* **Infect. Dis.** 53:386–389. doi: 10.1080/23744235.2020.1867763.

K. Ishraq Ibrahim, A. Juman Naser. *Corrosion inhibition of carbon steel in sodium chloride solution using artemisia plant extract.* **Plant Archives,** 20 (1),3315-3319,2020.

Jacek Ryl,Mateusz Brodowski, Marcin Kowalski ,Wiktoria Lipinska, Pawel Niedzialkowski and Joanna Wysocka ,*Corrosion inhibition mechanism and efficiency differentiation of dihydroxybenzene isomers towards aluminum alloy 5754 in alkaline media.* **Materials,** 12(19), 3067,2019.

Jasminka Talapko,Martina Juzbašić,Tatjana Matijević,Emina Pustijanac, Sanja Bekić, Ivan Kotris, Ivana Škrlec., *Candida albicans—The Virulence Factors and Clinical Manifestations of*

*Infection,***J Fungi (Basel).** 7(2)79, 2021Feb .Published online 2021 Jan 22. doi: 10.3390/jof7020079,PMCID: PMC7912069,PMID: 33499276

Javed Iqbal, Banzeer Ahsan Abbasi, Tabassum Yaseen, Syeda Anber Zahra, Amir Shahbaz, Sayed Afzal Shah, Siraj Uddin, Xin Ma, Blqees Raouf, Sobia Kanwal, Wajid Amin, Tariq Mahmood, Hamed A. El-Serehy & Parvaiz Ahmad,*Green synthesis of zinc oxide nanoparticles using Elaeagnus angustifolia L. leaf extracts and their multiple in vitro biological applications,***Scientific Reports** volume 11, Article number: 20988,2021.

Jingkuang Liu, Zhengjie Huang, Xuetong Wang. *Economic and Environmental Assessment of Carbon Emissions from Demolition Waste Based on LCA and LCC.* **Sustainability**,12, 6683, p. 6683,2020. https://doi.org/10.3390/su12166683,

J.O. Madu, C. Ifeakachukwu, U. Okorodudu, F.V. Adams, I.V. Joseph, *Corrosion Inhibition Efficiency of Terminalia Catappa Leaves Extracts on Stainless Steel in Hydrochloric Acid.* **Journal of Physics**: 1378, Issue,2,2019,1378 (2), 022092.**DOI** 10.1088/1742-6596.

A.Juman Naser, W. Zainab Ahmed, H.Enas Ali, *Plant Leaves Extracts as Green Inhibitors for Corrosion of Carbon Steel; a Review* **Annals of R.S.C.B**., ISSN:1583-6258, 25, 4, 2021, 5332 - 5340.

J. T. Nwabanne and V. N. Okafor, *Adsorption and thermodynamics study of the inhibition of corrosion of mild steel in H2SO4 medium using vernonia amygdalina*, **Journal of Minerals and Materials Characterization and Engineering,** vol. 11, no. 9, 2012.

K.Kanthavel ,Green Synthesis of Aluminium Oxide *Nanoparticles and its Applications in Mechanical and Thermal Stability of Hybrid Natural Composites*, **Journal of Polymers and the Environment** , 27, 10 ,2189–2200,2019.

Kausalya Tamalmani, Hazlina Husin (2020).*Review on Corrosion Inhibitors for Oil and Gas Corrosion* Issues, **Applied Sciences**, 10, 3389, 3389,ISSN 2076-3417, 2020 https://doi.org/10.3390/ app10103389. http://www.mdpi.com/journal/applsci

K. T. Dauda,Taiwo Felicia Owoeye ,Godwin Akande,Ojo Sunday Isaac Fayomi, *Evaluation of Corrosion Inhibition and Adsorption Effect of Aqueous Chrysophyllum Albidum Leaves and Peels Extract on Mild Steel in Acidic Medium*, **Protection of Metals and Physical Chemistry of Surfaces.** 59(6), December 2023, DOI:10.1134/S2070205123701137

Lisa Zimmermann , Andrea Dombrowski , Carolin Völker , Martin Wagner *Are bioplastics and plant-based materials safer than conventional plastics? In vitro toxicity and chemical composition* **Environment International,** 145,106066, 2020.

L. Gao, S. Peng, X. Huang, Z. Gong,*A combined experimental and theoretical study of papain as a biological eco-friendly inhibitor for copper corrosion in H2SO4 medium*,**Appl. Surf. Sci.**, 511 p. 145446,2020 10.1016/j.apsusc.2020.145446

ManikandanVelu, Balamuralikrishnan Balasubramanian,Palanivel Velmurugan,Hesam Kamyab, Arumugam Veera Ravi, Shreeshivadasan Chelliapan, Chew Tin Lee , Jayanthi Palaniyappan , *Fabrication of nanocomposites mediated from aluminium nanoparticles/Moringa oleifera gum activated carbon for effective photocatalytic removal of nitrate and phosphate in aqueous solution,* **Journal of Cleaner Production,** 281, 25, 124553, 2021 https://doi.org/10.1016/.

N.Mahmoud El-Haddad , A.S. Fouda , A.F. Hassan. *Data from Chemical, electrochemical and quantum chemical studies for interaction between Cephapirin drug as an eco-friendly corrosion inhibitor and carbon steel surface in acidic medium.* **Chemical Data Collections.** 22, 100251, 2019. https://doi.org/10.1016

ManikandanVelu, Balamuralikrishnan Balasubramanian, Palanivel Velmurugan,Hesam Kamyab, Arumugam Veera Ravi, Shreeshivadasan Chelliapan, Chew Tin Lee , Jayanthi Palaniyappan, *Fabrication of nanocomposites mediated from aluminium nanoparticles/Moringa oleifera gum activated carbon for effective photocatalytic removal of nitrate and phosphate in aqueous solution,* **Journal of Cleaner Production**, 281, 25 ,2021, 124553https://doi.org/10.1016/.

M. Gholamhosseinzadeh, H. Aghaie, M. Zandi, M. Giahi, *Rosuvastatin drug as a green and effective inhibitor for corrosion of mild steel in HCl and H_2SO_4 solutions.***Materials Research and Technology, 8,** 5314–5324,2019**.** DOI:10.1016

Muhammad Idrees,Saima Batool,Tanzila Kalsoom,Sadaf Raina,Hafiz M. Adeel Sharif,Summera Yasmeen., *Biosynthesis of silver nanoparticles using Sida acuta extract for anti-microbial actions and corrosion inhibition potential*, **Environmental Technology**, 40(8)1-26,2019.DOI:10.1080/09593330.

Muhammad Usman Sadiq , Afzal Shah , Abdul Haleem , Syed Mujtaba Shah , Iltaf Shah *Eucalyptus globulus Mediated Green Synthesis of Environmentally Benign Metal Based Nanostructures*: *A Review*, **Nanomaterials.** (Basel). 2023 Jul 6;13(13):2019. doi: 10.3390/nano13132019,PMCID: PMC10343597 PMID: 37446535

Muhammad Imran Din, Summiya Jabbar, Jawayria Najeeb, Rida Khalid, Tayabba Ghaffar, Muhammad Arshad, Safyan A. Khan, Shahid Ali, *Green synthesis of zinc ferrite nanoparticles for photocatalysis of methylene blue,* **Int J Phytoremediation** 22(13),1440-1447,2018. doi: 10.1080/15226514.2020.1781783.

Minlan Gao , Jie Zhang , Qiaona Liu , Jinling Li , Rongjun Zhang , Gang Chen *Effect of the alkyl chain of quaternary ammonium cationic surfactants on corrosion inhibition in hydrochloric acid solution.* **Comptes Rendus Chimie**, 22, 5, 355-362,2019.https://doi.org/10.1016/

Mahmoud Nasrollahzadeh, Mohaddeseh Sajjadi, S. Mohammad Sajadi *Green synthesis of Cu/zirconium silicate nanocomposite by using Rubia tinctorum leaf extract and its application in the preparation of N-benzyl-N-arylcyanamides,*Applied **Organometallic Chemistry** 33 (6),2018.DOI:10.1002/aoc.4705**.**

Minha Naseer , Usman Aslam , Bushra Khalid , Bin Chen *Green route to synthesize Zinc Oxide Nanoparticles using leaf extracts of Cassia fistula and Melia azadarach and their antibacterial potential* **Scientific Reports** 10, 9055,2020. DOI: 10.1038/s41598-020-65949-3

M.F. Shehata, A.M. El-Shamy, K.M. Zohdy, E.S.M. Sherif, S.Z. El Abedin,*Studies on the antibacterial influence of two ionic liquids and their corrosion inhibition performanc***Appl. Sci.,** 10 (2020), 10.3390/app10041444 doi:10.1016/j.molstruc.2021.131077.

N Naimi-Shamel , P Pourali , S Dolatabadi *Green synthesis of gold nanoparticles using Fusarium oxysporum and antibacterial activity of its tetracycline conjugant* **J Mycol Med**,29(1):2019,7-13.29.,DOI: 10.1016/j.mycmed**.(**2019).01.005

Naser Ali,Joao Amaral Teixeira, Abdulmajid Addali, *Aluminium Nanofluids Stability: A Comparison between the Conventional Two-Step Fabrication Approach and the Controlled Sonication Bath Temperature Method,* **Journal of Nanomaterials** 10.1155, 2019,Doi3930572

A.B.D.Nandiyanto, R.Oktiani, R.Ragadhita, R. *How to read and interpret FTIR spectroscope of organic material***. Indonesian Journal of Science and Technology**, 4(1), 97–118, 2019. doi:10.17509/ijost.v4i1.15806

Navid Rabiee , M. Bagherzadeh , Mahsa Kiani,Amir Mohammed Ghadiri *Rosmarinus officinalis directed palladium nanoparticle synthesis: investigation of potential anti-bacterial, anti-fungal and Mizoroki–Heck catalytic activities.* **Advance Powder Technology.** 31 ,4,1402-1411,2020. https ://doi. org/10.1016/

Nirmal Kumar Krishanu Biswas, Cryomilling: *An environment friendly approach of preparation large quantity ultra refined pure aluminium nanoparticles,* **Journal of Materials Research and Technology**, 8, 1, 63-74, 2019. https://doi.org/10.1016/j.jmrt.2017.05.017

P.Nithya,S Govindarajan , J.Simpson *Synthesis, crystal structure and Hirshfeld and thermal analysis of bis[benzyl 2-(heptan-4-yl-idene)hydrazine-1-carboxyl-ate-κ2 N 2,O]bis(thio-cyanato)-nickel(II).* **Acta crystallographica. Section E, Crystallographic Communications**, 76,Pt 5, 637-641,2020 DOI: 10.1107/s2056989020004260 .

N. Arrousse, E. Mabrouk, B. Hammouti, F. El hajjaji, Z. Rais, M. Taleb, *New strategy of synthesis, characterization, theoretical study and inhibition effect on mild steel corrosion in acidic solution,* **Mediterr. J. Chem**., 10 ,10.13171, 2020/mjc10502005151417feh

Nour Ahmad-Mansour, Paul Loubet, Cassandra Pouget, Catherine Dunyach-Remy, Albert Sotto, Jean-Philippe Lavigne, and Virginie Molle, *Staphylococcus aureus Toxins: An Update on Their Pathogenic Properties and Potential Treatments* **Toxins (Basel).** 13(10): 677, 2021.Published online 2021 Sep 23. doi:10.3390/toxins13100677,PMCID: PMC8540901,PMID: 34678970.

O.A. Akinbulumo, O.J. Odejobi, E.L. Odekanle, *Thermodynamics, and adsorption study of the corrosion inhibition of mild steel by Euphorbia heterophylla L. extract in 1.5M HCl,* **Results Mater.,** 5 , 10.1016, 2020/j.rinma.2020.100074 10074

Prince Clarance , Ben Luvankar , Jerin Sales , Ameer Khusro , Paul Agastian , J.-C. Tack , Manal M. Al Khulaifi , Hind A. AL-Shwaiman , Abdallah M. Elgorban , Asad Syed , H.-J. Kim *Green synthesis and characterization of gold nanoparticles using endophytic fungi Fusarium solani and its in-vitro anticancer and biomedical applications.* **Saudi Journal of Biological Sciences,** 27, 2, 706-712,2020, https://doi.org/10.1016/j.sjbs.

Pantea Ghahremania, Mohammad Ebrahim Haji Naghi Tehrani, Mohammad Ramezanzadeha, Bahram Ramezanzadeha , *Golpar leaves extract application for construction of an effective anti-corrosion film for superior mild-steel acidic-induced corrosion mitigation at different temperatures,* **Colloids and Surfaces** , 629, 127488, 2021**.**

A.Palani Manogar , A. Jobu Esther Morvinyabesh A, Ponnusamy Ramesh B, Gnanasekar Dayana Jeyaleela C, Venkatesan Amalan D, Jamaan S Ajarem E, Ahmed A Allam F, Jong Seong Khim G, Natesan Vijayakumar D, *Biosynthesis and antimicrobial activity of aluminium oxide*

nanoparticles using Lyngbya majuscula extract. **Materials Letters** Volume 311, 131569, 2022, https://doi.org/10.1016/j.matlet.2021.131569.

Peraman Manimegalai, Kuppusamy Selvam,Aboud Ahmed Awadh Bahajjaj,*Green synthesis of zinc oxide (ZnO) nanoparticles using aqueous leaf extract of Hardwickia binata: their characterizations and biological applications,* **Biomass Conversion and Biorefinery** (2023)

Pello Uranga, Cheng Jia Shang, Takehide Senuma, Jer Ren Yang, Ai Min Guo, Hardy Mohrbacher. *Molybdenum alloying in high-performance flat-rolled steel grades.* **Advances in Manufacturing,** 8,1, 15-34, 2020.

P. Vijaya Kumar, S. Mary Jelastin Kala , K.S. Prakash, *Green synthesis of gold nanoparticles using Croton Caudatus Geisel leaf extract and their biological studies.* **Materials Letters,** 236, 19-22,2019 https://doi.org/10.1016.

Qihui Wang , Bochuan Tan , Hebin Bao , Yuting Xie , Yixuan Mou , Pengcheng Li, Dabiao Chen , Ya nwei Shi , Xueming Li , Wenjing Yang *Evaluation of Ficus tikoua leaves extract as an eco-friendly corrosion inhibitor for carbon steel in HCl media.* **Bioelectrochemistry**,128, 49–55, 2019.

Ravi Mani, Parameswaran Vijayakumar, T.Stalin Dhas, Karthick Velu , D. Inbakandan , C. Thamarais elvi , Babett Greff , Murugesan Chandrasekaran , SaeedahMusaed Almutairi , Faris S Alharbi , DinaS. Hussein , Maisari Utami , *Synthesis of biogenic silver nanoparticles using butter fruit pulp extract and evaluation of their antibacterial activity against Providencia vermicola in Rohu* **Journal of King Saud University - Science,** 34, 3,101814,2022. https://doi.org/10.1016/j.jksus.2021.101814.

R. Farahati, S. M. Mousavi-khoshdel, A. Ghaffarinejad, H. Behzadi *Experimental and computational study of penicillamine drug and cysteine as water-soluble green corrosion inhibitors of mild steel.* **Progress in Organic Coatings** 105567,2020.DOI:10.1016.

C.Rodríguez-Cerdeira , E.Martínez-Herrera , M.Carnero-Gregorio , A.López-Barcenas A., Fabbrocini G., Fida M., El-Samahy M., González-Cespón J.L. *Pathogenesis and Clinical Relevance of Candida Biofilms in Vulvovaginal Candidiasis.***Front. Microbiol**. 11:2884, 2020. doi: 10.3389/fmicb.2020.544480.

Rijuta Ganesh Saratale , Indira Karuppusamy , Ganesh Dattatraya Saratale , Arivalagan Pugazhendhi , Gopalakrishanan Kumar , Yooheon Park , Gajanan S Ghodake , Ram Naresh Bharagava , J Rajesh Banu, Han Seung Shin. *A comprehensive review on green nanomaterials using biological systems: Recent perception and their future applications.* **Colloids Surf B ,**170, 20-35, 2018, doi: 10.1016.

Roland Tolulope Loto , Oluwatobilola Olowoyo *Synergistic effect of sage and jojoba oil extracts on the corrosion inhibition of mild steel in dilute acid solution.* **Procedia Manufacturing,** 35, 310-314, 2019.

Samira Shahriyari Rad , Ali Mohamadi Sani , Sharareh Mohseni , *Biosynthesis, characterization and antimicrobial activities of zinc oxide nanoparticles from leaf extract of Mentha pulegium* (L.).,**MicrobialPathogenesi**131,239 245,2019,https://doi.org/10.1016/j.micpath.2019.04.022

Santwana Padhi , Anindita Behera (2022), *Biosynthesis of Silver Nanoparticles: Synthesis, mechanism, and characterization, Agri-Waste and Microbes for Production of Sustainable Nanomaterials,* **Nanobiotechnology for Plant Protection,** 397-440, 2022 https://doi.org/10.1016/

S. Seetharaman, V.Indra M. Abdul Rahim *Green Synthesis and Analysis of Antioxidant Activity of Silver Nanoparticles Derived from Cissampelos pareira L. Leaves* **International Journal of Zoological Investigations**7, 2, 821-828, 2021. https://doi.org/10.33745/ijzi.2021.v07i02.069

N.S.Shashikumar, B.J. Gireesha, B. Mahanthesh, B.C.Prasannakumara, J.Ali Chamkha, *Entropy generation analysis of magneto-nanoliquids embedded withaluminium and titanium alloy nanoparticles in microchannel with partial slips and convective conditions,* **International Journal of Numerical Methods for Heat & Fluid Flow**,0961-5539,29, 10, .2019.

Shalini Anand, Jyoti Lamba, Pramod Kumar Rai,*Azolla microphylla extract ZnO nanoparticles and antibacterial activity: eco-friendly wastewater treatment, Nanotechnology for Environmental Engineering* ,**Journal of Inorganic and Organometallic Polymers and Materials** 2023

Shuaixuan Yinga Zhenru Guana Polycarp C.Ofoegbub Preston Clubbb Cyren Ricob Feng Hea JieHonga, *Green synthesis of nanoparticles: Current developments and limitations* **Environmental Technology & Innovation,** 26, 102336, 2022 https://doi.org/10.1016/ j.eti.2022.102336. ISSN:2352-1864**.**

Shveta Sharma, Ashish Kumar *Recent advances in metallic corrosion inhibition: A review,* **Journal ofMolecularLiquids** Volume 322, 2021, 114862, 2021.https://doi.org/10.1016/ j.molliq. 2020.114862

S. Bashir, A. Thakur, H. Lgaz, I.M. Chung, A. Kumar,*Corrosion inhibition performance of acarbose on mild steel corrosion in acidic medium: an experimental and computational study*,**Arab. J. Sci. Eng.,** 45, pp. 4773-4783,2020. 10.1007/s13369-020-04514-6

Surajit Dey, S.M.ASCE and Ravi Kiran, M.ASCE *Bio-Based Inhibitors to Mitigate Internal Corrosion in Crude Oil Pipelines*, **Pipelines** 2022, DOI:10.1061/9780784484289.009

S. Z. Salleh, A. H. Yusoff, Siti Koriah Zakaria, M. Taib, A. Abu Seman, M. N. Masri, M. Mohamad, S. Mamat, Sharizal Ahmad Sobri, Arlina Ali, P. Teo less. *Plant extracts as green corrosion inhibitor for ferrous metal alloys: A review*, **Journal of Cleaner Production**, 127030, 2021. https://doi.org/10.1016/

Taiwo F. Owoeye, Kehinde D. Akinlabu & Olayinka O. Ajani, *Proximate composition, phytochemical screening and mineral content studies of leaves extract of Adenanthera pavonina,* **Arab Journal of Basic and Applied Sciences**, 30:1, 317-328,2023. DOI: 10.1080/25765299.2023. 2215437

Tao Gao , Rongjun Bian , Stephen Joseph , Sarasadat Taherymoosavi , David R.G. Mitchell, Paul Munroe, Jianhong Xu, Jianrong Shi *Wheat straw vinegar: A more cost-effective solution than chemical fungicides for sustainable wheat plant protection.* **Science of the Total Environment,** 725,138359,2020. https://doi.org/10.1016.

Taye Kebede ,Eshetu Gadisa,,Abreham Tufa,, *Antimicrobial activities evaluation and phytochemical screening of some selected medicinal plants: A possible alternative in the treatment of multidrug-resistant microbes, **Pone**.0249253,*2021. ,https://doi.org/10.1371..

Tse-Lun Chen , Hyunook Kim , Shu-Yuan Pan , Po-Chih Tseng , Yi-Pin Lin , Pen-Chi Chiang *Implementation of green chemistry principles in circular economy system towards sustainable development goals: Challenges and perspectives.* **Science of the Total Environment,**716, 2020,136998. https://doi.org/10.1016

V. Saraswat, M. Yadav, *Carbon dots as green corrosion inhibitor for mild steel in HCl solution,* **ChemistrySelect**, 5, pp. 7347-7357,2020 10.1002/slct.202000625

P.Wei, W. Xue, Y.Zhao, G.Ning, J.Wang. *CRISPR-based modular assembly of a UAS-cDNA/ORF plasmid library for more than 5500 Drosophila genes conserved in humans*. **Genome Research.** 30 (1), 95-106, 2019.

Xianchun Zhu Kavitha Pathakoti, Huey-Min Hwang, *Green synthesis of titanium dioxide and zinc oxide nanoparticles and their usage for antimicrobial applications and environmental remediation,* **Micro and Nano Technologies** 223-263, 2019. https://doi.org/10.1016/B978-0-08-102579-6.000101.

X. He, J. Dan, and C. Hong, "Kinetics and thermodynamics studies of glycyrrhizic acid adsorption using s-8 macroporous resin," Asian Journal of Chemistry, vol. 25, no. 17, 2013, doi: 10.14233/ajchem.2013.15042.

Xuejie Li, Nixuan Gu,Teng Yi Huang,Feifeng Zhong, Gongyong Peng., *Pseudomonas aeruginosa: A typical biofilm forming pathogen and an emerging but underestimated pathogen in food processing*.**Front Microbiol**. 2022; 13: 1114199,Published online 2023,Jan 25. doi: 10.3389/fmicb.2022.1114199,PMCID: PMC9905436,PMID: 36762094

A.Yasser Selim, A. Maha Azb, Islam Ragab & H.M.Mohamed Abd El-Azim, *Green Synthesis of Zinc Oxide Nanoparticles Using Aqueous Extract of Deverra tortuosa and their Cytotoxic Activities,* **Scientific Reports** volume 10, Article number: 3445, 2020

Y. Al-Douri, K. Gherab, Khalid Mujasam Batoo, E. Raslan *Detecting the DNA of dengue serotype 2 using aluminium nanoparticle doped zinc oxide nanostructure: Synthesis, analysis and characterization,* **Journal of Materials Research and Technology** 9, 3, 5515-5523,2020. https://doi.org/10.1016/j.jmrt.2020.03.076

Yingchao Cui , Daosheng Wang , Clarissa,J. Nobile , Danfeng Dong , Qi Ni , Tongxuan Su , Cen Jiang , Yibing Peng, *Systematic identification and characterization of five transcription factors mediating the oxidative stress response in Candida albicans.* **micpath** ,Volume 187, 106507, 2024,https://doi.org/10.1016/

Yu Zhu, Li-Xiang Wang, Y. Behnamian, Shi-zhe Song, Ruiqi Wang, Zhiming Gao, Wenbin Hu, Da-Hai Xia less. *Metal pitting corrosion characterized by scanning acoustic microscopy and binary image processing.* **Corrosion Science**, 170, 2020, 108685.

Textbooks

[Lecture Text]Published: 21 November 2020, Strategies of metal corrosion protection,Su-Il Pyun, ChemTexts volume 7, Article number: 2 (2021)

Online Articles

Annual Global Cost of Corrosion: $2.5 Trillion | GlobalSpec, https://insights.globalspec.com/article/2340/annual-global-cost-of-corrosion-2-5-trillion

Corrosion costs the world an estimated $2.5 trillion USD – RCI | English (rcinet.ca), https://www.rcinet.ca/en/2021/04/24/corrosion-costs-the-world-an-estimated-2-5-trillion-usd/

Corrosion Prevention for Metals (thoughtco.com) https://www.thoughtco.com/

"Different Types of Corrosion: *Pitting Corrosion - Causes and Prevention".* corrosionclinic.com. **WebCorr** Corrosion Consulting Services.

Dynagard/Riserclad International Inc. Site Design. *Different-types-corrosion-inhibitors,* Available Online: https://www.dynagard.info/different-types-corrosion-inhibitors/

Factors Affecting Corrosion,https://unacademy.com/content/jee/study- material/chemistry/factors-affecting-corrosion/

Corrosion protection for car parts and safety (automotive-iq.com),https://www.automotive-iq.com/tag/automotive-corrosion, 02/08/2017.

Lug-All *Corrosive environments and factors* Available Online: (https://lug-all.com/blogs/blog/corrosive-environments-and-factors)

Syed Hasnain, Syed Hasnain Ali Pirzada,Corrosion in Oil and Gas Industries: A Review,November2022,https://www.researchgate.net/publication/365650732_Corrosion_in_Oil_and_Gas_Industries_A_Review.

What is Corrosion?: Factors Affecting, Types, Causes - Embibe What is Corrosion?: Factors Affecting, Types, Causes – Embibe,https://www.embibe.com/exams/corrosion

Marine Corrosion - Corrosion Types and What to Do About Them - PartsVu Xchange , https://www.partsvu.com/blog/marine-corrosion-corrosion-types-and-what-to-do-about-them/

Chapters in Book

Anass Nassef, Michael Keller, Shokrollah Hassani, Siamack Shirazi & Kenneth Roberts, A Review of Erosion-Corrosion Models for the Oil and Gas Industry Applications.Book Chapter, 2022. Recent Developments in Analytical Techniques for Corrosion Research pp 205–233, https://link.springer.com/chapter/10.1007/978-3-030-89101-5_10.

Derek Pletcher & Frank C. Walsh , Corrosion and its control, Book Chapter, **Industrial Electrochemistry** pp 481–542

Jennifer R. McCall , Ariel P. Brown , Kathryn T. Sausman , Samuel H. McCall IV. *Microalgae nanotechnology and drug development*.**Handbook of Microbial Nanotechnology,** Pages 169-190, 2022 https://doi.org/10.1016/B978-0-12-823426-6.00010-3,2022,.

Kisku, N. *Strengthening of High-Alloy Steel through Innovative Heat Treatment Routes.* **Welding-Modern Topics**. 2020. DOI:10.5772

L. K. M. O. Goni, M. Mazumder, **Materials Science** *Green Corrosion Inhibitors***,** Book Chapter , 2019,DOI:10.5772/INTECHOPEN.81376

R. Winston Revie and Herbert H. Uhlig, Corrosion and Corrosion Control, Book Copyright © 2008 John Wiley & Sons, Inc, Global web icon,https://onlinelibrary.wiley.com/doi/book/10.1002/9780470277270

The Monticello News, The Different Factors Affecting Corrosion, Book (2020), https://themonticellonews.com/the-different-factors-affecting-corrosion-p17173-147.htm

Uhlig, H H; Revie, R W,Corrosion and corrosion control. Third edition (Book) | OSTI.GOV, https://www.osti.gov/biblio/7195167, Publication Date:1985-01-01, OSTI Identifier:7195167

Appendix 1: Brief description of Plants used for the studies.

These are the various plants used

a) *Adonida merrilli*

b) Washingtonia robusta

c) Cassia javanica and

d) Casuarina equisetifolia.

Adonidia merrillii

Previously known as *Nomanbya merrilli* and *Veitchia merrillii*, the common names for *Adonidia merrilli* include Christmas palm, Dwarf Royal Palm, and Manila Palm. The Manila palm, also known as *Adonidia merrillii*, is a native of the Philippines (Palawan and Danjugan Island). (https://www.palmpedia.net/ /wiki/Adonidia_merrillii)

Washingtonia robusta

Washingtonia robusta, known by common name as the *Mexican fan palm, Mexican washingtonia*, or skyduster is a palm tree native to the Baja California peninsula and a small part of Sonora in northwestern Mexico. Despite its limited native distribution, W. robusta one of the most widely cultivated subtropical palms in the world. (https://plantcaretoday.com/washingtonia-robusta.html).

Cassia javanica

Cassia javanica

The Fabaceae family has a species of tree named *Cassia javanica*, sometimes referred to as the *Java cassia*, pink shower, or apple bloom tree and rainbow shower tree. While it originated in Southeast Asia, due to its stunning pink and red flower clusters, it has been widely planted as a garden tree across tropical regions of the world.(https://tropical.theferns.info/viewtropical.php?id =Cassia+javanica)

Casuarina equisetifolia

She-oak belonging to the Casuarina genus, *Casuarina equisetifolia*, is also known as the Outside of Australia, whistling pine trees or Australian pine trees. It is also known as Horsetail She-oak and Coastal She-oak. (https://www.cabidigitallibrary.org/doi/10.1079/cabicompendium.16718)

Appendix 2:Tables of various gravimetric results of Plant extracts and nanoparticles.

Table A: Weight loss and inhibition efficiency values for mild steel corrosion in 0.5 M H_2SO_4 at room temperature for day one

	Conc. Ppm (v/v)	Initial weight (g)	Final weight (g)	Weight loss (g)	Corrosion rate	Surface Coverage (Θ)	I.E (%)
BLANK		6.9664	3.5578	3.4086	10.6797	0	0
E	500	3.8129	1.2771	2.5358	7.9451	0.2561	25.6056
	1000	4.5554	3.7233	0.8321	2.6071	0.7559	75.5883
	1500	3.8824	0.6869	3.1955	10.0120	0.0625	6.2520
	2000	3.9728	0.6595	3.3133	10.3811	0.0279	2.7960
EZnO	500	5.8477	5.2100	0.6377	1.9980	0.8129	81.2916
	1000	4.1128	3.0350	1.0778	3.3769	0.6838	68.3802
	1500	5.8251	4.7561	1.069	3.3494	0.6864	68.6377
	2000	5.2321	4.5479	0.6842	2.1437	0.7993	79.9273
E-Al_2O_3	500	3.5171	0.3084	3.2087	10.0534	0.0586	5.8644
	1000	3.8125	0.4078	3.4047	10.6675	0.1142	1.1424
	1500	4.7516	1.6249	3.1267	9.7965	0.8261	8.2609
	2000	5.3273	2.3056	3.0217	9.4675	0.1135	11.3505

Table B : Weight loss and inhibition efficiency values for mild steel corrosion in 0.5 M H_2SO_4 at room temperature for day two.

	Conc. Ppm	Initial weight	Final weight	Weight loss (g)	Corrosion rate	Surface Coverage	I.E (%)

	(v/v)	(g)	(g)			(Θ)	
BLANK		6.9664	3.5578	3.4086	10.6797	0	0
E	500	7.9850	5.2340	2.7510	4.3097	0.3823	38.2255
	1000	7.440	6.0240	1.4160	2.2182	0.6820	68.2047
	1500	7.6280	4.0880	3.5400	5.5457	0.2051	20.5089
	2000	6.0760	3.2250	2.8510	4.4663	0.3598	35.9808
E-ZnO	500	6.0057	5.2601	0.7456	1.1680	0.8326	83.2581
	1000	8.9363	7.5866	1.3497	2.1144	0.6969	69.6930
	1500	6.3441	5.0466	1.2975	2.0327	0.7086	70.8638
	2000	5.4231	4.5264	0.8967	1.4048	0.7986	79.8638
E -Al_2O_3	500	7.2350	3.8420	3.3930	5.3154	0.2381	23.8099
	1000	6.2180	2.5859	3.6321	5.6900	0.1844	18.4405
	1500	5.8522	2.4725	3.3797	5.2946	0.2411	24.1081
	2000	7.100	4.1400	3.0400	4.7624	0.3174	31.7365

Table C: Table Weight loss and inhibition efficiency values for mild steel corrosion in 0.5 M H_2SO_4 at room temperature for day three.

	Conc. ppm	Initial weight	Final weight	Weight loss	Corrosion rate	Surface Coverage	I.E (%)

	(v/v)	(g)	(g)	(g)		(Θ)	
BLANK		6.4293	1.9760	4.4533	6.9765	0	0
E	500	13.5586	9.0339	4.5247	4.7256	0.2839	28.3881
	1000	7.1704	5.3716	1.7988	1.8787	0.7153	71.5301
	1500	6.9183	3.3062	3.6121	3.7724	0.4283	42.8329
	2000	9.8381	5.8641	3.9740	4.1504	0.3710	37.1047
E-ZnO	500	7.0078	6.1557	0.8521	0.8899	0.8651	86.5144
	1000	6.4532	4.5678	1.8854	1.9691	0.7016	70.1605
	1500	5.7432	4.0831	1.6601	1.7338	0.7372	73.7265
	2000	6.5642	5.3116	1.2526	1.3082	0.8017	80.1752
E- Al_2O_3	500	5.1210	1.0903	4.0307	4.2096	0.3627	36.2075
	1000	6.7355	2.6899	4.0456	4.2252	0.3597	35.9711
	1500	8.2627	4.1237	4.1390	4.3227	0.3449	34.4936
	2000	12.0056	7.7197	4.2859	4.4762	0.3217	32.1675

Table D: Table Weight loss and inhibition efficiency values for mild steel corrosion in 0.5 M H_2SO_4 at room temperature for day four

	Conc. ppm (v/v)	Initial weight (g)	Final weight (g)	Weight loss (g)	Corrosion rate	Surface Coverage (Θ)	I.E (%)

BLANK		16.1031	9.7847	6.3184	6.5989	0	0
E	500	7.0479	2.2755	4.7724	3.7382	0.3535	35.3543
	1000	5.8437	3.8305	2.0132	1.5769	0.7273	72.7303
	1500	9.3135	5.6070	3.7065	2.9033	0.4979	49.7925
	2000	8.8409	4.3892	4.4517	3.4869	0.3970	39.7001
E-ZnO	500	8.3236	7.3694	0.9542	0.7474	0.8708	87.0750
	1000	7.4466	5.3095	2.1371	1.6740	0.7105	71.0514
	1500	5.4631	3.6222	1.8409	1.4420	0.7506	75.0638
	2000	4.5231	3.4490	1.0741	0.8413	0.8545	85.4506
E- Al_2O_3	500	8.7906	4.3025	4.4881	3.5755	0.3921	39.2055
	1000	26.1108	21.9673	4.1435	3.2456	0.4387	43.8730
	1500	8.7906	4.3025	4.4881	3.5155	0.3921	39.2055
	2000	11.6848	6.7775	4.9073	3.8439	0.3353	33.5264

Table E: Table Weight loss and inhibition efficiency values for mild steel corrosion in 0.5 M H_2SO_4 at room temperature for day one.

	Conc. ppm (v/v)	Initial weight (g)	Final weight (g)	Weight loss (g)	Corrosion rate	Surface Coverage (Ɵ)	I.E (%)
BLANK		13.9454	6.5630	7.3824	5.7826	0	0

M	500	4.1978	0.9844	3.2134	10.0681	0.0575	5.7268
	1000	5.6139	2.7015	2.9124	9.1250	0.1456	14.5575
	1500	4.2849	1.8539	2.4310	7.6167	0.2868	28.6806
	2000	5.5530	3.5817	1.9713	6.1764	0.4217	42.1669
M-ZnO	500	3.0632	0.5231	2.5401	7.9586	0.2548	25.4792
	1000	3.2852	1.3050	1.9802	6.2043	0.4191	41.9056
	1500	4.8310	1.5292	3.3018	10.3451	0.3133	3.1330
	2000	3.6269	0.3457	3.2812	10.2806	0.3737	3.7370
M- Al_2O_3	500	3.4903	2.3168	1.1735	3.6768	0.5567	65.5721
	1000	3.9316	3.8062	0.1254	0.3929	0.9632	96.3211
	1500	3.0362	6.9702	2.2460	7.0371	0.3411	34.1077
	2000	3.8620	1.9707	1.8913	5.9258	0.4451	44.5134

Table F: Weight loss and inhibition efficiency values for mild steel corrosion in 0.5 M H_2SO_4 at room temperature for day two.

	Conc. ppm (v/v)	Initial weight (g)	Final weight (g)	Weight loss (g)	Corrosion rate	Surface Coverage (Θ)	I.E (%)
BLANK		13.9454	6.5630	7.3824	5.7826	0	0
M	500	4.1978	0.5547	3.6431	5.7072	0.1819	18.1939

	1000	23.0020	19.9888	3.0132	4.7204	0.3234	32.3386
	1500	8.4919	5.5467	2.9452	4.6139	0.3387	33.8651
	2000	7.9972	5.4651	2.5321	3.9668	0.4314	43.1405
M-ZnO	500	7.5580	4.7860	2.7720	4.3436	0.3775	37.7539
	1000	6.6581	4.6692	1.9889	3.1158	0.5534	55.3386
	1500	7.1704	1.4445	5.7259	8.9701	-0.2858	-28.5759
	2000	5.9309	1.1364	4.7945	7.5109	-0.0766	-7.6600
M- Al_2O_3	500	7.3185	5.5657	1.7528	2.7459	0.6064	60.6407
	1000	4.4470	1.4307	3.0163	0.0708	0.9899	98.9852
	1500	11.5340	8.5270	3.0070	4.7107	0.3248	32.4776
	2000	7.2135	4.7700	2.4435	3.8280	0.4513	45.1301

Table G: Weight loss and inhibition efficiency values for mild steel corrosion in 0.5 M H_2SO_4 at room temperature for day three.

	Conc. ppm (v/v)	Initial weight (g)	Final weight (g)	Weight loss (g)	Corrosion rate	Surface Coverage (Θ)	I.E (%)
BLANK		13.9454	6.5630	7.3824	5.7826	0	0
M	500	8.5921	4. 6421	3.9450	4.1201	0.3756	37.5638
	1000	9.6903	6.4563	3.2340	3.3776	0.4882	48.8157

	1500	7.4202	4.4057	3.0145	3.1483	0.5229	52.2905
	2000	12.4350	9.4937	2.9413	3.0719	0.5345	53.4483
M-ZnO	500	7.1665	2.8484	4.3181	4.5098	0.3166	31.6583
	1000	15.9011	13.7382	2.1629	2.2589	0.6577	65.7684
	1500	9.9950	4.5915	5.4035	5.6434	0.1448	14.4797
	2000	13.7014	9.3538	4.3476	4.5406	0.3119	31.1916
M- Al_2O_3	500	9.7386	7.1672	2.5714	2.6855	0.5930	59.3038
	1000	6.6309	6.5075	0.1234	0.1289	0.9805	98.0466
	1500	5.2868	0.3502	4.9366	5.1557	0.2187	21.8704
	2000	20.0722	15.9093	4.1629	4.3477	0.3411	34.1148

Table H: Weight loss and inhibition efficiency values for mild steel corrosion in 0.5 M H_2SO_4 at room temperature for day four.

	Conc. ppm (v/v)	Initial weight (g)	Final weight (g)	Weight loss (g)	Corrosion rate	Surface Coverage (Θ)	I.E (%)
BLANK		13.9454	6.5630	7.3824	5.7826		0
M	500	6.7826	2.5661	4.2135	3.3004	0.4293	42.9253
	1000	6.4467	2.5044	3.9423	3.0880	0.4659	46.5984
	1500	11.1798	7.7277	3.4521	2.7040	0.5324	53.2390

	2000	12.4350	9.1676	3.2674	2.5593	0.5574	55.7413
MZnO	500	6.6581	2.4632	4.1949	3.2856	0.4318	43.1778
	1000	12.3286	10.0946	2.2340	0.8864	0.6974	69.7385
	1500	7.1075	2.1201	4.9874	3.9066	0.3244	32.4422
	2000	8.0044	3.5598	4.4448	3.4816	0.3979	39.7918
M- Al_2O_3	500	6.7301	3.6268	3.1033	2.4308	0.5794	57.9356
	1000	13.5140	13.3594	0.1546	0.1211	0.9791	97.9056
	1500	9.6895	5.2301	4.4594	3.4930	0.3959	39.5946
	2000	6.7584	1.5583	5.2001	4.0732	0.2956	29.5611

Table I: Weight loss and inhibition efficiency values for mild steel corrosion in 0.5 M H_2SO_4 at room temperature for day one.

	Conc. ppm(v/v)	Initial weight (g)	Final weight (g)	Weight loss (g)	Corrosion rate	Surface Coverage (Ɵ)	I.E (%)
BLANK		13.9454	6.5630	7.3824	5.7826	0	0
NM	500	9.8978	5.9516	3.9462	12.3641	-0.1577	-15.7720
	1000	8.9540	4.9798	3.9742	12.4518	-0.1659	-16.5932
	1500	7.8455	4.2757	3.5698	11.1848	-0.0473	-4.7295
	2000	7.4732	4.4890	2.9842	9.3500	0.1245	12.4507

NM-ZnO	500	6.4789	2.4972	3.9817	12.4753	-16.8132	-0.1681
	1000	7.5568	3.9852	3.5716	11.1904	-4.7820	-0.04782
	1500	8.5462	4.9249	3.6213	11.3462	-6.2408	-0.0624
	2000	7.6232	4.0598	3.5634	11.1647	-4.5413	-0.0454
NM-Al_2O_3	500	8.6845	5.4505	3.234	10.1327	0.0512	5.1219
	1000	7.4532	4.4398	3.0134	9.4415	0.1222	12.2198
	1500	6.5533	3.7301	2.8232	8.8456	0.1717	17.1713
	2000	7.6502	5.3382	2.3120	7.2439	0.347	32.1713

Table J: Weight loss and inhibition efficiency values for mild steel corrosion in 0.5 M H_2SO_4 at room temperature for day two.

	Conc. ppm(v/v)	Initial weight (g)	Final weight (g)	Weight loss (g)	Corrosion rate	Surface Coverage (Θ)	I.E (%)
BLANK		13.9454	6.5630	7.3824	5.7826	0	0
NM	500	7.7846	2.7725	5.0121	7.8519	-0.1255	-12.5478
	1000	6.6654	1.6756	4.9848	7.8091	-0.1193	-11.9344
	1500	9.5540	4.9865	4.5675	7.1554	-0.0256	-2.5643
	2000	10.0120	5.9996	4.0124	6.2858	0.0449	4.4879
NM-	500	6.0084	1.0034	5.005	7.8408	-0.1239	-12.3887

ZnO	1000	6.7384	3.0171	3.7213	5.8297	0.1644	16.4380
	1500	6.0084	1.9952	4.0132	6.2870	0.0988	09.8832
	2000	7.2024	3.1366	4.0658	6.3694	0.0870	08.7021
NM-Al_2O_3	500	9.5432	5.5311	4.0121	6.2853	0.0991	09.9175
	1000	8.4722	4.559	3.9132	6.1304	0.1213	12.1279
	1500	7.3650	3.4666	3.8984	6.1072	0.1246	12.4604
	2000	8.4541	4.7757	3.6725	5.7625	0.1740	17.4013

Table K: Weight loss and inhibition efficiency values for mild steel corrosion in 0.5 M H_2SO_4 at room temperature for day three.

	Conc.ppm (v/v)	Initial weight(g)	Final weight(g)	Weight loss (g)	Corrosion rate	Surface Coverage (Θ)	I.E (%)
Blank		13.9454	6.5630	7.3824	5.7826	0	0
NM	500	10.9231	7.5099	3.4132	3.5647	0.4598	45.9804
	1000	11.8628	8.3427	3.5201	3.6764	0.4429	44.2877
	1500	12.7731	8.7868	3.9863	4.1633	0.3691	36.9092
	2000	10.6231	6.7219	3.9012	4.0744	0.3826	38.2564
NM-ZnO	500	7.3578	3.0064	4.3514	4.5446	0.3113	31.1309
	1000	7.36829	2.8947	4.4735	4.6721	0.2920	29.1988

	1500	7.3892	2.1845	5.2047	5.4357	0.176272	17.6272
	2000	6.7188	2.6597	4.0591	4.2393	0.3576	35.7575
NM-Al_2O_3	500	6.6094	1.4244	3.8942	4.0671	0.3837	38.3670
	1000	5.5389	0.3581	4.0012	4.1788	0.3667	36.6743
	1500	7.0319	3.0196	4.0123	4.1904	0.3650	36.4985
	2000	7.6554	2.1946	3.9876	4.1646	0.3689	36.8895

Table L: Weight loss and inhibition efficiency values for mild steel corrosion in 0.5 M H_2SO_4 at room temperature for day four.

	Conc. ppm(v/v)	Initial weight (g)	Final weight (g)	Weight loss (g)	Corrosion rate	Surface Coverage (Θ)	I.E (%)
BLANK		13.9454	6.5630	7.3824	5.7826	0	0
NM	500	12.4076	7.4838	4.9238	3.8568	0.3330	33.3034
	1000	11.5046	6.6344	4.8672	3.8124	0.3407	34.0712
	1500	9.6142	5.6400	3.9742	3.1130	0.4617	46.1661
	2000	8.7162	4.9368	3.7794	2,9604	0.4881	48.8050
NM-ZnO	500	10.7345	5.6131	5.1241	4.0116	30.6264	0.3063
	1000	9.8873	4.9341	4.9532	3.8798	0.3291	32.9056

	1500	8.7946	3.9202	4.8744	3.8181	0.3397	33.9726
	2000	9.6878	5.1044	4.5834	3.5901	0.3792	37.9155
NM-	500	9.8617	4.5165	5.3452	4.1869	0.2759	27.5949
Al_2O_3	1000	8.7780	4.3246	4.4534	3.4883	0.3968	39.6759
	1500	6.5754	2.611	3.9644	3.1053	0.4630	46.2992
	2000	5.6621	2.8523	2.8098	2.2009	0.6194	61.9393

Table M :Weight loss and inhibition efficiency values for mild steel corrosion in 0.5 M H_2SO_4 at room temperature for day one.

	Conc. ppm(v/v)	Initial weight(g)	Final weight(g)	Weight loss (g)	Corrosion rate	Surface Coverage (Θ)	I.E (%)
BLANK		13.9454	6.5630	7.3824	5.7826		0
C	500	6.7377	6.2101	0.5276	1.6531	0.8452	84.5211
	1000	4.7520	2.9616	1.7904	5.6096	0.4747	47.4742
	1500	5.2647	2.8238	2.4409	7.6476	28.3912	28.3912
	2000	6.3262	3.2046	3.2116	9.7805	0.8420	8.4197
C-ZnO	500	6.8843	3.7619	3.1224	9.7830	0.08396	08.3963
	1000	7.6542	4.8310	2.8232	8.8456	0.1717	17.1737
	1500	7.7712	5.4290	2.3422	7.3385	0.3129	31.2855

	2000	6.8845	4.9033	1.9812	6.2074	0.4188	41.8767
C-	500	9.9673	5.8752	4.0921	12.8212	-0.2005	-20.0521
Al_2O_3	1000	8.8656	5.0416	3.824	11.9812	-0.1218	-12.1867
	1500	9.9547	5.9631	3.9916	12.5064	-0.1710	-17.1044
	2000	7.8765	4.3121	3.5644	11.1679	-0.04571	-4.5713

Table N :Weight loss and inhibition efficiency values for mild steel corrosion in 0.5 M H_2SO_4 at room temperature for day two .

	Conc.ppm (v/v)	Initial weight(g)	Final weight(g)	Weight loss(g)	Corrosion rate	Surface Coverage (Θ)	I.E (%)
Blank		13.9454	6.5630	7.3824	5.7826		0
C	500	7.1051	6.2702	0.8349	1.3079	0.8125	81.2528
	1000	8.2234	5.6701	2.5533	3.9999	0.4266	42.6661
	1500	6.7521	3.5624	3.1897	4.9969	0.2838	28.3753
	2000	5.2867	1.5447	3.7420	5.8622	0.1597	15.9722
C-ZnO	500	6.6635	1.7332	4.9303	7.7237	-0.1071	-10.7102
	1000	6.1494	0.5628	5.5866	8.7519	-0.0255	-25.4483
	1500	8.6097	4.4100	4.1997	6.5792	0.05695	5.6948
	2000	5.6755	1.4078	4.2677	6.6857	0.04168	04.1783

C-Al_2O_3	500	6.0718	1.0215	5.0503	7.9117	-0.1340	-13.4050
	1000	7.1595	2.8356	4.3239	6.7738	0.0291	-02.9055
	1500	7.3000	3.3025	3.9975	6.2624	0.1024	10.2358
	2000	6.1547	1.4026	4.7521	7.4446	-0.06.710	-06.7097

Table O: Weight loss and inhibition efficiency values for mild steel corrosion in 0.5 M H_2SO_4 at room temperature for day three .

	Conc.ppm (v/v)	Initial weight(g)	Final weight(g)	Weight loss (g)	Corrosion rate	Surface Coverage (Θ)	I.E (%)
BLANK		13.9454	6.5630	7.3824	5.7826		0
C	500	8.0068	7.1456	0.8612	0.8994	0.8637	86.3705
	1000	6.0383	3.1630	2.8753	3.0029	0.5449	54.4939
	1500	6.2757	1.2512	5.0245	5.2475	0.2048	20.4792
	2000	8.9840	3.4814	5.1023	5.3288	0.1925	19.2471
C-ZnO	500	5.6203	0.1451	5.7654	6.0213	0.0875	08.7530
	1000	6.2643	0.3776	5.8867	6.1480	0.06833	06.8330
	1500	7.3602	1.7846	5.5756	5.8231	0.1178	11.7565
	2000	6.2114	1.5977	4.6137	4.8185	0.2698	26.9803
C-	500	7.0479	3.0930	3.9549	4.1305	0.3640	37.4062

Al_2O_3	1000	8.5007	2.8102	5.6905	5.9432	0.994	09.9365
	1500	6.8409	1.5699	5.2710	5.5050	0.1658	16.5770
	2000	6.7946	1.2894	5.5052	5.7496	0.1287	12.8703

Table P: Weight loss and inhibition efficiency values for mild steel corrosion in 0.5 M H_2SO_4 at room temperature for day four.

	Conc. ppm (v/v)	Initial weight (g)	Final weight (g)	Weight loss (g)	Corrosion rate	Surface Coverage (Ɵ)	I.E (%)
BLANK		13.9454	6.5630	7.3824	5.7826	0	0
C	500	9.3226	8.3582	0.9644	0.7554	0.8694	86.9367
	1000	8.0756	4.3620	3.7136	2.9088	0.49697	49.6974
	1500	7.7573	2.5472	5.2101	4.0810	0.2943	29.4262
	2000	9.7584	4.4853	5.2731	4.1304	0.2857	28.5719
C-ZnO	500	10.9245	6.3783	5.5462	4.3443	0.2487	24.8729
	1000	8.5876	4.6222	3.9654	3.1061	0.4629	46.2854
	1500	8.6792	4.8138	3.8654	3.0277	0.4764	47.6412
	2000	9.7745	6.9733	2.8012	2.1942	0.6206	62.0551
C- Al_2O_3	500	9.9846	4.8831	5.1015	3.9960	0.3090	30.8961

1000	12.1013	7.1501	4.9512	3.8782	0.3293	32.9333
1500	11.2330	6.3507	4.8823	3.8243	0.3386	33.8786
2000	12.9846	8.3022	4.6824	3.6677	0.3657	36.5735

Appendix 3 :Tables of various Electrochemical Results of Plant Extracts and Nanoparticles.

Table A.: Electrochemical Measurements of Inhibitors (Extracts) from 500 ppm, 1000 ppm, 1500 ppm, 2000 ppm of 0.5 M of H_2S0_4 Concentration.

Parameter	Concentration (ppm)	Ecorr	Jcorr	Corrosion rate (mm/yr)	Polarization I.E(μ)	I.E(%)	Surface coverage
M	500	-0.51307	1.4577E-10	1.6938E-06	4.5596E+06	-7.1744	-0.07171
M 500 1000 1500 2000	1000	-0.48786	3.7563E-10	4.3648E-06	3.3549E+06	-185.9164	-1.8592
	1500	-0.29104	6.3684E-10	7.4E-06	1.3374E+06	-384.7373	-3.8474
	2000	-0.26978	5.655E-10	6.5711E-06	1.2765E+06	-330.4402	-3.3044
NM	500	-0.41426	5.893E-10	6.8476E-06	2.17229E+06	-348.5523	-3.4853
1000 1500 2000	1000	-0.40256	2.2655E-10	2.6325E-06	2.7164E+06	-72.4420	-0.7244
	1500	-0.40101	3.2788E-10	3.8099E-06	1.863E+06	-149.5677	-1.4957
	2000	-0.628789	1.7757E-10	4.0275E-06	4.2276E+06	-163.8216	-1.6382

E	500	-0.48184	1.9598E-10	6.8476E-06	6.4503E+06	-49.1746	-0.4917
1000	1000	-0.47492	6.21835E-11	2.6325E-06	1.3191E+07	52.6687	0.5267
1500	1500	-0.36083	1.4338E-10	3.8099E-06	6.3507E+06	-99.1380	-0.9914
2000	2000	-0.4570	3..0788E-10	4.0275E-06	2.3726E+06	-134.3443	-1.3434
C	500	-0.45007	1.756E-11	2.0405E-07	1.9013E+07	86.6337	0.8663
1000	1000	-0.43348	1.1285E-10	1.3113E-06	4.789E+06	14.1032	0.1410
1500	1500	-0.47163	3.7399E-10	4.3457E-06	9.4162E+05	-184.6653	-1.8467
2000	2000	-0.43721	3.273E-10	3.8032E-06	2.1164E+06	-149.1288	-1.4913

Table B: Electrochemical Measurements of Inhibitors (Zinc Oxide Nanoparticles) from 500 ppm, 1000 ppm, 1500 ppm, 2000 ppm of 0.5 M of H_2SO_4 Concentration.

Parameter	Concentration	Ecorr (obs)U	Jcorr (A/cm^3)	Corrosion rate (mm/yr)	polarization Resistance (Ω)	I.E (%)	Surface Coverage ∅
M-ZnONP	500	-0.37757	$1.1967E^{-10}$	$1.3906E^{-06}$	$6.374E^{+06}$	8.9087	0.0890
	1000	-0.34812	$1.0559E^{-10}$	$1.2269E^{-06}$	$6.7422E^{+06}$	19.6318	0.1963
	1500	-0.35502	$2.4379E^{-10}$	$2.8328E^{-06}$	$2.5508E^{+06}$	-85.5627	-0.8556
	2000	-0.3389	$3.3302E^{-10}$	$3.8697E^{-06}$	$2.7241E^{+06}$	-153.485	-1.5348
NM-ZnONP	500	-0.34935	$3.1218E^{-10}$	$3.6275E^{-06}$	$4.3047E^{+06}$	-9014	-90.1400
	1000	-0.31966	$1.5764E^{-10}$	$1.8318E^{-06}$	$3.9899E^{-06}$	-137.62	-1.3762
	1500	-0.29715	$1.5605E^{-10}$	$1.8133E^{-06}$	$5.1555E^{+06}$	-19.9921	-0.1999
	20000	-0.31879	$1.4434E^{-10}$	$1.6772E^{-06}$	$4.5014E^{+06}$	-9.8651	-0.0987
E-ZnONP	500	-0.58703	9.2859E-12	1.079E-07	6.4551E07	92.9320	0.00939

	1000	-0.61863	2.4319E-11	2.8259E07	2.5937E07	81.4948	0.0081
	1500	-0.59679	2.2345E-11	2.5965E-07	2.6323E07	82.9916	0.0083
	2000	-0.57015	3.9457E-11	4.58.49E	1.7041E07	88.8373	0.0089
C-ZnONP	500	-048983	2.7237E-10	3.1649E-06	5.6036E06	-107.3169	-1.0732
	1000	-0.48322	4.0746E-10	4.7347E-06	1.7322E06	-210.1467	-2.1015
	1500	-0.44083	2.7636E-10	3.2113E-06	4.582E06	-110.3563	-1.1036
	2000	-0.38946	1.7017E-10	1.9774E-06	4.2827E06	30.0833	-0.3008
	Blank	0.61733	1.3138E-10	1.5266E-06	1.508E07	0	0

Table C:Electrochemical Measurements of Inhibitors (Aluminum Oxide Nanoparticles) from 500 ppm, 1000 ppm, 1500 ppm, 2000 ppm of 0.5 M of H_2SO_4 Concentration.

Parameter (ppm)	Ecorr (obs)v	Jcorr (A/cm^2)	Corrosion Rate(mm/yr)	Polarization Resistance (n)	I.E%	Surface coverage (θ)
M-AI_2O_3NP						
500	-0.55026	9.2801E-11	1.0783E-06	1.1417E+07	29.0000	0.2900
1000	-0.54783	5.0702E-11	5.8915E-07	1.3974E-07	61.4077	0.6141
1500	-0.51220	1.6118E-10	1.8729E-06	6.3811E-06	-22.6844	-0.2268
2000	-0.51300	1.4577E-10	1.6938E-06	4.5596E+06	-10.9524	-0.1095
NM-AI_2O_3NP						
500	-0.48786	3.7563E-10	4.3648E-06	3.3549E+06	-185.9164	-1.8592
1000	-0.48237	2.414E-10	2.8051E-06	2.2649E+06	-83.7482	-0.8375
1500	-0.47505	1.7515E-10	2.0352E-06	4.9149E+06	-33.3159	-0.3332
2000	-0.41366	3.4247E-10	3.9795E-06	2.7977E+06	-160.6773	-1.6068
E- AI_2O_3NP						
500	-0.3551	$1.3888E^{-10}$	$1.6138E^{-06}$	$8.5395E^{+06}$	-5.7120	-0.0571

1000	-0.2357	$2.8522E^{-10}$	$3.3142E^{-06}$	$3.3142E^{-06}$	-117.0968	-1.1709
1500	-0.2401	$2.6086E^{-10}$	$3.0312E^{-06}$	$3.043E^{+06}$	-99.5589	- 0.9955
2000	-0.26407	$2.5122E^{-10}$	$2.9199E^{-06}$	$2.4705E^{+06}$	-91.2695	-0.9127
C- AI_2O_3NP						
500	-0.50823	3.3677E-10	3.9132E-06	3.9132E-06	-156.3343	-1.5633
1000	0.21985	2.87.94E-10	3.3458E-06	2.9807E06	-119.1668	-1.1917
1500	0.22646	2.3259E-10	2.2027E-06	2.6248E06	-77.0405	-0.7704
2000	-0.3385	2.267E-10	2.6342E-06	3.5848E06	-72.5534	-0.7255

Bio-Data

A Personal Data

Full Names : Taiwo Felicia OWOEYE

Date of Birth : 3rd January 1976

Place of Birth : Omu-Aran

Local Government of Birth : Irepodun

State of Origin: Kwara State

Local Government Area : Irepodun

Nationality : Nigerian

Postal Address: Department of Chemistry, Covenant University, Km10, Idiroko Road, P.M.B.1023, Ota, Ogun, State,

Home Address: 1A, Bashiru Oshun street, New Iyesi lay-out, Iyesi, Ota.

Marital Status: Married

Religion : Christianity

E-Mail Address: felicia.owoeye@covenantuniversity.edu.ng

Alternative E-Mail: oluwaletofunmi@gmail.com

Mobile Phone Contact: +234-903-234-0113.

B Education Background

Lead City University, Ibadan PhD in view 2025

Bell University of Technology Ota M.Sc. (Industrial-Chemistry) 2021

Bell University of Technology Ota	B.Sc. (Chemistry)	2019
University of Ilorin, Ilorin.	HND	2001
Kwara State Polytechnic Ilorin.	OND	1997
West African Examinations Council	S.S.C.E	2015
Government Secondary School Afon, Kwara State	S.S.C.E.	1993
Zonal Education Board Primary School, Oke-Oyi		1981-1997

C Awards

- Most Outstanding Technologists in Chemistry during the **2012/2013** academic session.
- Most Outstanding Technologists in Chemistry during the **2013/2014** academic session.
- Winners of the 2nd Prize in the Individual (Research) by group of disciplines Agriculture and Veterinary Medicine Category At 6thNigerian Universities Research and Development Fair Organized by National Universities Commission at Nnamdi Azikiwe University, Awka. **(7th-11th March,2016).**
- Overall best Outstanding Presentation at Exhibition Competition held at the Bells University of Technology. **(2nd-4th November 2016).**
- Certificates of Patent Registration awarded by the Federal Government of through the Federal Ministry of Science Technology, Abuja in December. (**2018).**
- First Female Researcher in Covenant University to register Patent (Maiden Magazine Produced by CUCRID2019). (**2019).**
- Certificate of Gold Award in honour of the best Presentation and Outstanding Creativity and Innovativeness of the Invention Entitled ADPL Seed Extracts exhibited at World Invention Creativity Olympic 2020 (WICO).(**Aug 2020).**
- Certificate Of Gold award in honour of the best Presentation and outstanding Creativity of the invention entitled ADPL Seed extracts exhibited At Africa OCCIP Expo 2020 (Innovation for inclusive development in Africa),(**November 2020).**
- Certificate of Appreciation from Science Olympiad Nigeria Division A & B National Tournament during ‘’New Horizons of Discovery’’ **(July 2024)**

D Publications in Accredited/Peer-Reviewed Scientific Journals. (Scopus Indexed).

1) **Owoeye, T.F.**, Bamisaye, A., Adekoya, J.A., Afolalu, S.A., Monye, S.I., Oluwatoyin, O.A.2024,Biosynthesis, characterization, and antimicrobial study of zinc oxide nanoparticles using Adonida merrilli leaf extract, International Conference on Science, Engineering and Business for Driving Sustainable Development Goals, SEB4SDG 2024*, 2024*
2) **Owoeye, T.F**., Bamisaye, A., Eterigho, E.M., Afolalu,S.A., Monye, S.I., Oluwatoyin, O.A. 2024,Eco-friendly synthesis, characterization, and antimicrobial studies of Zinc

oxide nanoparticles using Cassia Javanica Leaf extract, International Conference on Science, Engineering and Business for Driving Sustainable Development Goals, SEB4SDG 2024, 2024

3) Akinlabu, KD Akinlabu, **TF Owoeye**, ME Emetere, HO Jonathan, DI Owoeye, PO Akinlabu.2024 Investigation of Proximate Analysis and Phytochemical Screening of Dry Orange Waste (Citrus sinensis) Extract: From Agrowaste to Sustainable Development,*IOP Conference Series: Earth and Environmental Science*, 2024, 1342(1), 012016
4) Dauda, K.T., **Owoeye, T.F**., Akande, I.G., Fayomi, O.S.I. 2023,Evaluation of Corrosion Inhibition and Adsorption Effect of Aqueous Chrysophyllum Albidum Leaves and Peels Extract on Mild Steel in Acidic Medium.*Protection of Metals and Physical Chemistry of Surfaces*, 2023, 59(6), pp. 1290–1297.
5) Dauda, K.T., **Owoeye, T.F**., Fayomi, O.S.I., Akande, I.G. 2023 Ethanolic extract of Chrysophyllum albidum leaves and peels as a green inhibitor for AISI 1015 carbon steel in 1M H_2SO_4 solution,*Vietnam Journal of Chemistry*, 2023, 61(2), pp. 178–186
6) **Owoeye, T.F**., Akinlabu, K.D., Ajani, O.O. 2023 Proximate composition, phytochemical screening and mineral content studies of leaves extract of Adenanthera pavonina
Arab Journal of Basic and Applied Sciences*, 2023, 30(1), pp. 317–328. Article* • Open access
7) **Owoeye T.F.,**Akinlabu D.K.,Ajayi O.O.,Afolalu S.A.,Popoola J.O.,Ajani O.O. 2022 Phytochemical constituents and proximate analysis of dry pineapple peels *IOP Conference Series: Earth and Environmental Science Open Access* Volume 993, Issue 129 March 2022 Article number 0120275th International Conference on Science and Sustainable Development, ICSSD 2021Ota, Virtual11 October 2021 through 13 October 2021Code 178213
8) Essien, Enobong R. Atasie, Violette N.;Nwude, Davies O.;Adekolurejo, Ezekiel;**Owoeye, Felicia T.** (2022)Characterisation of ZnO nanoparticles prepared using aqueous leaf extracts of Chromolaena odorata (L.) and Manihot esculenta (Crantz) *South African Journal of ScienceOpen Access*Volume 118, Issue 1122022 Article number #11225
9) Efemwenkiekie K.U.,Oyedepo S.O.Giwa S.O.·Sharifpur M.·**Owoeye T.F**.Akinlabu K.D.·Meyer J.P.(2021) Experimental investigation of heat transfer performance of novel bio-extract doped mono and hybrid nanofluids in a radiator.*Case Studies in Thermal EngineeringOpen Access*Volume 28December 2021 Article number 101494 Article• *Gold Open Access* Journal, 2214157X, 10.1016/j.csite.2021.101494
10) Olayinka O. Ajani,**Taiwo Felicia Owoeye**,Kehinde Deborah Akinlabu,Oladotun Bolade,Oluwatimilehin E.Aribisala,Bamidele M. Durodola.(2021). Sorghum extract: Phytochemical, proximate, and GC-MS analysesNovember 2021,Foods and Raw Materials 9(2):371-378,Follow journal DOI:10.21603/2308-4057-2021-2-371-378.
11) Banjo S.O. Fayomi O.S.I. Atayero A.A.A. Bolaji B.O .Dirisu J.O. ,Okeniyi J. Emetere M.E. Olorunfemi B.J., **Owoeye T.F** (2021). Effect of Fins spacing on the Performance Evaluation of a Refrigeration System using LPG as Refrigerantion OP Conference Series: Earth and Environmental Science,665(1), 012030
12) Emetere, M.E., Jack-Quincy, S., Aro, S.I., Okonwo O.D. **Owoeye, F.T**., Sanni, S.E. Biofuels, (2020) Validation of biodiesel quality of Monodora myristica and Moringa oleifera using regression and error analysis of UV absorption results 11(2), pp. 163–173
13) Emetere M.E.Jack-Quincy S.Aro S.I.Okonwo O.D. **Owoeye F.T**.,Sanni S.E. (2019). Validation of biodiesel quality of Monodora myristica and Moringa oleifera using regression and error analysis of UV absorption results*Journal of Physics: Conference SeriesOpen Access*Volume 1378, Issue 318 December Article number 0320573rd

International Conference on Engineering for Sustainable World, ICESW 2019, Ota, 3 July 2019 - 8 July 2019, 156325

14) Afolalu S.A., Olusegun S.D.,**Taiwo O.F**., Bello K.A.(2019)Morphological and mechanical behaviour of welded joint of a steel using nano-flux powder (MnO) from agrowaste (banana peel) during Mig welding*International Journal of Engineering Research and Technology*Volume 12, Issue 12, Pages 2884 – 28932019, Article, Journal,ISSN,09743154
15) Abioye A.A.,Rotimi D.O.,Fasanmi O.O.,Abioye O.P.,Afolalu S.A.,**Owoeye T.F**.,Ajayi O.O.,Obuekwe C.C. Synthesis and Characterization of Selected Starch Nanoparticles as Matrix Reinforcements for Low Density Polyethylene*Journal of Physics: Conference Series Open Access*Volume 1378, Issue 418 December 2019 Article number 0420703rd International Conference on Engineering for Sustainable World, ICESW 2019, Ota, 3 July 2019 - 8 July 2019, 156325
16) Ajayi O.O.,Ukasoanya D.E,.Ogbonnaya M,.Salawu E.Y.,Okokpujie I.P,.Akinlabi S.A.,Akinlabi E.T, **Owoeye F.T**.(2019)Investigation of the effect of R134a/Al_2O_3 -nanofluid on the performance of a domestic vapour compression refrigeration system*Procedia ManufacturingOpen Access*Volume 35, Pages 112 - 1172019 2nd International Conference on Sustainable Materials Processing and Manufacturing, SMPM 2019, Sun City, 8 March 2019 - 10 March 2019, 151557
17) Ajayi O.O.,Aba-Onukaogu C.C.,Salawu E.Y.,**Owoeye F.T**.,Akinlabu D.K.,Popoola A.P.I.,Afolalu S.A.,Abioye A.A. (2019) Effect of Biomaterial (Citrullus Lanatus Peels) Nanolubricant on the Thermal Performance and Energy Consumption of R600a in Refrigeration System *Minerals, Metals and Materials Series*Pages 91 - 1022019 Energy Technologies Symposium held at the TMS Annual Meeting and Exhibition, 2019, San Antonio, 10 March 2019 - 14 March 2019, 224859
18) Ajayi O.O.,Okolo T.I.,Salawu E.Y.,**Owoeye F.T**.,Akinlabu D.K.,Akinlabi E.T.,Akinlabi S.T.,Afolalu S.A. (2019)Performance and Energy Consumption Analyses of R290/Bio-Based Nanolubricant as a Replacement for R22 Refrigerant in Air-Conditioning System*Minerals, Metals and Materials Series*Pages 103 - 1122019 Energy Technologies Symposium held at the TMS Annual Meeting and Exhibition, 2019, San Antonio, 10 March 2019 - 14 March 2019, 224859
19) Ajani, O.O., Jolayemi, E.G., Owolabi, F.E., Aderohunmu, D.V., Akinsiku, A.A. and **Owoeye, F.T**. (2019). Dimethylformamide-mediated synthesis and characterization of novel pyrazole- and pyrimidine-based 3,4-dihydropyrimidine-2(1*H*)-thione derivatives. *IOP Conference Series: Journal of Physics*, 1299, 012117. http://dx.org/doi:10.1088/1742-6596/1299/1/012117 (Scopus Indexed).
20) Ajani, O.O., **Owoeye, F.T**., Owolabi, F.E., Akinlabu, D.K. and Audu, O.Y. (2019). Phytochemical screening and nutraceutical potential of sandbox tree.*(Hura crepitans* L.) seed oil. *Foods and Raw Materials* 7(1), 143-150.
21) Olanrewaju I.O.Mordi R.C.Echeme J.O. **Owoeye T.F**.Ejilude O.,Aruwajoye A.O.(2019) Anti-mycobacterial and GC-MS Studies of Irvingia gabonensis Baill Ex. Lanen Stem Extracts *Journal of Physics: Conference SeriesOpen Access*Volume 1378, Issue 418 December Article number 0421013rd International Conference on Engineering for Sustainable World, ICESW 2019, Ota, 3 July 2019 - 8 July 2019, 156325
22) Ajayi O.O,.Ukasoanya D.E,.**Owoeye F.T**,.Salawu E.Y,.Ohijeagbon I.O,.Oyawale F.A,.Agarana M.C,(2018)Experimental investigation into the effects of al-composite nanolubricants on the energy and exergy performance of vapour compression refrigerator compressor.*Lecture Notes in Engineering and Computer Science*Volume 2236, Pages 773 - 7772018 2018 World Congress on Engineering, WCE 2018, London, 4 July 2018 - 6 July 2018, 147866

23) Ajayi O.O,.Omowa O.F,.Abioye O.P,.Omotosho O.A,.Akinlabi E.T,.Akinlabi S.A,.Abioye A.A,. **Owoeye F.T**.Afolalu S.A.2018 Finite element modelling of electrokinetic deposition of zinc on mild steel with ZnO-citrus sinensis as nano-additive*Minerals, Metals and Materials Series*Volume Part F3, Pages 199 - 2112018 International Symposium on CFD Modeling and Simulation in Materials Processing, 2018, Phoenix, 11 March 2018 - 15 March 2018, 210849
24) Okeniyi, J.O., Okeniyi, E.T., Ogunlana, O.O., **Owoeye, T.F**., Ogunlana, O.E.(2017)Investigating biochemical constituents of Cymbopogon citratus leaf: Prospects on total corrosion of concrete steel-reinforcement in acidic-sulphate mediumMinerals, Metals and Materials Series,Part F6, pp. 341–351 Conference Paper.
25) **Owoeye T.F.,** Ajani O.O., Akinlabu D.K. and Ayanda O.I. (2017). Proximate composition, structural characterization and phytochemical screening of the seed oil of *Adenanthera pavonina* linn. *Rasayan Journal of Chemistry 10(3):* 807-814. (ISSN: 0974-1496); ISI Indexed (Thomson Reuter) and Scopus Index.
26) Ajanaku C.O., Echeme J.O., Mordi R.C., Ajani O.O., Olugbuyiro J.A.O., **Owoeye T.F**., Taiwo O.S. and Ataboh J.U. (2016). Phytochemical screening and antimicrobial studies of *Cratevaadasonii* leaf extract. *Covenant Journal of Physical & Life Sciences 4(2):* 35-41.
27) Okeniyi J.O.,Omotosho O.A.,Inyang M.A.,Okeniyi E.T.Nwaokorie I.T,.Adidi E.A.,**Owoeye T.F**.,Nwakudu K.C.,Akinlabu D.K.Gabriel O.O.,Taiwo O.S.,Awotoye O.A (2016) Investigating inhibition of microbes inducing microbiologically-influenced-corrosion by Tectona grandis based Fe-nanoparticle material *AIP Conference Proceedings*Volume 181423 February 2017 Article number 020034International Conference on Technologies and Materials for Renewable Energy, Environment and Sustainability Fall Meeting, TMREES 2016-Cnam, Paris, 16 November 2016 - 18 November 2016, 126555
28) Ajani O.O., **Owoeye T.F**., Olasehinde G.I., Audu O.Y., Owolabi F.E., Akinlabu D.K. and Edobor-Osoh, A. (2016). Preliminary studies on the seed oil of *Caryota mitis*: Proximate composition, phytochemical screening and evaluation of antimicrobial activity. *American Journal of Food Technology 11(6):* 253-263. (ISSN: 1557-4571). Scopus Indexed.
29) Ajani O.O., **Owoeye T.F.,** Olasehinde G.I., Akinlabu D.K., Owolabi F.E. and Audu O.Y. (2016). Characterization, proximate composition and evaluation of antimicrobial activity of seed oil of *Bauhinia tomentosa*. *Journal of Biological Sciences 16(4):* 102-111. (ISSN: 1727-3048); ISI (Thomson Reuter) and Scopus Indexed.
30) Okeniyi J.O.,Omotosho O.A.,Inyang M.A.,Okeniyi E.T.Nwaokorie I.T.,Adidi E.A.,**Owoeye T.F.**,Nwakudu K.C.,Akinlabu D.K.,Gabriel O.O.,Taiwo O.S.,Awotoye O.A. Effects of Dialium guineense based zinc nanoparticle material on the inhibition of microbes inducing microbiologically influenced corrosionIssue 9783319521312, Pages 21 – 312017
31) Okeniyi J.O.,John G.S.,**Owoeye T.F**.Okeniyi E.T.,Akinlabu D.K.,Taiwo O.S.,Awotoye O.A.Ige O.J.,Obafemi Y.D.(2017)Effects of Dialium guineense Based Zinc Nanoparticle Material on the Inhibition of Microbes Inducing Microbiologically Influenced Corrosion. February 2017,DOI:10.1007/978-3-319-52132-9_3,In book: Proceedings of the 3rd Pan American Materials Congress.
32) Okeniyi, J.O., Okeniyi, E.T., **Owoeye, T.F**.(2016)Bio-characterisation of Solanum aethiopicum leaf: prospect on steel-rebar total-corrosion in chloride-contaminated-environment.Progress in Industrial Ecology, 2016, 10(4), pp. 414–426. Conference Paper.

33) Olasehinde G.I.,Akinlabu D.K., **Owoeye F.T.**,Owolabi E.F.,Audu O.Y.,Mordi R.C.(2016) Phytochemical and antimicrobial properties of oil extracts from the seeds of Ricinodendron heudelotii *Research Journal of Medicinal PlantOpen Access* Volume 10, Issue 5, Pages 362 – 3652016
34) Mordi R.C.,Fadiaro A.E.,**Owoeye T.F**.,Olanrewaju I.O.,Uzoamaka G.C.,Olorunshola S.J. (2016)Identification by GC-MS of the components of oils of banana peels extract, phytochemical and antimicrobial analyses *Research Journal of PhytochemistryOpen Access* Volume 10, Issue 1, Pages 39 – 442016
35) Ajani O.O., Ajayi O., Adekoya J.A., **Owoeye T.F**., Durodola B.M. and Ogunleye O.M. (2016). Comparative study of microwave-assisted and conventional synthesis of 3-[1-(*s*-phenylimino)ethyl]-2*H*-chromen-2-ones and selected hydrazone derivatives. *Journal of Applied Sciences 16(3):* 77-87. (ISSN: 1812-5654); ISI Indexed (Thomson Reuter).
36) Ajani O.O., Isaac J.T., **Owoeye T.F**. and Akinsiku A.A. (2015). Exploration of the chemistry and biological properties of pyrimidine as a privileged pharmacophore in therapeutics. *International Journal of Biological Chemistry 9:* 148-177. (ISSN: 1819-155X); Scopus Indexed.
37) Okeniyi J.O.,Omotosho O.A.,Ogunlana O.O.,Okeniyi E.T.,**Owoeye T.F**.,Ogbiye A.S.,Ogunlana O.E.(2015)Investigating Prospects of Phyllanthus Muellerianus as Eco-friendly/Sustainable Material for Reducing Concrete Steel-reinforcement Corrosion in Industrial/Microbial Environment *Energy ProcediaOpen Access*Volume 74, Pages 1274 - 12812015 International Conference on Technologies and Materials for Renewable Energy, Environment and Sustainability, TMREES 2015, Beirut, 17 April 2015 - 20 April 2015, 114873
38) Akinlabu, D.K., **Owoeye, T.F**., Owolabi, F.E., Audu, O.Y., Ajanaku, C.O., Falope, F. and Ajani, O.O. (2019). Phytochemical and proximate analysis of African oil bean (*Pentaclethra macrophylla* Benth) seed. International Conference on Engineering for a Sustainable World, ICESW (Scopus Indexed).
39) Ajani, O.O., Jolayemi, E.G., Owolabi, F.E., Aderohunmu, D.V., Akinsiku, A.A. and **Owoeye, F.T**. (2019). Dimethylformamide-mediated synthesis and characterization of novel pyrazole- and pyrimidine-based 3,4-dihydropyrimidine-2(1H)-thione derivatives. Conference Proceeding of the International Conference on Science and Sustainable Development, ICSSD (Scopus Indexed).

Local Journals

1) Ajani, O.O., Owolabi, F.E., **Owoeye, F.T**., Olanrewaju, I.O. and Edobor-Osoh, A(2018).Acetic acid catalyzed synthesis and structural characterization of hydrazide hydrazone of 4,5,6-trisubstituted pyrimidin-2(1H)-one derivatives. Presentation at the 41st Annual CSN International Conference tagged Ibadan-2018, Held at University of Ibadan on 16 – 21st September, 2018.

2) Ajanaku C.O., Echeme J.O., Mordi R.C., Ajani O.O., Olugbuyiro J.A.O., **Owoeye T.F**., Taiwo O.S. and Ataboh J.U. (2016). Phytochemical screening and antimicrobial studies of *Crateva adansonii* leaf extract. International Conference tagged CUCIC-2016, Held at Ota in 29th June – 1st July 2016.

3) Ajani O.O., **Owoeye T.F**., Olanrewaju I.O., Adedapo A.E. and Ajanaku C.O. (2015). Heterogeneous catalytic efficiency of silica sulfuric acid toward the synthesis of substituted pyrimidin-2(1*H*)-one derivatives. CSN Conference tagged Abuja 2015 held at International Conference Centre Abuja on 7 – 11th September, 2015.

4) Ajani O.O., Familoni O.B.; Echeme J.O., **Owoeye T.F**., Akinsiku A.A. and Wu F. Facile synthesis, characterization and evaluation of antibacterial activities of 1-(benzylsulfonyl)pyrrolidine-2-carboxylic acid and other sulfonamide derivatives for future drug design. Presentation at the International CSN Conference tagged AKWA IBOM-2014, Held at Uyo on 7 – 12th September, 2014.

5) Paul Sanyaolu,O. C. 1Sanyaolu,A. O. Inegbenebor,**Taiwo Felicia Owoeye**,U.O Daniel,Akinlabu Deborah Kehinde,D.K,Oputa,S.E,P.E 0male,O. O. Ogundiran.(2017) International Conference & Workshop Of Chemical Society Of Nigeria,At: Kaduna-Kadacity 2017,Food Chemistry. Epistemological And Characterization Of Cassia Seed (Cassia Fisfula): Nutritional, Chemical Composition And Functional Importance For Industrial Applications,10.13140/RG.2.2.12927.10400,Conference: 2017

6) Paul Sanyaolu,O. C. Sanyaolu,A. O. Inegbenebor, **Taiwo Felicia Owoeye**,U.O Daniel, Akinlabu Deborah Kehinde,D.K, Omale,O.O,P.E,Okeniyi S.O.,Stephen Kayode Omotugba O.O Ogundiran.(2017)Phytochemical And In Vitro Analysis Of Cassia Fisfula Seed: Antimicrobial Activities For Industrial Applications, August 2017,DOI:10.13140/RG.2.2.11845.76004,Medicinal Chemistry.

E Selected Workshop / Training Attendances

- High Performance Liquid Chromatographic [HPLC] and Gas Chromatographic [GC] Techniques. **[May 2010]**
- Basic Hands on Training on Science Equipment maintenance and Management. **[May 2013]**
- Fire Hazard: Causes, Prevention And Basic Fire Fighting,
- Preparation of High Temperature Concrete/Monolithic for Application in Kiln and Furnaces and Testing**.** **[28th-1st July 2016].**
- Crystallizing the Synergy in Chemical Sciences Between Academia and Industry. **[17th-20th of June 2019].**
- Training workshop organized by National Health Research Ethics Committee in Nigeria in collaboration with Covenant University on Responsible conduct of research:Thinking Research, Thinking Humans **[November 2024]**
- Fire Safety Management System; Navigating the Benefits and Legal Requirements. **[March 2025]**

Referees

- Prof AJANI Olayinka O.
  Department of Chemistry Covenant University, Ota
  (08061670254)

- Prof Emetere, Moses E.
  Physics Department at Bowen University
  (08035267598)

- Engr. Adeboye, Yinka
  Centre for System and Information Services (C.S.I.S)
  Covenant University, Ota.
  (08030508636)

The University Compliance Certification

This is to certify that the Thesis written by Taiwo Felicia OWOEYE with matriculation number LCU/PG/002976 in the Department of Chemical Sciences, Faculty of Applied Sciences, Lead City University, Ibadan, Oyo State is in full compliance with approved University format and style.

Signature **Date**